

**EVALUATION OF STRUCTURE-FUNCTION RELATIONSHIP OF
PHOTOSYNTHETIC MACHINERY IN CYANOBACTERIA EXPOSED TO
CHROMIUM (VI) STRESS**

By

Ms. ALKA GUPTA

LIFE01201004003

Bhabha Atomic Research Centre, Mumbai, India

A thesis submitted to the

Board of Studies in Life Sciences

In partial fulfillment of requirements

for the Degree of

DOCTOR OF PHILOSOPHY

of

HOMI BHABHA NATIONAL INSTITUTE



July, 2013

Homi Bhabha National Institute

Recommendations of the Viva Voce Board

As members of the Viva Voce Board, we certify that we have read the dissertation prepared by Ms. Alka Gupta entitled “**Evaluation of Structure-Function Relationship of Photosynthetic Machinery in Cyanobacteria Exposed to Chromium (VI) Stress**” and recommend that it may be accepted as fulfilling the dissertation requirement for the Degree of Doctor of Philosophy.

_____ **Date:**
Chairman - Dr. S.F. D’Souza

_____ **Date:**
Guide/ Convenor - Dr. S.G. Bhagwat

_____ **Date:**
Member 1 – Dr. (Smt.) J.K. Sainis

_____ **Date:**
Member 2 – Dr. J.S. Melo

_____ **Date:**
Member 3 – Dr. H.N. Ghosh

Final approval and acceptance of this dissertation is contingent upon the candidate’s submission of the final copies of the dissertation to HBNI.

I hereby certify that I have read this dissertation prepared under my direction and recommend that it may be accepted as fulfilling the dissertation requirement.

Date:

Place:

Guide’s Signature

STATEMENT BY AUTHOR

This dissertation has been submitted in partial fulfillment of requirements for an advanced degree at Homi Bhabha National Institute (HBNI) and is deposited in the library to be made available to borrowers under rules of the HBNI.

Brief quotations from this dissertation are allowable without any special permission, provided that accurate acknowledgement of source is made. Requests for permission for extended quotation from or reproduction of this manuscript in whole or in part may be granted by the Competent authority of HBNI when in his or her judgment the proposed use of the material is in the interests of the scholarship. In all other instances, however, permission must be obtained from the author.

Alka Gupta

DECLARATION

I, hereby declare that the investigation presented in this thesis has been carried out by me. The work is original and has not been submitted earlier as a whole or in part for a degree/diploma at this or any other Institution/ University.

Alka Gupta

List of publications arising from the thesis

Journal

1. **Gupta A** and Sainis JK. Isolation of C-phycoyanin from *Synechococcus* sp., *Anacystis nidulans* BD1. J Appl Phycol. 2010;22(3): 231-233.
2. **Gupta A** Bhagwat SG, Sainis JK. *Synechococcus elongatus* PCC 7942 is more tolerant to chromate as compared to *Synechocystis* sp. PCC 6803; Biometals. 2013; 26(2):309-319.
3. **Gupta A**, Ballal A. Role of enzymatic antioxidants in contrasting tolerance of *Synechocystis* and *Synechococcus* to Cr (VI). *Under review in Biometals*
4. **Gupta A**, Bhagwat SG, Sainis JK. Differential modulation of photosynthetic apparatus in *Synechocystis* and *Synechococcus* grown with chromium (VI)". *In preparation*

Publication related to the thesis

1. Verma S, **Gupta A**, Sainis JK, Ghosh HN. Employing a photosynthetic antenna complex to interfacial electron transfer on ZnO quantum dot. J Phys Chem Lett. 2011; 2:858-862.

Conferences

1. **Gupta, A.** and Sainis J.K. (2008); Effect of chromate on photosynthesis and phycobilisome mobility in *Synechococcus* 7942 at conference on "Photosynthesis in the Global Perspective" organized by DAVV Indore between Nov 27-29, 2008. Poster No P-41.
2. **Gupta, A.**, Agarwal, R. and Sainis J.K. (2009); Effect of oxidative stress on phycobilisome mobility examined using fluorescence recovery after photobleaching (FRAP) at Conference-Frontiers in Photobiology, B. A. R. C, Mumbai. August 24 – 26, 2009, Abstract No. PB – 23, p66.
3. Verma, S., **Gupta, A.**, Sainis, J.K., and Ghosh, H.N. (2009); "Interfacial electron transfer dynamics in phycocyanobilin sensitized TiO₂ nanoparticles" at

Conference-Frontiers in Photobiology, B. A. R. C, Mumbai. August 24 – 26, 2009, Abstract No. PB – 23, p88.

4. Verma, S., **Gupta, A.**, Sainis, J.K., and Ghosh, H.N. (2010); “Interfacial electron transfer dynamics in photoactive Phycocyanin-allophycocyanin protein-pigment sensitized ZnO quantum dots” **In: the abstracts of the 3rd Asia Pacific Symposium on Radiation Chemistry**, PC 125, Lonavala, India.
5. **Gupta, A.**, Verma, S., Sainis, J.K., and Ghosh, H.N. (2011); “Comparative Studies on Interfacial Electron Transfer Dynamics in Phycocyanobilin Sensitized TiO₂ Nanoparticles and Phycocyanin Sensitized Quantum Dots” In: 2011 Photosynthesis, Bioenergy and Environment Gordon Research Seminar and Photosynthesis Gordon Research Conference, Davidson College, Davidson, NC, USA.

Courses, Workshops and Schools Attended

1. SERC School attended on LASER Spectroscopy and Applications in Science and Technology (3.11.08 – 21.11.08) conducted by Laser and Plasma Technology Division, BARC, Mumbai.
2. Workshop attended on “Intact Plant Fluorescence” (30.11.08 – 1.12.08) held at School of Life Sciences, DAVV, Indore.
3. Course attended on “Radiation and Photochemistry” conducted by Chemistry Group (Jan 2010 – May 2010).
4. Training on basic operation of Transmission Electron Microscope at Oberkochen, Germany (4.4.2011-8.4.2011).

Alka Gupta

DEDICATIONS

This thesis is dedicated to my teachers, family and friends

ACKNOWLEDGEMENTS

Reaching the stage of writing the acknowledgement is a feat in itself! What follows in this dissertation is the result of efforts of several people. All doctoral students must be fortunate, I find myself to be among the more fortunate ones who have been mentored by two guides, Dr.(Mrs.) J.K. Sainis and Dr. S.G. Bhagwat. Dr.(Mrs.) Sainis provided the vision, encouragement and guidance to proceed throughout the doctoral work. Dr. Bhagwat led my path during the later part; without his patience, kindness and encouragement; this dissertation would not have materialized. Today I find myself nurtured with the wisdom and vision of my guides.

Special thanks to Dr. S.K. Apte, Head, MBD & AD(BMG), Dr. K.B. Sainis, Director, BMG for providing the opportunity to carry out the doctoral work. I am also deeply grateful to Dr. A.D. Ballal, Head, BDRS for helping me take my doctoral work to completion. I am grateful to my organization, BARC, for providing each and every facility required to carry out my doctoral work.

I received generous support of my doctoral committee members, Dr. S.F. D'Souza, the committee chairman and other members; Dr.J.S. Melo and Dr. H.N. Ghosh. Their constructive comments and suggestions helped in bettering the thesis. One simply could not wish for a better committee!

I am deeply grateful to Dr. H. Pal, Dr. M. Kumbhakar, Dr. S.N. Jamdar, Dr. B.N. Pandey, Dr. P. Suprasanna, Dr. N. Jawali and Dr. H.S. Misra for extending their laboratory facilities for experiments. A vote of thanks to Dr. R. Mukhopadhyaya for arranging the radioisotopes. I am indebted to Manjoor and Vasumati for their assistance in carrying out confocal experiments and to Sameer, Sudhakar, Vikas for their timely help. I have greatly benefitted from Dr. H.N. Ghosh

and Dr. S. Verma with whom ultrafast experiments with photosynthetic pigments were conceptualized and performed.

I have been blessed with a friendly and cheerful group of colleagues. Dr. Rajani Kant C., Dr. R. Agarwal, Dr. M. Banerjee, Dr. V. Raut, Namrata, Narendra, Dhiman, Vijay, Jadhav ji extended their help and support. They have been ears to all my grievances that came across and helped me to get back to work.

I find myself short of words to express my feeling of gratitude to my dear friends; Bhanu, Chun Mei, Manish, Priya and Vinay simply for their friendship and all the good times we shared.

Heartfelt thanks to my lovely family; mom-dad, brother, sister-in-law for always being there by me; the newest members, my darling niece Bhuvi, my in-laws and my beloved life-partner Dr. Sanjeev Ranjan have unconditionally supported me. They have been the source of my energies.

Finally, I would take this opportunity to thank all my teachers. They made me what I am today and their teachings will be there with me for life.

Alka Gupta

CONTENTS

Contents	i-vi
Synopsis	vii-xxx
List of figures	xxxi-xxxiii
List of tables	xxxiv
List of abbreviations	xxxv-xxxvi
Chapter-1	1-31
1.1	2
1.2	3
1.3	6
1.3.1	7
1.3.2	13
1.3.3	15
1.3.4	15
1.3.5	16
1.3.6	16
1.3.7	17
1.3.8	17
1.4	18
1.4.1	18
1.4.2	18
1.4.2.1	19
1.4.2.2	19
1.4.3	22

1.5	Metals and living organisms	23
1.5.1	Ability of cyanobacteria to survive in inhospitable environment	23
1.5.2	Metal stress in cyanobacteria	25
1.5.3	Toxic metals in living organisms	26
	1.5.3.1 Chromate tolerance in microflora	27
1.5.4	Effect of chromium on photosynthesis	29
1.6	Aims and objective of the thesis	30
Chapter-2	Evaluation of Chromate Stress Tolerance in <i>Synechocystis</i> and <i>Synechococcus</i>	32-60
2.1	Introduction	33
2.2	Materials and Methods	34
2.2.1	Analysis of chromate toxicity of <i>Synechocystis</i> sp. PCC 6803 and <i>Synechococcus</i> elongatus PCC 7942	34
2.2.2	Determination of Cr (VI) reduction by <i>Synechocystis</i> and <i>Synechococcus</i>	34
2.2.3	Determination of ⁵¹ chromate accumulation	35
	2.2.3.1 Chromate uptake by <i>Synechocystis</i> and <i>Synechococcus</i> in light	35
	2.2.3.2 Sulfate dependence of chromate uptake by <i>Synechocystis</i> and <i>Synechococcus</i>	35
2.2.4	Determination of IC ₅₀ of chromate for ³⁵ sulfate uptake	35
2.2.5	Sequence comparison of sulfate and chromate transporters	36
2.3	Results	36
2.3.1	Analysis of chromate toxicity in <i>Synechocystis</i> and <i>Synechococcus</i>	36
2.3.2	Cr (VI) reduction by <i>Synechocystis</i> and <i>Synechococcus</i>	42
2.3.3	Chromate uptake by <i>Synechocystis</i> and <i>Synechococcus</i>	44
	2.3.3.1 Chromate uptake by <i>Synechocystis</i> and <i>Synechococcus</i> in light	44
	2.3.3.2 Sulfate dependence of chromate uptake by <i>Synechocystis</i> and <i>Synechococcus</i>	45
2.3.4	Determination of IC ₅₀ of chromate for ³⁵ sulfate uptake	46

2.3.5	Sequence comparison of sulfate and chromate transporters in <i>Synechocystis</i> and <i>Synechococcus</i>	48
2.3.5.1	Sulfate-thiosulfate transporters	51
2.3.5.2	Chromate transporters	56
2.4	Discussion	58
Chapter-3	Oxidative Stress Markers in <i>Synechocystis</i> and <i>Synechococcus</i> in Response to Chromate	61-76
3.1	Introduction	62
3.2	Materials and Methods	63
3.2.1	Preparation of cell free extract	63
3.2.2	Assay of catalase content	63
3.2.3	Monitoring 2-Cys-Peroxiredoxin content	64
3.2.4	Monitoring oxidized (carbonylated) protein content	64
3.2.5	<i>In vivo</i> detection of ROS	64
3.2.6	Determination of Superoxide dismutase (SOD) activity	65
3.2.7	Oxidative stress tolerance of <i>Synechocystis</i> and <i>Synechococcus</i> grown with or without potassium chromate	65
3.3	Results	66
3.3.1	Comparison of oxidative stress tolerance between <i>Synechocystis</i> and <i>Synechococcus</i>	66
3.3.2	Effect of growth with chromate on oxidative stress markers in <i>Synechocystis</i> and <i>Synechococcus</i>	68
3.3.2.1	Determination of (ROS)	68
3.3.2.2	Determination of SOD, catalase and peroxiredoxin levels	70
3.3.3	Oxidative stress tolerance of <i>Synechocystis</i> and <i>Synechococcus</i> grown with or without potassium chromate	72
3.4	Discussion	74

Chapter-4	Evaluation of Structure-Function Relationship of Photosynthetic Machinery in <i>Synechocystis</i> and <i>Synechococcus</i> grown with chromate	77-140
4.1	Introduction	78
4.2	Materials and Methods	79
4.2.1	Cell morphology and ultrastructure of <i>Synechocystis</i> and <i>Synechococcus</i> grown with or without chromate	79
4.2.2	Effect of chromate on photosynthetic pigments in <i>Synechocystis</i> and <i>Synechococcus</i>	80
4.2.2.1	Absorption measurement	80
4.2.2.2	Room temperature and 77K fluorescence emission measurement in <i>Synechocystis</i> and <i>Synechococcus</i> grown with or without chromate	80
4.2.3	Studies on phycobilisome redistribution by Confocal Laser Scanning Microscope (CLSM) of <i>Synechocystis</i> and <i>Synechococcus</i> grown with or without chromate	81
4.2.4	Fluorescence Recovery After Photobleaching (FRAP) of <i>Synechocystis</i> and <i>Synechococcus</i> grown with or without chromate by CLSM	81
4.2.5	Assay of photochemical activities of <i>Synechocystis</i> and <i>Synechococcus</i> grown with or without chromate	82
4.2.5.1	Preparation of cell free extract	82
4.2.5.2	PS II activity	82
4.2.5.3	PS I activity	83
4.2.6	Assay of biochemical activities of <i>Synechocystis</i> and <i>Synechococcus</i> grown with or without chromate	83
4.2.6.1	CO ₂ fixation activity	83
4.2.6.2	R-5-P + ATP dependent CO ₂ fixation activity	83
4.2.7	Assay of photosynthetic parameters of <i>Synechocystis</i> and <i>Synechococcus</i> grown with or without chromate by PAM fluorometry	84
4.2.7.1	Measurement of PSII and PSI quantum efficiencies	84
4.2.7.2	Recording of slow induction curve under constant actinic light	85

4.2.7.3	Recording of light curves of ETR(I) and ETR(II)	85
4.2.8	Blue Native Polyacrylamide Gel Electrophoresis (BN PAGE) analysis of thylakoid membrane fractions of <i>Synechocystis</i> and <i>Synechococcus</i> grown with or without chromate	86
4.2.8.1	Preparation of thylakoid membrane fractions	86
4.2.8.2	BN PAGE	86
4.2.9	Studies on thylakoid membrane damage and repair in <i>Synechocystis</i> and <i>Synechococcus</i> grown with or without chromate	87
4.3	Results	88
4.3.1	Effect of chromate on morphology and ultrastructure of <i>Synechocystis</i> and <i>Synechococcus</i> grown with or without chromate	88
4.3.2	Effect of growth with chromate on absorption and fluorescence characteristics of <i>Synechocystis</i> and <i>Synechococcus</i>	92
4.3.2.1	Absorption measurement	92
4.3.2.2	Content of photosynthetic pigments	94
4.3.2.3	Fluorescence emission spectra	96
4.3.2.4	Phycobilisome (PBS) fluorescence redistribution by CLSM	102
4.3.2.5	Phycobilisome mobility by FRAP	104
4.3.3	Effect of growth with chromate on biochemical and photochemical activities in <i>Synechocystis</i> and <i>Synechococcus</i>	108
4.3.3.1	Photosynthetic CO ₂ fixation activity	108
4.3.3.2	PS II activity	110
4.3.3.3	PS I activity	111
4.3.3.4	Partial reactions of Calvin-Benson cycle enzymes in <i>Synechocystis</i> and <i>Synechococcus</i> grown with or without chromate	112
4.3.4	Assay of photosynthetic parameters in the cyanobacteria by PAM fluorometry	113
4.3.4.1	Effect of growth with chromate on maximal quantum yield of PSII (F _v /F _m) and maximal P700 change (P _m)	115
4.3.4.2	Complementary quantum yields of energy conversion in PSI and PSII	117

4.3.4.3	Effect of growth with chromate on cyclic electron flow	119
4.3.4.4	Effect of growth with chromate on ETR in PS I and PS II	122
4.3.4.5	Light curves of electron transport rate of PS I and PS II	123
4.3.4.6	Effect of growth with chromate on parameters of light response reaction in the cyanobacteria	125
4.3.5	Heterogeneity in thylakoids of <i>Synechocystis</i> and <i>Synechococcus</i> grown with or without chromate	127
4.3.6	Thylakoid membrane damage and repair in <i>Synechocystis</i> and <i>Synechococcus</i> in response to growth with chromate	130
4.4	Discussion	136
Chapter-5	Analysis of Phycocyanin Isolated from Cyanobacteria Grown With or Without Chromate	141-158
5.1	Introduction	142
5.2	Materials and Methods	143
5.2.1	Isolation of phycocyanobilin	143
5.2.2	Characterization of PCB	144
5.2.3	Isolation of phycocyanin	144
5.2.4	Characterization of phycocyanin	145
5.3	Results	145
5.3.1	Isolation and characterization of phycocyanobilin	145
5.3.2	Isolation of phycocyanin from <i>Synechococcus</i> grown with or without chromate	149
5.4	Discussion	154
5.5	Application of the phycocyanobilin and phycocyanin	155
Chapter-6	Summary and Future Directions	159-168
	List of references	169
	Reprints of published articles	180

**Evaluation of Structure-Function Relationship of
Photosynthetic Machinery in Cyanobacteria Exposed to
Chromium (VI) Stress**

A

SYNOPSIS

Ms. Alka Gupta

**Enrolment No.: LIFE01201004003, HBNI
Molecular Biology Division, BARC, Mumbai**

INTRODCUTION

Cyanobacteria are the most ancient microorganisms capable of carrying out oxygenic photosynthesis like plants and were responsible for converting the original atmosphere of earth from reducing to oxidizing. They are ubiquitous organisms; found to grow under the most inhospitable ecological niches and have evolved mechanisms to thrive under several abiotic stresses like extreme pH, high and low temperatures, extreme light intensities, oxygen tensions, excessive UV, imbalances in salt concentrations and presence of toxic metal ions etc. Understanding the resistance mechanisms of cyanobacteria to stresses is one of the frontier areas of research. According to current paradigm, essential metal ion deficiency, high light, UV irradiation, desiccation and salinity directly or indirectly lead to oxidative stress (Latifi et al. 2009). The relatively simple form with plant like photosynthetic apparatus of cyanobacteria makes them a suitable system for studying effect of a stress factor on the structure–function relation of their photosynthetic machinery.

A comparison between organisms exhibiting contrasting tolerance to a toxicant is one of the ways of understanding the mechanism of tolerance. Most of such studies are carried out by giving acute stress. It was earlier observed that two unicellular cyanobacteria, *Synechocystis* sp. PCC 6803 and *Synechococcus* sp. BD1, showed contrasting D_{10} values of 800 and 257 Gy for γ irradiation from ^{60}Co source (Agarwal et al. 2011). Ionizing radiations are known to impart oxidative stress. Since these two cyanobacteria showed differences in survival after acute exposure to $^{60}\text{Co}\gamma$ radiations, it was interesting to explore the effect of chronic oxidative stress in the cyanobacteria. Cr (VI) is one such toxicant which can impart chronic oxidative stress by undergoing reduction from Cr (VI) to Cr (III) using intracellular reductants (Cheung and Gu 2007).

Hexavalent chromium (Cr^{6+}) is highly soluble and toxic to most organisms as it causes oxidative damage to biomolecules (Cervantes et al. 2001). However, several microorganisms such as bacteria, fungi and photoautotrophs grow in aquatic bodies contaminated with chromate by adopting various strategies. Some of them reduce Cr (VI) to its less soluble and less toxic form Cr (III) by reductases (Cervantes et al. 2001). Another strategy which prokaryotes employ is efflux of chromium using a plasmid encoded gene, *chrA*. Some of the aquatic biota adsorb chromate on their surface and reduce concentration of chromate in aquatic bodies in which they are growing (Ozturk et al. 2009). Such organisms find use in bioremediation.

Aims and objectives of the thesis

The present thesis contains investigation on tolerance responses of standard strains of two unicellular cyanobacteria, *Synechococcus elongatus* PCC 7942 and *Synechocystis* sp. PCC 6803 (referred to as *Synechococcus* and *Synechocystis* hereafter) to Cr (VI) stress since these two cyanobacteria showed contrasting tolerance to chromate. In addition to investigating a possible general tolerance mechanism, emphasis is given to studies on structure-function of photosynthetic machinery of the cyanobacteria when grown in presence of Cr (VI) as photosynthesis is intrinsically attenuated by the oxidative stress generated during the assimilation of light.

Objectives of the thesis

- 1. Evaluation of chromate stress tolerance in *Synechococcus* and *Synechocystis***
- 2. Assessment of oxidative stress markers in *Synechococcus* and *Synechocystis* in response to chromate**
- 3. Effect of chromate on structure-function of photosynthetic machinery in *Synechococcus* and *Synechocystis***

- Effect of chromate on ultrastructure, especially of thylakoids of *Synechococcus* and *Synechocystis*
 - Biochemical and biophysical characterization of components of photosynthetic electron transport chain
 - Evaluation of phycobilisomes and phycobilisome mobility by Confocal Laser Scanning Microscopy (CLSM)
 - Analysis of heterogeneity in thylakoids isolated from cells grown in presence or absence of chromate
 - Analysis of photosynthetic supercomplexes using Blue Native PAGE (BN PAGE)
 - Evaluation of thylakoid membrane repair in chromate grown cells
- 4. Analysis of phycocyanin isolated from cyanobacteria grown with or without chromate**

Experimental

Log phase cultures of *Synechococcus elongatus* PCC 7942 and *Synechocystis* sp. PCC 6803 were used for all the experiments. Tolerance to chromate in the two cyanobacteria was determined by growing them in the presence of increasing concentration of potassium dichromate and following effect on growth for 20-30 days. Growth in the cultures after 9 days was used to define tolerance as EC₅₀. Chromium uptake by the cyanobacteria was determined by using ⁵¹Cr labeled chromate. Interplay of sulfate and chromate uptake was dissected by using ³⁵S labeled sulfate as tracer. Cr (VI) is known to cause free radical generation in the cells. The oxidative stress was monitored by following the ROS generated in the chromate grown cells using DCFHDA. Antioxidant enzyme levels were also monitored in cell free extracts. Protein damage caused due to ROS was monitored by measuring protein carbonylation. Photosynthetic electron transport process inevitably causes free radical generation and an imbalance between free radical generation and scavenging adversely affects this vital function. Total

photosynthetic CO₂ fixation, PSII, PSI and partial Calvin cycle enzyme activities were monitored in the cells grown in presence of chromate. PSII, PSI contents and light harvesting functions were analyzed biophysically by following room temperature and 77 K fluorescence emission from PSII and phycobilisomes in the chromate grown cells. Phycobilisome mobility was monitored by Fluorescence Recovery after Photobleaching (FRAP) using CLSM. BN PAGE analysis of thylakoid fractions obtained by differential ultracentrifugation was carried out to probe changes in the membrane super complexes. The changes in cell morphology and ultrastructure were determined by performing transmission electron microscopy of the cells grown with or without chromate. Whether chromate grown cells developed better ability to combat oxidative stress was studied by subjecting control and chromate grown cells to high light stress followed by incubation under normal illumination and photosynthetic functions like total CO₂ fixation, room temperature and 77 K fluorescence were measured. Phycocyanin and phycocyanobilin were isolated from *Synechococcus* and interfacial electron transport from phycocyanobilin to TiO₂ nanoparticles was studied using ultrafast transient absorption spectroscopy.

Results and Discussion

➤ Evaluation of tolerance to chromate stress in *Synechococcus* and *Synechocystis*

Comparative studies on chromate tolerance and understanding of mechanism of chromate tolerance in *Synechococcus* and *Synechocystis* were undertaken. Growth and growth rate of *Synechocystis* and *Synechococcus* were measured in the presence or absence of chromate. The capacity of cells to reduce chromate concentration in medium, its accumulation in cells and its effect on inhibition of sulfate uptake were monitored.

- *EC₅₀ values for chromate in *Synechocystis* and *Synechococcus**

The two strains were grown with different concentrations of chromate for 30 days. Both showed a lag of 4-5 days followed by exponential growth up to 14 days. Chromate tolerance was monitored as EC₅₀ values which is the concentration of potassium dichromate at which number of cells ml⁻¹ was 50% as compared to control. Growth on 9th day after inoculation was used to compare chromate tolerance. *Synechococcus* and *Synechocystis* showed contrasting responses to chromate stress with 9 day EC₅₀ of 150 ± 15 µM and 12 ± 2 µM potassium dichromate respectively. Interestingly, *Synechococcus* showed stimulation of growth at concentrations of chromate less than 100 µM. This contrasting tolerance was specific to chromate as tolerance of *Synechococcus* and *Synechocystis* to other metal oxyanions like molybdate, tungstate and arsenate was similar.

- *Intracellular accumulation of chromate in *Synechocystis* and *Synechococcus**

There was no reduction in Cr (VI) concentration in the growth medium after growth of cyanobacteria as determined by Di Phenyl Carbazide (DPC) reduction assay, suggesting that the tolerance could not be attributed to reduction of Cr (VI) to Cr (III). Using ⁵¹Cr labeled chromate, low level of light dependent accumulation (< one nanomole/10⁸ cells) was observed in live cells of *Synechocystis* over 24 hour incubation with medium containing ~ 100 µM chromate. No accumulation of chromate was observed in *Synechococcus* under these conditions.

- *Competitive inhibition of sulfate uptake by chromate in *Synechocystis* and *Synechococcus**

Chromate oxyanion is known to enter the cells using sulfate uptake channels. Inhibition of sulfate uptake was observed in both the cyanobacteria when log phase cells were incubated with increasing concentration of chromate at two different concentrations of

^{35}S labeled sulfate. Sulfate uptake was competitively inhibited by chromate and IC_{50} of chromate for uptake of sulfate was higher in *Synechococcus* as compared to *Synechocystis*. The results suggested that the sulfate transporters in *Synechococcus* have lower affinity to chromate than those from *Synechocystis*.

- *Bioinformatic analysis of sulfate and chromate transporters in Synechocystis and Synechococcus*

Genomes of these two cyanobacteria have been sequenced and annotated and are available in Cyanobase (<http://genome.microbedb.jp/cyanobase/>). Translated amino acid sequences of chromate and sulfate transporter genes in *Synechocystis* and *Synechococcus* were compared. Both the cyanobacteria have typical sulfate and chromate transporters with conserved motifs. Although bioinformatic comparison of chromate and sulfate transporters revealed identity to a varying extent, the differences in their primary sequences could account for the difference in IC_{50} of chromate. Thus in addition to these differences, the other putative sulfate permease annotated in these two organisms may play a role in their distinct chromate response. Chromate resistance of *Synechococcus* would give it growth advantage in chromate contaminated sites over sensitive species such as *Synechocystis*. Thus the multifarious interaction of sulfate/chromate transporters could be the basis or form an important component of contrasting response of *Synechococcus* and *Synechocystis* to chromate.

In summary the results suggested that the differential sensitivity of *Synechococcus* and *Synechocystis* to chromate may be attributed partly to the differences in affinity of their sulfate transporters to chromate. Lack of accumulation of chromate in *Synechococcus* can be due to presence of active efflux system. The variability observed in the non-conserved regions of sulfate and chromate transporters may have a role in their differential response to chromate. The large difference in response to chromate by the two organisms may be

attributed to a multi-component process. Although the comparison is between two genera, the difference in chromate resistance between the two makes it a suitable system for investigations on the resistance contributing factors and their interplay (*Gupta et al. 2013).

➤ **Evaluation of oxidative stress in *Synechocystis* and *Synechococcus* in response to chromate**

Chromate is known to impart oxidative stress by reduction of Cr (VI) to Cr (III) using cellular reductants which results in generation of reactive oxygen species (ROS). Reactive oxygen species are detoxified enzymatically by antioxidants like catalases, superoxide dismutase (SOD) and peroxidases. An imbalance between ROS production and their detoxification causes damage to protein, lipids and DNA which in turn leads to physiological malfunctions. *Synechococcus* and *Synechocystis* grown with respective EC₅₀ concentration of chromate for 9-10 days showed presence of 4-6 n moles chromate/10⁸ cells. Therefore level of oxidative stress markers was evaluated in these cells. In addition, induction of these markers in response to chromate was studied by giving acute stress of chromate to normally grown cyanobacteria.

- *Effect of chronic chromate stress on oxidative stress markers in *Synechocystis* and *Synechococcus**

Effect of growth with chromate on ROS levels, protein carbonylation, SOD and catalase was monitored in *Synechocystis* and *Synechococcus*. ROS content increased in *Synechocystis* when grown with increasing chromate concentration ranging from 0 to 100 μM. In case of *Synechococcus*, ROS increase was pronounced only at chromate concentrations higher than 200 μM at which growth was drastically reduced. An increase in catalase and SOD levels was observed in both the cyanobacteria when

grown in the presence of respective EC₅₀ chromate concentrations. In addition, *Synechocystis* inherently showed lower levels of catalase and 2-Cys Peroxiredoxin as compared to *Synechococcus* on equal protein basis. *Synechocystis* also showed higher number of carbonylated proteins as detected by immunoblotting with anti-2,4-dinitrophenylhydrazine antibody.

When the cells of these cyanobacteria grown with or without chromate were exposed to different concentrations of H₂O₂ for 24 hours, the chromate grown cells of *Synechocystis* showed higher adaptation to extra stress due to H₂O₂. In case of *Synechococcus*, however, there was no additional advantage of growth with chromate to their susceptibility to oxidative stress. This suggested that when grown with chromate *Synechocystis* developed adaptive mechanisms which could combat extra oxidative stress. This feature was not observed in *Synechococcus*.

- *Effect of acute chromate stress on oxidative stress markers in Synechocystis and Synechococcus*

To study the effect of acute chromate stress on the induction of catalase, SOD and on protein carbonylation, log phase cells of *Synechocystis* and *Synechococcus* were incubated with 0, 50 or 300 µM potassium dichromate up to 48 hours. These concentrations were determined on the basis of effect of 24 hour light incubation with chromate on ¹⁴CO₂ fixation rates in *Synechococcus* and *Synechocystis*. ¹⁴CO₂ fixation rates were reduced to half of control at 50 µM chromate in *Synechocystis* and at 300 µM chromate in *Synechococcus*. Increase in catalase and SOD activities in *Synechocystis* and *Synechococcus* along with marginal increase in carbonylated proteins was observed in these samples incubated with chromate.

In summary, *Synechococcus* inherently had higher level of antioxidative enzymes as compared to *Synechocystis*. However in both the cyanobacteria, the levels of these

enzymes rose on growth or incubation with chromate. These results along with more ROS content in chromate grown *Synechocystis* indicated that chromate caused oxidative stress because of its transient presence inside the cells. Due to lower inherent level of antioxidants and relatively higher chromate inside, *Synechocystis* may be less tolerant to chromate stress as shown by a low EC₅₀.

➤ **Evaluation of chromate stress on structure function of photosynthetic apparatus in *Synechocystis* and *Synechococcus***

Photoautotrophic growth in the presence of Cr (VI) would be a metabolic challenge to the organism. When grown with chromate, photosynthetic machinery of cyanobacteria would be required to be adjusted to additional chronic oxidative stress in addition to normal oxidative stress produced in photosynthetic electron transport. Therefore, biophysical and biochemical parameters, pigment protein complexes and ultrastructure were evaluated in *Synechocystis* and *Synechococcus* grown with chromate. In addition photoinhibition and thylakoid membrane repair was studied in cells of *Synechocystis* and *Synechococcus* grown with or without chromate.

- *Effect of chromate on morphology and ultrastructure*

Effect of chromate on morphology and ultrastructure was determined by transmission electron microscopy of the cells grown with chromate. In *Synechocystis*, growth with 12 μM potassium dichromate damaged the ultrastructure and thylakoid organization with deformation from regular spherical shape. In *Synechococcus* slight reduction in average length of cells was observed on growth in presence of 150 μM potassium dichromate, thylakoid structure was not affected.

- *Effect of chromate on pigment composition*

Chlorophyll, phycocyanin and carotenoids were measured in *Synechocystis* and *Synechococcus* grown with chromate on per cell basis. *Synechocystis* showed up to 50 % decrease in chlorophyll and phycocyanin per cell in cells grown with 10 μM potassium dichromate as compared to control. In *Synechococcus*, pigment concentration on per cell basis was not affected in 75 μM potassium dichromate, but it decreased when grown in presence of 150 μM potassium dichromate.

- *Effect of chromate on biophysical parameters*

Biophysical parameters like absorption and fluorescence emission characteristics are indicative of overall state of the photosynthetic apparatus. Absorption spectra showed a decrease in pigment content per cell in *Synechocystis* and *Synechococcus* grown in the presence of their respective EC_{50} chromate concentrations. An increase in the allophycocyanin to PSII fluorescence ratio in *Synechococcus* grown with 150 μM chromate indicated a dissociation of phycobilisomes from PSII when fluorescence at room temperature was monitored by excitation with 580 nm.

Further, 77 K fluorescence emission was monitored in the two cyanobacteria grown with or without chromate. In both, decrease in the PSII/PSI fluorescence ratio was observed in the cells grown with chromate suggesting a relative increase in PSI content or decrease in PSII content. On excitation of phycobilisome at 580nm, characteristic peaks of allophycocyanin, PSII and PSI were observed in the two cyanobacteria at 77 K. In both the cyanobacteria, changes in the association of phycobilisome (PBS) to PSII and PSI were observed in chromate grown cells as compared to control cells. In *Synechocystis*, an increase in PSII/PSI fluorescence indicated more PBS-PSII association in chromate grown cells. In *Synechococcus*, cells grown with 75 μM potassium dichromate showed enhanced energy transfer from PBS to PSII as compared to PSI whereas in cells grown with 150 μM potassium dichromate, a drastic reduction in

PSII/PSI ratio occurred which suggested higher energy transfer from phycocyanin to PSI as compared to PSII.

- *Effect of chromate on phycobilisome mobility*

Phycobilisomes are the light harvesting complexes of cyanobacteria located on the outer surface of thylakoid membrane and are known to diffuse rapidly on the surface to allow the cells to adapt to varying light conditions (Mullineaux et al. 1997). Phycobilisomes are a possible target of ROS and have been shown to undergo dissociation and decoupling with reaction centres in presence of oxidative stress (Liu et al. 2005). Fluorescence Recovery after Photobleaching (FRAP) was used to study mobility of phycobilisomes. Phycobilisome mobility was not affected in *Synechocystis* cells grown with or without chromate. However in *Synechococcus*, growth with 150 μM potassium dichromate resulted in reduction in phycobilisome mobility. This is in agreement with drastic reduction in PSII/PSI fluorescence on 580 nm excitation at 77 K. The ratio of absorbance at 680/620 in control and chromate grown cells did not change indicating no change in antenna sizes.

- *Effect of chromate on biochemical parameters*

Rate of CO_2 fixation on equal chlorophyll basis was higher in *Synechocystis* as compared to *Synechococcus* suggesting subtle differences in the abilities of their photosynthetic machinery. CO_2 assimilation rates followed the response of growth pattern to chromate in the two cyanobacteria. The cells grown at their EC_{50} concentration showed a marginal decline in rate of CO_2 fixation on chlorophyll basis. *Synechococcus* grown in presence of 75 μM potassium dichromate showed a higher rate of CO_2 fixation on chlorophyll basis as compared to control indicating higher efficiency of photosynthetic machinery.

PSII is generally considered to be more sensitive to various stresses. *Synechocystis* grown with 12 μM chromate showed a ~70% decline in PSII activity as compared to control whereas *Synechococcus* showed a decline up to 30 % in cells grown with 150 μM chromate on chlorophyll basis. However as observed in CO_2 fixation, 75 μM potassium dichromate grown cells showed a higher PSII activity as compared to control in *Synechococcus*. PSI activity was reduced by 20 % in *Synechocystis* grown in presence of 12 μM potassium dichromate and was maintained as good as control in *Synechococcus* grown in presence of 150 μM potassium dichromate on chlorophyll basis, whereas 75 μM potassium dichromate grown cells of *Synechococcus* showed a higher PSI activity as compared to control. Fluorescence data also showed that PSII/PSI fluorescence ratio decreased in chromate treated cells.

R-5-P dependent $^{14}\text{CO}_2$ fixation monitors activity of three sequential Calvin cycle enzymes, phosphoriboisomerase, phosphoribulokinase and RuBP carboxylase. This R-5-P dependent $^{14}\text{CO}_2$ fixation activity decreased in *Synechocystis* grown with 12 μM chromate on equal chlorophyll basis. In contrast, in *Synechococcus*, this partial activity was unaffected in cells grown with 75 μM chromate and increased by ~ 60 % in cells grown with 150 μM chromate suggesting differential response of Calvin cycle enzymes to chromate.

- *Effect of chromate on pigment protein complexes analyzed on BN PAGE*

Cell free extracts of the cyanobacteria can be separated by differential ultracentrifugation in three fractions sedimenting at 40,000 x g, 90,000 x g and 1,50,000 x g. These membrane fractions show differences in proteomic and biophysical properties suggesting thylakoid membrane heterogeneity in *Synechococcus* and *Synechocystis* (Dani and Sainis 2005, Agarwal et al., 2010, 2012). Membrane heterogeneity in the two cyanobacteria grown in presence of chromate was studied. Thylakoid membranes isolated from *Synechocystis*

and *Synechococcus* cells grown with chromate were subjected to differential ultracentrifugation at 40,000 x g, 90,000 x g and 1,50,000 x g and three fractions were obtained. The three thylakoid fractions from control and chromate grown cells were subjected to Blue Native PAGE. Alteration in the profile of super complexes from cells grown with or without Cr (VI) was observed in terms of mobility and quantity. Qualitative and quantitative differences in pigment-protein complexes from thylakoid membranes of chromate grown and control cells indicated differences in assembly of components of the supercomplexes. This suggested that growth with chromium probably results in modification of supercomplexes.

- *Effect of chromate on membrane biogenesis and repair*

Photosynthesis is affected by high light intensity, this is termed as photoinhibition. It involves damage to thylakoid membranes along with their repair and recovery after incubation with low light. The effect of high light on *Synechocystis* and *Synechococcus* grown with or without chromate was measured by following $^{14}\text{CO}_2$ fixation and fluorescence characteristics to monitor thylakoid membrane damage and repair. High light inhibited CO_2 fixation in *Synechocystis*, but not in *Synechococcus*. The extent of inhibition of CO_2 fixation after high light stress was higher in cells grown with chromate as compared to the respective controls. After photoinhibition, the cultures were incubated in normal illumination conditions ($\sim 30 \mu\text{mol m}^{-2}\text{s}^{-1}$) for 2 hours to undergo recovery. In the cultures grown with chromate, recovery was lower as compared to control cells. The extent of photoinhibition was more in the cells exposed to high light in presence of chloramphenicol suggesting active role of protein synthesis in the process of recovery.

The reduction in photosynthetic activity is mainly due to damage to photosystems, especially photosystem II. Absorption and fluorescence emission spectra of the above

samples were monitored to study the damage caused to PSII. Fluorescence was reduced in all the samples in response to light stress and recovery was poor in case of cells grown with chromate. In *Synechocystis*, the characteristic peak and shape of the absorption spectra were maintained after light stress and recovery, whereas in case of *Synechococcus* emergence of fluorescence at 655 nm, characteristic of allophycocyanin was observed after light stress. This allophycocyanin fluorescence was higher in case of *Synechococcus* cells grown with chromate. These observations showed that PSII is affected by light stress both in control and chromate grown cells. Fluorescence emission spectra after excitation of phycobilisome at 580 nm were monitored in all the samples. In both the cyanobacteria, control cells showed allophycocyanin and PSII characteristic peaks at 655 nm and 686 nm respectively. After light stress, PSII peak disappeared in both cyanobacteria. This indicated uncoupling of phycobilisomes and PSII. These changes in the fluorescence emission spectra along with study of ^{14}C fixation rates showed that thylakoid membrane damage and repair was affected in the cells grown with chromate and the two cyanobacteria showed differences in the extent of damage and repair of thylakoid membranes.

In summary studies on structure function of photosynthetic machinery showed that thylakoid organization was affected by growth with chromate in *Synechocystis*, but not in *Synechococcus*. There was no effect of growth with chromate on pigment composition although PSII/PSI ratios and activities were affected. Phycobilisome mobility was affected in *Synechococcus* cells grown with chromate. Thus although there was reduction in pigments of photosynthesis on per cell basis, major photosynthetic functions were maintained to reasonable level on growth with chromate. This may be due to adjustments in the photosynthetic apparatus as seen by the alterations in pigment

protein complexes on BN PAGE. The general growth retardation around EC_{50} may be due to reduced amounts of pigments in cells in presence of chromate.

➤ **Analysis of phycocyanin isolated from *Synechococcus* grown with or without chromate**

There is considerable interest in exploring the natural light harvesting complexes (LHC) for their potential use in artificial photosynthesis. The aim is to use these antenna complexes in “fabrication of robust micron-scale biohybrid light harvesting systems to drive chemical processes or to generate photocurrent”. In cyanobacteria the antenna system comprises of water soluble mobile pigment protein complexes *viz* phycocyanin and allophycocyanin organized in phycobilisomes. These pigment protein complexes have covalently attached chromophore phycocyanobilin which is open chain tetrapyrrole. The potential of phycocyanobilin to act as sensitizer of semiconductor TiO_2 nanoparticles was analyzed. In addition, as *Synechococcus* cells could grow in presence of chromate and with adjustments in the photosynthetic apparatus major photosynthetic functions were maintained, the possibility of differences in their light harvesting complexes was explored.

- *Isolation and characterization of phycocyanobilin from Synechococcus spp.*

Isolation of pigment phycocyanobilin was optimized from *Synechococcus* spp. by HCl treatment followed by extraction in chloroform. This pigment preparation was characterized by absorption spectroscopy and also by HPLC. TiO_2 nanoparticles were sensitized with isolated phycocyanobilin and the electron transfer dynamics was studied by ultrafast transient absorption spectroscopy. The results showed that phycocyanobilin sensitized the TiO_2 semiconductor nanoparticles and electron injection from photo-excited states of phycocyanobilin was observed to take place. However, multi

exponential back electron transfer was also observed and the pigment was not stable. Therefore phycocyanin-allophycocyanin was used for further studies.

- *Isolation of phycocyanin from Synechococcus spp.*

A simple and efficient procedure was developed to isolate phycocyanin from *Anacystis nidulans* (BD1), a local isolate of *Synechococcus* spp. using lysozyme treatment of the cells. The purity ($A_{620/280}$) of phycocyanin obtained after lysozyme treatment was up to 2.18, which was improved up to 4.72 after incubation with activated charcoal and chitosan. The yield of phycocyanin was 80–100 mg·g⁻¹ dry weight of cells (*Gupta and Sainis 2010). Using this procedure, phycocyanin-allophycocyanin from the tolerant strain under study, *Synechococcus elongatus* PCC 7942 grown with or without chromate was isolated and analyzed. The antenna functionality of phycocyanin-allophycocyanin isolated from *Synechococcus* spp. as sensitizer of semiconductor was carried out using ZnO quantum dots (Verma et al. 2011).

The phycocyanin-allophycocyanin complexes isolated from chromate grown and control cells showed similar subunit composition, in addition to similar biophysical properties suggesting that the antenna function of light harvesting complexes was not altered by chromate, although *in vivo* mobility of phycobilisomes was affected in cells grown with 150 μM chromate.

The results opened a new vista in use of antenna complexes in biohybrid photocurrent generating systems. Although the photosynthetic apparatus shows considerable changes after growth with chromate, the antenna systems do not show any significant structural-functional alterations.

➤ Summary and future directions

In the present study, contrasting tolerance of the two unicellular cyanobacteria to chromate stress and its effect on the structure and function of the photosynthetic apparatus was investigated. Evaluation of chromate stress tolerance in *Synechococcus* and *Synechocystis* showed that *Synechococcus* was more tolerant as compared to *Synechocystis*; this differential tolerance was specific to chromate oxyanion and not general to other metal oxyanions like molybdate, tungstate or arsenate. The differential tolerance was explained by dissecting the mechanism of chromate uptake and efflux systems which further explained the structural and functional changes occurring in the cyanobacteria in response to chromate. It is known that chromate ion enters the cells using sulfate transporters present in cell membrane as chromate ion is nearly identical in size shape and charge as sulfate ion. Decrease in uptake of chromate due to its similarity with sulfate along with seemingly more efficient chromate efflux in *Synechococcus* may make it more tolerant. The results suggested that *Synechococcus* possesses efficient strategies to prevent entry and to remove chromate from the cell as compared to *Synechocystis*. Since the cells were continuously exposed to chromate during their growth, there may be transient presence of chromate inside the cells to varying levels in *Synechocystis* and also in *Synechococcus*. Assessment of oxidative stress markers in *Synechococcus* and *Synechocystis* in response to chromate showed *Synechococcus* to be inherently better equipped to deal with oxidative stress as compared to *Synechocystis*. Studies on effect of growth with chromate on ultrastructure, especially of thylakoids showed that more damage to the cellular structure was observed in *Synechocystis* as compared to *Synechococcus* in response to growth with chromate which is in agreement with ability to combat the stress. Experiments on effect of chromate on photosynthetic machinery in *Synechococcus* and *Synechocystis* showed that there was no effect of

growth with chromate on pigment composition although PSII and PSI activities were affected differentially. PSII was affected more as compared to PSI. Phycobilisome mobility was affected in *Synechococcus* cells grown with chromate. Biophysical studies suggested that chromate treatment altered PII/PSI content as well as energy transfer from light harvesting complexes to photosystems. Major photosynthetic functions were maintained in *Synechococcus* cells on growth with chromate by making adjustments in the photosynthetic apparatus. Analysis of heterogeneity in thylakoids isolated from cells grown in presence or absence of chromate carried out by BN PAGE analysis showed alterations in pigment protein complexes. The studies in thylakoid membrane damage and repair revealed a new paradigm. *Synechocystis* which was more sensitive to chromate showed decreased sensitivity to high light stress in its chromate grown cells. However, *Synechococcus* which was inherently more resistant to photoinhibition succumbed more to high light if cells were grown with chromate. The results suggested that in *Synechococcus* the cellular machinery was engaged in tolerating high levels of chromate in medium and therefore did not have enough resources to tolerate any additional oxidative stress. The results on H₂O₂ tolerance also showed similar phenomenon, where *Synechocystis* showed more adaptation to higher oxidative stress as compared to *Synechococcus* although the later can grow with fold more chromate than the former. Thus both these cyanobacteria appear to be intrinsically different in their responses to chromate and the resultant oxidative stress. Evaluation of phycobilisomes and phycobilisome mobility by CLSM showed that growth of *Synechococcus* cells in chromate affected phycobilisome mobility. Therefore the light harvesting complex from these tolerant cyanobacteria was studied. The phycocyanin isolated from *Synechococcus* cells grown with or without chromate showed similar subunit composition and comparable spectral features.

In future, the contrasting characteristics observed in the two cyanobacteria would be useful in understanding the complex relationship of chromate and sulfate transporters. Further studies are needed to comprehend the phenomenon of stimulation of growth and morphological changes in *Synechococcus* at low concentration of chromate although no chromate uptake is observed in this organism. Identification of chromate sensitive mutant of *Synechococcus* or chromate resistant mutant in *Synechocystis* may be an approach to identify gene(s) for chromate tolerance. Although at this stage it appears that the multifarious interaction of sulfate/chromate transporters could be the basis of contrasting response of *Synechococcus* and *Synechocystis* to chromate and isolation of single mutations may not be possible. It will be interesting to explore the transcriptome, proteomes and metabolome in these two taxonomically related cyanobacteria in response to chromate stress. Further studies on molecular mechanisms of chromate tolerance in cyanobacteria may accentuate our knowledge about mechanisms of chromate tolerance in higher plants.

Organization of the Thesis

The thesis is organized into six chapters. In the first chapter information about the chromate tolerance in general and in microorganisms in particular is presented. The literature related to effect of chromate on photosynthesis is also reviewed. Second chapter deals with comparison of chromate tolerance in *Synechococcus elongatus* PCC 7942 and *Synechocystis* sp. PCC 6803 with respect to growth, chromate uptake and its relation with sulfate uptake. Cr (VI) is known to cause oxidative stress by production of ROS. Third chapter of the thesis deals with comparative studies on oxidative stress in *Synechococcus* and *Synechocystis*. Photosynthesis is the site of production of ROS which cause damage to the photosynthetic machinery. Fourth chapter of the thesis elaborates the effect of

chromate stress on structure function of photosynthetic apparatus in the two cyanobacteria under study. Fifth chapter is on analysis of phycocyanobilin and phycocyanin isolated from *Synechococcus* spp. in addition to isolation and characterization of phycobiliproteins isolated from *Synechococcus* grown with or without chromate. The last chapter includes summary and future directions.

References

- Agarwal R (2011) Physico-chemical Characterization and Biogenesis of Photosynthesome and Thylakoid Membranes from *Synechocystis* 6803, Ph D Thesis Homi Bhabha National Institute, Mumbai, (LIFE01200704003) Chapter 5: 140-166
- Agarwal R, Maralihalli G, Sudarsan V, Choudhury SD, Vatsa RK, Pal HK, Melzer M, and Sainis JK (2012) Differential Distribution of Pigment-Protein Complexes in the Thylakoid Membranes of *Synechocystis* 6803, *Journal of Bioenergetics and Biomembranes*, 44:399-409
- Agarwal R, Melzer M, Matros A, Mock H-P, and Sainis JK (2010) Heterogeneity in thylakoid membrane proteome of *Synechocystis* 6803, *Journal of Proteomics* 73: 976 – 991
- Cervantes C, Garcia JSC, Devars S, Gutierrez-Corona F, Loza-Tavera H, Torres-Guzma JC, and Moreno-Sanchez R (2001) Interactions of chromium with microorganisms and plants. *FEMS Microbiol Reviews* 25: 335-347
- Cheung KH, and Gu JD (2007) Mechanism of hexavalent chromium detoxification by microorganisms and bioremediation application potential: A review. *International Biodeterioration & Biodegradation* 59: 8–15

- Dani DN, and Sainis JK (2005) Isolation and characterization of a thylakoid membrane module showing partial light and dark reactions. *Biochim. Biophys. Acta* 1969: 43-52.
- Latifi A, Ruiz M, and Zhang CC (2009) Oxidative stress in cyanobacteria. *FEMS Microbiology Reviews* 33: 258–278
- Liu XG, Zhao JJ, and Wu QY (2005) Oxidative stress and metal ions effects on the cores of phycobilisomes in *Synechocystis* sp. PCC 6803. *FEBS Letters* 579: 4571–4576
- Mullineaux CW, Tobin MJ, and Jones GR (1997) Mobility of photosynthetic complexes in thylakoid membranes. *Nature* 390: 421-424
- Ozturk S, Aslim B, and Suludere Z (2009) Evaluation of chromium (VI) removal behavior by two isolates of *Synechocystis* sp. in terms of exopolysaccharide (EPS) production and monomer composition. *Bioresource Technology* 100: 5588-5593
- Verma S, Gupta A, Sainis JK, Ghosh HN (2011) Employing a Photosynthetic Antenna Complex to Interfacial Electron Transfer on ZnO Quantum Dot. *Journal of Physical Chemistry Letters*, 2: 858-862

Publications

1. ***Gupta A** and Sainis JK, (2010) Isolation of C-phycoyanin from *Synechococcus* sp., *Anacystis nidulans* BD1. *Journal of Applied Phycology* 22, 3: 231-233.
2. ***Gupta A**, Bhagwat SG, Sainis JK. *Synechococcus elongatus* PCC 7942 is more tolerant to chromate as compared to *Synechocystis* sp. PCC 6803; *Biometals*. 2013; 26(2):309-319.

Posters and Oral Presentations

1. **Gupta A** and Sainis JK (2008); Effect of chromate on photosynthesis and phycobilisome mobility in *Synechococcus* 7942 at conference on Photosynthesis in the Global Perspective” organized by DAVV Indore between Nov 27-29, 2008. Poster No P-41.
2. **Gupta A**, Agarwal, R and Sainis JK (2009); Effect of oxidative stress on phycobilisome mobility examined using fluorescence recovery after photobleaching (FRAP) at Conference-Frontiers in Photobiology, B. A. R. C, Mumbai. August 24 – 26, 2009, Abstract No. PB – 23, p66.
3. Verma S, **Gupta A**, Sainis JK, and Ghosh HN (2009); “Interfacial electron transfer dynamics in phycocyanobilin sensitized TiO₂ nanoparticles” at Conference-Frontiers in Photobiology, B. A. R. C, Mumbai. August 24 – 26, 2009, Abstract No. PB – 23, p88.
4. Verma S, **Gupta A**, Sainis JK, and Ghosh HN (2010); “Interfacial electron transfer dynamics in photoactive Phycocyanin-allophycocyanin protein-pigment sensitized ZnO quantum dots” **In: the abstracts of the 3rd Asia Pacific Symposium on Radiation Chemistry**, PC 125, Lonavala, India.
5. **Gupta A**, Verma S, Sainis JK, and Ghosh HN (2011); “Comparative Studies on Interfacial Electron Transfer Dynamics in Phycocyanobilin Sensitized TiO₂ Nanoparticles and Phycocyanin Sensitized Quantum Dots” In: 2011 Photosynthesis, Bioenergy and Environment Gordon Research Seminar and Photosynthesis Gordon Research Conference, Davidson College, Davidson, NC, USA.

Courses, Workshops and Schools Attended

1. SERC School attended on LASER Spectroscopy and Applications in Science and Technology (3.11.08 – 21.11.08) conducted by Laser and Plasma Technology Division, BARC, Mumbai.
2. Workshop attended on “Intact Plant Fluorescence” (30.11.08 – 1.12.08) held at School of Life Sciences, DAVV, Indore.
3. Course attended on “Radiation and Photochemistry” conducted by Chemistry Group (Jan 2010 – May 2010).
4. Training on basic operation of Transmission Electron Microscope at Oberkochen, Germany (4.4.2011-8.4.2011).

List of figures

Figure No.	Title
Figure 1.1	A typical cyanobacterial cell
Figure 1.2	A simplified Z scheme of electron transport in cyanobacteria
Figure 1.3	Components of photosynthetic electron transport chain in cyanobacteria
Figure 1.4	Sources of ROS generation in the photosynthetic electron transport chain of cyanobacteria
Figure 1.5	Photodamage and repair of PSII
Figure 2.1	Growth curve of <i>Synechocystis</i> and <i>Synechococcus</i> grown with potassium dichromate
Figure 2.2	Tolerance of <i>Synechocystis</i> and <i>Synechococcus</i> to potassium dichromate
Figure 2.3	Effect of inoculum size on EC ₅₀ value of potassium dichromate for <i>Synechocystis</i> and <i>Synechococcus</i>
Figure 2.4	Chromium (VI) reduction by <i>Synechocystis</i> and <i>Synechococcus</i>
Figure 2.5	Uptake of ⁵¹ chromate by <i>Synechocystis</i> and <i>Synechococcus</i> in light
Figure 2.6	Sulfate dependence of chromate uptake by <i>Synechocystis</i> and <i>Synechococcus</i>
Figure 2.7	Effect of chromate on uptake of ³⁵ S labeled sulfate by <i>Synechocystis</i> and <i>Synechococcus</i>
Figure 2.8	Sequence comparison of Sbp, a periplasmic sulfate binding protein
Figure 2.9	Sequence comparison of CysA, the ATPase subunit of the SulT permease
Figure 2.10	Sequence comparison of CysT, transport channel protein of the SulT permease
Figure 2.11	Sequence comparison of CysW, transport channel protein of the SulT permease
Figure 2.12	Sequence comparison of chromate transporters
Figure 3.1	Catalase, 2-cys peroxiredoxin and protein carbonylation levels in

Synechocystis and *Synechococcus*

- Figure 3.2 ROS content in *Synechocystis* and *Synechococcus* grown with increasing concentration of potassium dichromate
- Figure 3.3 Catalase levels in *Synechocystis* and *Synechococcus* grown with or without potassium chromate
- Figure 3.4 Effect of growth with chromate on 2-cys peroxiredoxin levels in *Synechocystis* and *Synechococcus*
- Figure 3.5 Effect of incubation with H₂O₂ on *Synechocystis* and *Synechococcus* grown with chromate
- Figure 4.1 Ultrastructure of *Synechocystis* and *Synechococcus* cells grown with or without potassium dichromate
- Figure 4.2 Changes in cell size and shape of *Synechocystis* and *Synechococcus* cells grown with or without potassium dichromate
- Figure 4.3 Absorption spectra of *Synechocystis* and *Synechococcus* cells grown with or without potassium dichromate
- Figure 4.4 Room temperature fluorescence emission spectra of *Synechocystis* and *Synechococcus* cells grown with or without potassium dichromate
- Figure 4.5 77K fluorescence emission spectra of *Synechocystis* and *Synechococcus* cells grown with or without potassium dichromate
- Figure 4.6 Association of phycobilisomes with thylakoid membranes using CLSM in *Synechocystis* and *Synechococcus* grown with or without chromate
- Figure 4.7 Phycobilisome Mobility by FRAP in *Synechococcus*
- Figure 4.8 ¹⁴CO₂ fixation in *Synechocystis* and *Synechococcus* and grown with or without chromate
- Figure 4.9 PSII activity in *Synechocystis* and *Synechococcus* grown with or without chromate
- Figure 4.10 PSI activity in *Synechocystis* and *Synechococcus* grown with or without chromate
- Figure 4.11 Linked activity of three Calvin cycle enzymes in *Synechocystis* and *Synechococcus* grown with or without chromate

- Figure 4.12 Quantum yield of cyclic electron flow in *Synechocystis* and *Synechococcus* grown with or without chromate
- Figure 4.13 Effect of growth with chromate on ratios of Y(CEF)/Y(I), Y(CEF)/Y(II) and Y(II)/Y(I) on *Synechocystis* and *Synechococcus*
- Figure 4.14 Effect of growth with chromate on ETR of PSI and PSII
- Figure 4.15 Light curves of electron transport rate of PSI and PSII in the cyanobacteria grown with or without chromate
- Figure 4.16 BN PAGE images of thylakoid fractions from *Synechocystis* and *Synechococcus* grown with or without chromate
- Figure 4.17 $^{14}\text{CO}_2$ fixation rates after thylakoid membrane damage and repair in *Synechocystis* and *Synechococcus* grown with or without chromate
- Figure 4.18 Absorption spectra of *Synechocystis* and *Synechococcus* grown with or without chromate incubated under high light followed by incubation under normal illumination
- Figure 4.19 Room temperature fluorescence emission spectra of *Synechocystis* and *Synechococcus* grown with or without chromate exposed to high light followed by recovery. Excitation wavelength = 440nm
- Figure 4.20 Room temperature fluorescence emission spectra of *Synechocystis* and *Synechococcus* grown with or without chromate exposed to high light followed by recovery. Excitation wavelength = 580nm
- Figure 5.1 Absorption spectrum of phycocyanobilin in chloroform
- Figure 5.2 Elution profile of phycocyanobilin in chloroform
- Figure 5.3 Absorption spectra of phycocyanin
- Figure 5.4 Fluorescence emission spectra of phycocyanin
- Figure 5.5 Protein profile of the phycocyanin
- Figure 5.6 Excited state dynamics of PCB and PCB-TiO₂ in chloroform
- Figure 6.1 Interaction of chromate with *Synechococcus* and *Synechocystis*

List of tables

Table No.	Title
Table 1.1	Major complexes involved in photosynthetic electron flow in thylakoid membranes of cyanobacteria
Table 2.1	EC ₅₀ values measured at different time points of growth of <i>Synechocystis</i> and <i>Synechococcus</i>
Table 2.2	Comparative analysis of sulfate and chromate transporter genes in <i>Synechococcus</i>
Table 2.3	Comparative analysis of sulfate and chromate transporter genes in <i>Synechocystis</i>
Table 3.1	SOD activity in <i>Synechocystis</i> and <i>Synechococcus</i> grown with or without potassium chromate
Table 4.1	Effect of chromate on pigment composition
Table 4.2	Relative contents of PSII / PSI and energy transfer characteristics in <i>Synechocystis</i> and <i>Synechococcus</i> grown with or without chromate
Table 4.3	Fluorescence Recovery after Photobleaching in cells of <i>Synechocystis</i> and <i>Synechococcus</i> grown with or without chromate
Table 4. 4	Data analysis parameters used for PAM Fluorimetry in this study
Table 4.5	Effect of growth with chromate on maximal quantum yield of PSII (Fv/Fm) and maximal P700 change (Pm) in the cyanobacteria
Table 4.6	Complementary quantum yields of energy conversion in PSII and PSI of <i>Synechocystis</i> and <i>Synechococcus</i> grown with or without chromate
Table 4.7	Effect of growth with chromate on parameters of light response reaction in the cyanobacteria
Table 5.1	Isolation and purification of phycocyanin from <i>Synechococcus</i> grown with or without chromate

List of abbreviations

APC	allophycocyanin
BN PAGE	blue native PAGE
BSA	bovine serum albumin
CLSM	confocal laser scanning microscopy
Cyt <i>b₆f</i>	cytochrome <i>b₆f</i>
DCFH	2',7'-Dichlorofluorescein diacetate
DCFH-DA	2',7'-Dichlorofluorescein diacetate
DCMU	3-(3,4-dichlorophenyl)-1,1-dimethylurea
DCPIP	dichlorophenolindophenol
DNP	2,4-dinitrophenylhydrazone
DNPH	2,4 dinitrophenyl hydrazine
DSSC	dye sensitized solar cell
DTT	dithiothreitol
ETR	electron transport rate
FRAP	fluorescence recovery after photobleaching
HEPES	4-(2-hydroxyethyl)-1-piperazineethanesulfonic acid
LASER	light amplification by stimulated emission of radiation
LHC	light harvesting complex
LMP	low melting point
NBT-BCIP	nitro blue tetrazolium chloride -5-Bromo-4-chloro-3-indolyl phosphate
OD	optical density
OEC	oxygen evolving complex

PAGE	polyacrylamide gel electrophoresis
PAM	Pulse amplitude modulated
PBS	phycobilisomes
PC	phycocyanin
PCB	phycocyanobilin
PMSF	phenylmethylsulfonyl fluoride
PSI	photosystemI
PSII	photosystemII
ROS	reactive oxygen species
SOD	superoxide dismutase
TES	2-[(2-Hydroxy-1,1-bis(hydroxymethyl)ethyl)amino]ethanesulfonic acid, N- [Tris(hydroxymethyl)methyl]-2-aminoethanesulfonic acid
UV	ultraviolet

Chapter 1

Introduction

1.1 Introduction to cyanobacteria

Evolution of life on Earth is a marvel of nature where bio-molecules have interacted to evolve into complicated networks leading to the emergence of the most advanced creatures like us: the human beings. The credit of aerobic life as we know it today goes to the oxygen evolution by cyanobacteria *ca* 3.2 billion years ago. The creation of a photosynthetic apparatus capable of splitting water into oxygen (O₂), protons, and electrons was the pivotal innovation in the evolution of life on Earth. Use of water as a reductant freed photosynthesis from other chemical reductants and this opened new environments for photosynthesis to occur leading to accumulation of atmospheric oxygen. This sequence of evolutionary events enabled the emergence of complex, multicellular, energy efficient, eukaryotic organisms (Dismukes et al. 2001).

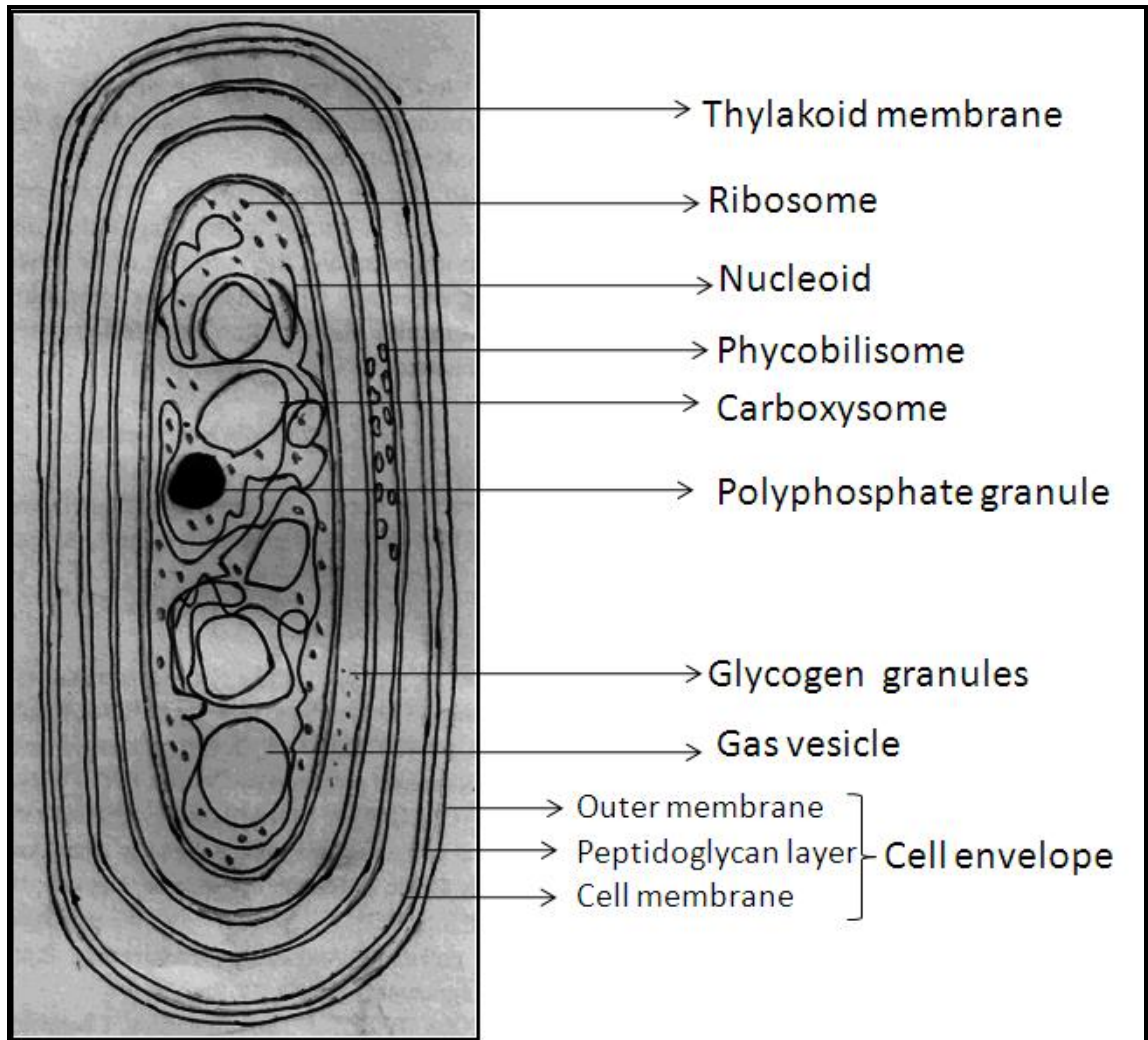
Cyanobacteria (formerly known as blue green algae) are prokaryotic oxygenic phototrophs found in almost every conceivable habitat on earth. They are either unicellular existing as single cells, suspended, benthic, in aggregates or filamentous types existing as single trichome or bundles with or without a sheath and are able to perform different modes of metabolism with the capacity to switch from one mode to another (Abed et al. 2009). The unifying property of the cyanobacteria is their ability to perform oxygenic photosynthesis. Moreover, to adapt in varying environmental conditions; some species have developed ability to fix nitrogen using nitrogenase complex and cell types like akinetes, baeocytes and hormogonia for dissemination and reproduction of the species. The nitrogenase complex gets irreversibly inactivated by oxygen; one of the major products of photosynthesis in these prokaryotic organisms. To overcome this difficulty, some filamentous cyanobacteria have spatially separated photosynthesis and nitrogen fixation in highly specialized nitrogen-fixing cells, called

heterocysts (Tandeau de Marsac and Houmard 1993). Nitrogen fixation capability makes cyanobacteria very important organisms for plants and the overall nitrogen cycle of the Earth.

1.2 Cellular organization of cyanobacteria

All cyanobacterial cells have a uniform and distinctive prokaryotic cell structure in general; however, many cyanobacteria have extracellular layers. **Figure 1.1** shows schematic representation of a typical cyanobacterial cell. The cell wall is bilayered, similar in structure and composition with that of gram-negative prokaryotes and has distinguishable layers. Cells of most cyanobacteria have mucilaginous sheath made of microfibrils. A thicker peptidoglycan layer as compared to typical gram negative bacteria is present and it makes the major portion of the cell wall. The outer membrane layer contains both proteins and lipopolysaccharides and is in contact with the outermost mucilaginous sheath. Periplasmic space is bound between the outer membrane and the peptidoglycan layer. Although cyanobacteria do not have flagella typical of most bacteria, many cyanobacteria are able to translocate over surfaces by gliding movement.

Figure 1.1: A typical cyanobacterial cell



Schematic representation of a cyanobacterial cell. Major subcellular entities are shown with respect to their location and roughly to their relative size.

The cell membrane or the cytoplasmic membrane is usually simple and separates the periplasm from the cytoplasm. A major portion of the cytoplasm is occupied by the components of the photosynthetic apparatus. The photosynthetic apparatus is located in a series of flattened, membranous sacs or thylakoids where photosynthetic pigments, the photochemical reaction centers, and the photosynthetic electron transport chains are located. These thylakoid membranes are located in the cell periphery with a central cytoplasmic region largely devoid of thylakoid membranes. Unlike plants, where light harvesting complex is located in the thylakoid membranes, in cyanobacteria, major light harvesting complexes, the phycobilisomes are extrathylakoidal in location; they are attached in regular rows to the outer surfaces of the thylakoids. Phycobilisomes are disc shaped entities about 40nm in diameter; they are constituted by phycobiliproteins which are brilliantly colored blue or red pigment proteins capable of absorbing specific wavelengths of visible light and are arranged in rows. Adjacent thylakoids are therefore separated from one another by a space of about 50nm. Cyanobacterial phycobilisomes are typically hemidiscoidal with a diameter of ~32 – 70nm.

Thylakoids are arranged in different fashions in a cyanobacterial cell. In *Synechococcus*, which is a cylindrical cell, they are arranged in a cortical array of two to five thylakoids aligned parallel to each other and to the long axis of the cell. *Synechocystis* cells are spherical and have thylakoid membranes organized primarily as three or more concentric layers around the cell periphery. In cyanobacteria the typical grana stacks which are characteristic of higher plant chloroplasts are not observed although the photosynthetic machinery of cyanobacteria resembles the photosynthetic machinery in higher plants. Phycobilisomes are never attached to the inner surface of the cell membrane implying that photosynthesis does not take place in the cell membrane and

thylakoid membranes are distinctly dedicated to carry out photosynthesis. A typical cyanobacterium cell contains inclusions like polyphosphate granules, glycogen granules, cyanophycin granules and carboxysomes. Gas vesicles are present in some cyanobacteria (Stanier and Cohen-Bazire 1977).

Cyanophycin is a nitrogenous non protein arginine and aspartate rich organic reserve material synthesized by almost all cyanobacteria. It is accumulated in the form of granules in the cytoplasm during phosphate or sulfur starvation, generally in the early and mid-stationary phase. Carboxysomes may be termed as micro-compartments in a cyanobacterial cell which contains enzymes involved in carbon fixation. They are thought to concentrate carbon dioxide to overcome the inefficiency of RuBisCO - the predominant enzyme in carbon fixation and the rate limiting enzyme in the Calvin cycle. Glycogen granules are reserves of carbon and energy, while polyphosphate bodies are stores of phosphate. The central part of the cell contains the nucleoid or the DNA material. It is present in the form of circular fibrils of DNA which is devoid of histones. 70S ribosomes are dispersed but are most populous in the central region around nucleoid material of the cell.

1.3 Photosynthetic apparatus of cyanobacteria

One of the most important reasons for ubiquitous occurrence of cyanobacteria is their combination of metabolic pathways and metabolic flexibility. Unlike plants and eukaryotic photosynthetic organisms, where there are specialized compartments to carry out photosynthesis and respiration, cyanobacteria are among the very few groups of organisms that perform oxygenic photosynthesis and respiration simultaneously in the same compartment. The thylakoid membrane harbors both photosynthetic and

respiratory electron transport chains which intersect and partially use the same components in the membrane. The cytoplasmic membrane contains the respiratory electron chain but not photosynthetic complexes in most cyanobacteria. Therefore, in most cyanobacteria, photosynthetic electron transport chain occurs solely in thylakoids whereas respiratory electron flow takes place in both the thylakoid and cytoplasmic membrane systems (Vermaas 2001). Almost all the cyanobacteria possess thylakoid membranes with two photosystems (photosystem I and photosystem II). However, unlike most of the photosynthetic eukaryotes, they do not contain chlorophyll *b* but harvest light energy primarily through unique multimolecular structures called phycobilisomes.

1.3.1 Basic scheme of photosynthesis: Photosynthesis is essentially a process in which light energy driven charge separation and electron flow leading to conversion of light energy to chemical energy takes place where water provides the electron. Highly organized and coordinated activity of the components of membrane complexes and electron carriers makes this process possible. In cyanobacteria the electron transfer path is:

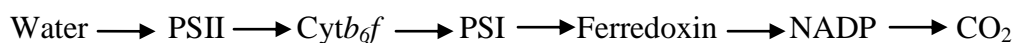
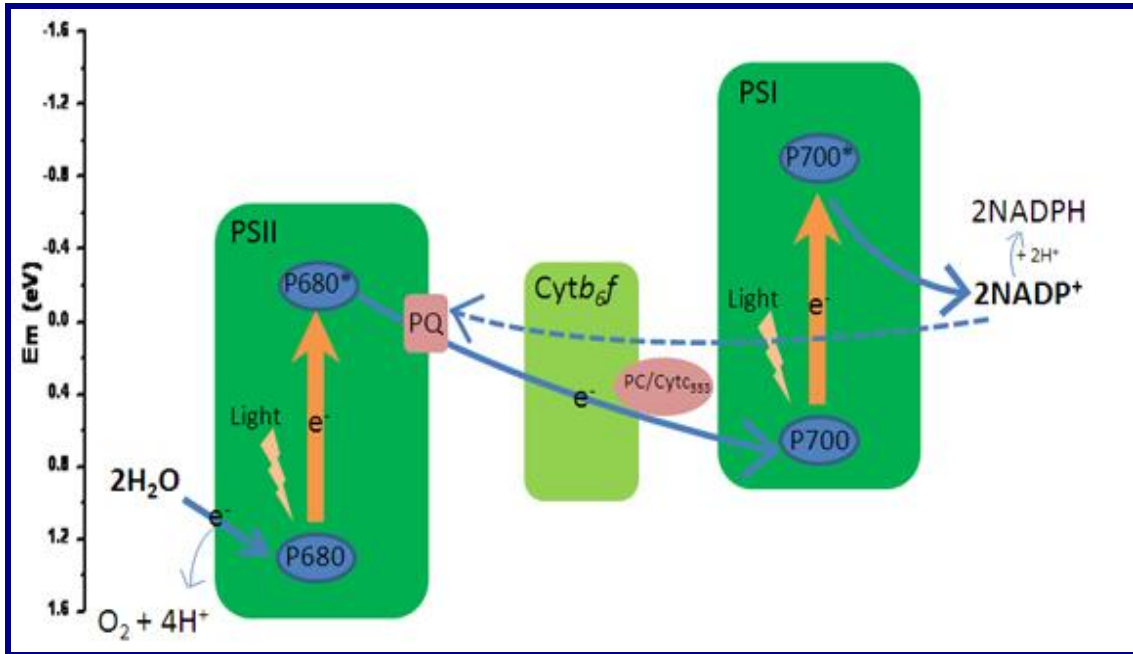


Figure 1.2 shows the simplified Z scheme of electron flow typical of cyanobacteria.

Specific energy photons excite the specialized chlorophyll of the reaction centers, P680 for photosystem II (PSII), and P700 for photosystem I (PSI) which eject an electron from their respective excited states. The electron then passes through a series of electron carriers and eventually reduces P700 (for electrons from PSII) or NADP^+ (for electrons from PSI). Four major protein complexes are involved in this process: photosystem II, cytochrome *b_{6f}* (cyt *b_{6f}*) complex, photosystem I, and the ATP synthase. These four complexes are arranged in an organized manner in the thylakoid membrane.

Photosystem II uses light energy to split water and to reduce the plastoquinone pool. Electrons are transported from the plastoquinone pool to the *cyt b₆f* complex and from there to a soluble electron carrier, plastocyanin or cytochrome *c₅₅₃* on the luminal side of the thylakoid membrane. This in turn reduces the oxidized PSI reaction centre chlorophyll, P700⁺ which is formed by a light-induced transfer of an electron from PSI to ferredoxin (Fd) and eventually to NADP which is used for CO₂ fixation (Vermaas 2001).

Figure 1.2: A simplified Z scheme of electron transport in cyanobacteria



The scheme of electron transport in cyanobacteria after excitation of reaction centre chlorophyll a (P680 or P700) in response to the absorption of light through the antenna system. Abbreviations: E_m (eV): redox potential at pH 7 in electron volts; e^- : electron; PQ: plastoquinone; Cyt b_6/f : cytochrome b_6/f complex; Cyt c_{553} : cytochrome c_{553} ; PC: plastocyanin; PSII; photosystemII; PSI: photosystemI. Based on Govindjee and Shevela 2011.

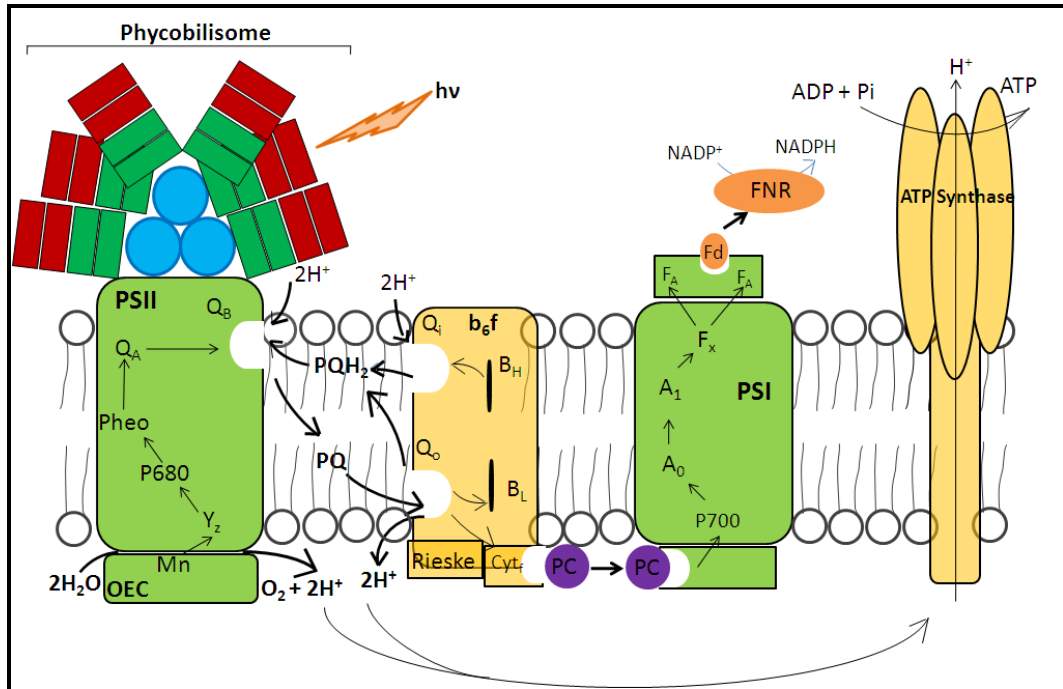
Cyanobacteria show linear transfer of electrons from NADP using PSII, *Cyt_b₆f* and PSI resulting in oxygen evolution and reduction of NADP and formation of ATP. In addition, there is also cyclic electron flow around PSI to drive additional ATP production. Plastocyanin or cytochrome *c₅₅₃* can reduce the oxidized PS I reaction centre chlorophyll P700, which is oxidized by a light-induced transfer of an electron from PSI to ferredoxin (Fd) and eventually to NADP. Reduced NADP can be used for CO₂ fixation. The proton gradient created across thylakoid membranes by electron transport is used for ATP synthesis. The photosynthetic complexes in the thylakoid membrane of cyanobacteria are shown in **table 1.1** and **figure 1.3**. The components are briefly described in the following subsections.

Table 1.1: Major complexes involved in photosynthetic electron flow in thylakoid membranes of cyanobacteria

Complex	Gene designation	Major proteins	Cofactors	Function
Photosystem II	<i>psb</i>	D1, D2, CP43, CP47, PsbO	Mn, Ca, Cl, Fe, PQ, chlorophyll, cyt <i>b</i> ₅₅₉ , pheophytin	Light-induced water splitting and PQ reduction
Cytochrome <i>b₆f</i>	<i>pet</i>	Cyt <i>b</i> ₆ , cyt <i>f</i> , Rieske, subunit IV	2cyt <i>b</i> , cyt <i>f</i> (cyt <i>c</i>), FeS	PQH ₂ oxidation and PC/cyt <i>c</i> ₅₅₃ reduction
Photosystem I	<i>psa</i>	PsaA, PsaB and other Psa proteins	Chlorophyll, vitamin K1, FeS centres	Light-induced PC/cyt <i>c</i> ₅₅₃ oxidation and Fd reduction

The major complexes involved in photosynthetic electron flow in cyanobacteria, their gross composition, set of genes expressing major complex proteins and function of the complexes are mentioned. Based on Vermaas 2001.

Figure 1.3: Components of photosynthetic electron transport chain in cyanobacteria



Schematic representation of components of photosynthetic electron transport chain in the thylakoid membrane with their relative positions and path of electron flow along with generation of proton motive force leading to synthesis of ATP. Phycobilisomes are known to act as antenna complex for PSI also; here they are shown for representation as associated with PSII. Abbreviations: PSII: Photosystem II, PSI: Photosystem I, P680: PSII Reaction centre chlorophyll, Pheo: Pheophytin, Q_A and Q_B : Plastoquinones, OEC: Oxygen evolving complex, b_{6f} : Cytochrome b_{6f} - cytochromes bH, bL, b6, and heme x, cyt_f : cytochrome f, PC: plastocyanin, P700: PSI reaction centre chlorophyll, A_0 : Chlorophyll a molecule, A_1 : phylloquinone, 4Fe-4S clusters: F_X , F_A , and F_B , ferredoxin (Fd), FNR: ferredoxin-NADP reductase.

1.3.2 Light harvesting complexes: Photosynthetic organisms use antenna systems to capture light energy and transfer the energy to reaction centers where photochemistry occurs. Antenna complexes are structurally diverse and highly specialized among the various classes of photosynthetic organisms and are optimized to allow the maximal absorption of light energy available in their environmental niche (Blankenship 2002). Cyanobacteria use a combination of membrane -intrinsic and -extrinsic antennae to harvest sunlight over a wide spectral range. Phycobilisomes (PBS) are the major light harvesting antennae in red algae and in most cyanobacteria. These are complex, highly structured assemblies of brilliant colored phycobiliproteins (PBPs) and colorless linker polypeptides. In contrast to eukaryotic systems, PBS are composed of predominantly hydrophilic polypeptides. PBPs are composed of two dissimilar subunits, α and β , with molecular weights of 14 – 20 kDa and covalently attached open chain tetrapyrrole chromophores known as phycobilins. Five major classes of PBPs are known – phycocyanin, phycoerythrin, allophycocyanin, allophycocyanin B and phycoerythrocyanin. Most of the cyanobacteria contain phycocyanin, allophycocyanin and allophycocyanin B. PBPs owe their brilliant color to the phycobilins, -cyanins have covalently attached bilin called phycocyanobilin and –erythrins have phycoerythrobin. PBS structure is variable; the general assembly scheme is that there is a central core composed of allophycocyanins and specific linker polypeptides. There are two distinct regions, a core composed mainly of trimeric discs of allophycocyanin and peripheral rods composed of stacked trimeric discs. In the rods, a hexameric phycocyanin complex is always located at the rod-core linkage position, while the other end of the rod may contain phycocyanin, phycoerythrocyanin or phycoerythrin hexamers (Liu et al. 2005).

A number of rods composed of discs of phycocyanins and/or phycoerythrin held together by specific linker polypeptides radiate from the core. Their function is to absorb light energy and transfer it to chlorophyll of photosystems. The whole arrangement is such that it allows unidirectional energy transfer as:

Phycoerythrin → Phycocyanin → Allophycocyanin → Reaction Center

PBS absorb green-orange (550–650 nm) light excitation principally; this portion of solar spectrum is not intercepted by chlorophyll a. Their efficiency in light-harvesting and energy transfer is close to 100% (Tandeau de Marsac and Houmard 1993). The entire assembly of PBS has a typical molecular mass of 7 – 15 MDa.

It is well known now that PBS are mobile over thylakoid membranes and are associated to PSII under normal conditions, but these structures are highly flexible and their location and composition vary with changing environmental conditions. Nutrition levels, light quality and quantity alter PBS structure and function. Generally, low light intensities stimulate the synthesis

of PBS and increase in length of the rods. Increased PBP content is observed when PSI light is more. This adjustment helps the cyanobacteria in striking a balance of electron flow between the two photosystems (Grossman et al. 1993). The rapid configuration changes in the light harvesting apparatus in response to changing light conditions are known as state transitions; these take place in higher plants as well as cyanobacteria. Illumination conditions which lead to excess excitation of PSII compared with PSI induce a transition to State 2, in which more absorbed excitation energy is diverted to PSI. When PSI is over-excited relative to PSII this induces a transition to State 1, in which more energy is transferred to PSII. Thus state transitions appear to act as a

mechanism to balance excitation of the two photosystems under changing light regimes (Allen and Forsberg 2001).

1.3.3 Photosystem II: PSII is the light-driven water : plastoquinone oxidoreductase of oxygenic photosynthesis found in the thylakoid membrane of chloroplasts and cyanobacteria (Nixon et al. 2010). It is a multi-subunit, pigment-protein complex; an active and native PSII is dimeric in nature. The core of PSII consists of a heterodimer of two homologous proteins D1 and D2. Among all subunits of PSII, D1 is most prone to the photodamage and is continuously replaced by newly synthesized D1. The antenna proteins transfer the excitation energy to the photochemical reaction center with primary electron donor P680 formed by chlorophyll *a* (Chl *a*) molecule(s). The excited primary donor is oxidized to P680⁺, and the released electron travels along the electron transfer chain composed of two pairs of chlorophyll *a*, one pair of pheophytin *a* and two plastoquinones (Q_A and Q_B). P680⁺ is re-reduced via redox-active tyrosine (TyrZ) by an electron from a Mn-cluster that catalyzes the oxidation of water to atmospheric oxygen (Biesiadka et al. 2004). Oxygen - evolving complex (OEC) is associated with the core of PSII that acts as the active site of the water oxidation centre. In the case of higher plants, the water-splitting Mn₄CaO₅ cluster is stabilized by three extrinsic proteins on the luminal side of PSII *viz* PsbO (33 kDa), PsbP (23 kDa), and PsbQ (17 kDa). In cyanobacteria the smaller proteins are substituted by cytochrome *c*₅₅₀ (PsbV, 17 kDa) and PsbU (12 kDa) (Govindjee and Shevela 2011).

1.3.4 Cytochrome *b₆f* supercomplex: The cyt *b₆f* complex is a large multisubunit protein with several prosthetic groups. It is involved in electron transfer from PSII to PSI via mobile electron carriers. This complex accepts electrons from reduced plastoquinone (plastohydroquinone) and releases oxidized plastoquinone; the

mechanism of this function is known as Q cycle. In this mechanism, plastoquinone is oxidized, and one of the two electrons is passed along a linear electron transport chain toward photosystem I, while the other electron goes through a cyclic process that increases the number of protons pumped across the membrane. The net result is that two protons are picked up from the cytosolic side of the thylakoid membrane and four protons are released into the lumen contributing to the pH gradient (Berry et al. 2000).

1.3.5 Photosystem I: The PSI complex is organized in cyanobacterial membranes preferentially in trimeric form and participates in electron transport. It is also involved in dissipation of excess energy thus protecting the complex against photodamage. Charge separation in the PSI reaction center is the fastest of all known reaction centers. The reaction center of PSI catalyzes the oxidation of reduced plastocyanin and reduction of soluble ferredoxin or flavodoxin. The excitation energy is transferred from the antenna pigments to P700 which then passes through a chain of electron carriers *viz.* A₀ (Chlorophyll a molecule), A₁ (phylloquinone) and the three (4Fe-4S) clusters F_X, F_A, F_B and finally to the soluble electron carrier ferredoxin (Fromme et al. 2001). Oxidised P700 is re-reduced by the soluble electron carrier plastocyanin or cytochrome c₆ in cyanobacteria which act as electron donors to PSI.

1.3.6 ATP Synthase: It is located in thylakoid membranes and synthesizes ATP from ADP and Pi by utilizing the electrochemical proton gradient formed by photosynthetic electron flow. It is a rotary motor enzyme that couples transmembrane flow of protons through it to formation of ATP. ATP synthase is composed of 8 types of subunits, of which 5 (α , β , γ , δ and ϵ) form the catalytic hydrophilic F₁ portion. The proton translocating F₀ portion is composed of subunits of 3 types named *a*, *b* and *c*. A binding

change mechanism has been suggested for the synthesis of ATP through this complex (Boyer 2000).

1.3.7 Carbon fixation: Using reducing power generated in the form of NADPH by the photosynthetic electron flow, carbon-dioxide fixation takes place by sequential activity of cytosolic enzymes through a pathway known as 'Calvin cycle'. The reducing power in the form of NADPH or reduced ferredoxins and ATP generated by photosynthetic electron transport systems is ultimately used in several metabolic processes occurring in the cytosol. Many of these processes such as photosynthetic carbon assimilation were hypothesized to be solely occurring in the cytosol. This assumption was based on the fact that these enzymes can be isolated from cytosol. However, immune-electron microscopy has shown that many of these soluble enzymes are located in the vicinity of thylakoid membranes which results in channelized functioning of light dependent generation of reducing power, ATP generation and carbon fixation (Agarwal et al. 2010, Sainis and Melzer 2005).

1.3.8 Effect of stressors on photosynthesis: Photosynthesis is a vital process in all photoautotrophs; abiotic or biotic stressors affect components of photosynthetic machinery or they indirectly affect photosynthesis by causing oxidative stress. Some stressors such as high light affect the process of repair of the components of photosynthetic apparatus. Extensive investigations have been carried out on the effect of acute environmental stresses on structure and function of photosynthetic apparatus (Ashraf and Harris 2013). Since photosynthetic apparatus is highly sensitive to oxidative stress effect of oxidative stress on photosynthesis is discussed in the following section.

1.4 Oxidative stress and photosynthetic system

1.4.1 Oxidative stress: The term reactive oxygen species (ROS) is used to describe a variety of molecules and free radicals (chemical species with one unpaired electron) derived from molecular oxygen. The reduction of oxygen by one electron at a time produces relatively stable intermediates. Superoxide anion is the precursor of most ROS and a mediator in oxidative chain reactions (Turrens 2003). Dismutation of superoxide anion produces hydrogen peroxide, which in turn may be fully reduced to water or partially reduced to hydroxyl radical, one of the strongest oxidants in nature. The formation of hydroxyl radical is catalyzed by reduced transition metals, which in turn may be re-reduced by superoxide anion, propagating this process (Liochev and Fridovich 1999). This reduction of hydrogen peroxide to hydroxide radical by interaction with reduced transition metal like Fe^{2+} is known as Fenton's reaction. Living organisms have developed enzymatic and non enzymatic defenses against ROS damage. Examples of enzymatic defenses are catalases, superoxide dismutases and peroxidases. Common non enzymatic defenses are glutathione, vitamin A, C, E and carotenoids. Oxidative stress results from an imbalance between the excessive formation of ROS and limited antioxidant defenses. Uncontrolled increase in the ROS leads to damaging effects on proteins, lipids, carbohydrates and DNA; although low levels of ROS have been proposed to play role in intracellular signaling (Foyer and Shigeoka 2011).

1.4.2 Sources of oxidative stress in cyanobacteria: Photosynthetic organisms face ROS produced by the photosynthetic electron transport in addition to ROS generated by respiratory mechanism. In the respiratory electron transport chain, various respiratory complexes leak electrons to oxygen producing primarily superoxide anion which may be converted to hydrogen peroxide and oxygen. Increased concentrations of superoxide

ion may reduce transition metals which in turn react with hydrogen peroxide producing hydroxyl radicals by Fenton's reaction. The sources of ROS generation in the photosynthetic electron transport chain of cyanobacteria are depicted in **figure 1.4**.

1.4.2.1 ROS generation at PSII level: There are several stages in photosynthetic electron flow at PSII where ROS generation has been reported:

(i) Light absorption excites PSII reaction centre chlorophyll P680 to its singlet excited state P680* which under normal course transfers its electron to plastoquinone, but it may also pass its energy to molecular oxygen converting it to singlet oxygen ($^1\text{O}_2$); this happens more when due to excess light intensity, plastoquinone pool is reduced. $^1\text{O}_2$ is thought to inhibit the repair of PSII inactivated by light (Latifi et al. 2009).

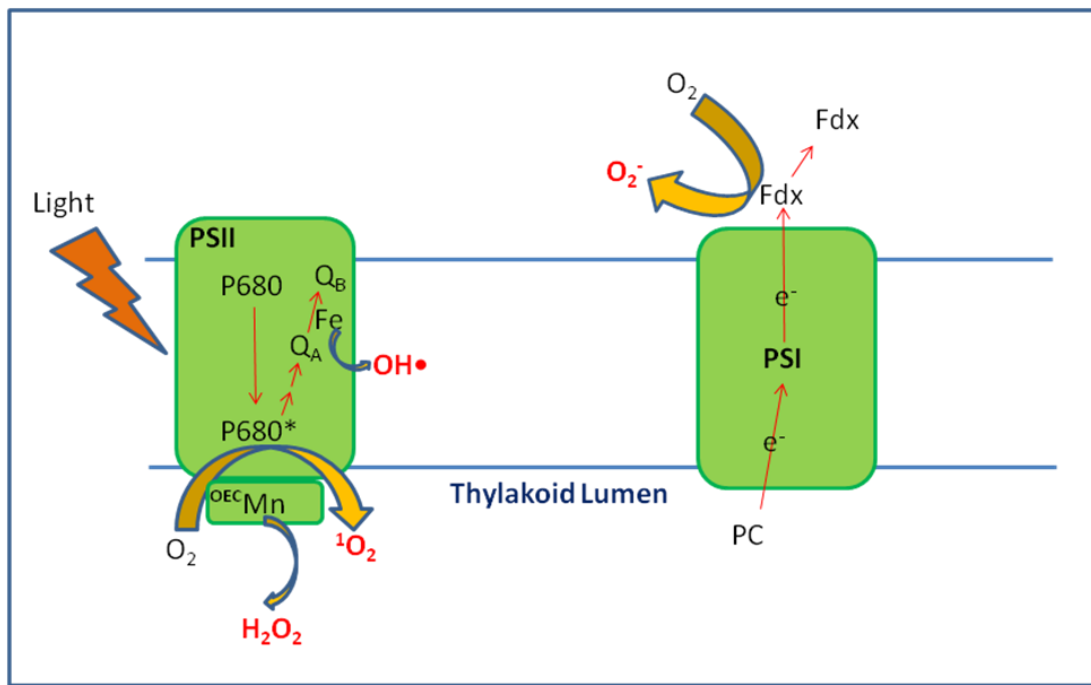
(ii) When pH in the thylakoid drops, the extrinsic protein protection of Mn cluster stops; one of the consequences of impaired Mn cluster activity is production of hydrogen peroxide instead of oxygen (Krieger and Rutherford 1998).

(iii) Under high light intensity, electrons may be transferred from PSII to oxygen instead of plastoquinone leading to formation of superoxide which can interact with a non-heme iron present between two plastoquinones (Q_A and Q_B) by Fenton's reaction thus producing hydroxide radicals (Pospisil et al. 2004).

1.4.2.2 ROS generation at PSI level: When light intensity is high, PSI mediated ROS generation also takes place by Mehler reaction where oxygen rather than ferredoxin is used as electron acceptor, which generates a superoxide anion as a primary product (Latifi et al. 2009). If membrane bound SOD is present as is in the case in higher plants and many cyanobacteria, its dismutation activity leads to hydrogen peroxide generation which in turn can interact with Fe-S clusters of PSI by Fenton chemistry (Shcolnick and

Keren 2006). However, whether Mehler reaction takes place in cyanobacteria to the same extent as in higher plants is controversial (Latifi et al. 2009).

Figure 1.4: Sources of ROS generation in the photosynthetic electron transport chain of cyanobacteria



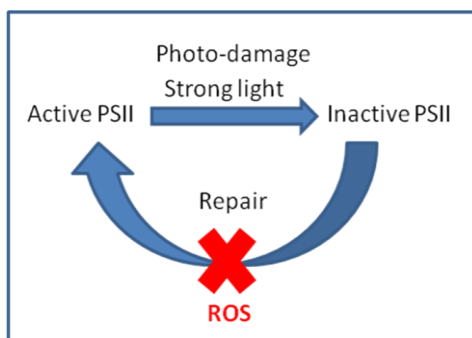
Schematic representation of ROS generation at the level of PSII and PSI in photosynthetic electron transport chain of cyanobacteria. The sizes of PSII and PSI are not to scale and portions of electron transport chain where ROS generation has been reported are depicted in the figure.

PSII: Photosystem II, PSI; Photosystem I, OEC: Oxygen Evolving Complex, P680: Reaction centre chlorophyll of PSII, Q_A and Q_B: plastoquinones, Fdx: ferredoxins.

1.4.3: Targets of ROS damage in the photosynthetic apparatus of cyanobacteria:

The most widely studied target of ROS mediated damage is PSII. Exposure of photosynthetic organisms to high light causes inactivation of PSII, a phenomenon termed as photo-inhibition. The main reason of photo-inhibition is degradation of D1 and D2 of the reaction centre of PSII. Photosynthetic organisms are able to overcome photodamage by rapid and efficient repair of PSII (Nishiyama et al. 2006). As shown in **figure 1.5**, the extent of photo-inhibition is dependent on balance between photo-damage of PSII and its repair. Recent studies have shown that photo-inhibition is an exclusively light dependent process and ROS only target the *de novo* synthesis of D1 at the repair step (Nishiyama et al. 2004).

Figure 1.5 Photodamage and repair of PSII



The extent of activity of PSII is dependent on balance between photo-damage of PSII and its repair. It has been established that ROS only target the repair process of PSII by hampering D1 synthesis.

Phycobilisomes are reported to be possible targets of ROS in the photosynthetic apparatus of cyanobacteria. Liu et al. (2005) have reported hydrogen peroxide induced energy transfer between the core and the terminal emitter of phycobilisomes suggesting that phycobilisome core was disassembled under oxidant conditions. Another general

source of oxidative source in all organisms is metals. Whereas metals play a key role as cofactors in oxygenic photosynthesis, they pose at the same time a major oxidative risk factor due to their deleterious interaction with oxygen (Shcolnick and Keren 2006). In the following section, interaction of metals with living organisms is elaborated.

1.5 Metals and living organisms

All life forms have evolved using compounds made of elements known as bio-molecules which form the major structural and functional framework of life, e.g. protein, DNA, carbohydrates, lipids and numerous others in relatively smaller quantities. Similarly, to carry out specific functions, metals are used by all living organisms and depending upon the quantity they have been classified as macro- or micro- nutrients; therefore as an analogy to bio-molecules they may be referred to as 'bio-metals'. As elaborated in the above section on photosynthesis, metals like Mg, Mn, Fe, Na, K etc. in their appropriate ionic forms are indispensable to functioning of protein super-complexes involved in photosynthesis. All metals are toxic beyond certain concentrations; there are metals which are either non-required or are toxic at all concentrations. In general, aquatic environments have a milieu of various metallic ions due to anthropogenic activities and also natural leaching from mineral rocks, soil etc. Therefore, various degrees of tolerance or adaptive measures to non-essential and/or toxic metals in addition to other inhospitable conditions are found to occur in organisms of aquatic ecosystems.

1.5.1 Ability of cyanobacteria to survive in inhospitable environment:

Cyanobacteria are ubiquitous organisms; they are found to grow under the most inhospitable ecological niches; the long time of 3.5 billion years elapsed since their

origin has allowed cyanobacteria to adapt to almost all habitats. They have evolved mechanisms to thrive under several abiotic stresses like extreme pH, high and low temperatures, light intensities, oxygen tensions, excessive UV, imbalances in salt concentrations and presence of toxic metal ions etc. One of the main reasons for the evolutionary hardiness of cyanobacteria is their successful combination of effective metabolic pathways (Vermaas 2001). They have developed capacity to adjust their photosynthetic apparatus to suit the environment. Studies on effect of acute environmental stress on structure and function of photosynthetic apparatus have been reported. Campbell et al. (1998) showed that upon exposure to UV-B *Synechococcus* rapidly changes expression of the *psbA* genes which encode D1 protein. The exposure of cells for 15mins to UV-B results in accumulation of transcripts of *psbAII* and *psbAIII* transcripts replacing the *psbAI* transcripts of wild type. The wild type D1:1 (coded by *psbAI*) protein of PSII is replaced by D1:2 (coded by *psbII* and *III*). The D1:2 isoform has 25% higher quantum yield and is more resistant to photoinhibition (Campbell et al. 1995). This switch imparts UV resistance to *Synechococcus*. During their long evolution, cyanobacteria have adapted to aquatic habitats with various salt concentrations. High salt concentrations in the environment challenge the cell with reduced water availability and high contents of inorganic ions. The basic mechanism of salt acclimation involves the active extrusion of inorganic ions and the accumulation of compatible solutes, including sucrose, trehalose, glucosylglycerol, and glycine betaine (Hagemann 2011). Earlier it was shown by Jeanjean et al. (1993) that metabolic adjustments with respect to electron transport rates involving respiration and photosynthesis in response to salt stress occur in *Synechocystis* PCC 6803. In order to survive and to grow in the presence of a high salinity (550 mM NaCl) it increases its

energetic capacity by increasing electron transport rates around cytochrome *c* oxidase and PSI.

1.5.2 Metal stress in cyanobacteria: As discussed above metals are required for a variety of functions. Fe, Mn, Mg and Cu are essential cofactors for photosynthetic apparatus. To ensure an adequate supply of metals, photosynthetic organisms from cyanobacteria to vascular plants have developed efficient strategies for metal uptake and accumulation. However, the photosynthetic apparatus presents unique challenges to metal homeostasis as they pose a major oxidative risk factor due to their deleterious interaction with oxygen (Shcolnick and Keren 2006).

When cells encounter metals in small excess, mechanisms of avoidance occur, such as exclusion, sequestration or compartmentation and at sub-lethal concentrations, the oxidative stress triggered by toxic metals leads to persistent active oxygen species. Biomolecules are then destroyed and metabolism is highly disturbed. In plants, at the chloroplast level, changes in pigment content and lipid peroxidation are observed. The disorganized thylakoids impair the photosynthetic efficiency, Calvin cycle becomes less efficient and the photosynthetic organism grows slowly. When an essential metal is given together with a harmful one, the damages are less severe than with the toxic element alone. Combined metals and phytochelatin may act against metal toxicity (Bertrand and Poirier 2005). Cyanobacteria are known to exhibit tolerance to several heavy and toxic metals by using variety of mechanisms like extracellular binding or precipitation, impermeability and exclusion, internal detoxification and metal transformations. Lead granules deposition on the cell wall of *Plectonema boryanum* exposed to lead and cadmium adsorption by *Gloeothece* ATCC27152 has been reported. Decreased metal transport, impermeability or metal efflux systems have been observed

in cyanobacteria. The active transport of Ni^{2+} in *Anabaena cylindrica* was observed to be dependent on the membrane potential, is decreased in the dark, and is inhibited by metabolic uncouplers and electron transport inhibitors. In *Synechocystis* PCC6803 the toxicity of Cs^+ was suggested to be due to replacement of cellular K^+ by Cs^+ . Internal detoxification mechanisms like formation of polyphosphate bodies accumulating aluminium and titanium in *Anabaena cylindrica* and *Anacystis nidulans* has been observed (Fiore and Trevors 1994). Photosynthesis becomes a major target of metal toxicity mainly due vulnerability of the process to free radicals.

1.5.3 Toxic metals in living organisms: Trace amount of some heavy metals such as cobalt, copper, manganese, molybdenum, vanadium, strontium and zinc are required for living organisms whereas mercury, lead and cadmium have no known vital role or beneficial effect on organisms and their accumulation can cause serious defects. The term heavy metal refers to any metallic element that has specific gravity more than four and is toxic or poisonous at low concentrations (Duffus 2002). Industrial waste and excessive mining and natural distribution of metals in environment are the major sources of the heavy metal contamination in the environment (Kamaludeen et al. 2003). At low pH the metal salts are more mobile as the solubility of metal increases. Heavy metals can be 'locked up' in the sediments at the bottom of water bodies where they remain for many years. Unlike organic matter heavy metals cannot be degraded or destroyed. Among toxic metals, chromate contamination causes considerable risk in aquatic ecosystems as it is present in effluents of several industries such as tanning, paint, electroplating, printing, metal finishing, oil industry as well as matches and firework factories.

Chromium is known to impart oxidative stress. Effects of chromium on human health and microorganisms like bacteria and fungi are well documented in the literature. Chromium is nonessential and toxic to humans and the toxicity depends on the oxidation states. Cr (VI) is the most reactive and toxic form which is widely recognized as cytotoxic, carcinogenic, and mutagenic (Langård 1990). However Cr (III) has been shown to be present in some animal tissues and has been shown to be essential for human development (Bielicka et al. 2005). Chromium is not essential in plants and accumulates in plant tissues in the order root > leaves > stem > flowers (Vajpayee et al. 1999, Vajpayee et al. 2000, Davies et al. 2001, Ali et al. 2004, Choo et al. 2006). There are no reports of presence Cr (VI) reducing enzymes in plants (Cervantes et al. 2001).

1.5.3.1 Chromate tolerance in microflora: Chromium is a member of transition metals and exhibits various oxidation states from +2 to +6, of which +3 and +6 are predominant in chromium compounds. Hexavalent chromium (Cr^{6+}) is highly soluble and hence toxic and usually exists as oxyanions such as chromate (CrO_4^{2-}) and dichromate ($\text{Cr}_2\text{O}_7^{2-}$) whereas the trivalent form (Cr^{3+}) is less soluble, less toxic and is found in the form of oxides, hydroxides or sulfates (Cheung et al. 2007). Among the environmental pollutants, chromium pollution is one of the major concerns in environmental science as hexavalent chromium is known to be associated with variety of health disorders including cancer. Chromium has been given higher ranking in list of inorganic pollutants (USEPA 1998). Cr (VI) is highly mobile and hence available, resulting in biological toxicity mainly due to oxidative damage to biomolecules (Cervantes et al. 2001). Microorganisms inhabiting the chromate contaminated sites have developed different strategies to thrive in the presence of Cr (VI) in the aquatic environment. One of these strategies deals with reduction of Cr (VI) to the less toxic Cr

(III); this reduction being carried out by chromate reductase identified in diverse bacterial species (Cervantes et al. 2001). Another strategy in prokaryotes uses chromate (VI) efflux system using a plasmid encoded gene, *chrA*. Its product ChrA belongs to a small family of proteins (CHR), which occur in bacteria and archaea and represents a novel kind of prokaryotic PMF driven chromate transporters. Several members of CHR superfamily have been shown to confer resistance to chromate (Nies et al. 1995; Alvarez et al. 1999; Ramírez-Díaz et al. 2008).

Among photoautotrophs, cyanobacteria and algae isolated from chromate contaminated sites or some mutants are able to tolerate chromate to different extent (Garnham and Green 1995; Khattar et al. 2004; Yewalkar et al. 2007; Anjana et al. 2007; Kiran et al. 2007; 2008, Ozturk et al. 2009). Some of these were shown to adsorb chromate on the surface or reduce Cr (VI) to Cr (III). Recently an investigation into mechanism of chromate resistance in *Synechococcus elongatus* showed that this cyanobacterium possesses a homologue of chromate transporter gene *srpC* on pANL plasmid which harbors genes of sulfur metabolism (Aguilar-Barajas et al. 2012). Although overexpression of *srpC* conferred chromate resistance to *E. coli* by reducing chromate uptake, it did not complement *E. coli cysA* sulfate uptake mutant, suggesting that *srpC* is not sulfate transporter. Since chromate (VI) oxyanion is structurally related to sulfate, chromate actively crosses biological membranes by means of the sulfate uptake pathway (Ramírez-Díaz et al. 2008, Aguilar-Barajas et al. 2011). This results in sulfate deficiency as well as in creating oxidative stress in bacterial cells. Thus a complex and enigmatic relation is known to exist between sulfate and chromate transporters *vis a vis* the effect of chromate in prokaryotes.

1.5.4 Effect of chromium on photosynthesis: Physiological responses of cyanobacteria to chromium stress have been investigated extensively and it has been found that photosynthetic apparatus is one of the sensitive targets of chromium toxicity. Prasad et al. (1991) reported that in *Nostoc*, PSII was more sensitive to chromate as compared to PSI and it also suppressed phycocyanin fluorescence. Appentroth et al. (2001) had studied effect of chromate on photosynthetic parameters on fronds of *Spirodela polyrhiza*, common aquatic duckweed. The fronds were exposed for 10 days to different concentrations chromate and oxygen evolution and photosynthetic parameters were examined using JIP test for chlorophyll a fluorescence. It was observed that chromate affected several targets in PSII, especially the total number of active reaction centers, efficiency of electron transport, yield of primary photochemistry and oxygen evolving complex. Inhibition of PS II in *Lemna gibba* due to chromate stress was caused by decrease in D1 protein content and oxygen evolving complex; the functional alteration in PSII was correlated with structural changes in the complex (Ali et al. 2006). *In vivo* chlorophyll fluorescence was used to monitor the effect of fluorescence on PSII of *Synechocystis* (Pan et al. 2009). JIP test and Q_A^- reoxidation showed that chromate induced inhibition of electron transport from Q_A^- to Q_B/Q_B^- and accumulation of P_{680}^+ . Perrault et al. (2009) showed that treatment of *Chlamydomonas reinhardtii* affected energy dissipation process via PSII and PSI showing that dichromate affects PSI, PSII and energy dissipation beyond PSI. Short term accumulation of chromium in *Lemna gibba* and *Lemna minor* was shown to induce different responses of photosynthetic electron transport system (Olah et al. 2010). Recently effect of acute chromate stress on photosystems in *Microcystis* was examined by Wang et al. (2013). The cells were grown normally and exposed to chromate for 12

hours. This affected several photosynthetic parameters such as quantum yield of PSII and inhibited efficiency of PSII. Electron transport rate in PSI was affected to lesser extent than PSII and cyclic electron flow was stimulated by chromate. All these changes were observed in response to acute chromate stress.

1.6 Aims and objective of the thesis

A comparison between organisms exhibiting contrasting tolerance to a toxicant is one of the ways of understanding the mechanism of tolerance. It was earlier observed that two unicellular cyanobacteria, *Synechocystis* sp. PCC 6803 and *Synechococcus* sp. BD1, showed contrasting D_{10} values of 800 and 257 Gy for γ irradiation from ^{60}Co source (Agarwal 2011). Ionizing radiations are known to impart oxidative stress. Since these two cyanobacteria showed differences in survival after acute exposure to ^{60}Co γ radiations, it was interesting to explore the effect of chronic oxidative stress in cyanobacteria. Cr (VI) is one such toxicant which can impart chronic oxidative stress by undergoing reduction from Cr (VI) to Cr (III) using intracellular reductants (Cheung and Gu 2007). Therefore a comparative study on chromate tolerance of *Synechocystis* sp. PCC 6803 and *Synechococcus elongatus* PCC 7942 was undertaken with an aim to study metabolic adjustments in photosynthetic machinery in cyanobacteria grown with or without chromate.

In this thesis, in the present chapter of introduction, a brief overview of the photosynthetic system of cyanobacteria followed by a review of chromium interaction with photosynthetic organisms is given. Comparison of chromate tolerance in *Synechococcus elongatus* PCC 7942 and *Synechocystis* sp. PCC 6803 with respect to growth, chromate uptake and its relation with sulfate uptake is the subject of the second

chapter. Cr (VI) is known to cause oxidative stress by production of ROS. Third chapter of the thesis deals with comparative studies on oxidative stress in *Synechococcus* and *Synechocystis*. Photosynthesis is the site of production of ROS which cause damage to the photosynthetic machinery. Fourth chapter of the thesis elaborates the effect of chromate stress on structure function of photosynthetic apparatus in the two cyanobacteria under study. Fifth chapter describes isolation and analysis of phycocyanin isolated from *Synechococcus* when grown in presence of chromate and application of phycocyanobilin to study charge transfer to TiO₂ nanoparticles. The last chapter includes summary and future directions.

Chapter 2

*Evaluation of Chromate Stress Tolerance in *Synechocystis* and *Synechococcus**

2.1 Introduction

Chromium is a member of transition metals and exhibits various oxidation states from +2 to +6, of which +3 and +6 are predominant in chromium compounds. Hexavalent chromium (Cr^{6+}) is highly soluble and hence toxic; it usually exists as oxyanions such as chromate (CrO_4^{2-}) and dichromate ($\text{Cr}_2\text{O}_7^{2-}$) whereas the trivalent form (Cr^{3+}) is less soluble, less toxic and is found in the form of oxides, hydroxides or sulfates (Cheung and Gu 2007). Microorganisms have developed different strategies to thrive in the presence of chromate in the aquatic environment. One of these strategies deals with reduction of chromate to the less toxic Cr (III) by chromate reductase identified in diverse bacterial species (Cervantes et al. 2001). Another strategy in prokaryotes uses chromate efflux system using a plasmid encoded gene, *chrA*. ChrA belongs to a small family of proteins (CHR), which occur in bacteria and archaea and represents a novel kind of prokaryotic proton motive force driven chromate transporters.

A comparison between organisms exhibiting contrasting tolerance to a toxicant is one of the ways of understanding the mechanism of tolerance. Most of such studies are carried out by giving acute stress. It was earlier observed that two unicellular cyanobacteria, *Synechocystis* sp. PCC 6803 and *Synechococcus* sp. BD1, showed contrasting D_{10} values of 800 and 257 Gy for γ irradiation from ^{60}Co source (Agarwal 2011). Ionizing radiations are known to impart oxidative stress. Since these two cyanobacteria showed differences in survival after acute exposure to ^{60}Co radiations, it was interesting to explore the effect of chronic oxidative stress in cyanobacteria. Cr (VI) is one such toxicant which can impart chronic oxidative stress by undergoing reduction from Cr (VI) to Cr (III) using intracellular reductants (Cheung and Gu 2007). In this chapter, a comparison of chromate tolerance of *Synechocystis* sp. PCC 6803 and *Synechococcus elongatus* PCC 7942 has been carried out followed by chromate uptake and interplay of chromate and sulfate

uptake by the cells. Sequence comparison of chromate and sulfate transporters has also been performed.

2.2 Materials and Methods

2.2.1 Analysis of chromate toxicity in *Synechocystis* sp. PCC 6803 and *Synechococcus elongatus* PCC 7942

Log phase cultures of *Synechocystis* sp. PCC 6803 and *Synechococcus elongatus* PCC 7942 (referred to as *Synechocystis* and *Synechococcus* respectively hereafter) were used for all the experiments. The two strains were inoculated in 50 ml of BG-11 medium (Rippka et al. 1979) and grown at 30°C under continuous white light of intensity 21 W·m⁻². To study the effect of chromate on growth, ~10⁸ cells of log phase culture were inoculated in BG-11 medium containing K₂Cr₂O₇ ranging from 0 to 200 µM and growth was monitored periodically as cell density and expressed as number of cell ml⁻¹ using Neubauer's hemacytometer in the Zeiss Axio imager digital microscope. Growth was monitored as OD₇₃₀ up to 30 days. EC₅₀ value represents the concentration of potassium dichromate at which number of cells ml⁻¹ was 50 % as compared to control.

2.2.2 Determination of Cr (VI) reduction by *Synechocystis* and *Synechococcus*

Cr (VI) concentration in the BG-11 medium in which the cyanobacteria were grown was determined by Di Phenyl Carbazide (DPC) reduction assay as described by Urone (1955). Cells were removed from the culture by centrifugation at 6000 x g for 10 minutes at room temperature and the cell free medium was used for determination of Cr (VI) concentration. Briefly, an aliquot of 200 µL of the medium containing Cr (VI) was mixed with 600 µL of 0.2 N H₂SO₄ and 200 µL of 0.25 % DPC prepared in 50 % acetone. OD₅₄₀ was measured immediately using spectrophotometer. Concentration of Cr (VI) was determined by plotting a standard curve from 0 to 100 µM solutions of potassium dichromate. On the day of

inoculation and after 10 days of growth of the cyanobacteria with increasing concentration of potassium dichromate, Cr (VI) concentration was determined in the medium.

2.2.3 Determination of ^{51}Cr chromate accumulation

2.2.3.1 Chromate uptake by *Synechocystis* and *Synechococcus* in light: Chromate uptake was determined by using ^{51}Cr chromium labeled chromate as a tracer. Log phase cultures of *Synechocystis* and *Synechococcus* were washed and incubated (10^8 cells/ml) in light (21 W m^{-2}) for 24 h at room temperature in fresh BG-11 medium containing $10 \mu\text{M}$ or $100 \mu\text{M}$ $\text{K}_2\text{Cr}_2\text{O}_7$ with $20 \mu\text{Ci}$ ^{51}Cr labeled sodium chromate ($0.24 \mu\text{Ci/nmole}$). Cells were washed with BG-11 medium followed by 1 mM EDTA, resuspended in 90 % methanol and mixed with $175 \mu\text{L}$ of Perkin Elmer's Hidex aqualight cocktail. ^{51}Cr chromate in the cells was estimated by counting β emission by using liquid scintillation counter.

2.2.3.2 Sulfate dependence of chromate uptake by *Synechocystis* and *Synechococcus*: Sulfate dependence of chromate uptake was determined by incubating the cultures with different sulfate concentrations containing medium. Log phase cultures of *Synechocystis* and *Synechococcus* (10^8 cells/ml) were incubated in BG-11 medium containing (i) Low SO_4^{2-} ($30 \mu\text{M}$) (ii) Normal SO_4^{2-} ($300 \mu\text{M}$) or (iii) High SO_4^{2-} ($3000 \mu\text{M}$) and $10 \mu\text{M}$ potassium dichromate with ^{51}Cr as tracer for 24h in light. ^{51}Cr uptake by *Synechocystis* 6803 and *Synechococcus* 7942 was measured after incubation.

2.2.4 Determination of IC_{50} of chromate for ^{35}S sulfate uptake

Inhibitory concentration (IC_{50}) of chromate for sulfate uptake was determined by monitoring uptake of ^{35}S labeled sodium sulfate. Log phase cultures of *Synechococcus* and *Synechocystis* were washed and suspended in fresh BG-11

medium (10^8 cells/ml) containing 30 μ M or 300 μ M sulfate along with 40 μ Ci 35 sodium sulfate (28.6 μ Ci/ μ mole) and increasing concentration of chromate (0 to 10 mM) for 2 h in light at room temperature. Cell pellets were washed with BG-11 medium followed by 1 mM EDTA. The washed cells were resuspended in 90 % methanol and mixed with 175 μ l of Perkin Elmer's Hidex aqualight cocktail. 35 Sulfate in the cells was measured by liquid scintillation counting.

2.2.5 Sequence comparison of sulfate and chromate transporters

A comparison of sulfate transport and chromate efflux system of *Synechocystis* and *Synechococcus* were carried out. Amino acid sequences of sulfate and chromate transporters from *Synechocystis* and *Synechococcus* were downloaded from Cyanobase (<http://genome.kazusa.or.jp/cyanobase>) and compared with similar well characterized genes from other bacteria. Alignment and analyses of proteins were performed using BioEdit v7.0.8. Conserved domains were obtained using (CDD) Conserved Domain Database available at <http://www.ncbi.nlm.nih.gov/Structure/cdd/cdd.shtml> with CDDv2.3.CDD) and SMART (Simple Modular Architecture Research Tool) available at (<http://smart.embl-heidelberg.de>).

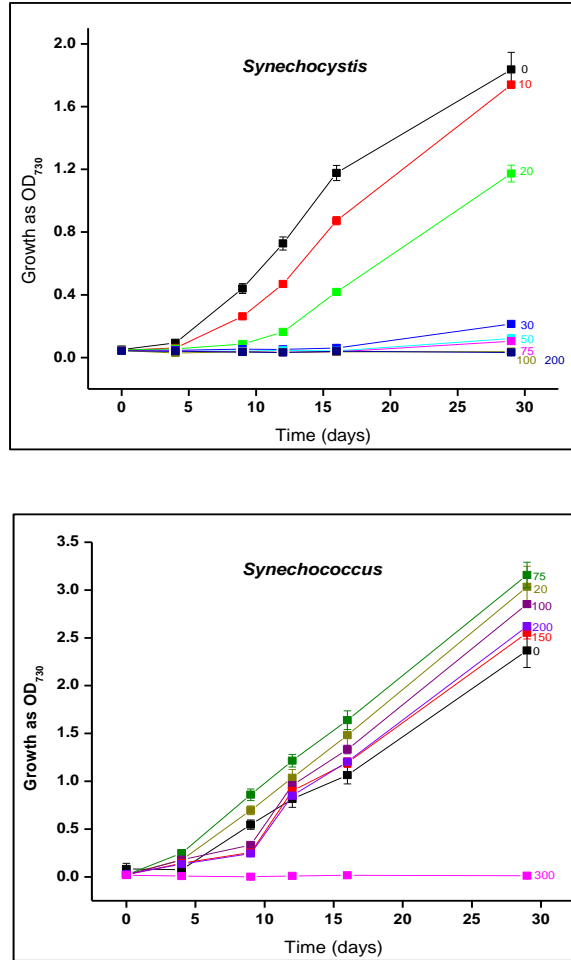
2.3 Results

2.3.1 Analysis of chromate toxicity in *Synechocystis* and *Synechococcus*

When log phase cultures of *Synechocystis* and *Synechococcus* were inoculated in 50 ml of BG-11 medium, the exponential growth phase started after four days and lasted for about 30 days in untreated *Synechococcus* where as in case of untreated *Synechocystis* the log phase lasted for 15 days after which slow decline in growth was observed under similar growth conditions. The two organisms showed comparable growth rates in absence of chromate with doubling time in the range of 40–50 hours

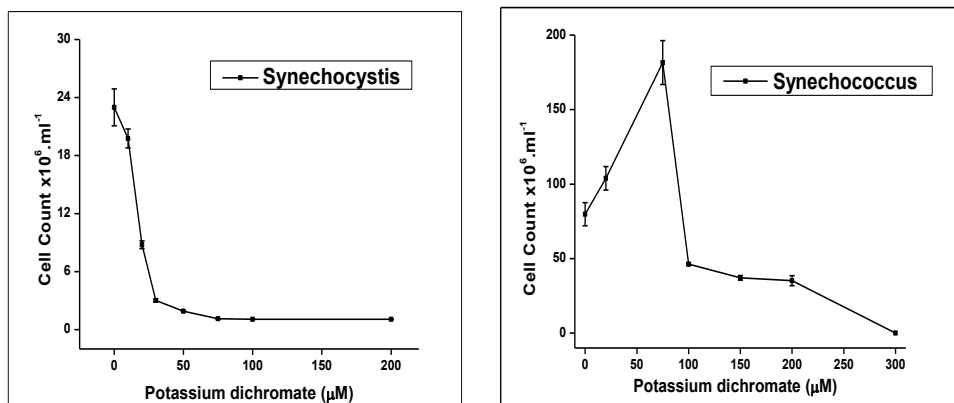
till 15 days period indicating that both were growing normally under the conditions used for their growth. Growth was monitored as OD₇₃₀ and also by measuring number of cells ml⁻¹. *Synechococcus* cultures showed over twice the number of cells at equivalent OD₇₃₀ as compared to *Synechocystis* culture suggesting difference in scattering properties of the cells. To measure the effect of chromate on cell survival and growth, ~ 10⁸ cells were inoculated in BG-11 medium containing different concentrations of chromate and growth was monitored by cell count. **Figure 2.1** shows growth curve of the two cyanobacteria cultured in presence of increasing concentration of potassium dichromate.

Figure 2.1: Growth curve of *Synechocystis* and *Synechococcus* grown with potassium dichromate



Growth curve of *Synechocystis* and *Synechococcus* grown with increasing concentration of potassium dichromate was obtained by monitoring growth as absorbance at 730nm up to 30 days. X axis denotes time in days and Y axis denotes growth as OD₇₃₀. The chromate concentrations are shown at the end of each curve in µM.

In case of *Synechocystis* survival was reduced in the presence of potassium dichromate at concentration as low as 10-20 μM . On the contrary, *Synechococcus*, cells could grow even in presence of 200 μM potassium dichromate (**Figure 2.2**). In *Synechococcus* inclusion of potassium dichromate up to 100 μM in growth medium stimulated growth; highest stimulation was observed with 70-80 μM potassium dichromate. Concentration of potassium dichromate required to inhibit growth completely in *Synechococcus* was 300 μM . In case of *Synechocystis*, survival declined with increasing concentration of chromate and was completely inhibited in presence of 30 μM potassium dichromate. Since both cultures showed exponential growth from 4 to 15 days, the concentration of potassium dichromate at which number of cells ml^{-1} was 50 % as compared to control was monitored after 9 days of inoculation and was used to compare the tolerance of *Synechococcus* and *Synechocystis* to chromium stress. The 9 day EC_{50} of potassium dichromate was 12 ± 2 μM for *Synechocystis* and 150 ± 15 μM for *Synechococcus* (**figure 2.2**). The EC_{50} values increased with time after inoculation as well as with increase in the size of inoculum (**table 2.1, figure 2.3**).

Figure 2.2: Tolerance of *Synechocystis* and *Synechococcus* to potassium dichromate

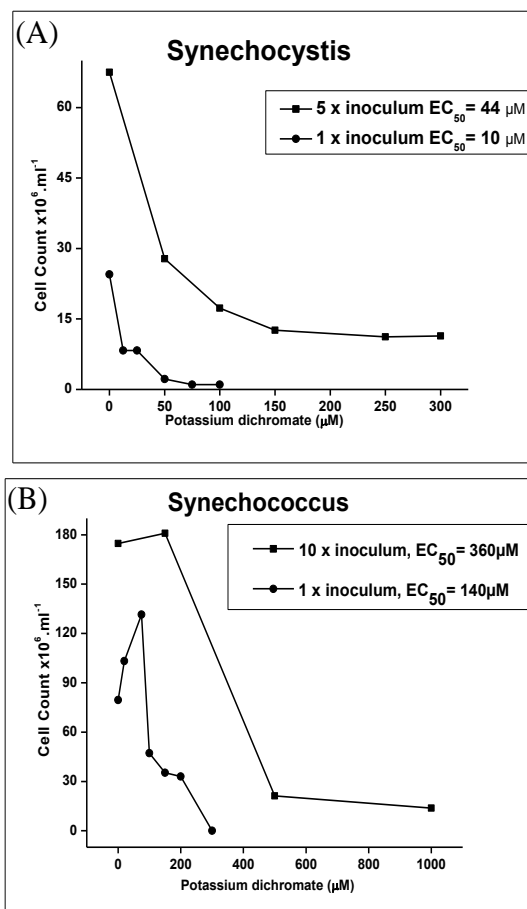
BG-11 medium containing increasing concentration of potassium dichromate was inoculated with log phase cultures of *Synechocystis* and *Synechococcus* containing $\sim 10^8$ cells/ml. Growth was monitored as number of cells ml⁻¹. EC₅₀ for potassium dichromate was calculated after growth for 9 days. The points represent average of four experiments and bars represent SE.

Table 2.1: EC₅₀ values measured at different time points of growth of *Synechocystis* and *Synechococcus*

Day after inoculation	<i>Synechococcus</i> EC ₅₀ (μM K ₂ Cr ₂ O ₇)	<i>Synechocystis</i> EC ₅₀ (μM K ₂ Cr ₂ O ₇)
09	150	12
12	242	14
16	259	16
29	253	23

Log phase cultures of *Synechocystis* and *Synechococcus* containing $\sim 10^8$ cells/ml were inoculated in BG-11 medium containing increasing concentration of potassium dichromate and EC₅₀ value represents the concentration of potassium dichromate at which number of cells ml⁻¹ was 50 % as compared to control.

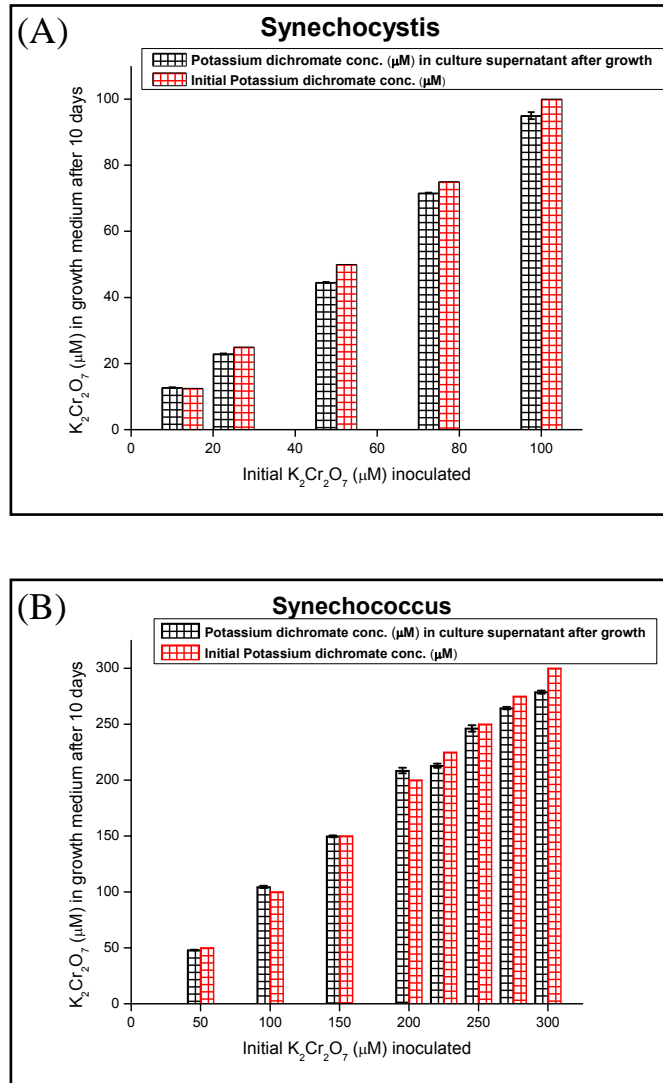
Figure 2.3: Effect of inoculum size on EC₅₀ value of potassium dichromate for *Synechocystis* and *Synechococcus*



Synechocystis and *Synechococcus* were inoculated with 1ml of 1x inoculum containing $\sim 10^8$ cells and 5x (5×10^8 cells) or 10x (10×10^8 cells) inoculum respectively in 50ml of BG-11 medium containing varying concentrations of $\text{K}_2\text{Cr}_2\text{O}_7$ ranging from 0 to 300 μM as indicated in figures. The cultures were grown under continuous white light of intensity $21 \text{ W}\cdot\text{m}^{-2}$ at 30°C . EC₅₀ value represents the concentration of potassium dichromate at which number of cells ml^{-1} was 50 % as compared to control after 9 days of inoculation. X axis denotes the chromate concentration in growth medium and Y axis shows cell number ml^{-1} .

2.3.2 Cr (VI) reduction by *Synechocystis* and *Synechococcus*

Synechocystis and *Synechococcus* were grown in the presence of increasing concentration of potassium dichromate. Cell free medium from each culture was obtained and chromate concentration in the medium was determined using Di Phenyl Carbazide (DPC) reduction assay. As shown in **figure 2.4**, there was no change in chromate concentration in the supernatant of the growth medium indicating that chromate was not absorbed or reduced by both the cyanobacteria.

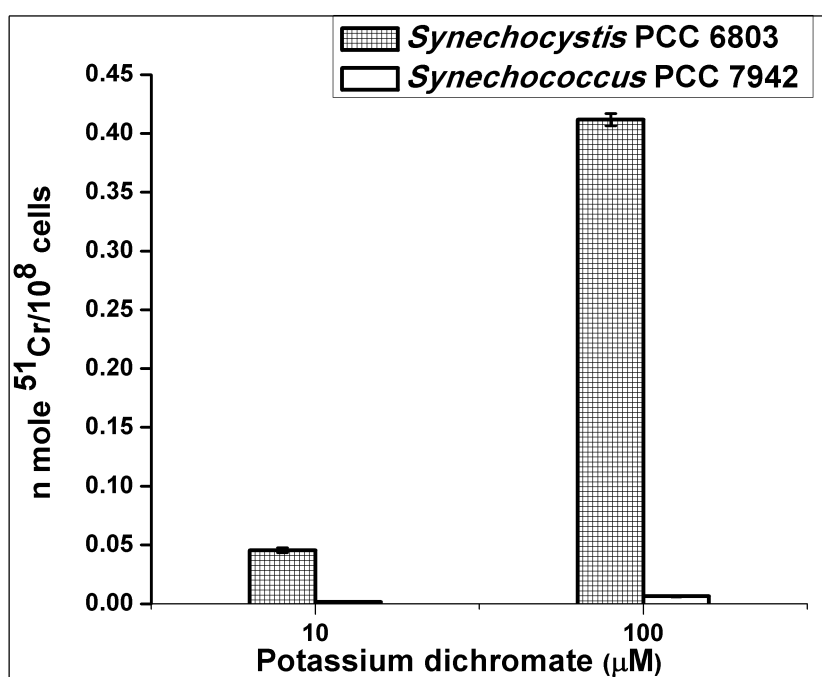
Figure 2.4: Chromium (VI) reduction by *Synechocystis* and *Synechococcus*

Log phase cultures of *Synechocystis* and *Synechococcus* containing 10^8 cells/ml were inoculated in BG-11 medium containing increasing concentration of potassium dichromate. Cr (VI) concentration in the medium at the time of inoculation did not show any significant decrease after 10 days of growth. X axis shows chromate concentration added to growth medium and Y axis shows chromate concentration in growth medium after growth for 10 days.

2.3.3 Chromate uptake by *Synechocystis* and *Synechococcus*

2.3.3.1 Chromate uptake by *Synechocystis* and *Synechococcus* in light: Chromate accumulation was monitored using radiolabeled chromate as a tracer. **Figure 2.5** shows that in *Synechocystis*, chromate accumulation up to 0.04 - 0.05 nmoles/ 10^8 cells was observed after 24 h of incubation in light, when extracellular concentration of chromate was 10 μ M. This increased to 0.4 nmole/ 10^8 cells when chromate concentration in the medium was increased to 100 μ M. In contrast, there was no accumulation of chromate in *Synechococcus* cells under these conditions.

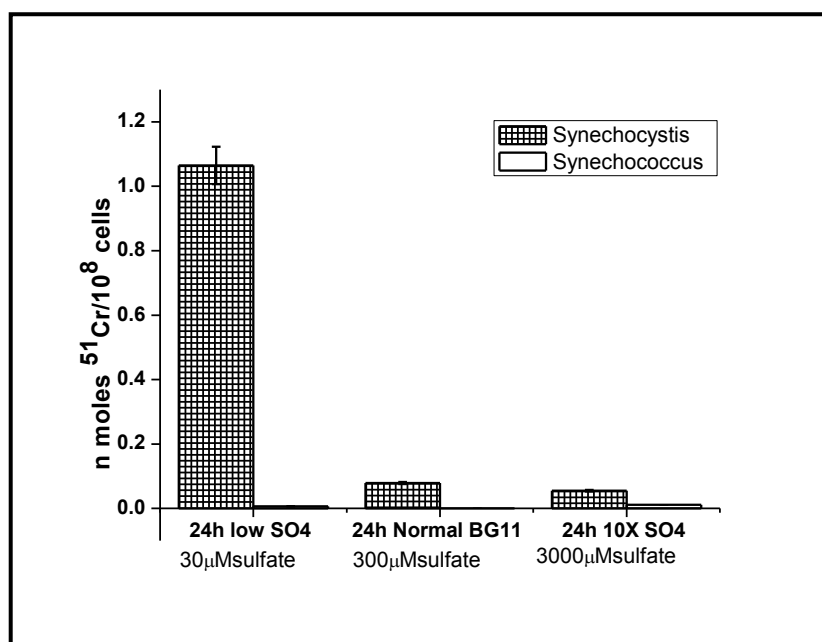
Figure 2.5: Uptake of 51 chromate by *Synechocystis* and *Synechococcus* in light



Log phase cultures of *Synechocystis* and *Synechococcus* (10^8 cells \cdot ml $^{-1}$) were incubated in BG-11 medium containing 10 μ M or 100 μ M of potassium dichromate with 51 Cr as tracer. The intracellular 51 Cr was measured after incubation for 24 hours in light at room temperature. X axis denotes the chromate concentration in growth medium and Y axis shows chromate uptake.

2.3.3.2 Sulfate dependence of chromate uptake by *Synechocystis* and *Synechococcus*: Sulfate dependence of chromate uptake was determined by carrying out 24 h uptake as described above in presence of sulfate concentrations containing medium. **Figure 2.6** shows that chromate uptake in *Synechocystis* decreased with increase in sulfate concentration in the medium indicating an interplay between sulfate and chromate uptake. No chromate uptake could be observed in *Synechococcus* in the sulfate concentrations used.

Figure 2.6: Sulfate dependence of chromate uptake by *Synechocystis* and *Synechococcus*

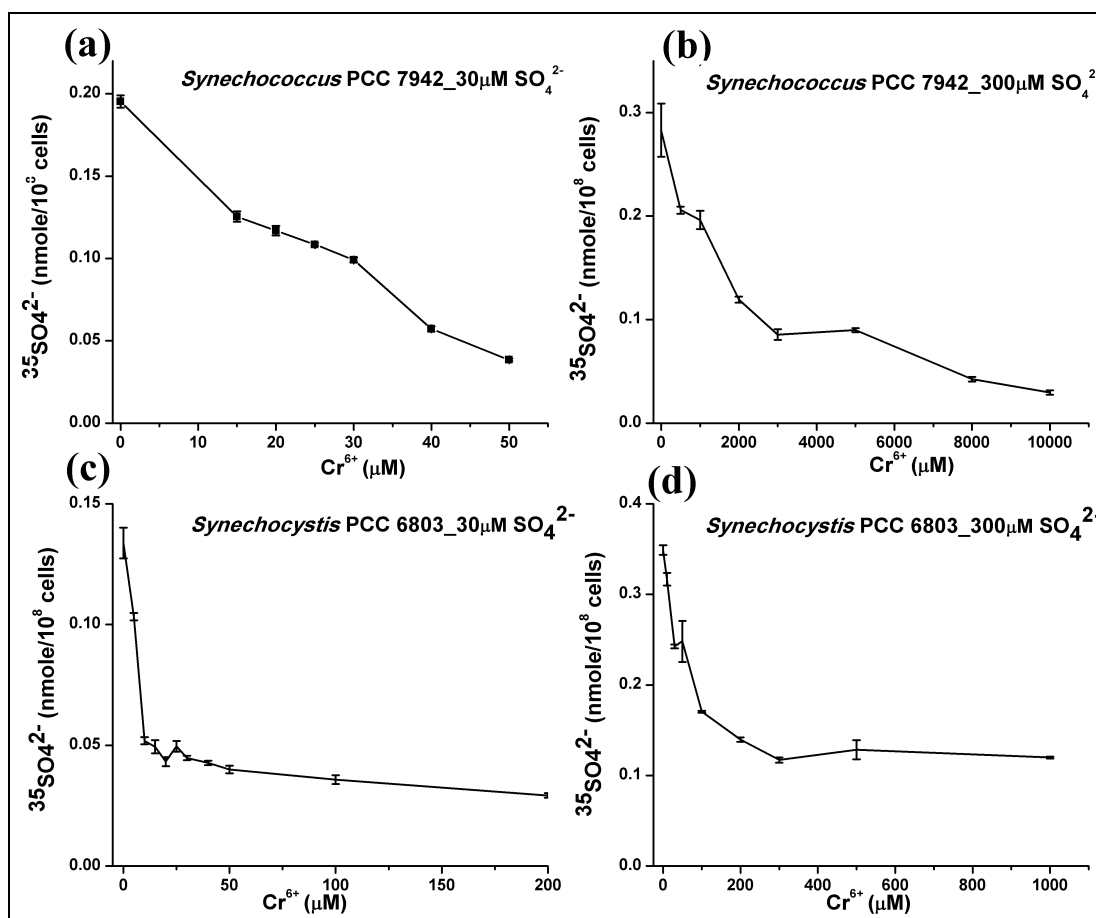


Log phase cultures of *Synechocystis* and *Synechococcus* (10^8 cells ml^{-1}) were incubated in BG-11 medium containing (i) Low SO_4^{2-} (30 μM) (ii) Normal SO_4^{2-} (300 μM) or (iii) High SO_4^{2-} (3000 μM) and 10 μM potassium dichromate with ^{51}Cr as tracer for 24 h in light. ^{51}Cr uptake by *Synechocystis* and *Synechococcus* was measured after incubation. X axis denotes sulfate concentration in growth medium and Y axis shows chromate uptake.

2.3.4 Determination of IC₅₀ of chromate for ³⁵S sulfate uptake

Sulfate uptake using ³⁵S labeled sodium sulfate in the presence of varying concentrations of chromate was monitored in *Synechocystis* and *Synechococcus* incubated in the medium containing 30 μM or 300 μM sodium sulfate (**figure 2.7**). Chromate was found to decrease the uptake of sulfate in *Synechococcus* and *Synechocystis*. When concentration of sulfate was increased from 30 to 300 μM the concentration of chromate required for IC₅₀ was increased from 30.35 μM to 1.7 mM in case of *Synechococcus*. In *Synechocystis* when concentration of sulfate was increased from 30 to 300 μM the concentration of chromate required for IC₅₀ was increased from 8.6 μM to 99 μM.

Figure 2.7: Effect of chromate on uptake of ^{35}S labeled sulfate by *Synechocystis* and *Synechococcus*



Log phase cultures of *Synechocystis* and *Synechococcus* ($10^8/\text{ml}$ cells) were incubated in BG-11 medium containing 30 or 300 μM sodium sulfate with ^{35}S labeled sodium sulfate as tracer and different concentrations of potassium dichromate as mentioned in figure. Uptake of ^{35}S sulfate was monitored after 2 hours. The average of four estimations is shown. Bars represent SE. X axis denotes chromate concentration in growth medium and Y axis shows sulfate uptake.

a: *Synechococcus* incubated in medium containing 30 μM sodium sulfate. **b:** *Synechococcus* incubated in medium containing 300 μM sodium sulfate. **c:** *Synechocystis* incubated in medium containing 30 μM sodium sulfate and **d:** *Synechocystis* incubated in medium containing 300 μM sodium sulfate.

2.3.5 Sequence comparison of sulfate and chromate transporters in *Synechocystis* and *Synechococcus*

To investigate if the differences in the IC₅₀ of chromate for sulfate uptake in the two organisms could be attributed to the differences in primary structure of the sulfate and chromate transporters, a comparative sequence analysis of amino acid sequences of these proteins from *Synechococcus* and *Synechocystis* was carried out (**table 2.2, table 2.3**) and (**figure 2.8–2.12**). The analysis included SulT permease constituting the permease, membrane proteins and ATPase; and chromate transporter ChrA. Their sequences were also compared with the sequences of well characterized sulfate and chromate uptake related proteins from other prokaryotic organisms.

Table 2.2: Comparative analysis of sulfate and chromate transporter genes in *Synechococcus*

Sulfate transporters in <i>Synechococcus</i> PCC 7942							
Sr. No	ORF ID	Gene Symbol	Definition	Aa	TM	Homologue in <i>Synechocystis</i>	% Identity
1	Synpcc79_42_1681	<i>sbpA</i>	Thiosulfate-binding protein	350	nil	slr1452	58.9
2	Synpcc79_42_1680	<i>cysA</i>	Sulfate transport system permease protein 1	338	nil	slr1455	63.3
3	Synpcc79_42_1688	<i>cysW</i>	Sulfate ABC transporter, permease protein CysW	286	6	slr1454	51.9
4	Synpcc79_42_1685	<i>cysW</i>	Sulfate transport system permease protein 2	286	6	slr1454	62.8
5	Synpcc79_42_1682	<i>cysT</i>	Sulfate transport system permease protein 2	278	6	slr1453	62.5
6	Synpcc79_42_1687	<i>cysT</i>	Sulfate ABC transporter, permease protein CysT	288	7	slr1453	46.1
7	Synpcc79_42_1722		Thiosulfate-binding protein	361	nil	slr1452	54.5
8	Synpcc79_42_1686		Thiosulfate-binding protein	341	nil	slr1452	42.4
9	Synpcc79_42_0366		putative sulfate transporter	727	11	slr0096	22.9
10	Synpcc79_42_1380		sulfate permease	574	11	slr1776	32.8
Chromate transporters in <i>Synechococcus</i> PCC 7942							
1	Synpcc794_2_0390		Chromate transporter	383	9	slr1457	40.2
2	Synpcc794_2_B2622_plasmid 1 ^a	<i>srpC</i>	probable chromate transport transmembrane protein	393	12	slr1457	29.2

Translated amino acid sequences annotated as sulfate and chromate transporters as given in Cyanobase were used for comparative analysis of *Synechococcus* PCC 7942 with *Synechocystis* PCC 6803. The values of Aa (Amino acid chain length), TM (Number of Transmembrane helices) and % Identity (as in orthologue search) for individual genes have been obtained from Cyanobase. ^a indicates that gene is located on plasmid. ORF ID (Open Reading Frame Identity).

Table 2.3: Comparative analysis of sulfate and chromate transporter genes in *Synechocystis*

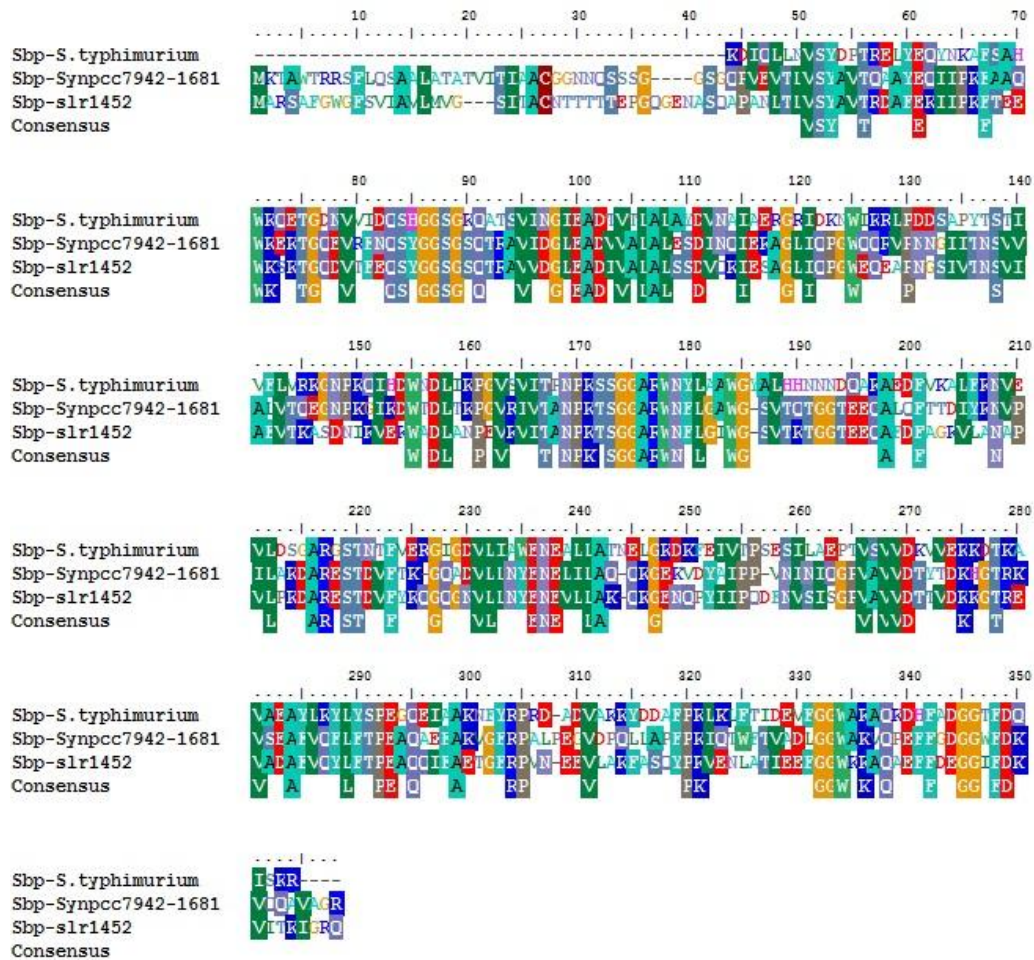
Sulfate transporters in <i>Synechocystis</i> PCC 6803							
Sr. No	ORF ID	Gene Symbol	Definition	Aa	TM	Homologue in <i>Synechococcus</i>	% Identity
1	slr1452	<i>sbpA</i>	sulfate transport system substrate-binding protein	352	nil	Synpcc7942_1681	58.9
2	slr1455	<i>cysA</i>	sulfate transport system ATP-binding protein	355	nil	Synpcc7942_1680	63.3
3	sll1041	<i>cys A</i>	similar to sulfate transport ATP-binding protein CysA	260	nil	Synpcc7942_0350	53.1
4	slr1454	<i>cysW</i>	sulfate transport system permease protein	276	6	Synpcc7942_1685	62.8
5	slr1453	<i>cysT</i>	sulfate transport system permease protein	286	6	Synpcc7942_1682	62.5
6	slr1229		sulfate permease	453	9	Synpcc7942_1380	22.7
7	slr0096		low affinity sulfate transporter	556	11	Synpcc7942_1380	25
8	sll0834		low affinity sulfate transporter	564	12	Synpcc7942_1380	29.1
9	slr1776		high affinity sulfate transporter	566	11	Synpcc7942_1380	32.9
Chromate transporters in <i>Synechocystis</i> PCC 6803							
1	slr1457	<i>chrA</i>	chromate transport protein	399	9	Synpcc7942_0390	40.5
2	slr5038 pSYSM ^a		chromate transporter	412	11	Synpcc7942_0390	36.4

Translated amino acid sequences annotated as sulfate and chromate transporters as given in Cyanobase were used for comparative analysis of *Synechocystis* PCC 6803 with *Synechococcus* PCC 7942. The values of Aa (Amino acid chain length), TM (Number of Transmembrane helices) and % Identity (as in orthologue search) for individual genes have been obtained from Cyanobase. ^a indicates that gene is located on plasmid. ORF ID (Open Reading Frame Identity).

2.3.5.1 Sulfate-thiosulfate transporters

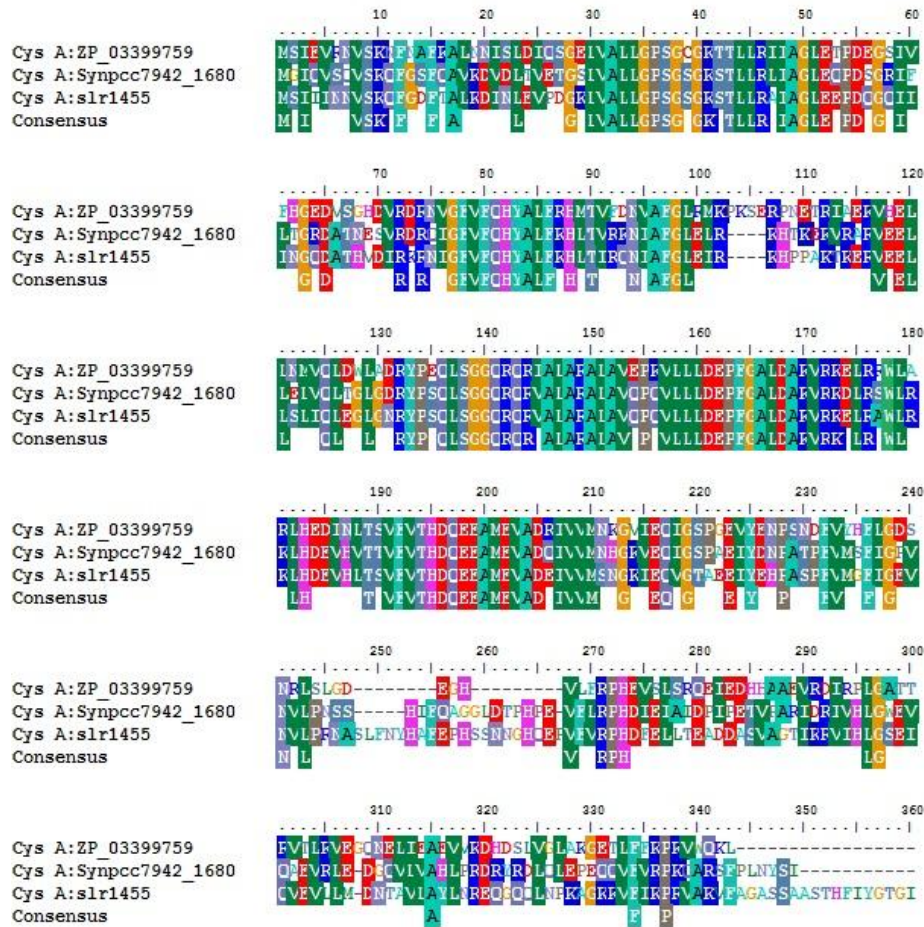
Sulfate-thiosulfate (SulT) permease complex from some bacteria is well characterized and typically consists of sulfate or thiosulfate binding protein Sbp or CysP, and the proteins of ABC transporter viz CysA, ATPase, CysW and CysT. These were used as reference to identify differences among the corresponding proteins in the two organisms under study. Ten and nine genes for sulfate transporters are identified in *Synechococcus* and *Synechocystis* respectively in Cyanobase (**tables 2.2 and 2.3**). The sulfate binding proteins (SbpA) in *Synechococcus* and *Synechocystis* have ~ 58.9 % identity. SbpA from these organisms showed 99 conserved amino acid residues with SbpA from *Salmonella typhimurim* (**figure 2.7**). Cys A, the ATPase subunit of the SulT permease of *Synechococcus* and *Synechocystis* have ~ 63 % identity. **Figure 2.8** shows that there were 148 conserved amino acid residues among them and the CysA from *Pseudomonas syringae*. Bacterial CysT and CysW constitute the transport channel of the SulT permease typically with six transmembrane helices which are also present in CysT and CysW from *Synechocystis*. *Synechococcus* CysT and CysW show ~ 46 to 64 % identities with homologs from *Synechocystis*. All of these have six transmembrane helices except Synpcc7942_1687 (Cys T) which has seven transmembrane helices. *Synechocystis* and *Synechococcus* CysT and CysW showed 70 and 96 conserved amino acid residues with CysT and CysW from *E. coli*. (**figure 2.9 and 2.10**).

In addition to the conserved SulT components, the genomes of *Synechococcus* PCC 7942 and *Synechocystis* PCC 6803 show presence of some putative sulfate transporters, thiosulfate binding protein, low and high affinity sulfate transporter and sulfate permease (**tables 2.2 and 2.3**). Some of these have transmembrane domains suggesting a possible membrane location for them.

Fig 2.8: Sequence comparison of Sbp, a periplasmic sulfate binding protein

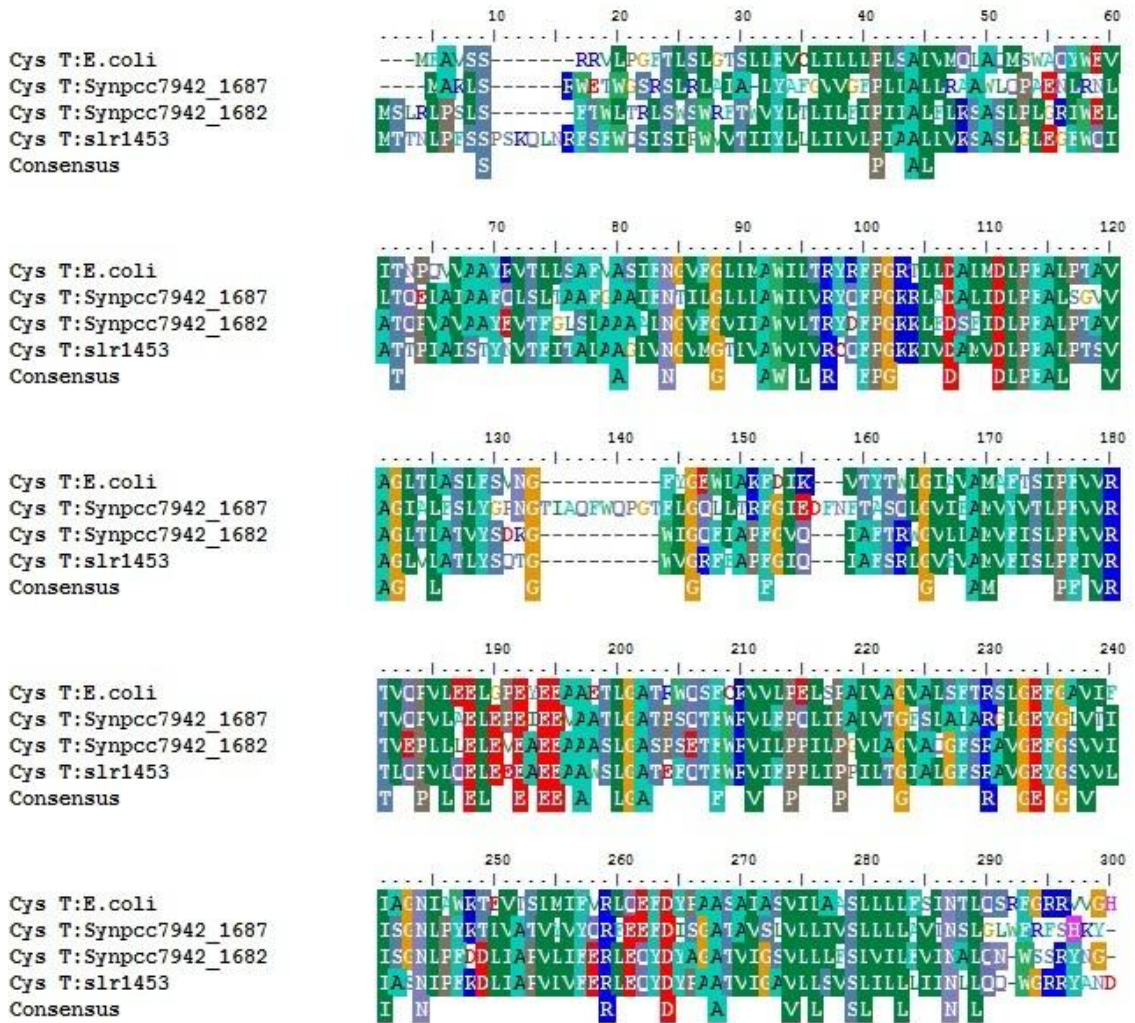
Translated amino acid sequences from Cyanobase were used for comparative analysis of the periplasmic sulfate binding protein of *Synechococcus* and *Synechocystis*. Synpcc7942_1681 is a sulfate-thiosulfate binding protein (Sbp) from *Synechococcus*. slr1452 is sulfate-thiosulfate binding protein (Sbp) from *Synechocystis*. The standard protein sequences used was from *Salmonella typhimurium* ISBP:A|PDBID|CHAIN|SEQUENCE. The three sequences showed 99 conserved residues depicted as consensus in the figure. The active site residues such as Glu 57, Asp 68, Arg 134, Lys 232, Glu 23 and N termini of some of the α helices from *Salmonella typhimurium* are conserved in Sbp from *Synechococcus* and *Synechocystis* although they have about 43 extra amino acids at the N terminus.

Figure 2.9: Sequence comparison of CysA, the ATPase subunit of the SulT permease



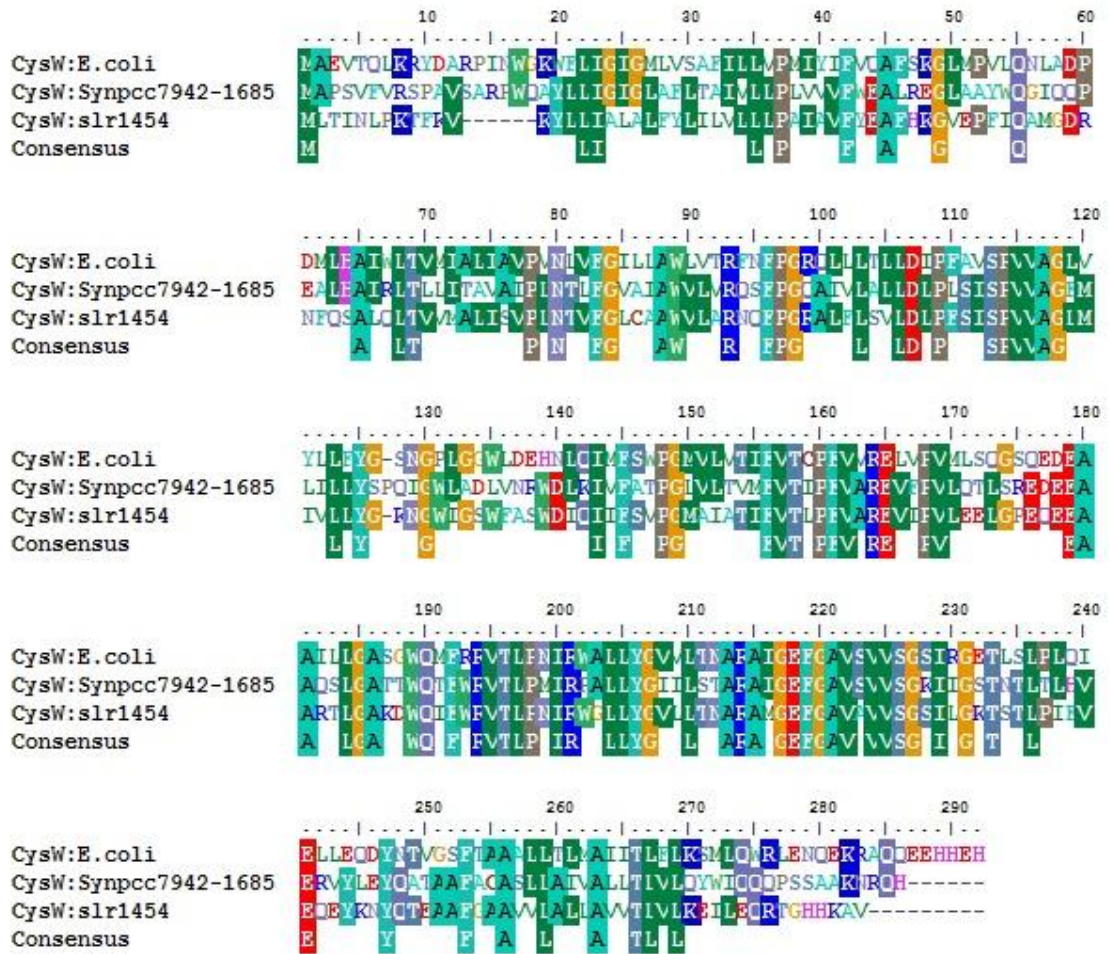
Translated amino acid sequences from Cyanobase were used for comparative analysis of CysA, the ATPase subunit of the SulT permease from *Synechococcus* and *Synechocystis*. Synpcc7942_1680 is CysA protein from *Synechococcus*. slr1455 is CysA from *Synechocystis*. The standard protein is from *Pseudomonas syringae* ZP_03399759: sulfate ABC transporter, ATP-binding protein CysA. The three sequences showed 148 conserved residues depicted as consensus in the figure. ABC transporters are a subset of nucleotide hydrolases that contain a signature Walker A motif with sequence *GXXGXGKS/T*, Walker B motif with sequence *hhhhD* in which h stands for hydrophobic amino acid and ABC signature motif *LSGGQ* (also called C-loop). All these typical motifs were present in the three sequences.

Figure 2.10: Sequence comparison of CysT, transport channel protein of the SulT permease



Translated amino acid sequences from Cyanobase were used for comparative analysis of CysT which constitutes the transport channel of the SulT permease from *Synechococcus* and *Synechocystis*. Synpcc7942_1682 and 1687 are the two CysT proteins from *Synechococcus*. slr1453 is CysT from *Synechocystis*. The standard protein is from *E.coli*, E. coli-CysT B2424 P16701. The four sequences showed 70 conserved residues depicted as consensus in the figure.

Figure 2.11: Sequence comparison of CysW, transport channel protein of the SulT permease



Translated amino acid sequences from Cyanobase were used for comparative analysis of CysW which also is also a component of the transport channel of the SulT permease from *Synechococcus* and *Synechocystis*. Synpcc7942_1685 is CysW protein from *Synechococcus*. slr1454 is CysW from *Synechocystis*. The standard protein is from *E.coli* sulfate transport system permease protein CysW (P0AEB0). The three sequences showed 96 conserved residues depicted as consensus in the figure.

2.3.5.2 Chromate transporters

Chromate resistance in prokaryotes has been attributed to ChrA which is a chemiosmotic pump responsible for chromate efflux using proton motive pump (Alvarez et al. 1999). Two ORFs have been annotated as chromate transporters in *Synechococcus* and *Synechocystis*, one on plasmid and other on chromosome (**tables 2.2 and 2.3**). These showed ~ 29 – 40 % identity, and presence of two CHR domains containing homologous halves with membrane spanning regions which is a feature of long chain CHR family proteins in bacteria. The cyanobacterial chromate transporters showed 37 conserved amino acid residues when compared with chromate transporter from *Pseudomonas aeruginosa* (**figure 2.12**).

2.4 Discussion

Chromate toxicity in aquatic organisms is mainly examined by exposing cultures to different concentrations of chromate for a given time, followed by investigations on physiological parameters. We compared two non-nitrogen fixing unicellular aquatic cyanobacteria belonging to order *Chroococcales* for their sensitivity to chromate when included in their growth media. Comparative analysis of chromate tolerance in *Synechococcus elongatus* PCC 7942 and *Synechocystis* PCC 6803 revealed that the former showed ~ 12 times higher tolerance to chromate than the latter, with EC₅₀ values of 150±15 µM and 12±2 µM respectively. The EC₅₀ values were dependent on the inoculum size in both cases indicating stoichiometric relation between chromate receptors per cell and number of chromate ions available in the growth medium. Thompson et al. (2002) have compared *Synechococcus* PCC 7942 and *Nostoc* PCC 7120 for resistance to chromate under high and low density conditions and have shown that there is general decrease in toxicity in dense cultures. Interestingly, stimulation in growth at less than 100 µM potassium dichromate was observed in *Synechococcus*. Lesser extent of ultrastructural damage in *Synechococcus* supports this argument.

In bacteria, two mechanisms of chromate tolerance are known: reduction of Cr (VI) to Cr (III) and efflux of chromate ions from cytoplasm (Ramírez-Díaz et al. 2008). DPC assays showed that these two cyanobacteria were not chromate reducers. Only nanomolar concentration of chromate accumulation was detected in *Synechocystis* using ⁵¹chromate. Although in *Synechococcus*, no chromate accumulation was observed under these conditions, there was stimulation of growth. This entailed that *Synechococcus* was able to sense the presence of low concentration of chromate in the growth medium. These observations indicated that in *Synechococcus* there are efficient mechanisms for sensing and efflux of chromate.

It is known that chromate ion enters the cells using sulfate transporters present in cell membrane as chromate ion is nearly identical in size shape and charge as sulfate ion (Riedel 1985). IC_{50} values of chromate in both *Synechococcus* and *Synechocystis* were dependent on sulfate concentration in medium indicating that sulfate uptake was competitively inhibited by chromate in both the cases. The inhibition of sulfate uptake by chromate suggested an interaction of chromate ions with sulfate uptake mechanism. However, the IC_{50} value of chromate was much higher in *Synechococcus* as compared to *Synechocystis* showing that *Synechocystis* has higher affinity for chromate as compared to *Synechococcus*. Sequence analysis showed that both the cyanobacteria have similar type of sulfate uptake channels and also contain similar genes related to efflux of chromate having typical bi-domain structure of LCHR. The differences in IC_{50} value of chromate suggested that the sequence variation in the non-conserved regions of sulfate uptake systems in both these organisms may be contributing to higher affinity of the sulfate uptake system for chromate in *Synechocystis* 6803 as compared to *Synechococcus* 7942. *Synechococcus elongatus* PCC 7942 possesses a plasmid (pANL) that contains a gene (*srpC/chrA*) conferring chromate resistance. The higher chromate susceptibility of *Synechocystis* cannot be attributed to absence of pANL as the sequence analysis shows that it has *chrA* homologues on its chromosome. Whether the location of *chrA* is responsible for the differential tolerance remains to be explored.

IC_{50} of chromate for sulfate uptake was higher in *Synechococcus* as compared to *Synechocystis* indicating that differential affinity of sulfate transporters for chromate may be contributing to the chromate tolerance in *Synechococcus* 7942 as compared to *Synechocystis* 6803. While IC_{50} for chromate at 10 fold increase in sulfate needed ~ 50 fold increase in chromate in case of *Synechococcus*, in case of *Synechocystis* with similar increase in sulfate, IC_{50} was attained by only ~ 12 fold increase in chromate concentration. Thus in *Synechococcus* the sulfate limitation by chromate

would be avoided by the its sulfate transporters which have lower affinity to chromate as well as by the efficient chromate efflux systems resulting in higher EC₅₀ for chromate. Although bioinformatic comparison of chromate and sulfate transporters revealed identity to a varying extent, the differences in their primary sequences could account for the difference in IC₅₀ of chromate. Thus in addition to differences mentioned above, the different putative sulfate permease in these two organisms may play a role in their distinct chromate response. Chromate resistance of *Synechococcus* would give it growth advantage in chromate contaminated sites over *Synechocystis*.

Thus the multifarious interaction of sulfate/chromate transporters could be the basis of contrasting response of *Synechococcus* and *Synechocystis* to chromate.

Bioinformatic analysis of sulfate and chromate transporters of *Synechococcus* and *Synechocystis* show the complexity of these transporters. Chromate resistance is a manifestation of numerous biochemical processes governed by different genes and their homologues. The complexity in composition of sulfate and chromate transporters and subsequent metabolic adjustments to sulfate deficiency in these two strains may be the cause of differential response of these two cyanobacteria. Cr (VI) is known to cause generation of free radicals inside the cells thus leading to oxidative stress which is dealt with in the next chapter.

Chapter 3

Oxidative Stress Markers in Synechocystis and Synechococcus in Response to Chromate

3.1 Introduction

The most stable state of any system is when its component molecules are in chemically reduced state as it is the minimum energy state. A living system though always stays in a dynamic state with a milieu of reduction-oxidation reactions going on at any particular time and there exists balance between reduced and oxidized molecules. Whenever oxidants increase in a cell, it is termed as under “oxidative stress”. The photosynthetic and respiratory electron transport processes lead to formation of free radicals, which include reactive oxygen species (ROS). Living organisms have developed various defenses to protect themselves against ROS damage (Latifi et al. 2009). ROS are detoxified enzymatically by antioxidants like catalases, superoxide dismutase (SOD) and peroxidases. An imbalance between ROS production and their detoxification causes damage to protein, lipids and DNA which in turn leads to physiological malfunctions. However, it is also well established now that ROS play important role as signaling molecules in eukaryotic cells.

In cyanobacteria, high light is one of the most prominent causes of oxidative stress. Apart from this, in the aquatic environment, heavy metals and toxic chemicals are known to impart oxidative stress to aquatic flora and fauna. As described in the literature overview, Cr (VI) leads to generation of free radicals by undergoing reduction to Cr (III) by using intracellular reductants. Therefore, ROS and common antioxidants were assayed in *Synechocystis* and *Synechococcus* grown with or without potassium dichromate.

3.2 Materials and Methods

3.2.1 Preparation of cell free extract

Synechocystis and *Synechococcus* were grown in BG-11 medium containing 0 or 12 μM and 0, 75 and 150 μM potassium dichromate respectively for 9-10 days as described in section 2.2.1. Cells were harvested from 50 ml culture by centrifugation at 8000 x g for 5 minutes at room temperature. The pellet was washed with tris buffer (50 mM, pH 8.0) and finally suspended in 100 μl of the same buffer. Glass beads (100 μm size, acid washed) were added to the suspension and vortexed 3 to 5 times for 1 minute with intermittent incubation on ice to break the cells. Cell free extract was obtained by centrifugation of the suspension at 9300 x g for 5 minutes at 4°C. The extracts were maintained at 4°C and used the same day or the following day for enzyme assays. Total protein estimation in the extracts was carried out using standard Lowry's method (Lowry et al. 1951). BSA was used as standard in protein estimation.

3.2.2 Assay of catalase content: Catalase content was compared between *Synechocystis* and *Synechococcus* by in gel activity assay according to Weydert and Cullen (2010). Protein (10 μg) of the samples were resolved on 8 % native PAGE at 4-7°C following Laemmli's buffer system (Laemmli 1970). The gel was rinsed with distilled water, followed by incubation with 0.003 % solution of H_2O_2 for 15 min at room temperature on rocker. After rinsing with distilled water, the gel was incubated in equal volume of solution of 1 % ferric chloride (FeCl_3) and 1 % potassium ferricyanide for 5-10 minutes. These two solutions were prepared separately and poured over the gel simultaneously. Yellow bands were observed as catalase activity in a Prussian blue background.

The assay is based on the removal of peroxide from the area of the gel where catalase is present. Removal of peroxide does not allow potassium ferricyanide which is a yellow substance to be reduced to potassium ferrocyanide which reacts with ferric chloride to form a Prussian blue precipitate. Therefore a yellowish clear area is visualized on the gel where catalase is present in the otherwise Prussian blue background.

3.2.3 Monitoring 2-Cys-Peroxiredoxin content: Content of 2-Cys-Peroxiredoxin was determined by Western blotting with *Anabaena* anti-alr 4641 (2-Cys Prx) antibody. Preparation of cell free extract and determination of protein concentration were carried out as described in section 3.2.1. Total protein (50 µg) of *Synechocystis* and *Synechococcus* were resolved on 12 % SDS PAGE using Laemmli's buffer (Laemmli 1970) followed by transfer to nitrocellulose membrane. Western blotting was done using 1:50,000 dilution of the anti-2-Cys Prx antibody. The detection of 2-Cys Peroxiredoxin was carried out by NBT-BCIP which gives a bluish precipitate on being acted on by alkaline phosphatase attached to the secondary antibody.

3.2.4 Monitoring oxidized (carbonylated) protein content: Content of carbonylated proteins was determined by Western blotting with anti-2, 4-dinitrophenylhydrazone antibody using Millipore S7150 kit. Preparation of protein sample and western blotting were carried out as described in sections 3.2.1 and 3.2.3 respectively. Before resolving the proteins on SDS PAGE, they were derivatized to 2,4-dinitrophenylhydrazone (DNP).

3.2.5 *In vivo* detection of ROS: ROS was detected by using 2',7'-Dichlorofluorescein diacetate (DCFH-DA). This nonpolar compound is converted to the polar derivative 2',7'-Dichlorofluorescein diacetate (DCFH) by cellular esterases when it is taken up. DCFH is nonfluorescent; it is converted to a highly fluorescent form DCF when oxidized by intracellular ROS and other peroxides. DCF

fluorescence is used as indicator of ROS (He and Häder 2002). Cultures of *Synechocystis* and *Synechococcus* cells, 1 ml each, grown with or without potassium dichromate and containing about 3 µg of chlorophyll were incubated with 5 µM of DCFHDA for 1h in dark at room temperature on a rocker. DCFHDA stock solution of 5 mM prepared in absolute ethanol was used for the assay. ROS was quantified by measuring fluorescence with λ excitation of 485 nm and λ emission at 520 nm using Hitachi F-4010 fluorimeter.

3.2.6 Determination of Superoxide dismutase (SOD) activity: The activity of SOD was assayed according to Beauchamp and Fridovich (1971) with some modifications. The assay is based on ability of SOD to inhibit the photochemical reduction of nitrobluetetrazolium (NBT). Briefly, the assay was carried out in 1ml reaction mixture containing 40 mM phosphate buffer (pH 7.8), 13 mM methionine, 75 µM NBT, 2 µM riboflavin, 0.1 mM EDTA and 5 µl of cell free extract. The tubes containing the reaction mixture were shaken and placed on a light box consisting of fluorescent lights for 15 to 20 minutes. The absorbance was measured at 560 nm. The activity of SOD was expressed as units mg^{-1} protein. One unit of activity is the amount of protein required to inhibit 50 % initial reduction of NBT under light.

3.2.7 Oxidative stress tolerance of *Synechocystis* and *Synechococcus* grown with or without potassium chromate: To determine the tolerance of the cyanobacteria to oxidative stress after growth with chromate, equal number (about 10^8 cells/ml) of cells of 9 day old cultures of *Synechocystis* and *Synechococcus* grown with 0 or 12 µM and with 0, 75 or 150 µM potassium dichromate respectively were subjected to 24 h light incubation with 0, 5, 10, 15, 20 or 30 mM of H_2O_2 . Chlorophyll *a* concentration in the cells was determined as a measure of survival. Chlorophyll extraction and estimation was carried out in the methanolic extract according to Tandeau de Marsac and Houmard (1988). Cells from 1ml of culture were pelleted

down by centrifugation at ~6000 x g for 5 minutes. The pellet was suspended in 1ml of 90 % methanol and allowed to stand in dark for 10 minutes. Clear methanolic extract of chlorophyll *a* was obtained by centrifuging the suspension at 10,000 x g for 5 minutes. Chlorophyll *a* was quantified by recording optical density of the extract at 665 nm (OD₆₆₅) in spectrophotometer and calculating the concentration as:

$$\text{Chlorophyll } a (\mu\text{g}\cdot\text{ml}^{-1}) = \text{OD}_{665} \times 13.9$$

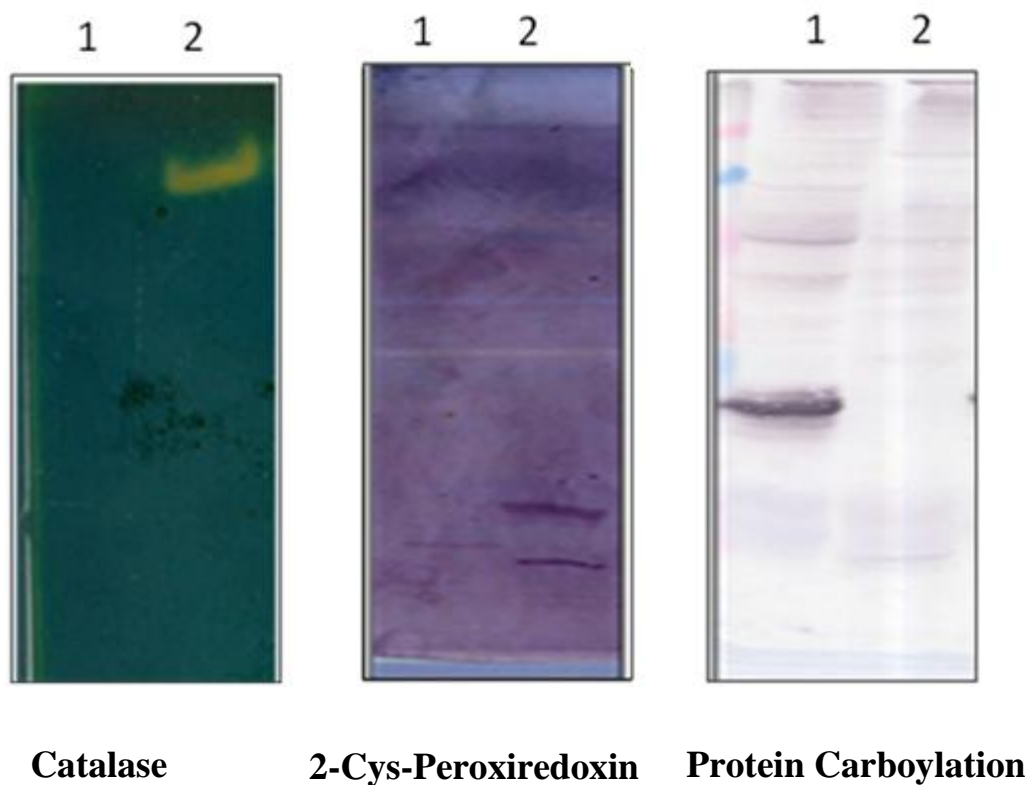
3.3 Results

3.3.1 Comparison of oxidative stress tolerance between *Synechocystis* and

Synechococcus

Since *Synechocystis* and *Synechococcus* showed differences in tolerance to chromate, to check if the possibility of the antioxidants being involved in detoxifying the ROS was contributing to the difference, levels of general antioxidant enzymes and protein carbonylation in the two cyanobacteria under control growth conditions were compared to ascertain the inherent levels. **Figure 3.1** shows a comparison of catalase, 2-Cys-Prx and level of protein carbonylation between *Synechocystis* and *Synechococcus* grown under control conditions. Activities of both the H₂O₂ detoxifying enzymes on equal total protein basis were found to be lower in *Synechocystis* as compared to *Synechococcus*. Content of carbonylated proteins, which is proteins in oxidized condition, was higher in *Synechocystis* as compared to *Synechococcus* showing that *Synechococcus* was better equipped to mitigate general oxidative stress.

Figure 3.1: Catalase, 2-Cys Peroxiredoxin and protein carbonylation levels in *Synechocystis* and *Synechococcus*

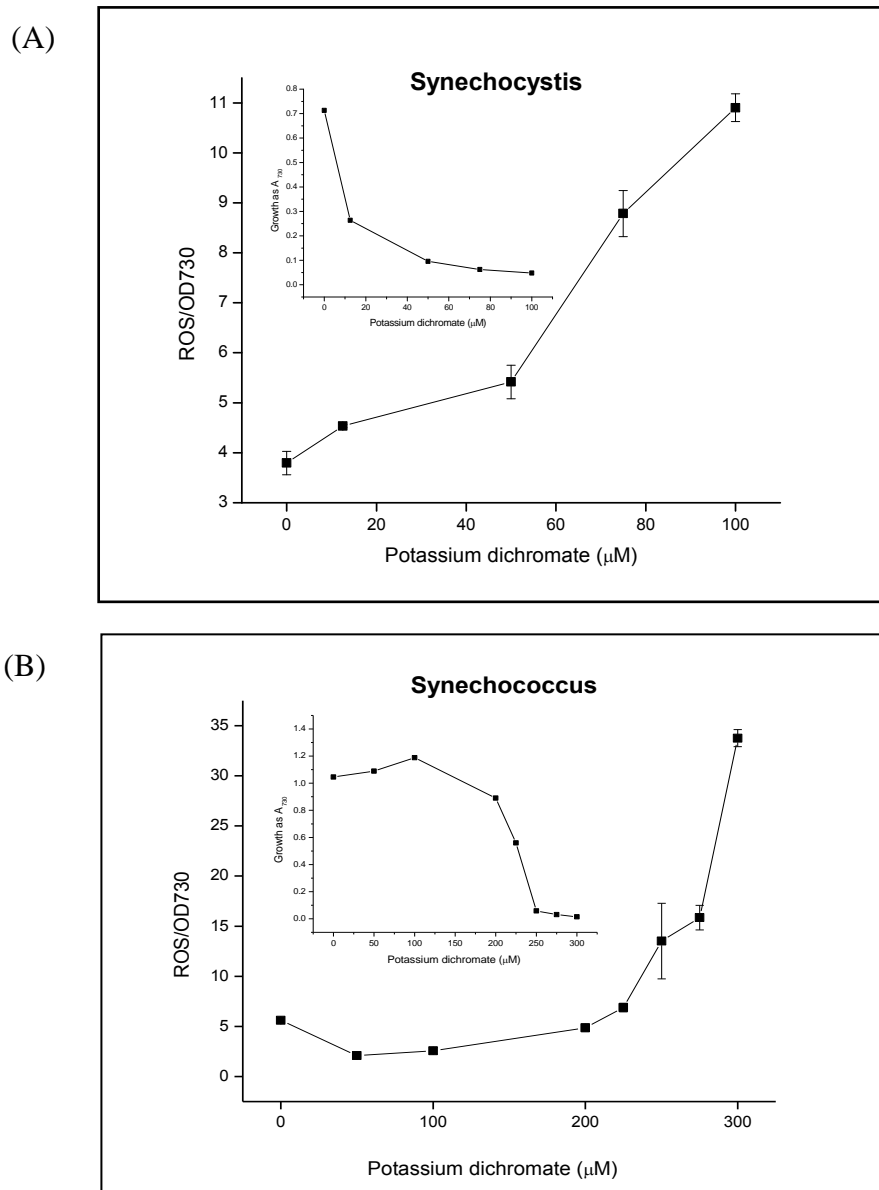


Catalase activity, 2-Cys Peroxyredoxin and carbonylated proteins were monitored in 1 *Synechocystis* and 2 *Synechococcus* grown under normal conditions. Catalase activity was determined by in gel activity assay, 2-Cys-Peroxiredoxin was immunodetected using *Anabaena* anti-alr 4641 (2-Cys Prx) antibody and protein carbonylation was monitored by immunodetection with anti-2,4-dinitrophenylhydrazone antibody.

3.3.2 Effect of growth with chromate on oxidative stress markers in *Synechocystis* and *Synechococcus*

3.3.2.1 Determination of ROS: Presence of free radicals and antioxidant enzymes are indicative of a cell being exposed to oxidative stress condition and therefore are termed as markers of oxidative stress. **Figures 3.2 A and B** show the ROS content in the two cyanobacteria after growth for nine days with increasing concentration of potassium dichromate and in the inset growth pattern of the cultures are shown. In *Synechocystis*, an almost linear increase in ROS content with increasing potassium dichromate was observed whereas a reverse trend was followed in the growth pattern (**figure 3.2A**). In *Synechococcus*, a significant increase in ROS content per cell as compared to control culture was observed in cultures grown with potassium dichromate $\geq 200 \mu\text{M}$. A drastic reduction in growth as compared to control cultures was also observed under these conditions (**figure 3.2 B**). In cultures grown with lower concentrations of potassium dichromate where ROS content was low, growth was observed.

Figure 3.2 ROS content in *Synechocystis* and *Synechococcus* grown with increasing concentration of potassium dichromate



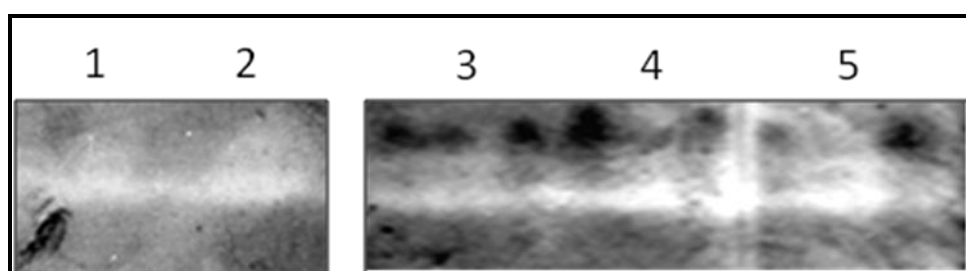
ROS content was measured as described in section 3.2.5 in (A) *Synechocystis* and (B) *Synechococcus* grown with increasing concentration of potassium dichromate for 9 days. The inset shows growth pattern of the same cultures after growth. X axis shows potassium dichromate concentration and Y axis shows ROS content and growth as OD_{730} on Y axis of the inset.

3.3.2.2 Determination of SOD, catalase, and peroxiredoxin levels: The levels of anti-oxidative stress markers were monitored in *Synechocystis* and *Synechococcus* cells grown with 0 or 12 μM chromate and 0, 75 or 150 μM potassium dichromate respectively and cell free extracts were prepared from 9 day old cultures. The most common enzymes involved in detoxification of ROS are SOD and catalase; SOD reduces superoxide radical to form oxygen and hydrogen peroxide. Catalase catalyzes the decomposition of hydrogen peroxide to water and oxygen. Activities of SOD and catalase were measured in the cell free extracts. **Table 3.1** shows levels of SOD activities in the two cyanobacteria grown with or without potassium dichromate. In case of *Synechocystis* the increase in level of SOD was not significant when cells were grown with or without 12 μM chromate; same was the case in *Synechococcus* grown with 0 or 75 μM chromate. However, level of SOD was significantly higher in *Synechococcus* cells grown with 150 μM chromate. **Figure 3.3** shows the zymogram of catalase activity which was higher in *Synechococcus* on equal protein basis. There was slight increase in catalase activity in both the cyanobacteria after growth with chromate. The level of 2-Cys-Peroxiredoxin was also determined in response to chromate. As shown in **figure 3.1 and 3.4**, the level of 2-cys-peroxiredoxin was low in *Synechocystis* grown under control conditions and no change in its levels could be detected in response to chromate. However, *Synechococcus* showed an increase in the level of the peroxiredoxin when grown in presence of 75 and 150 μM potassium dichromate (**figure 3.4**).

Table 3.1 SOD activity in *Synechocystis* and *Synechococcus* grown with or without potassium chromate

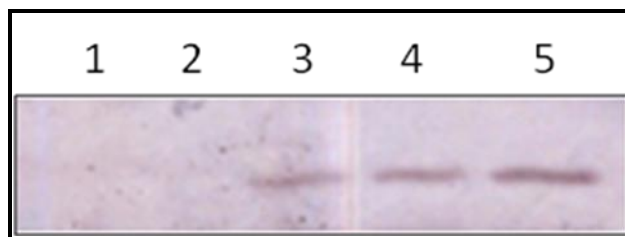
Sample	SOD (Units/mg protein)
<i>Synechocystis</i> _0 μ M K ₂ Cr ₂ O ₇	27.36 \pm 0.86
<i>Synechocystis</i> _12 μ M K ₂ Cr ₂ O ₇	28.90 \pm 0.38
<i>Synechococcus</i> _0 μ M K ₂ Cr ₂ O ₇	8.02 \pm 0.52
<i>Synechococcus</i> _75 μ M K ₂ Cr ₂ O ₇	8.94 \pm 1.01
<i>Synechococcus</i> _150 μ M K ₂ Cr ₂ O ₇	19.76 \pm 0.06

SOD activity was measured in the cell free extracts of *Synechocystis* and *Synechococcus* grown with 0, 12 μ M and 0, 75, 150 μ M respectively, by photoreduction of NBT caused by SOD on equal protein basis in the cell free extracts as described in section 3.2.6.

Figure 3.3 Catalase levels in *Synechocystis* and *Synechococcus* grown with or without potassium chromate

Catalase activity was measured in the cell free extracts of *Synechocystis* grown with 0 or 12 μ M (1, 2) and *Synechococcus* grown with 0, 75 or 150 μ M potassium dichromate (3, 4, 5). The assay was carried out on the cell free extract resolved on 8 % colourless native PAGE run on equal protein basis as described in section 3.2.2.

Figure 3.4 Effect of growth with chromate on 2-Cys Peroxiredoxin levels in *Synechocystis* and *Synechococcus*

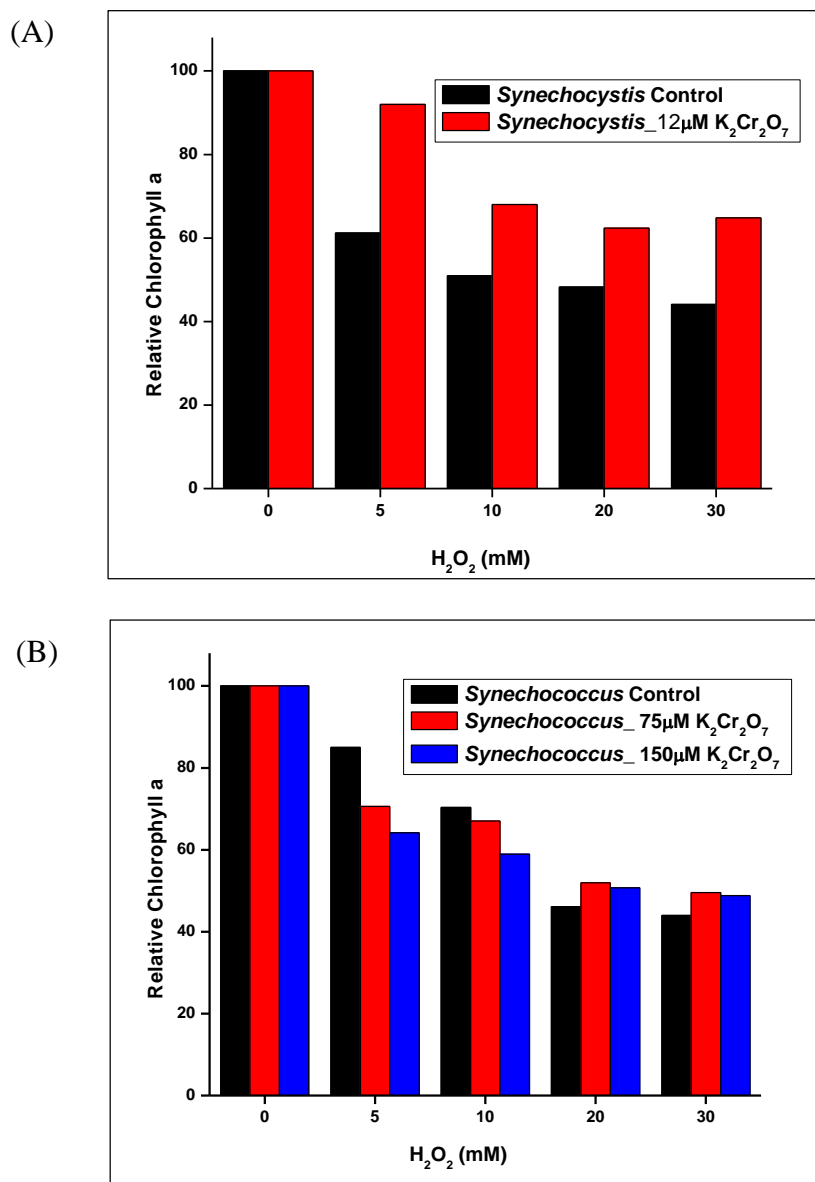


2-cys-peroxiredoxin was immunodetected using *Anabaena* anti-alr 4641 (2-Cys Prx) antibody in the cell free extracts of *Synechocystis* grown with 0 or 12 μM (1, 2) and *Synechococcus* grown with 0, 75 or 150 μM potassium dichromate (3, 4, 5).

3.3.3 Oxidative stress tolerance of *Synechocystis* and *Synechococcus* grown with or without potassium chromate

Since there was only marginal difference in antioxidant enzymes in chromate grown cells, whether growth with chromate gave any advantage to cells to tolerate additional oxidative stress was evaluated. *Synechocystis* grown with 0 or 12 μM chromate and *Synechococcus* grown with 0, 75 or 150 μM chromate were exposed to different concentrations of H_2O_2 for 24 h in light. **Figure 3.5** shows the relative chlorophyll a contents in *Synechocystis* and *Synechococcus* after incubation with different concentrations of H_2O_2 . *Synechocystis* showed higher adaptation to extra stress due to H_2O_2 as chlorophyll a contents were higher at all H_2O_2 concentrations in cells grown with chromate as compared to control cells (**figure 3.5 A**). Although there was higher SOD activity in *Synechococcus* cells grown with 150 μM chromate, there was no additional advantage of growth with chromate in their susceptibility to oxidative stress at all H_2O_2 concentrations as there was no significant difference between control and chromate grown cells (**figure 3.5 B**). Thus, although *Synechococcus* showed higher resistance to chromate, the chromate grown cells had no further benefit in their response to extra oxidative stress.

Figure 3.5 Effect of incubation with H_2O_2 on *Synechocystis* and *Synechococcus* grown with chromate



Equal number of cells of 9 day old cultures of *Synechocystis* and *Synechococcus* grown with 0 or 12 μ M and 0, 75 or 150 μ M and potassium dichromate respectively were subjected to 24 h light incubation with 0, 5, 10, 15, 20 or 30 mM of H_2O_2 . Chlorophyll a concentration in the cells was determined after incubation as a measure of survival. X axis represents H_2O_2 concentration in the medium and Y axis represents relative chlorophyll concentration.

3.4 Discussion

Free radicals are byproducts of aerobic metabolism; for cyanobacteria, the sources are respiratory and photosynthetic electron transport chains. All cells have strategies to deal with the free radicals as they are cytotoxic beyond a certain level. Cyanobacteria come across different stresses in their environment that expose them to conditions leading to generation of more of free radicals. The experiments on oxidative stress were based on the question: whether growth of the two cyanobacteria which showed contrasting tolerance to potassium dichromate with chromium (VI) exposes them to oxidative stress? And if so, what is the tolerance level to the oxidative stress? Therefore, markers of oxidative stress, ROS and general antioxidant enzyme activities were determined in the cells grown with or without chromate. Basal levels of the antioxidant activities in the two cyanobacteria were compared to understand the basis of contrasting tolerance. Further, whether growth with chromate gives additional advantage to the cyanobacteria to deal with oxidative stress was examined.

In *Synechococcus* as shown in the chapter 2, a relatively tolerant response to potassium dichromate was observed with stimulation in growth at low concentration of chromate. The increase in ROS at higher chromate concentrations where growth is reduced indicated that the reason for such a response could be the ability of *Synechococcus* to cope with the chromate toxicity which manifests itself by causing oxidative stress inside the cells. Also, another plausible reason could be a better chromate efflux mechanism working in *Synechococcus* which keeps chromium out or under tolerable limits up to 150 μM . Hence a better machinery to keep chromate out and a better machinery to take care of oxidative stress make it more tolerant as compared to *Synechocystis*. In contrast, *Synechocystis* showed higher chromium content inside cells which would lead to free radical generation, therefore the

response was observed from low chromate concentrations. The results showed that chromate causes oxidative stress in both the cyanobacteria and induces an antioxidant response in both. An increase in antioxidant enzyme activities like SOD and catalase when grown with chromate indicated that both the cyanobacteria were exposed to oxidative stress due to chromate.

These results suggested that *Synechocystis* has lower level of some antioxidants which could be one of the reasons of being less tolerant to chronic stress of chromate. This difference in strategies to deal with stressors is common in cyanobacteria. *Synechocystis* 6803 and *Anabaena* 7120 have different strategies to deal with H₂O₂. *Synechocystis* 6803 has low content of less sensitive 2 Cys Prx and high catalase activity and *Anabaena* 7120 has abundant and sensitive 2 Cys Prx but low catalase activity (Pascual et al. 2010).

Synechocystis grown with EC₅₀ concentration of potassium dichromate showed adaptation to oxidative stress by H₂O₂ whereas *Synechococcus* did not exhibit such a response. As discussed in the chapter 2, there is more probability of chromium being present in the cells of *Synechocystis* than in *Synechococcus*, thus allowing the live cells to develop adaptation to oxidative stress generated by chromium exposes them to. Also, in *Synechococcus*, most of the 'efforts' in terms of resources could be channelized to keep chromium out as lower chromium was found to be present inside the cells and no adaptive mechanisms observed in them.

Thus in conclusion, the results showed that *Synechococcus* cells were inherently more resistant to oxidative stress as compared to *Synechocystis*. Chromate imparted oxidative stress to both the cyanobacteria and *Synechocystis* showed adaptive response to oxidative stress after growth with chromate. *Synechococcus* did not show such adaptation.

The effect of prolonged oxidative stress due to growth with chromate on structure function of photosynthetic apparatus in *Synechocystis* and *Synechococcus* was explored and results are presented in the next chapter.

Chapter 4

*Evaluation of Structure-
Function Relationship of
Photosynthetic Machinery in
Synechocystis and
Synechococcus Grown With
Chromate*

4.1 Introduction

In the earlier chapters contrasting responses of *Synechocystis* and *Synechococcus* to chromate is described. Since there were differences in susceptibility to chromate and in oxidative stress tolerance in *Synechocystis* and *Synechococcus*, investigations on the long term effect of growth with chromate on the photosynthetic apparatus of these two cyanobacteria were carried out. Photosynthetic apparatus is one of the targets of chromate. Effects of acute stress of chromate on photosynthetic apparatus have been studied as discussed in detail in chapter 1.

Acute stress of chromate is known to affect PSII function in various photoautotrophs. The inhibitory effect was mainly observed on D1 protein and oxygen evolving complex of PSII in *Chlamydomonas reinhardtii*. (Ali et al. 2006, Perreault et al. 2009). Effect of acute stress on photosynthesis on fronds of *Spirodela polyrhiza* and on *Microcystis* was examined by Appenroth et al. (2001) and Wang et al. (2013) using chlorophyll fluorescence analysis. It was observed that chromate affected several targets in PSII, especially the total number of active reaction centers, efficiency of electron transport, yield of primary photochemistry and oxygen evolving complex. Electron transport rate in PSI was affected to lesser extent than PSII and cyclic electron flow was stimulated by chromate. In nature, aquatic microflora rarely comes across such acute metal stress; rather it is chronically exposed toxic metals. To thrive in the contaminated sites, the microflora adapts to the continuous presence of toxic metals. Therefore, structure-function relationship of the photosynthetic machinery in *Synechocystis* and *Synechococcus* grown with Cr (VI) was explored and the results are presented in this chapter.

4.2 Materials and Methods

Log phase cultures of *Synechocystis* and *Synechococcus* were used for all the experiments. The cultures were grown as described in 2.2.1. 50 ml of sterilized BG-11 medium containing 0 or 12 μM potassium dichromate was inoculated with 10^8 cells for *Synechocystis*. Similarly BG-11 medium containing 0, 75 or 150 μM potassium dichromate was inoculated with $\sim 10^8$ cells for *Synechococcus*. Cultures were grown under continuous illumination of $\sim 15 \mu\text{mol m}^{-2}\text{s}^{-1}$ at $26 \pm 2^\circ\text{C}$. For BN PAGE, cultures were scaled up in 500 ml BG-11 medium containing proportionate potassium dichromate and inocula concentration.

4.2.1 Cell morphology and ultrastructure of *Synechocystis* and *Synechococcus* grown with or without chromate

Cells were harvested and washed with sodium phosphate buffer (100 mM pH 7.4), fixed with 0.5 % glutaraldehyde – 2 % paraformaldehyde for 2 h at room temperature followed by washing with water. The cells were immobilized in 1.5 % low melting point molten agarose and dehydrated by incubation in graded series of ethanol (35, 50, 75 and 100 %) for 30 minutes each. Ethanol was removed by incubation with propylene oxide for 3 h followed by further incubation with 3:1, 1:1, 1:3 (v/v propylene oxide: araldite resin/embedding medium) for 2 h each. The araldite resin was prepared by mixing 10 ml of araldite (CY212), 10 ml of 2-Dodecen-1 γ l succinic Anhydride (DDSA), 1 ml of dibutylphthalate and 7-8 drops of (Dimethylamino-methyl) phenol (DMP 30). The samples were infiltrated with araldite resin (embedding medium) for 16 h under slow rocking conditions. Freshly prepared embedding medium was then poured into moulds with the agarose blocks immersed near the bottom of the moulds and were incubated at 60°C for 72 h for hardening and blocks containing embedded samples were obtained. Thin (70 nm) sections cut from the hardened blocks using diamond knife fitted in Leica

ultramicrotome were lifted on formvar coated copper grids and spread using chloroform. The sections were contrasted with 10 % uranyl acetate prepared in 50 % methanol for 15 min followed by lead citrate (Reynolds, 1963) for 2 minutes. The sections were viewed under Carl Zeiss Libra 120 KeV transmission electron microscope.

4.2.2 Effect of chromate on photosynthetic pigments in *Synechocystis* and *Synechococcus*

4.2.2.1 Absorption measurement: Absorption spectra of the cultures were recorded from 400–800 nm using Shimadzu UV-1800 spectrophotometer. Data on pigments and pigment protein contents like chlorophyll, carotenoid and phycobiliproteins on per cell basis were retrieved from absorption spectra by picking peaks specific to pigments at 680, 489 or 630 nm respectively.

4.2.2.2 Room temperature and 77K fluorescence emission measurement in *Synechocystis* and *Synechococcus* grown with or without chromate

Room temperature fluorescence emission spectra of the cultures were recorded using Hitachi F-4010 fluorescence spectrophotometer. Cultures were incubated in dark for about 10 min before recording the spectra. PSII fluorescence emission was obtained by exciting the sample at 440 nm and collecting emission between 600–800 nm. To study phycobilisome to PSII energy transfer, phycobilisomes were excited at 580 nm and emission was collected between 600–800 nm. 77 K fluorescence emission spectra of the cultures were recorded using Hitachi F-4500 fluorescence spectrophotometer with the set up modified for recording fluorescence from sample maintained at liquid nitrogen temperature. Far red sensitive photomultiplier tube was used as detector and all the emission spectra were corrected for the detector response in red and far red region.

4.2.3 Studies on phycobilisome redistribution by Confocal Laser Scanning Microscopy (CLSM) of *Synechocystis* and *Synechococcus* grown with or without chromate

LSM 510 Meta Confocal Laser Scanning Microscope (CLSM) from Carl Zeiss was used for analysis of phycobilisome redistribution in *Synechocystis* and *Synechococcus* grown with or without potassium dichromate. Cells were mixed with 2 % low melting point (LMP) molten agarose brought down to ambient temperature and immediately spread on a clean glass slide with the help of a cover slip. Under the CLSM, cells were visualized by exciting phycobilisomes with He-Ne laser at 633 nm and fluorescence was collected between 651-672 nm at 23 % laser power. By using the Z stack function, middle of the cell was reached and fluorescence coming from the phycobilisome was imaged.

4.2.4 Fluorescence Recovery After Photobleaching (FRAP) of *Synechocystis* and *Synechococcus* grown with or without chromate by CLSM

Cells were mixed with 2 % molten agarose brought down to ambient temperature and immediately spread on a clean glass slide with the help of a cover slip. Phycobilisomes were excited with 633 nm He-Ne LASER and fluorescence was monitored using 650 nm long pass filter. Phycocyanin was bleached in the central ~ 0.5 μm region of cell by increasing the laser power to 17.8 % with 500 iterations. The bleached area of the cell was seen as dark and non-fluorescent. The laser power was then decreased to 1.07 % and the whole cell was imaged repeatedly at 3 seconds interval over several seconds following bleaching. The mobility of phycobilisomes was monitored as recovery of fluorescence in the bleached area. PSII is known to be immobile; this was confirmed by exciting PSII using 458 nm Ar LASER and monitoring its fluorescence using 650 nm long pass filter.

4.2.5 Assay of photochemical activities of *Synechocystis* and *Synechococcus* grown with or without chromate

4.2.5.1 Preparation of cell free extract: *Synechocystis* and *Synechococcus* cells grown with or without chromate for 9 days were harvested from 50 ml culture by centrifugation at 8000 x g for 5 minutes at room temperature. The pellet was washed with buffer 1 (30mM sodium phosphate, pH 7.0) followed by wash with buffer 2 (600 mM sucrose, 30 mM sodium phosphate, pH 6.8). The pellet was finally suspended in 100 µl buffer 3 (15 mM TES/NaOH pH 7.0, 600 mM sucrose, 5 mM MgCl₂, 10 mM NaCl). Glass beads (100 µm size, acid washed) were added to the suspension and vortexed 3 to 5 times for 1 minute with intermittent incubation on ice to break the cells. Cell free extract was obtained by centrifugation of the suspension at 9300 x g for 5 minutes at 4°C.

4.2.5.2 PSII activity: PSII activity was assayed spectrophotometrically by following reduction of DCPIP at OD₆₀₀ according to Xiao et al. (1997) with some modifications. The reaction mixture consisted of cell free extract containing 8 – 10 µg chlorophyll in 20 µl suspended in 1480 µl Tricine-KOH buffer (50mM Tricine-KOH pH 7.6 containing 50 mM MgCl₂, 50 mM KCl) and 50 µM DCPIP which was added last. This mixture was incubated under saturating white light or dark with continuous stirring and OD₆₀₀ was followed for 5 minutes immediately after addition of DCPIP. Reaction mixture without DCPIP was taken as reference. PSII activity was calculated as units. One unit of photosystem activity is defined as the sample quantity which photoreduced 1 µmol of DCPIP per minute in the reaction conditions.

4.2.5.3 PSI activity: PSI activity was assayed polarographically by following oxygen consumption in light and dark using Clarke type electrode in Oxytherm system from Hansatech Instruments. The reaction mixture consisted of cell free

extract containing 8 – 10 µg chlorophyll suspended in Tricine-KOH buffer (50 mM Tricine-KOH pH 7.6 containing 50 mM MgCl₂, 50 mM KCl), 50 µM DCPIP, 2 mM sodium ascorbate, 2 mM sodium azide, 5 mM ammonium chloride, 5 µM DCMU and 50 µM methyl viologen in a 2 ml reaction volume. Buffer and buffer containing cell free extract were taken as blank.

4.2.6 Assay of biochemical activities of *Synechocystis* and *Synechococcus* grown with or without chromate

4.2.6.1 CO₂ fixation activity: CO₂ fixation activity was determined by using ¹⁴C labeled NaHCO₃ as tracer. The cell suspension consisting of 0.5 – 1 µg chlorophyll in 200 µl of BG-11 medium containing the respective concentration of potassium dichromate was taken in transparent scintillation vials. NaH¹⁴CO₃ (20 mM, specific activity 0.5 mCi mmole⁻¹) was added to the culture and the reaction mixture was incubated for 10 min in light (21 W m⁻²) at room temperature and the reaction was stopped by addition of 400 µl of 6 N acetic acid. The vials were dried. The acid stable labeled product was re-suspended in 100 µl of distilled water and 3 ml of alcohol was added followed by 5 ml of scintillation cocktail (0.4 % BBOT in toluene) and the ¹⁴C labeled product was measured in liquid scintillation counter. The rate of CO₂ fixation was expressed as nmoles ¹⁴CO₂ fixed µg⁻¹ chl h⁻¹.

4.2.6.2 R-5-P + ATP dependent CO₂ fixation activity: Permeabilized cells were used for this activity assay. Cell permeabilization was carried out according to Tabita (1978) wherein cells equivalent to 200 µg chlorophyll were suspended in HEPES buffer (100 mM HEPES pH 8.0) and treated with half the volume of toluene for 10 min on ice bath. Permeabilized cells obtained by centrifugation of the mixture at 6000 x g for 5 min at 4 °C. Cell pellet was washed with the HEPES buffer and finally suspended in 160 µl of assay buffer (100 mM HEPES pH 8.0, 40 mM MgCl₂,

10 mM DTT and 20 mM NaHCO₃) and incubated for 15 min in transparent scintillation vial. Reaction was started by adding 2 mM ATP and 2 mM R-5-P and incubating the mixture in light for 10 minutes; total reaction volume was adjusted to 220 µl. The reaction was stopped by adding 400 µl of 6 N acetic acid. Acid stable product was counted as described above in the section (4.2.6.1).

4.2.7 Assay of photosynthetic parameters of *Synechocystis* and *Synechococcus* grown with or without chromate by PAM fluorometry

The effect of growth with chromate on photosynthesis in the cyanobacteria was also studied by analysis of chlorophyll fluorescence using a dual wavelength pulse amplitude modulated fluorescence monitoring system (Dual-PAM-100, Heinz Walz GmbH, Germany). Responses of PSII and PSI activities were simultaneously measured. Quantification of PSII and PSI activities was carried out by chlorophyll fluorescence and P700⁺ absorbance changes respectively.

4.2.7.1 Measurement of PSII and PSI quantum efficiencies: Measurement of PSII and PSI efficiencies was carried out by placing around 2 ml of cell suspension (containing ~10 µg.ml⁻¹ chlorophyll) in a fluorescence quartz cuvette between emitter head and detector head of the system. The sample was dark adapted for 5 min and saturation pulse method was used for detection of maximal PSII fluorescence and maximal change in P700⁺ signal (Klughammer and Schreiber 1994, 2008b). Briefly, after dark adaptation minimum fluorescence (F₀) was measured with measuring light of intensity 24 µmol.m⁻².s⁻¹ followed by determination of maximum fluorescence (F_m) by applying a saturating pulse of irradiance 10,000 µmol.m⁻².s⁻¹ for 300 ms. The corresponding maximal change in P700⁺ signal (P_m) was determined by application of the saturation pulse after far red pre-illumination

for 10s. For P700 analysis, redox signal obtained by dual wavelength (830/875) unit was used.

4.2.7.2 Recording of slow induction curve under constant actinic light: Induction curve based on the saturation pulse method was recorded for 240 s using the slow kinetics sequence of the Dual PAM software. Saturating pulses were applied after each 20 s interval after the onset of actinic light of $53 \mu\text{mol m}^{-2}\text{s}^{-1}$ for determination of maximum fluorescence (F_m') and maximum P700⁺ (P_m') signal under the actinic light. The data derived after the 4th saturating pulse was used for determination of parameters of PSII and PSI efficiencies. A steady state of the photosynthetic apparatus was reached after the 3rd saturating pulse. The quantum yields of PSII and PSI along with cyclic electron flow (CEF) and electron transport rates (ETR) in PSI and PSII were calculated as described in instrument manual and by Wang et al. (2013). The parameters used in calculation are given in Table 4.4.

4.2.7.3 Recording of light curves of ETR(I) and ETR(II): Additional information on the photosynthetic performance of the cyanobacteria was obtained by light response curves. Light response curves of ETR(I) and ETR(II) from intensity (PAR) 0 to $363 \mu\text{mol photons m}^{-2}\text{s}^{-1}$ were recorded using the routine of the Dual PAM software after the recording of induction curve. Saturating pulse of $10,000 \mu\text{mol photons m}^{-2}\text{s}^{-1}$ for 300 ms was given after 1 min exposure to each PAR and ETR(I) and ETR(II) were determined.

4.2.8 Blue Native Polyacrylamide Gel Electrophoresis (BN PAGE) analysis of thylakoid membrane fractions of *Synechocystis* and *Synechococcus* grown with or without chromate

4.2.8.1 Preparation of thylakoid membrane fractions: Thylakoid membranes were prepared by following method described by Murata et al. (1981) with some modifications described in Dani and Sainis (2005). Cells from 1 L culture were harvested by centrifugation at 6000 x g for 10 minutes at room temperature. Cell pellet was washed and resuspended in 5 ml of membrane isolation buffer (10 mM Tris-HCl pH 7.8, 10 mM MgCl₂, 50 mM NaHCO₃, 1 mM EDTA, 12 mM β-mercaptoethanol and 10 % sucrose containing 3 mg PMSF). Cells were broken by sonication of the suspension by giving 6 cycles of 4 minutes run (each 4 minute run was of 6 seconds on, 2 seconds off). Cell free extract was obtained by centrifugation of the lysate at 6000 x g for 10 minutes at 4 °C to remove unbroken cells. The lysate was subjected to ultracentrifugation at 40,000 x g for 1 h at 4 °C. The pellet thus obtained was designated as 40k fraction. The supernatant was subjected to 90,000xg followed by 1,50,000 x g, each for 1 h at 4 °C and the pellets were designated as 90 k and 150 k fraction respectively. The pellets were suspended in 200 – 500 µl of solubilization buffer (50 mM NaCl, 50 mM imidazole/HCl, 2 mM 6-aminohexanoic acid, 1 mM EDTA, pH 7.0) and stored at -70 °C until further use.

4.2.8.2 BN PAGE: The BN PAGE analysis of native protein supercomplexes was carried out according to Wittig et al. (2006). Thylakoid membrane fractions equivalent to 25 µg chlorophyll (which contains around 250 µg protein) were solubilized with 250 µg of dodecyl- β-D-maltoside for 30 min at 4°C and gentle rocking followed by incubation at room temperature for 10 min with continuous shaking followed by centrifugation at 16,000 x g for 2 minutes at 4 °C. Supernatant was harvested and 5 % v/v glycerol and 5 % Serva Blue G-250 (Coomassie Blue G-250) were added to the solubilized membranes. The membrane supercomplexes were resolved on 4-13 % gradient polyacrylamide gel with 3.5 % stacking gel at 4 °C at 100 V till the samples entered the gel followed by further electrophoresis at 15

mA. Anode buffer was 25 mM imidazole pH 7.0; cathode buffer containing 50 mM Tricine, 7.5 mM Imidazole, 0.02 % w/v Coomassie blue G-250 pH 7.0 was used for one third of the run followed by cathode buffer containing 0.002 % Coomassie blue G-250 for further run. The blue gels were scanned immediately after run to visualize green colored chlorophyll containing supercomplexes followed by fixation in solution containing 50 % v/v methanol, 10 % v/v acetic acid and 100 mM ammonium acetate at room temperature for a few hours. The gels were stained with 0.025 % coomassie blue G-250 prepared in 10 % acetic acid for a few hours to visualize the bands containing membrane supercomplexes.

4.2.9 Studies on thylakoid membrane damage and repair in *Synechocystis* and *Synechococcus* grown with or without chromate

Cells were harvested from 9 day old cultures by centrifugation at 6000 x g for 10 minutes at room temperature and suspended in BG-11 medium containing respective potassium dichromate concentrations; OD₇₃₀ of all the cultures was adjusted to 0.5. The cultures were incubated under 1500 $\mu\text{mol}\cdot\text{m}^{-2}\cdot\text{s}^{-1}$ of light with intermittent shaking at room temperature in presence or absence of 200 $\mu\text{g}\cdot\text{ml}^{-1}$ chloramphenicol followed by incubation under normal illumination conditions (~ 30 $\mu\text{mol}\cdot\text{m}^{-2}\cdot\text{s}^{-1}$) for 2 h. Aliquots were removed after each 1 h interval and CO₂ fixation, absorbance spectra, fluorescence spectra at room temperature was monitored in all the samples as described in Section 4.2.2.2.

4.3 Results

Synechocystis and *Synechococcus* showed contrasting tolerance to potassium dichromate as described in chapter 2. The presence of potassium dichromate in

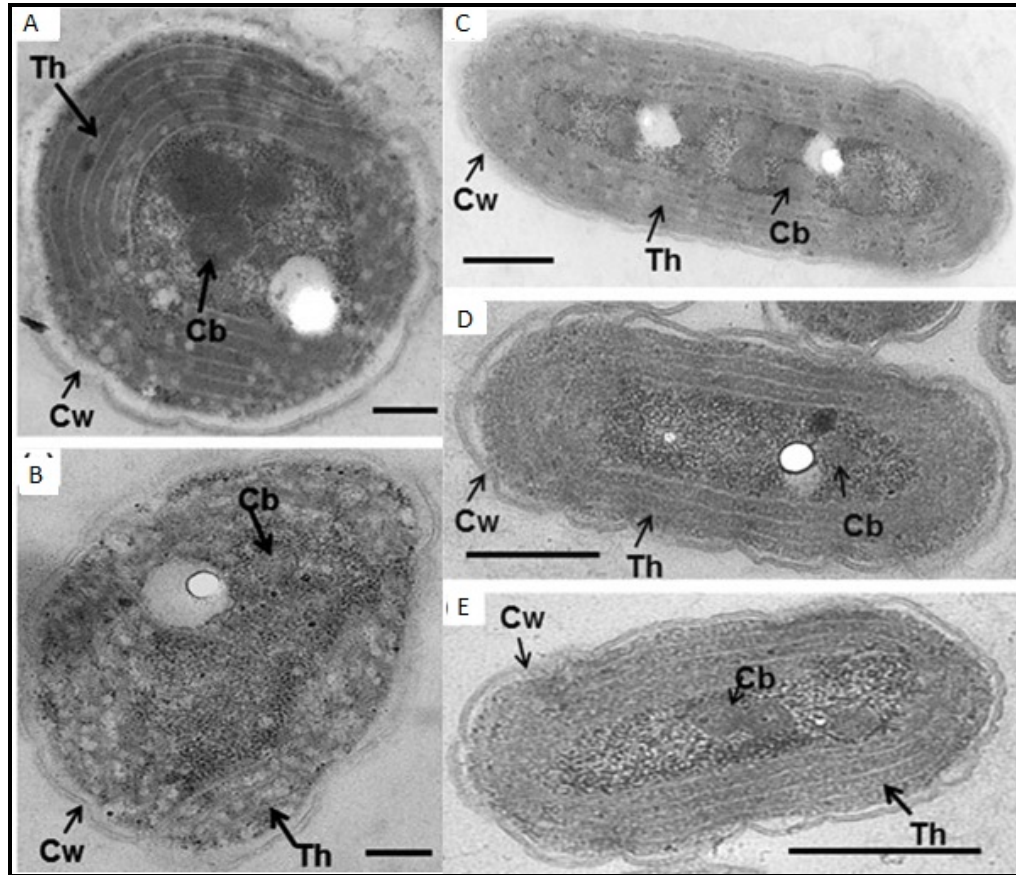
growth media exacerbated the oxidative stress. Both these cyanobacteria could grow in the presence of potassium dichromate albeit at different concentrations depending on their sensitivity, it was therefore interesting to study how the photosynthetic apparatus acclimatizes to prolonged exposure to potassium dichromate in growth medium. *Synechocystis* and *Synechococcus* were grown in the presence of their respective EC₅₀ concentrations *i.e* 12 µM and 150 µM of potassium dichromate for 9 days. Since *Synechococcus* showed stimulation of growth at 75 µM of potassium dichromate, the culture grown at this concentration was also included in study. Several factors related to photosynthesis such as ultrastructure of thylakoids, pigment contents, photosynthetic functions and biophysical parameters were studied and analysis of photosynthetic supercomplexes was carried out.

4.3.1 Effect of chromate on morphology and ultrastructure of *Synechocystis* and *Synechococcus* grown with or without chromate

Ultrastructural changes in *Synechocystis* and *Synechococcus* grown at their respective EC₅₀ concentrations of potassium dichromate were observed by transmission electron microscopy. In *Synechocystis*, growth in the presence of chromate resulted in distortions in thylakoid membranes and damage to cell wall in addition to slight elongation of regular spherical shape with increase in length to breadth (L/B) ratio (**figure 4.1 A, B, figure 4.2 A**). In *Synechococcus* the cells grown with chromate did not show extensive damage to ultrastructure (**figure 4.1 C-E**). The cell wall, thylakoids and carboxysomes were not affected by the presence of dichromate in medium. However, growth in the presence of chromate resulted in reduction in cell length and length to breadth (L/B) ratio (**figure 4.2 A**), whereas there was slight elongation of cells in case of *Synechocystis* while the cell width was not affected (**figure 4.2 A**). The results showed that growth with chromate affected the ultrastructure and morphology of *Synechocystis* and *Synechococcus*. **Figure 4.2**

B shows the fluorescence images of *Synechocystis* and *Synechococcus* cells grown with chromate. The morphological changes seen in electron micrographs were also perceived in the fluorescence images.

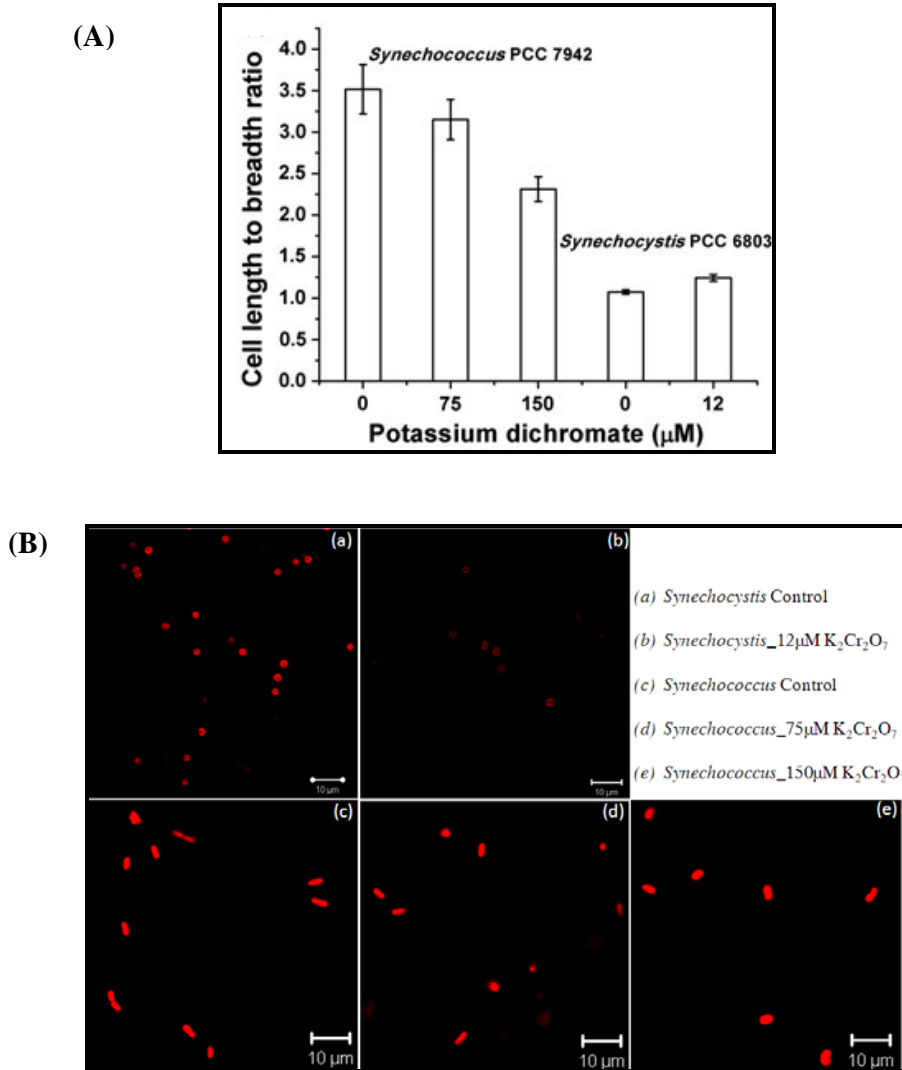
Figure 4.1: Ultrastructure of *Synechocystis* and *Synechococcus* cells grown with or without potassium dichromate



Log phase cultures of *Synechocystis* and *Synechococcus* containing 10^8 cells/ml were inoculated in BG-11 medium containing potassium dichromate as mentioned below. Cells were harvested after 9 days of growth and were processed for transmission electron microscopy as described in material and methods.

A: *Synechocystis* control **B:** *Synechocystis* grown with 12 μM of potassium dichromate. Bars represent 200 nm. **C:** *Synechococcus* control **D:** *Synechococcus* grown with 75 μM of potassium dichromate **E:** *Synechococcus* grown with 150 μM of potassium dichromate. Bars represent 500 nm. Th: Thylakoids, Cb: Carboxysomes, Cw: Cell wall

Figure 4.2: Changes in cell size and shape of *Synechocystis* and *Synechococcus* grown with or without potassium dichromate



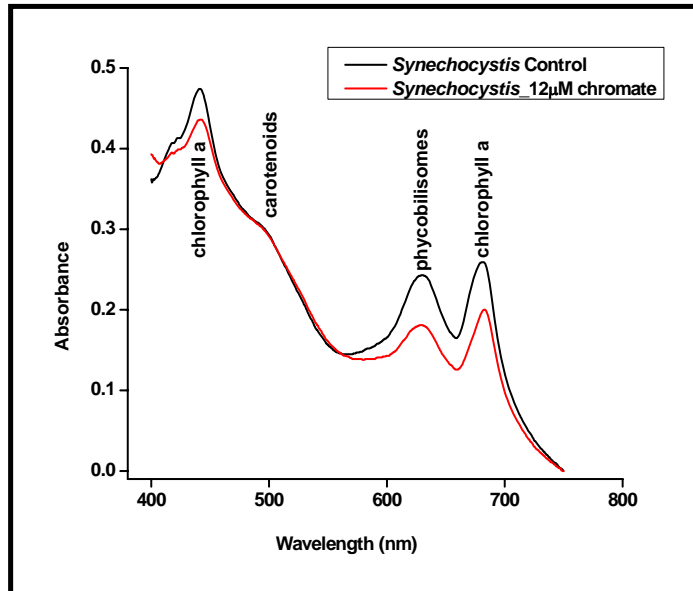
Log phase cultures of *Synechocystis* and *Synechococcus* containing 10^8 cells/ml were inoculated in BG-11 medium containing potassium dichromate concentrations 0 or 12 µM for *Synechocystis* and 0, 75 or 150 µM for *Synechococcus*. Cells were harvested after 9 days of growth and were processed for (A) transmission electron microscopy as described section 4.2.1 Length to breadth ratio of *Synechocystis* and *Synechococcus* grown with above mentioned chromate concentrations in the growth medium were measured. The values represent mean ratio obtained from micrographs of 15-20 cells and bars represent SE. (B) Fluorescent cells visualized under CLSM as described in section 4.2.3.

4.3.2 Effect of growth with chromate on absorption and fluorescence characteristics of *Synechocystis* and *Synechococcus*

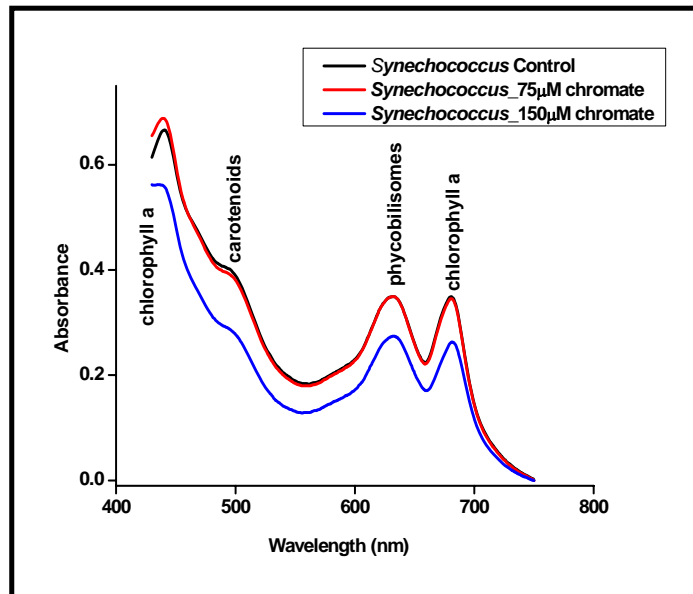
4.3.2.1 Absorption measurement: Absorption spectra of the cultures grown in presence or absence of potassium dichromate are shown in **figure 4.3**. The absorption spectra of whole cells showed peak at 440 nm due to soret band of chlorophyll *a*. Cyanobacteria do not have chlorophyll *b*, instead they have phycobilisomes containing phycocyanin and allophycocyanin which showed absorption at 630 nm. An absorption peak belonging to chlorophyll *a* was also observed at 680 nm. All the spectra were normalized to OD₇₃₀. Chromate grown cells showed no change the pattern or shape of absorption spectra in both *Synechocystis* and *Synechococcus*. Growth with 12 μ M chromate reduced chlorophyll and phycocyanin on equal OD₇₃₀ basis in *Synechocystis* (**figure 4.3A**). In case of *Synechococcus* growth with 75 μ M chromate did not show any effect of phycocyanin and chlorophyll content. These cells when grown with 150 μ M chromate showed reduction in chlorophyll and phycocyanin (**figure 4.3 B**). The results confirmed the findings that growth with chromate quantitatively reduced the pigment complexes per cell without affecting their quality.

Figure 4.3: Absorption spectra of *Synechocystis* and *Synechococcus* cells grown with or without potassium dichromate

(A)



(B)



10^8 cells of *Synechocystis* and *Synechococcus* from log phase cultures were inoculated in 50 ml BG-11 medium containing different concentrations of potassium dichromate. Absorption spectra of the cultures were recorded after 9 days of growth.

Peak₄₄₀: Chlorophyll *a*; Peak₄₉₆: carotenoid; Peak₆₃₀: Phycocyanin; Peak₆₈₀: Chlorophyll *a*

4.3.2.2 Content of photosynthetic pigments: Chlorophyll, phycocyanin and carotenoids were measured in *Synechocystis* and *Synechococcus* grown with chromate on per cell basis from the absorption spectra shown in **figure 4.3**. **Table 4.1** shows that in *Synechocystis* there was up to 23 % decrease in chlorophyll content per cell when grown with 12 μM potassium dichromate. In *Synechococcus*, chlorophyll concentration on per cell basis was not affected in 75 μM potassium dichromate, but it decreased by 25 % when grown in presence of 150 μM potassium dichromate. Presence of EC_{50} concentration of chromate in growth medium reduced the carotenoid and phycocyanin content on per cell basis in *Synechococcus*. Thus growth with chromate differentially affected the content of photosynthetic pigments in *Synechocystis* and *Synechococcus*.

Table 4.1: Effect of chromate on pigment composition

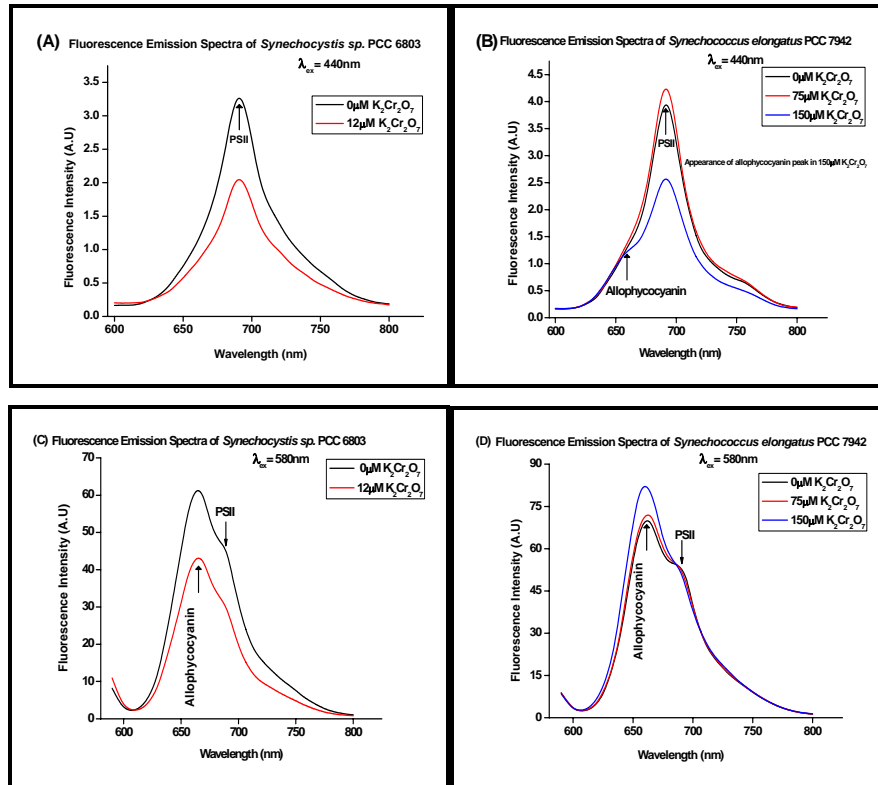
K ₂ Cr ₂ O ₇ concentration (μM)_Sample	Chlorophyll a (OD ₆₈₀ /10 ⁷ cells)	Carotenoids (OD ₄₉₆ /10 ⁷ cells)	Phycocyanin (OD ₆₃₀)/10 ⁷ cells	Phycocyanin to chlorophyll ratio
0 μM <i>Synechocystis</i>	0.260	0.309	0.243	0.938
12 μM <i>Synechocystis</i>	0.200	0.308	0.181	0.905
0 μM <i>Synechococcus</i>	0.349	0.414	0.349	1.000
75 μM <i>Synechococcus</i>	0.345	0.406	0.349	1.012
150 μM <i>Synechococcus</i>	0.263	0.303	0.273	1.038

10⁸ cells of *Synechocystis* and *Synechococcus* from log phase cultures were inoculated in 50ml BG-11 medium containing different concentrations of potassium dichromate. Pigment concentrations were measured per 10⁷ cells after 9 days of growth.

4.3.2.3 Fluorescence emission spectra: Steady state fluorescence emission spectra of dark incubated cultures were recorded at room temperature and at 77 K by excitation at 440 nm which excites chlorophylls in photosystems and at 580 nm which excites phycocyanin and allophycocyanin of phycobilisome complex. The room temperature fluorescence after excitation with 440 nm is supposed to arise from PSII. There was a decrease in fluorescence from PSII (F690) both in *Synechocystis* and *Synechococcus* cultures which were grown in presence of 12 or 150 μ M potassium dichromate (**figure. 4.4 A and B**). The intensity of fluorescence was slightly higher as compared to control for *Synechococcus* grown in presence of 75 μ M potassium dichromate. Emergence of characteristic peak of allophycocyanin at 665 nm (**figure. 4.4 B**) in *Synechococcus* grown in presence of 150 μ M potassium dichromate suggested back transfer of electrons from PSII to phycobilisomes.

On excitation of phycobilisomes at 580 nm (**figure 4.4 C**), a decrease similar to that in F690 was observed at F653 in *Synechocystis* grown with 12 μ M potassium dichromate as compared to control. In case of *Synechococcus*, F654 was found to increase as compared to control; F654 peak intensity was same as control for *Synechococcus* grown with 75 μ M potassium dichromate. An increase in the allophycocyanin to PSII fluorescence ratio (F664/F688) in *Synechococcus* grown with 150 μ M chromate indicated a dissociation of phycobilisomes from PSII when fluorescence at room temperature was monitored by excitation with 580 nm (**figure 4.4D**).

Figure 4.4: Room temperature fluorescence emission spectra of *Synechocystis* and *Synechococcus* grown with or without potassium dichromate

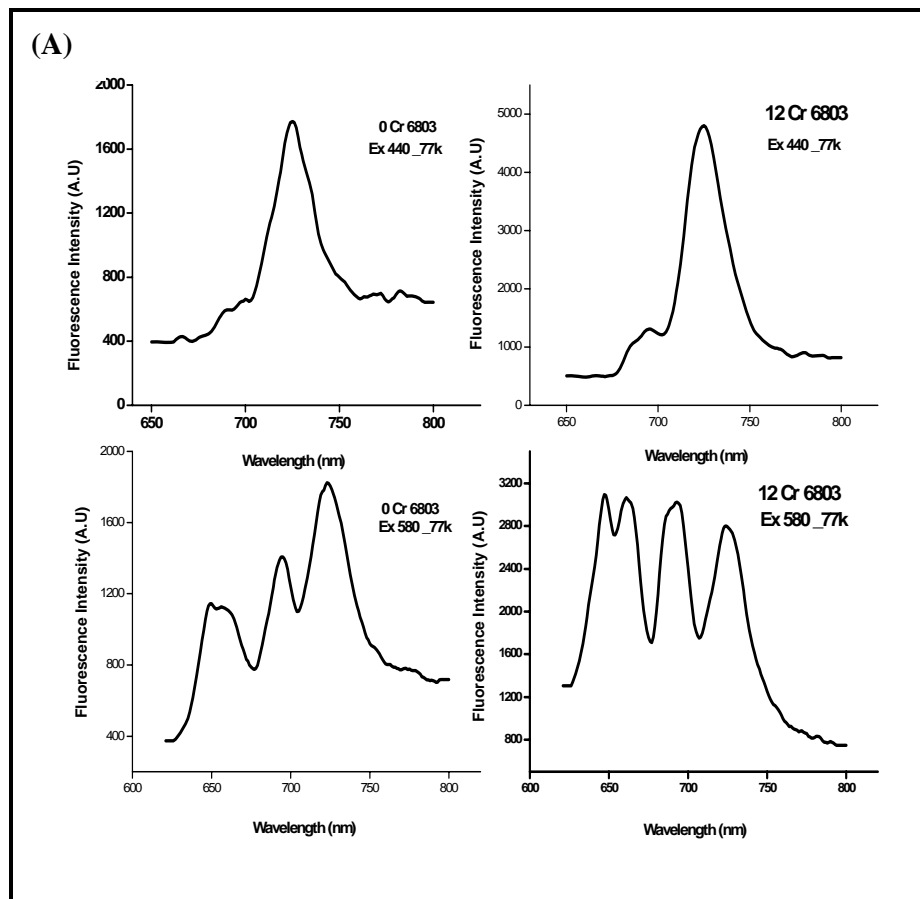


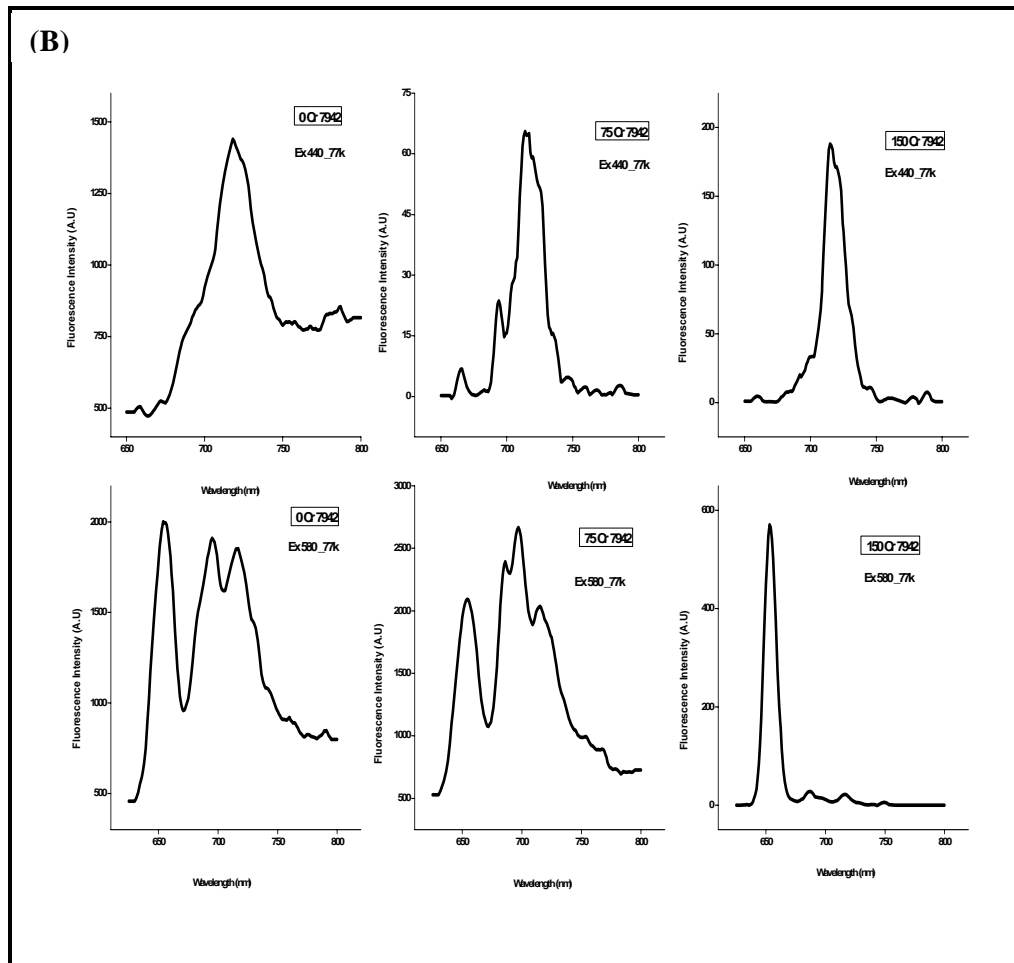
Room temperature fluorescence emission spectra of *Synechocystis* and *Synechococcus* grown with 0 or 12 μM and 0, 75 or 150 μM potassium dichromate respectively in the media for 9 days. (A, B) excitation at 440 nm and (C, D) excitation at 580 nm.

Further, 77 K fluorescence emission was monitored in the two cyanobacteria grown with or without chromate is shown in **figure 4.5**. On excitation at 440 nm, characteristic PSII and PSI emission peaks were shown by the two cyanobacteria at 690 (F690) and 725 nm (F725) respectively in *Synechocystis*. For *Synechococcus*, the PSI fluorescence emission maximum was observed at 714 nm (F714). On 580 nm excitation, three peaks showing characteristic emission from allophycocyanin or terminal emitter of phycobilisome (F653), PSII (F690) and PSI (F725) were observed. In *Synechococcus* for 440 nm excitation, the PSI peak was observed at 714 nm (F714) on 580 nm excitation also. Unlike absorption spectra where spectral characteristics were unaltered after growth with chromate, fluorescence emission spectra showed drastic changes in the relative peak intensities, although peak positions were not altered indicating disturbances in the integrity of the photosynthetic apparatus. On exciting phycobilisomes at 580 nm, emission characteristic of PSII and PSI were observed indicating coupling of phycobilisome to the photosystems. This coupling was disturbed in both the cyanobacteria on growth with chromate and was seen as increase in phycobilisome specific emission and relative decrease in PSII or PSI specific emissions. The relative contents of PSII, PSI and energy transfer are indicated by the analysis of fluorescence intensity ratios which are shown in **table 4.2**. Decrease in the PSII/PSI fluorescence ratio in the cells grown with chromate was observed suggesting a relative increase in PSI content or decrease in PSII content. On excitation of phycobilisome at 580 nm, changes in the intensity of characteristic peaks of allophycocyanin, PSII and PSI were observed in the two cyanobacteria. In both the cyanobacteria, changes in the association of phycobilisome (PBS) to PSII and PSI were observed in chromate grown cells as compared to control cells. In *Synechocystis*, an increase in PSII/PSI fluorescence indicated more PBS-PSII association in chromate grown cells. In *Synechococcus*, cells grown with 75 μ M

potassium dichromate showed enhanced energy transfer from PBS to PSII as compared to PSI whereas in cells grown with 150 μ M potassium dichromate, a drastic reduction in PSII/PSI ratio occurred which suggested higher energy transfer from phycocyanin to PSI as compared to PSII. Thus growth with chromate altered the PSII/PSI ratios as well as energy transfer from phycobilisomes.

Figure 4.5: 77 K fluorescence emission spectra of *Synechocystis* and *Synechococcus* grown with or without potassium dichromate





77 K fluorescence emission spectra of log phase *Synechocystis* (A) cultures grown in BG-11 media for 9 days with 0 and 12 μM potassium dichromate and *Synechococcus* (B) grown in BG-11 media for 9 days with 0, 75 and 150 μM potassium dichromate on excitation at 440 nm and 580 nm. The upper panels are emission spectra obtained after 440 nm excitation and lower panels are emission spectra obtained on 580 nm excitation.

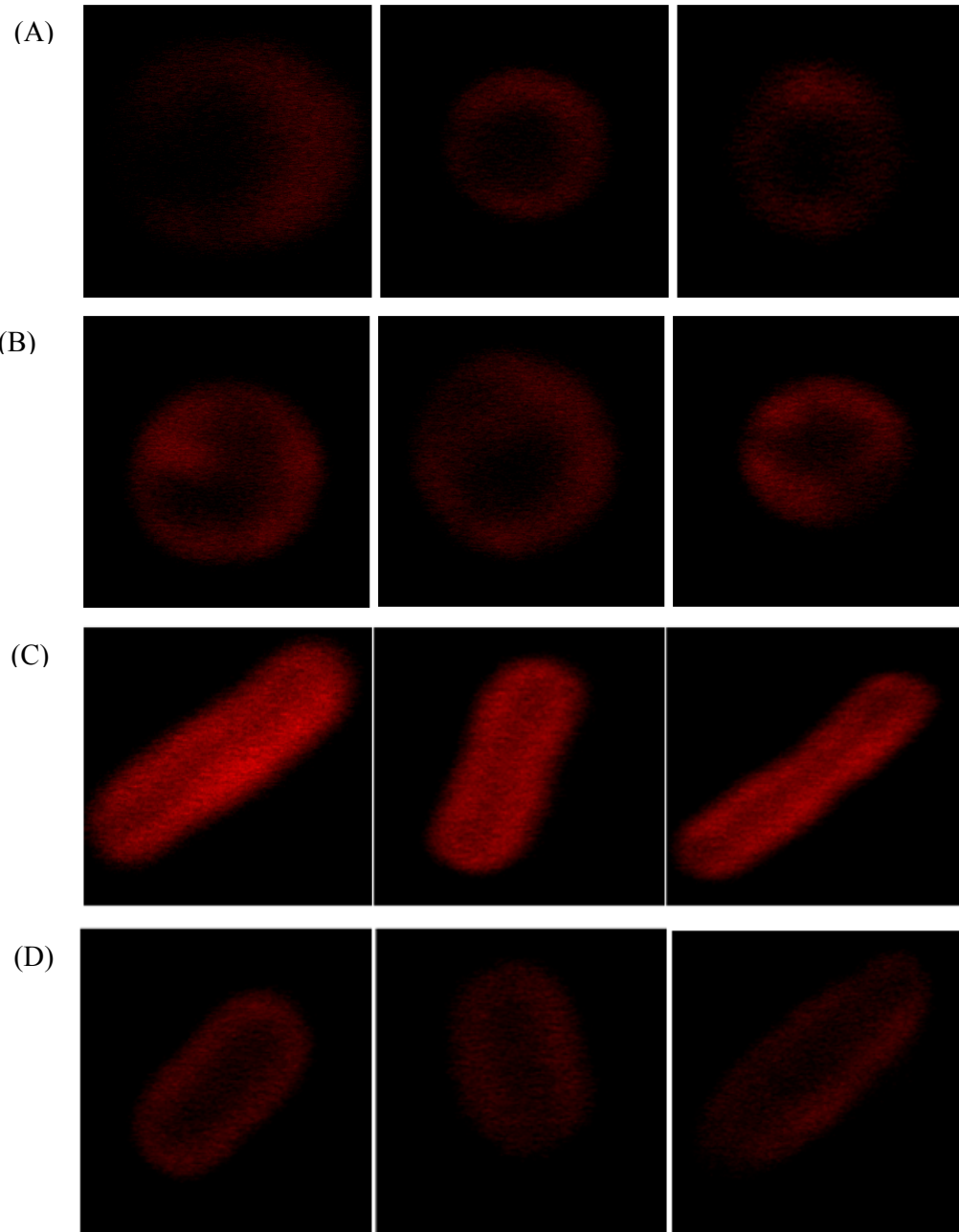
Table 4.2: Relative contents of PSII / PSI and energy transfer characteristics in *Synechocystis* and *Synechococcus* grown with or without chromate

Sample	440 Ex (Ratio of PSII/PSI)	580 Ex (Ratio of PSII/PSI)
0 μ M <i>Synechocystis</i>	0.33	0.79
12 μ M <i>Synechocystis</i>	0.27	1.12
0 μ M <i>Synechococcus</i>	0.53	0.83
75 μ M <i>Synechococcus</i>	0.43	1.28
150 μ M <i>Synechococcus</i>	0.29	0.38

Fluorescence emission spectra of *Synechocystis* and *Synechococcus* grown with 0 or 12 μ M and 0, 75 or 150 μ M potassium chromate were recorded at 77 K by exciting the samples at 440 or 580 nm. Ratios of the fluorescence emission peaks (F690/F714 or F725) obtained on 440 nm excitation were used to estimate relative contents of PSII-PSI and those obtained on 580 nm excitation to estimate the energy transfer from PSII to PSI (F690/ F714 or F725).

4.3.2.4 Phycobilisome (PBS) fluorescence redistribution by CLSM: Fluorescence emission spectra indicated uncoupling of PBS from PSII and rearrangements in the energy transfer to the photosystems. PBS fluorescence redistribution is another way of probing the PBS association status with thylakoid membranes. **Figure 4.6A** shows that in *Synechocystis* PBS fluorescence is maintained in the periphery of the cells as is expected due the arrangement of thylakoids in concentric rings in the periphery of the cell and PBS being physically associated to the thylakoid membranes. When *Synechocystis* cells were grown with 12 μM potassium dichromate, the fluorescence was no longer confined to the periphery of the cell but extended towards the central region of the cell where thylakoid are not present indicating partial uncoupling of phycobilisomes with pigment protein complexes of photosystems. In case of *Synechococcus*, due to high overall fluorescence of control cells, PBS location in the periphery was not clear. In the cells grown with 150 μM potassium dichromate, there was reduction in overall PBS fluorescence, but no visible physical uncoupling was observed (**figure 4.4 C and D**).

Figure 4.6 Association of phycobilisomes with thylakoid membranes using CLSM in *Synechocystis* and *Synechococcus* grown with or without chromate

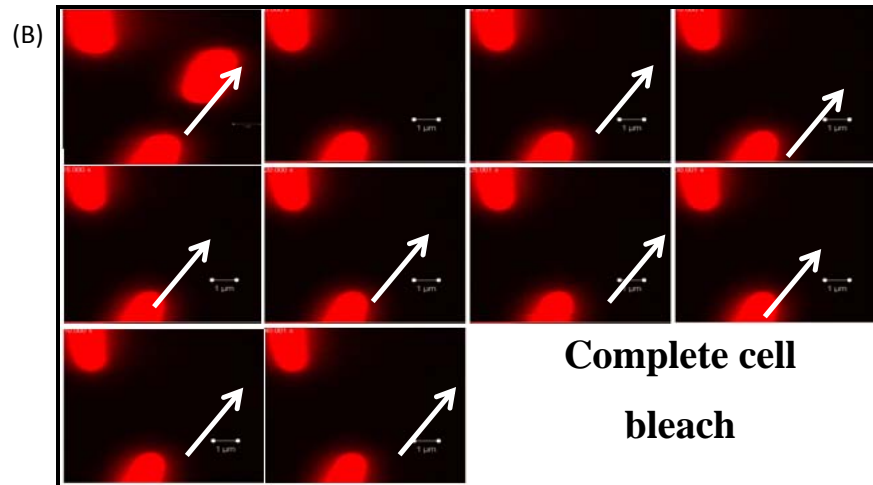
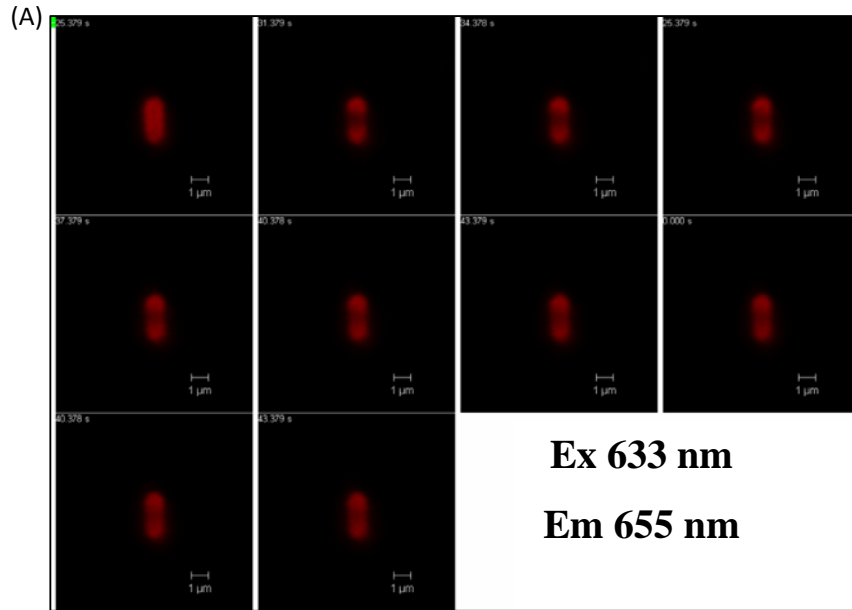


Synechocystis (A, B) and *Synechococcus* (C, D) cells were grown with 0 or 12 μM (A, B) and 0 or 150 μM (C, D) potassium dichromate respectively for 9 days and immobilized in 1.5 % low melting agarose and overlaid on a glass slide. Cells were visualized under CLSM by exciting phycobilisomes at 633 nm and collecting fluorescence in 651-672 nm range.

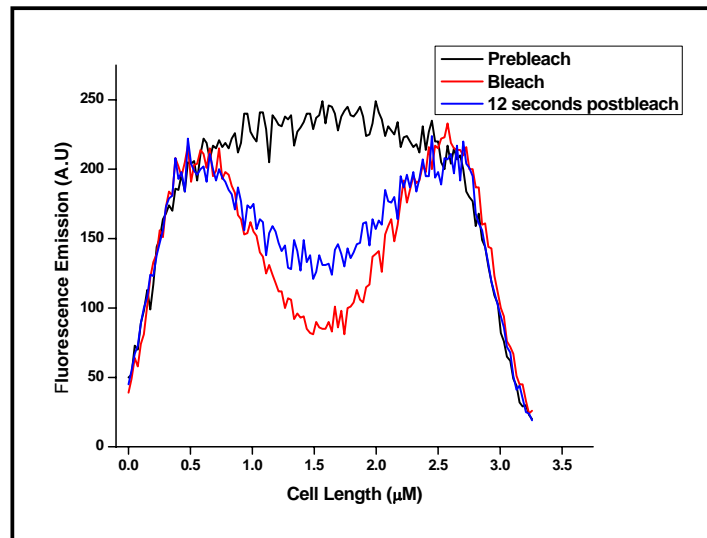
4.3.2.5 Phycobilisome mobility by FRAP: Phycobilisomes in cyanobacteria are mobile and are known to be involved in adaptation responsible for state transitions. Their movement over thylakoid membrane can be studied by FRAP. It involves laser-bleaching of phycobilisome in the central region of cell by increasing the laser power. This bleached is seen as dark and non-fluorescent. Then the laser power is decreased and the whole cell is imaged repeatedly over several seconds (**figure 4.7A**). The mobility of phycobilisomes is monitored as recovery of fluorescence in the bleached area (**figure 4.7B**). In addition, PBS fluorescence of the complete cell is also bleached to confirm that recovery of fluorescence in the bleached area is not due to emergence of fluorescence from the fluorophores of the same location but is due to movement from the adjacent areas. The results (**figure 4.7C**) showed that there was no recovery of fluorescence after complete bleaching of cell suggesting that there was no internalization of phycobilisomes after bleaching. The PSII complexes are supposed to be immobile. When part of the area was bleached with 458 nm laser, there was no recovery of fluorescence (**figure 4.7D**) indicating that PSII complexes were indeed non mobile.

FRAP can be performed more conveniently on *Synechococcus* as compared to *Synechocystis* due to thylakoid membrane geometry. FRAP was also attempted in *Synechocystis*. Both control cells and cells grown with chromate were used for experiments. **Table 4.3** shows results of the FRAP experiment on *Synechocystis* and *Synechococcus* in response to growth with chromate. Phycobilisome mobility was not affected significantly in *Synechocystis* cells on growth with chromate. However in *Synechococcus*, growth with 150 μ M potassium dichromate caused a reduction in phycobilisome mobility. This is in agreement with drastic reduction in PSII/PSI fluorescence on 580 nm excitation at 77 K.

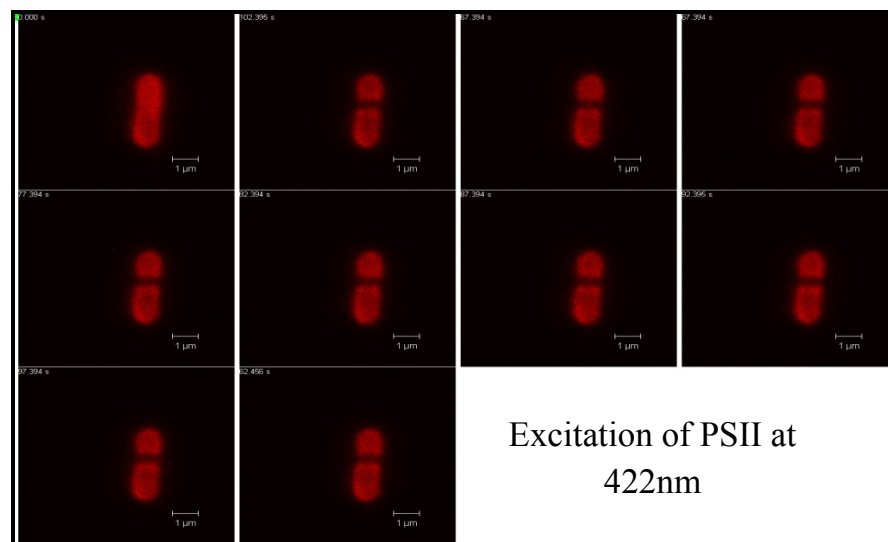
Figure 4.7: Phycobilisome mobility by FRAP in *Synechococcus*



(C)



(D)



Synechococcus cells were immobilized in 1.5 % low melting agarose and overlaid on a glass slide and visualized under CLSM by exciting phycobilisomes at 633 nm and collecting fluorescence at 665 nm. Fluorescence was bleached in the central region of the cell by increasing laser power and number of iterations. The mobility of phycobilisomes was monitored by scanning the whole cell repeatedly up to 30 seconds. Fluorescence intensity in the bleached area was used to estimate the phycobilisome mobility

A: Typical experiment of PBS bleaching and recovery, B: Bleaching of whole cells, arrow indicates completely bleached cell which does not recover its fluorescence in 30 seconds, C; Scans of pre bleach, post bleach and after recovery used for calculation of data given in table 4.3, D: PSII mobility was monitored by exciting PSII at 458 nm and collecting fluorescence using long pass 650 nm filter.

Table 4.3 Fluorescence Recovery After Photobleaching in cells of *Synechocystis* and *Synechococcus* grown with or without chromate

Sample	Mean recovery of fluorescence 12 seconds post bleach expressed as % of prebleach
0 μ M <i>Synechocystis</i>	72.1 \pm 6.6
12 μ M <i>Synechocystis</i>	80.1 \pm 6.9
0 μ M <i>Synechococcus</i>	59.6 \pm 3.8
75 μ M <i>Synechococcus</i>	58.6 \pm 4.9
150 μ M <i>Synechococcus</i>	30.6 \pm 9.7

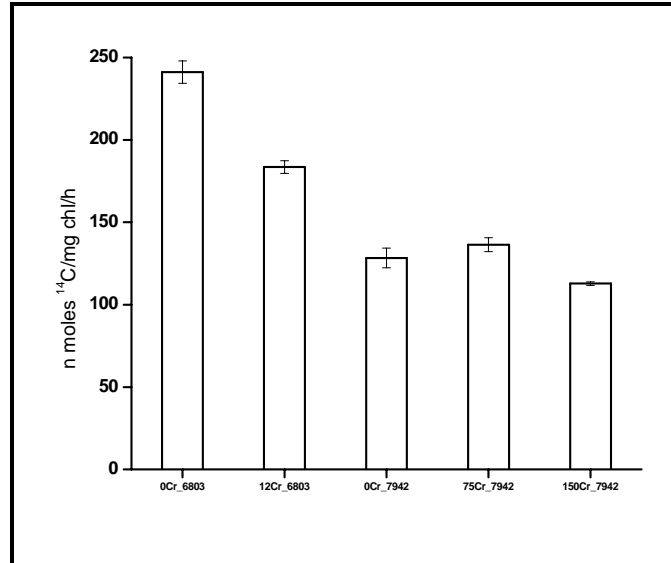
Synechocystis and *Synechococcus* control and after growth with chromate were subjected to FRAP to study phycobilisome mobility. Post bleach scans were taken up to 30 seconds. Phycobilisome mobility was determined by recovery of its specific fluorescence in the bleached area as percentage of prebleach (native) fluorescence in the same area.

4.3.3 Effect of growth with chromate on biochemical and photochemical activities in *Synechocystis* and *Synechococcus*

PSI and PSII activities were assayed in *Synechocystis* and *Synechococcus* grown with or without chromate along with total carbon fixation and certain Calvin cycle enzyme activities.

4.3.3.1 Photosynthetic CO₂ fixation activity: Light dependent CO₂ fixation was carried out in both the cyanobacteria grown with or without chromate (**figure 4.8**). In general, *Synechocystis* showed higher rates of CO₂ fixation as compared to *Synechococcus* on equal chlorophyll basis suggesting subtle differences in their photosynthetic machinery. Both the cyanobacteria grown at their EC₅₀ concentration showed a marginal decline in rate of CO₂ fixation. *Synechococcus* grown in presence of 75 µM potassium dichromate showed a higher CO₂ fixation rate on chlorophyll basis as compared to control. Thus CO₂ assimilation rates mimicked the response of growth pattern to chromate in these two cyanobacteria.

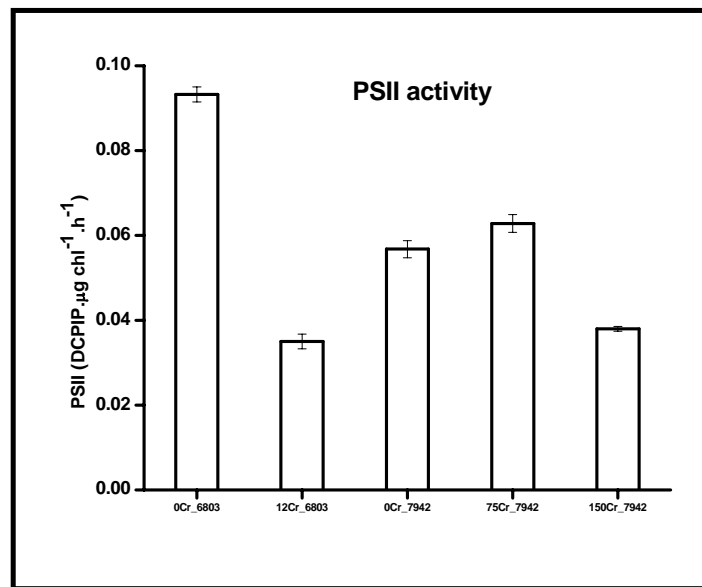
Figure 4.8: $^{14}\text{CO}_2$ fixation in *Synechocystis* and *Synechococcus* grown with or without chromate



Total photosynthetic activity determined as $^{14}\text{CO}_2$ fixation rate on per mg chlorophyll basis in *Synechocystis* grown with 0 or 12 μM and *Synechococcus* grown with 0, 75 or 150 μM potassium dichromate for 9 days. Y axis represents rate of CO_2 fixation (nanomoles of ^{14}C fixed $\cdot\text{mg chl}^{-1}\cdot\text{h}^{-1}$) and X axis represents the sample; *Synechocystis* is denoted as 6803 and *Synechococcus* as 7942.

4.3.3.2 PSII activity: PSII activity was measured as DCPIP photoreduction. *Synechocystis* grown with 12 μM chromate showed a $\sim 70\%$ decline in PSII activity as compared to control whereas *Synechococcus* showed a decline up to 30% in cells grown with 150 μM chromate (**figure 4.9**). However, as observed in CO_2 fixation (**figure 4.8**), 75 μM potassium dichromate grown cells showed a higher PSII activity as compared to control in *Synechococcus*.

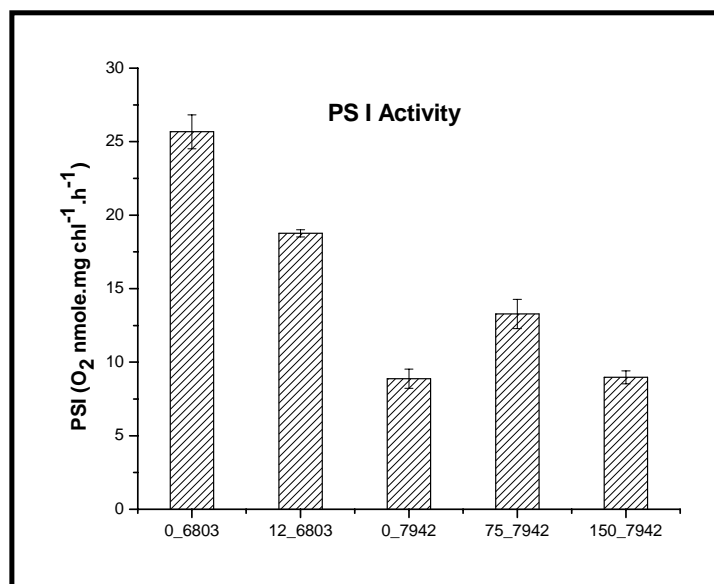
Figure 4.9: PSII activity in *Synechocystis* and *Synechococcus* grown with or without chromate



PSII activity determined as DCPIP reduction rate on per mg chlorophyll basis in the cell free extracts of *Synechocystis* grown with 0 or 12 μM and *Synechococcus* grown with 0, 75 or 150 μM and potassium dichromate for 9 days. Y axis represents PSII activity determined as rate of DCPIP reduction and X axis represents the sample; *Synechocystis* is denoted as 6803 and *Synechococcus* as 7942.

4.3.3.3 PSI activity: PSI activity was monitored as oxygen consumption in light in presence of methyl viologen. **Figure 4.10** shows that PSI activity was reduced by 20 % in *Synechocystis* grown in presence of 12 μM potassium dichromate and was maintained as good as control in *Synechococcus* grown in presence of 150 μM potassium dichromate; 75 μM potassium dichromate grown cells showed a higher PSI activity as compared to control. The overall rates of PSII and PSI activities were higher in *Synechocystis* as compared to *Synechococcus* on chlorophyll basis (**figures 4.9 and 4.10**).

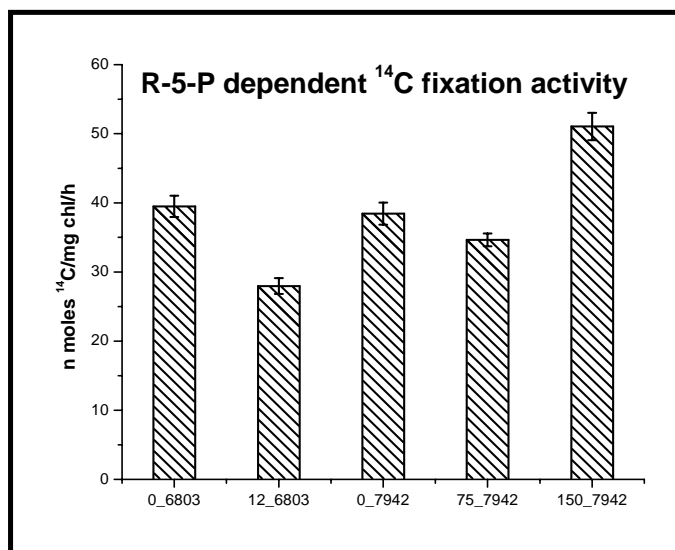
Figure 4.10: PSI activity in *Synechocystis* and *Synechococcus* grown with or without chromate



PSI activity was determined as oxygen consumption rate on per mg chlorophyll basis in the cell free extracts of *Synechocystis* grown with 0 or 12 μM and *Synechococcus* grown with 0, 75 or 150 μM and potassium dichromate for 9 days. Y axis represents rate of O_2 consumed (nanomoles of O_2 fixed $\text{mg chl}^{-1}.\text{h}^{-1}$) and X axis represents the sample; *Synechocystis* is denoted as 6803 and *Synechococcus* as 7942.

4.3.3.4 Partial reactions of Calvin-Benson cycle enzymes in *Synechocystis* and *Synechococcus* grown with or without chromate: Partial reactions of Calvin-Benson cycle enzymes viz phosphoriboisomerase, phosphoribulokinase and Rubisco were measured using linked assay as R-5-P + ATP dependent CO₂ fixation activity. **Figure 4.11** shows that R-5-P dependent ¹⁴C fixation activity decreased in *Synechocystis* grown with 12 μM chromate on equal chlorophyll basis. In contrast, in *Synechococcus*, it remained unaffected in cells grown with 75 μM chromate and increased by ~60% in cells grown with 150 μM chromate suggesting differential response of Calvin cycle enzymes to chromate.

Figure 4.11: Linked activity of three Calvin cycle enzymes in *Synechocystis* and *Synechococcus* grown with or without chromate



Linked activity of three Calvin cycle enzymes viz. phosphoriboisomerase, phosphoribulokinase and RubisCo was determined as CO₂ fixed on per mg chlorophyll basis in permeabilized cells of *Synechocystis* grown with 0 or 12 μM and *Synechococcus* grown with 0, 75 or 150 μM potassium dichromate for 9 days. Y axis represents rate of CO₂ fixation (nanomoles of ¹⁴C fixed mg chl⁻¹h⁻¹) and X axis represents the sample; *Synechocystis* is denoted as 6803 and *Synechococcus* as 7942.

4.3.4 Assay of photosynthetic parameters in the cyanobacteria by PAM fluorometry

Pulse amplitude modulated fluorescence monitoring system (Dual-PAM-100, Heinz Walz GmbH, Germany) was used for further analysis of responses of photosynthetic apparatus of the cyanobacteria to growth with chromate. Using the Dual PAM system software, responses of PSII and PSI activities were simultaneously measured. The parameters used in the study are defined in **table 4.4**.

Table 4.4: Data analysis parameters used for PAM fluorometry in this study.

Parameter	Definition of parameter	Calculation of parameter
F _o	Fluorescence yield of dark adapted sample	
F _o '	Fluorescence yield of illuminated sample	
F	Average fluorescence after application of saturated pulses	
F _m	Fluorescence yield of dark adapted sample after application of saturation pulse	
F _m '	Fluorescence yield of Illuminated sample after application of saturation pulse	
F _v /F _m	Maximal Quantum yield of PSII	$F_v/F_m = (F_m - F_o)/F_m$
Y _{II}	Effective quantum yield of PSII	$Y(II) = F_m' - F/F_m$
Y(NO)	Quantum yield of non regulated energy dissipation	$Y(NO) = F/F_m$
Y(NPQ)	Quantum yield of regulated energy dissipation	$Y(NPQ) = F/F_m' - F/F_m$
ETR II	Electron transport rate PSII	$ETR(II) = Y(II) \times PAR \times 0.84 \times 0.5$
P	P700 signal recorded just before saturation pulse	
P _m	Maximal P700 change	
P _m '	Maximal P700 change in P _m ' in analogy with F _m '	
Y _I	Photochemical quantum yield of PSI	$Y(I) = 1 - Y(ND) - Y(NA)$
Y(ND)	Non photochemical quantum yield of PSI (Donor side limitation)	$Y(ND) = 1 - P700 \text{ red.}$
Y(NA)	Non photochemical quantum yield of PSI (Acceptor side limitation)	$Y(NA) = (P_m - P_m')/P_m$
ETR I	Electron transport rate PSI	$ETR(I) = Y(I) \times PAR \times 0.84 \times 0.5$
Y CEF	Quantum yield of cyclic electron flow	$Y(CEF) = Y(I) - Y(II)$
Y(CEF)/Y(I)	Contribution of CEF to Y(I)	
Y(CEF)/Y(II)	Relation between quantum yield of CEF and LEF	
Y(II)/Y(I)	Contribution of LEF to Y(I)	

4.3.4.1 Effect of growth with chromate on maximal quantum yield of PSII

(F_v/F_m) and maximal P700 change (P_m): The maximal quantum yields of *Synechocystis* and *Synechococcus* grown with or without chromate were determined by measuring fluorescence (F_0) of the dark adapted sample followed by application of a saturation pulse to determine F_m . Maximal P700 change (P_m) was determined by redox signal obtained on application of the saturation pulse after far red pre-illumination. F_v/F_m and P_m values thus determined are shown in **table 4.5**. The F_v/F_m and P_m values were compared by independent t-test and significance of difference was determined at 0.05 level of confidence. The maximal quantum yield of PSII (F_v/F_m) was significantly higher in *Synechocystis* as compared to *Synechococcus*. In both *Synechocystis* and *Synechococcus*, growth with respective EC_{50} concentrations of potassium dichromate caused significant decrease in the (F_v/F_m) as compared to their respective controls. However, growth with 75 μ M dichromate did not cause significant decrease in the maximal quantum yield of PSII. The amplitude of P_m depends on the P700 content and the mean path length of measuring light. Therefore, in case of sample with same optical properties, P_m value will depend of the P700 content. P_m was also significantly higher in *Synechocystis* as compared to *Synechococcus*. On growth with chromate, P_m of both cyanobacteria showed variable behavior. In *Synechocystis*, P_m showed 50 % reduction in response to growth with chromate while in *Synechococcus*, 75 μ M dichromate caused significant increase in P_m whereas 150 μ M dichromate caused marginal decrease in the P_m .

Table 4.5: Effect of growth with chromate on maximal quantum yield of PSII (Fv/Fm) and maximal P700 change (Pm) in the cyanobacteria

Sample	Fv/Fm	Pm
<i>Synechocystis</i> Control	0.245 ± 0.005	0.453 ± 0.015
<i>Synechocystis</i> _12 μM K ₂ Cr ₂ O ₇	0.172 ± 0.014	0.223 ± 0.001
<i>Synechococcus</i> Control	0.186 ± 0.011	0.360 ± 0.006
<i>Synechococcus</i> _75 μM K ₂ Cr ₂ O ₇	0.160 ± 0.013	0.493 ± 0.005
<i>Synechococcus</i> _150 μM K ₂ Cr ₂ O ₇	0.144 ± 0.002	0.368 ± 0.021

Fv/Fm and Pm were determined in the cultures dark adapted for 5 mins by applying the saturation pulse method using the Dual PAM software.

4.3.4.2 Complementary quantum yields of energy conversion in PSI and PSII:

Complementary quantum yields of energy conversion in PSI and PSII determined at steady state from the slow induction curve are shown in **table 4.6**. The effective quantum yield of PSII [Y(II)] in *Synechocystis* was three times higher as compared to that of *Synechococcus* with reverse in Y(NO), the quantum yield of non-regulated energy dissipation in PSII. The value of Y(NPQ), the quantum yield of regulated energy dissipation in PSII was zero in all the samples. Y(II) decreased by 24 % on growth with chromate in *Synechocystis* along with minor increase in the Y(NO). In contrast, in *Synechococcus*, more than two fold increase was observed in Y(II) on growth with potassium dichromate, both at 75 and 150 μM along with corresponding decrease in Y(NO).

The effective quantum yield of PSI, Y(I), was also twice in *Synechocystis* as compared to that in *Synechococcus*. Y(ND) and Y(NA), the quantum yield of non-photochemical quenching due to donor or acceptor side limitation, respectively, showed smaller values in *Synechocystis* as compared to those in *Synechococcus*. In *Synechocystis*, growth with chromate did not change the Y(I) significantly, but quantum yields of non-photochemical quenching showed changes. In *Synechococcus*, however, growth with chromate caused increase in the Y(I) with concomitant decrease in the quantum yields of non-photochemical quenching.

Table 4.6: Complementary quantum yields of energy conversion in PSII and PSI of *Synechocystis* and *Synechococcus* grown with or without chromate

Sample	Quantum yields in PSII		
	Y(II)	Y(NO)	Y(NPQ)
<i>Synechocystis</i> Control	0.234± 0.002	0.792± 0.001	0.00± 0.00
<i>Synechocystis</i> _12 µM K ₂ Cr ₂ O ₇	0.173± 0.016	0.848± 0.001	0.00 ± 0.00
<i>Synechococcus</i> Control	0.076± 0.008	0.948 ± 0.001	0.00 ± 0.00
<i>Synechococcus</i> _75µM K ₂ Cr ₂ O ₇	0.184± 0.005	0.882± 0.004	0.00 ± 0.00
<i>Synechococcus</i> _150 µM K ₂ Cr ₂ O ₇	0.165± 0.001	0.866± 0.001	0.00 ± 0.00

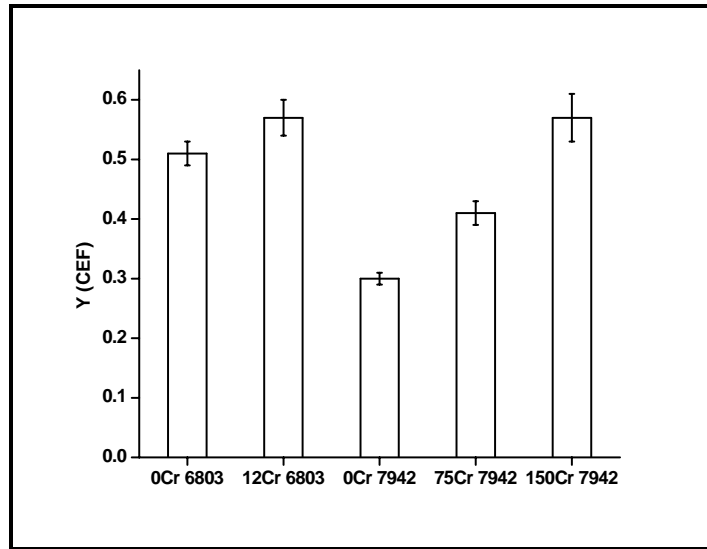
Sample	Quantum yields in PSI		
	Y(I)	Y(ND)	Y(NA)
<i>Synechocystis</i> Control	0.741 ± 0.019	0.207± 0.008	0.052± 0.025
<i>Synechocystis</i> _12 µM K ₂ Cr ₂ O ₇	0.740 ± 0.026	0.117 ±0.006	0.143± 0.026
<i>Synechococcus</i> Control	0.373 ± 0.002	0.313± 0.019	0.313± 0.020
<i>Synechococcus</i> _75 µM K ₂ Cr ₂ O ₇	0.594 ± 0.023	0.288± 0.014	0.118± 0.014
<i>Synechococcus</i> _150 µM K ₂ Cr ₂ O ₇	0.731 ± 0.041	0.216± 0.032	0.072± 0.050

Quantum yields of energy conversion in PSI and PSII were determined at steady state under actinic light during the recording of slow induction curve as described in table 4.4.

4.3.4.3 Effect of growth with chromate on cyclic electron flow: The quantum yield of cyclic electron flow (CEF), $Y(\text{CEF})$ was calculated from $Y(\text{II})$ and $Y(\text{I})$ values obtained at steady state from the slow induction curve. As observed for $Y(\text{II})$ and $Y(\text{I})$, $Y(\text{CEF})$ was also higher in *Synechocystis* as compared to that in *Synechococcus*. $Y(\text{CEF})$ increased in both the cyanobacteria on growth with chromate (**figure 4.12**); however the increase was more pronounced in *Synechococcus*.

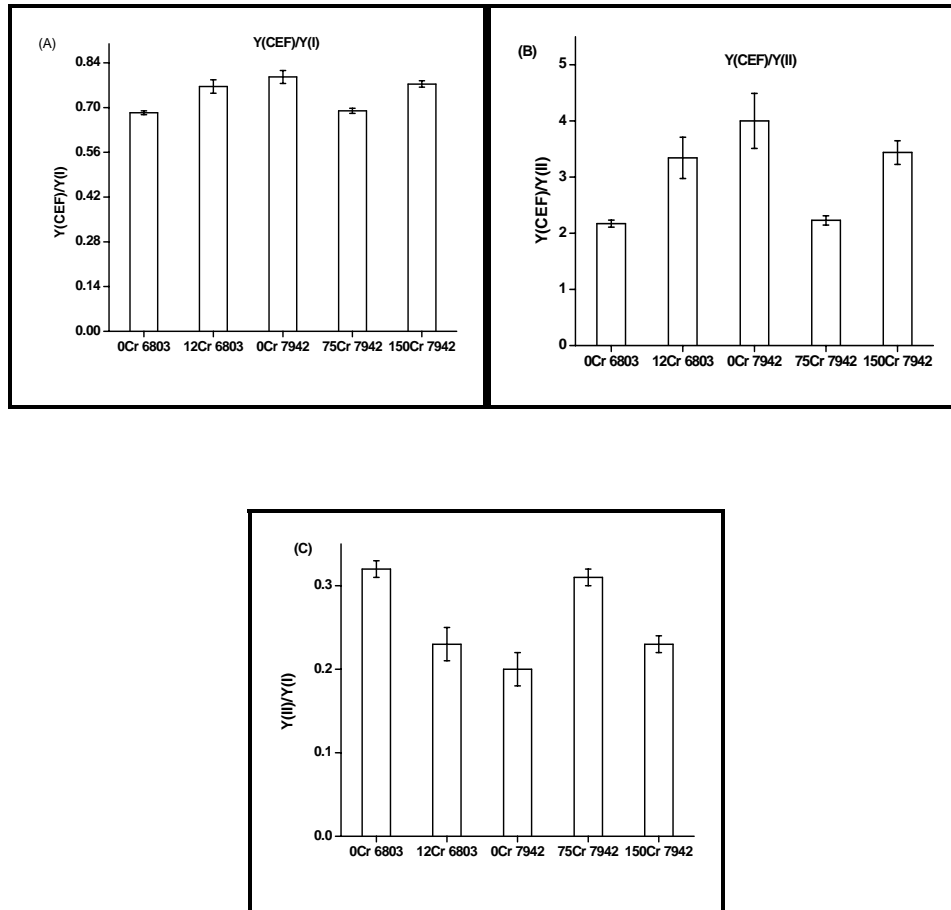
The ratio $Y(\text{CEF})/Y(\text{I})$ which indicates contribution of CEF to $Y(\text{I})$ increased marginally in *Synechocystis* in response to chromate and decreased marginally in *Synechococcus* (**figure 4.13 A**). Similar trend was shown in the ratio $Y(\text{CEF})/Y(\text{II})$, which indicates relation between quantum yield of CEF and LEF (**figure 4.13 B**). The ratio $Y(\text{II})/Y(\text{I})$, which indicates contribution of LEF to $Y(\text{I})$ decreased in *Synechocystis* in response to growth with chromate (**figure 4.13 C**). In *Synechococcus*, growth with 75 μM caused increase in this ratio and decrease on growth with 150 μM potassium dichromate.

Figure 4.12: Quantum yield of cyclic electron flow in *Synechocystis* and *Synechococcus* grown with or without chromate



The quantum yield of cyclic electron flow (CEF) [Y(CEF)] of the cultures was calculated from the respective Y(I) and Y(II) values detected at steady state during recording of the slow induction curve as described in table 4.4. *Synechocystis* is denoted as 6803 and *Synechococcus* as 7942.

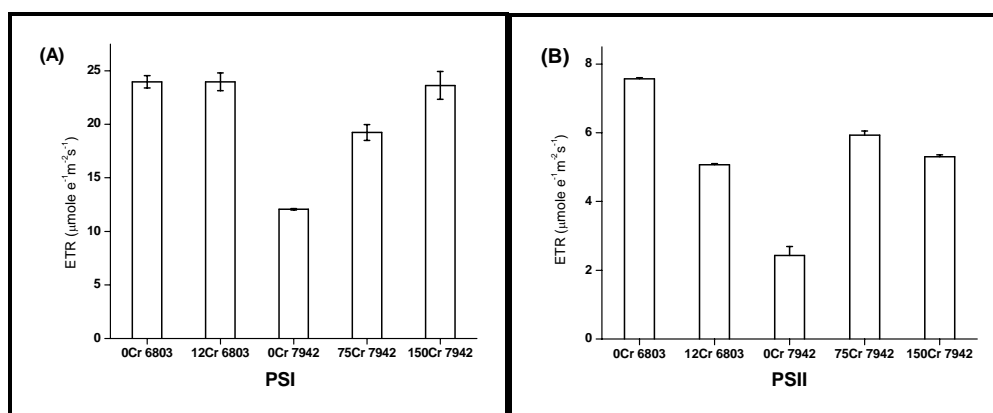
Figure 4.13: Effect of growth with chromate on ratios of $Y(\text{CEF})/Y(\text{I})$, $Y(\text{CEF})/Y(\text{II})$ and $Y(\text{II})/Y(\text{I})$ on *Synechocystis* and *Synechococcus*



The ratios were calculated from the values of $Y(\text{I})$, $Y(\text{II})$ and $Y(\text{CEF})$ detected at steady state during recording of the slow induction curve as described in methods. (A) $Y(\text{CEF})/Y(\text{I})$ indicates contribution of CEF to $Y(\text{I})$. (B) $Y(\text{CEF})/Y(\text{II})$ indicates relation between quantum yield of CEF and LEF. (C) $Y(\text{II})/Y(\text{I})$ indicates contribution of LEF to $Y(\text{I})$. *Synechocystis* is denoted as 6803 and *Synechococcus* as 7942.

4.3.4.4 Effect of growth with chromate on ETR in PSI and PSII: Response of ETR to chromate is shown in **figure 4.14**. ETRs in both PSI and PSII were higher in *Synechocystis* as compared to *Synechococcus*. In response to growth with chromate, ETR(I) did not change in *Synechocystis* whereas in *Synechococcus*, ETR(I) increased with increase in dichromate concentration from 75 to 150 μM . ETR (II), however showed 50 % decrease in response to chromate in *Synechocystis* and up to 50 % increase in *Synechococcus* on growth in presence of chromate.

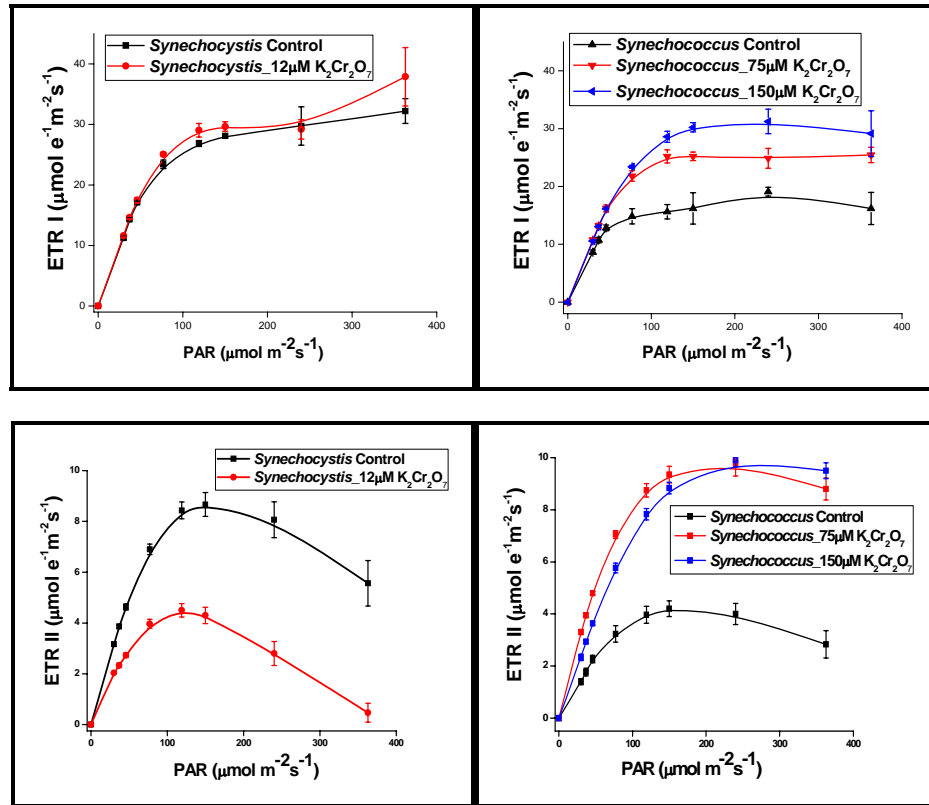
Figure 4.14: Effect of growth with chromate on ETR of PSI and PSII



The electron transport rates (ETR) in (A) PSI and (B) PSII were calculated from the respective Y(I) and Y(II) values detected at steady state during recording of the slow induction curve as described in methods. *Synechocystis* is denoted as 6803 and *Synechococcus* as 7942.

4.3.4.5 Light curves of electron transport rate of PSI and PSII: The response of ETR(I) and ETR(II) with increasing photosynthetically active radiation (PAR) was recorded using the light curve function of the Dual PAM software (**figure 4.15**). ETR of *Synechocystis* and *Synechococcus* showed contrasting responses to increasing PAR when grown with chromate. Light curve of ETR(I) in response to chromate did not change in *Synechocystis* whereas ETR(II) values showed a decline at all PARs; the decrease was more pronounced at $\text{PAR} > 77 \mu\text{mol photons}\cdot\text{m}^{-2}\cdot\text{s}^{-1}$. In *Synechococcus*, both ETR(I) and ETR(II) showed an increase beyond $77 \mu\text{mol photons}\cdot\text{m}^{-2}\cdot\text{s}^{-1}$ PAR in response to growth with 75 and 150 μM potassium dichromate. ETR(I) was lower in *Synechococcus* grown with 150 μM .

Figure 4.15: Light curves of electron transport rate of PSI and PSII in the cyanobacteria grown with or without chromate



Light curves of electron transport rate (ETR) of PSI and PSII [designated as ETR(I) and ETR(II) respectively] in the cultures were recorded by exposing them to increasing photosynthetically active radiation (PAR) from 0 – 363 $\mu\text{mol photons m}^{-2}\text{s}^{-1}$ using the Dual PAM software. X axis represents PAR and Y axis represents ETR.

4.3.4.6 Effect of growth with chromate on parameters of light response reaction

in the cyanobacteria: Parameters indicating the index of light adaptation of PSI or PSII (I_k), photochemical efficiency (α) and maximal electron transport rates in PSI or PSII (ETR_{max}) were calculated from the light curves and are shown in **table 4.7**. The parameters of PSI showed a general increase in response to growth with chromate in both the cyanobacteria. I_k showed a marginal increase in *Synechocystis* whereas it was significantly higher in *Synechococcus* in response to growth with chromate. Similar trend was shown by α and ETR_{max} also. The parameters of PSII showed varied responses in the two cyanobacteria. I_k marginally decreased in *Synechocystis* whereas it increased significantly in *Synechococcus* grown with 150 μ M potassium dichromate. α and ETR_{max} decreased drastically in *Synechocystis* whereas in *Synechococcus* increased in response to chromate with higher values in cells grown with 75 μ M.

Table 4.7: Effect of growth with chromate on parameters of light response reaction in the cyanobacteria

Sample	Parameters of RLCs of ETR(I)		
	I_k ($\mu\text{mol photon m}^{-2}\cdot\text{s}^{-1}$)	α ($\text{e}^{-1}\text{ photon}^{-1}$)	ETR_{max} ($\mu\text{mol e}^{-1}\cdot\text{m}^{-2}\cdot\text{s}^{-1}$)
<i>Synechocystis</i> Control	88.785 ± 6.288	0.376 ± 0.006	32.23 ± 2.022
<i>Synechocystis</i> _12 $\mu\text{M K}_2\text{Cr}_2\text{O}_7$	98.525±13.580	0.385 ± 0.004	37.86 ± 4.827
<i>Synechococcus</i> Control	67.787 ± 3.208	0.284 ± 0.010	19.20 ± 0.819
<i>Synechococcus</i> _75 $\mu\text{M K}_2\text{Cr}_2\text{O}_7$	74.948 ± 1.817	0.366 ± 0.012	27.43 ± 1.147
<i>Synechococcus</i> _150 $\mu\text{M K}_2\text{Cr}_2\text{O}_7$	92.144 ± 6.082	0.351± 0.002	32.40± 2.344

Sample	Parameters of RLCs of ETR(II)		
	I_k ($\mu\text{mol photon}\cdot\text{m}^{-2}\cdot\text{s}^{-1}$)	α ($\text{e}^{-1}\text{ photon}^{-1}$)	ETR_{max} ($\mu\text{mol e}^{-1}\cdot\text{m}^{-2}\cdot\text{s}^{-1}$)
<i>Synechocystis</i> Control	84.673 ± 3.688	0.102 ± 0.003	8.667 ± 0.470
<i>Synechocystis</i> _12 $\mu\text{M K}_2\text{Cr}_2\text{O}_7$	72.849 ± 2.175	0.062 ± 0.002	4.500 ± 0.265
<i>Synechococcus</i> Control	89.233 ± 4.712	0.048 ± 0.004	4.233 ± 0.285
<i>Synechococcus</i> _75 $\mu\text{M K}_2\text{Cr}_2\text{O}_7$	93.814 ± 4.506	0.108 ± 0.002	10.100 ± 0.503
<i>Synechococcus</i> _150 $\mu\text{M K}_2\text{Cr}_2\text{O}_7$	126.406±0.868	0.078± 0.002	9.900± 0.252

Parameters of light response reaction were derived from rapid light curves (RLCs) of ETR(I) and ETR(II) measured in the cyanobacteria grown with or without chromate

α : initial slope of RLCs of ETR(I) and ETR(II)

I_k : $\text{ETR}_{\text{max}}/\alpha$

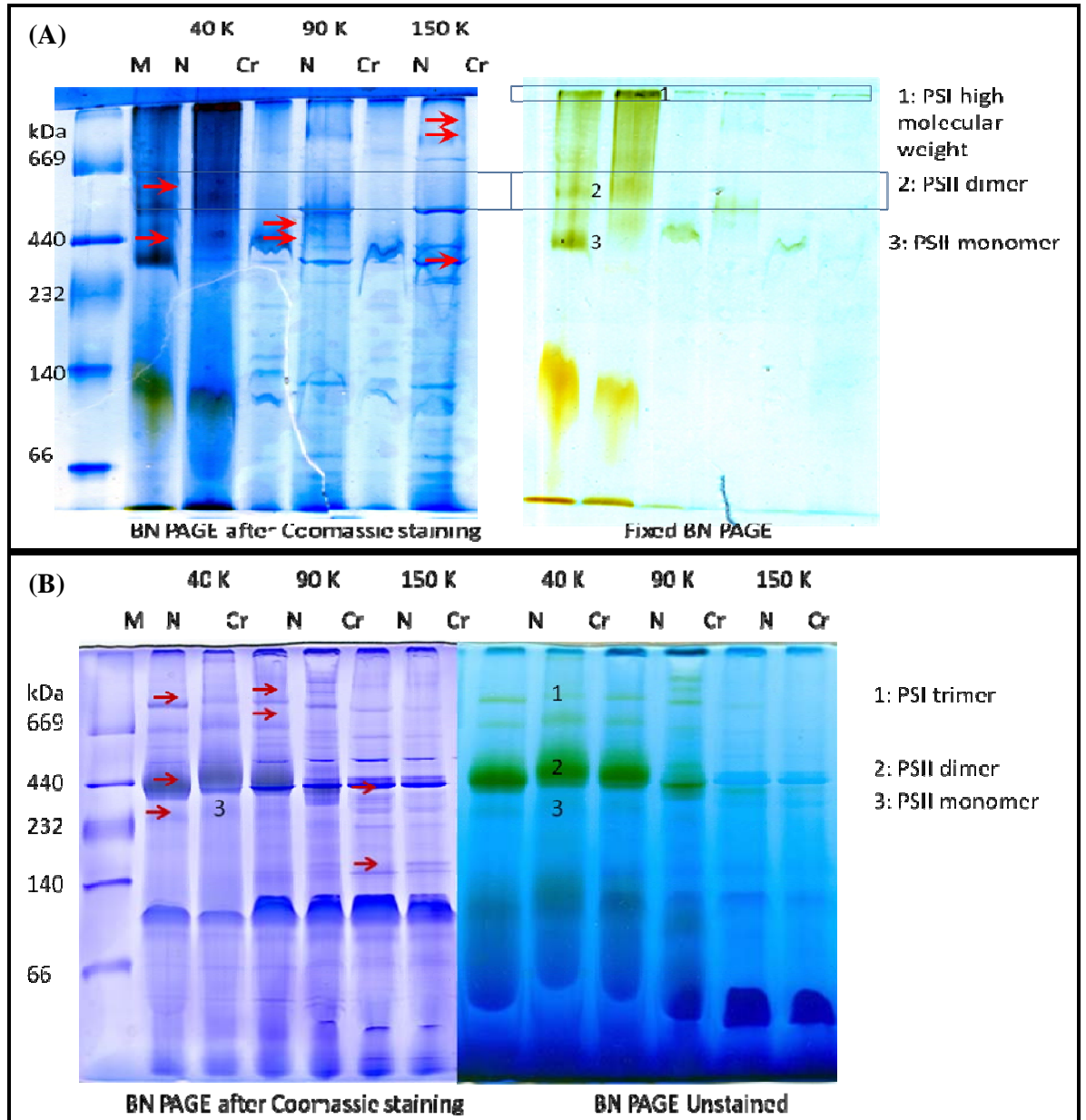
ETR_{max} : maximal electron transport rates in PSI or PSII

4.3.5 Heterogeneity in thylakoids of *Synechocystis* and *Synechococcus* grown with or without chromate

Since there are no visible differences in thylakoids in cyanobacteria, it is considered that all the membranes are homogeneous. However, previous studies had shown that thylakoids in cyanobacteria can be fractionated from cell free extracts in different fractions by ultracentrifugation. These membrane fractions show differences in proteomic and biophysical properties suggesting thylakoid membrane heterogeneity in *Synechocystis* and *Synechococcus* (Dani and Sainis 2005, Agarwal et al., 2010, 2012). It was interesting to explore whether growth with chromate affects the heterogeneity in thylakoids of cyanobacteria. Thylakoid membranes isolated from *Synechocystis* and *Synechococcus* cells grown with chromate were subjected to differential ultracentrifugation at 40,000 x g, 90,000 x g and 150,000 x g and three fractions were obtained. The three thylakoid fractions from control and chromate grown cells were subjected to Blue Native PAGE. **Figure 4.16A** shows the stained and unstained Blue Native PAGE of the three membrane fractions isolated from *Synechocystis*. The three fractions showed heterogeneity with respect to composition. Most of the chlorophyll containing membrane super complexes were present in the heaviest (40 k) fraction as shown by the green band observed in the unstained gel image. The distribution was different in the fractions obtained from *Synechocystis* grown with chromate. The PSII dimer and monomer were more in control cells as shown in the 40 k fraction. The PSI high molecular weight monomer was higher in quantity in the 40 k fraction of chromate grown cells. 40 k fraction from chromate grown cells also showed decomposition evident by a pronounced green color in upper portion of the lane. Apart from the chlorophyll containing complexes, appearance of a few protein complexes was observed in the 150 k fraction from chromate grown cells. **Figure 4.16 B** shows the stained and unstained Blue Native page of the three membrane fractions isolated from

Synechococcus control cells and after growth with chromate. As in case of *Synechocystis*, heterogeneity was observed in the three fractions obtained from both control and chromate grown cells. However, chlorophyll containing supercomplexes were relatively more in the 90 k fraction as compared to that in *Synechocystis*. PSII monomer, dimer and PSI trimer were observed in the 40 and 90 k fractions. The stained gel image showed presence of more non chlorophyll membrane protein complexes. In both *Synechocystis* and *Synechococcus*, a new protein complex was observed in the 150 k fraction of the chromate grown cells at ~440 kDa. Thus alteration in the profile of super complexes from cells grown with or without Cr (VI) was observed in terms of mobility and quantity. Qualitative and quantitative differences in pigment-protein complexes from thylakoid membranes of chromate grown and control cells indicated differences in assembly of components of the supercomplexes. This suggested that growth with chromium probably results in modification of supercomplexes.

Figure 4.16: BN PAGE images of thylakoid fractions from *Synechocystis* and *Synechococcus* grown with or without chromate



Thylakoid fractions obtained by differential ultracentrifugation of cell free lysate from *Synechocystis* (A) and *Synechococcus* (B) grown with or without chromate were solubilised and resolved on BN PAGE. The arrows indicate the qualitative differences in the supercomplexes in the three fractions in response to growth with chromate. N represents fractions obtained from normal or control cells and Cr represents the corresponding fractions obtained from cells grown with chromate. Arrows represent the bands that show difference in mobility or intensity between fractions from control and chromate grown cells.

4.3.6 Thylakoid membrane damage and repair in *Synechocystis* and *Synechococcus* in response to growth with chromate

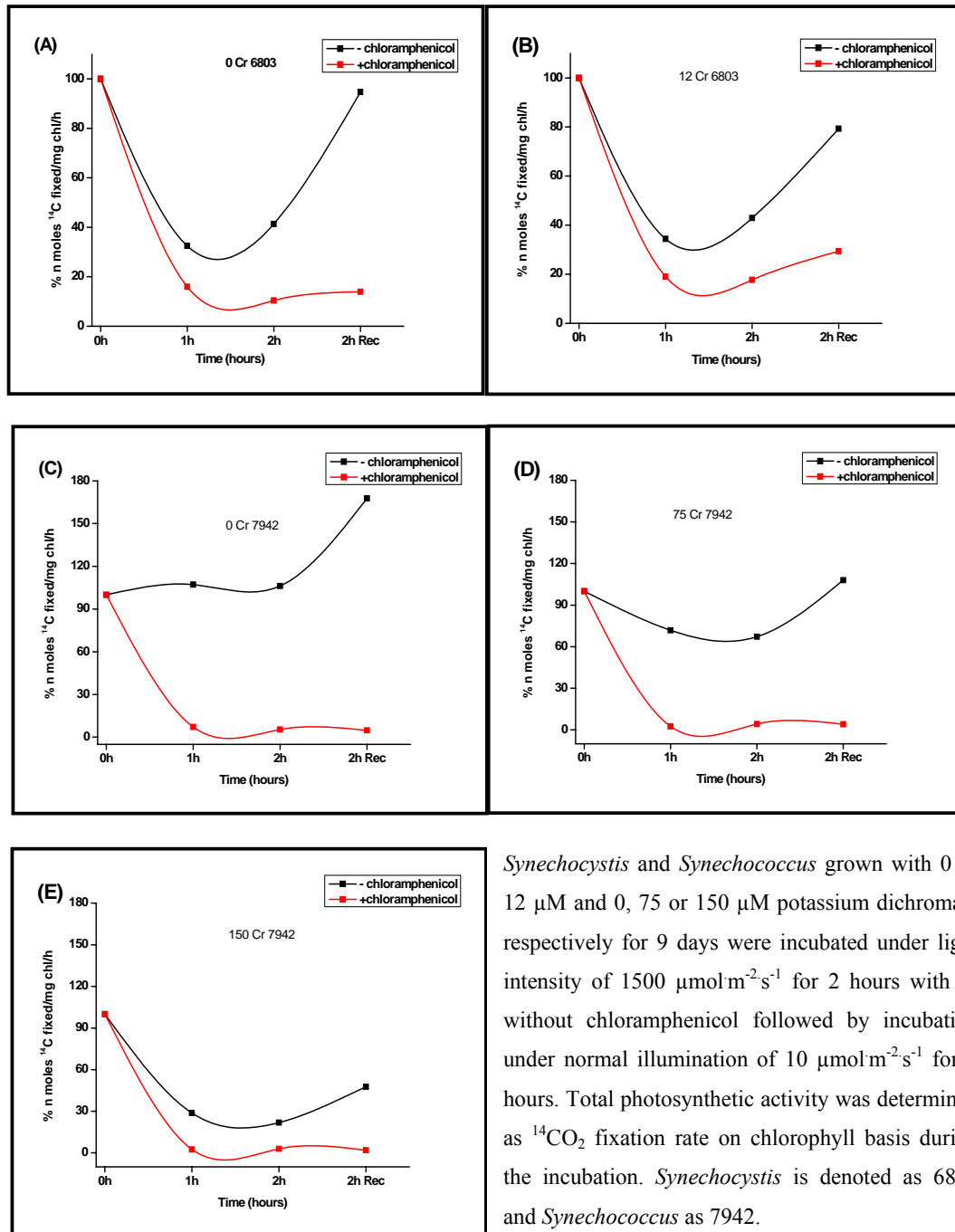
The activity of photosynthesis is affected by high light due to damage to thylakoids which is termed as photoinhibition. In these experiments photoinhibition was used to explore the effect of growth with chromate on thylakoid membrane damage and repair. *Synechocystis* and *Synechococcus* grown with or without chromate were incubated under $1500 \mu\text{mol m}^{-2}\text{s}^{-1}$ of light at 25°C with intermittent shaking at room temperature followed by incubation under normal illumination conditions for repair of the photodamage ($\sim 30 \mu\text{mol m}^{-2}\text{s}^{-1}$) for 2 h in water bath at 25°C . Repair of thylakoid is known to require efficient protein synthesis. Therefore, thylakoid membrane damage and repair was also examined in these samples in the presence and absence of chloramphenicol. $^{14}\text{CO}_2$ fixation, absorption and fluorescence characteristics were monitored during exposure to high light and after recovery phase with low light. **Figure 4.17A, C** show that high light inhibited CO_2 fixation in *Synechocystis*, but not in *Synechococcus*. Inclusion of chloramphenicol exacerbated the photoinhibition in *Synechocystis*, and resulted in photoinhibition in *Synechococcus*. After high light stress, the cultures were incubated in normal illumination conditions ($\sim 30 \mu\text{mol m}^{-2}\text{s}^{-1}$) for 2 hours to undergo recovery. Incubation with low light resulted in recovery in case of *Synechocystis* and showed much higher rates in *Synechococcus*. The samples treated with chloramphenicol showed very little recovery. The extent of inhibition was higher in cells grown with chromate as compared to the respective controls and recovery was lower as compared to control cells. Although control cells of *Synechococcus* did not show any reduction in rates of CO_2 fixation after exposure to high light, the cells which were grown with $75 \mu\text{M}$ and $150 \mu\text{M}$ chromate showed photoinhibition which was higher in cells grown with $150 \mu\text{M}$ as compared to cells grown with $75 \mu\text{M}$.

Similarly recovery was less in cells grown with 150 μM as compared to cells grown with 75 μM . As against this recovery of chromate grown cells of *Synechocystis* was higher.

PSII is damaged by high light stress and the repair process is known to be hampered by oxidative stress. Absorption and fluorescence emission spectra of the above samples were monitored. **Figure 4.18** shows the absorption spectra of the samples exposed to photodamage and repair. There was no discernible difference in absorption spectra after exposure to high light suggesting that there was no degradation of photosystems or phycobilisomes. **Figure 4.19** shows the room temperature fluorescence of these samples. Fluorescence was reduced in all the samples in response to light stress and recovery was poor in case of cells grown with chromate. In *Synechocystis*, the characteristic peak and shape of the spectra were maintained after light stress and recovery whereas in case of *Synechococcus*, emergence of fluorescence at 655 nm, characteristic of allophycocyanin was observed after light stress. This allophycocyanin fluorescence was higher in case of *Synechococcus* cells grown with chromate. These observations showed that PSII is affected by light stress in these cyanobacteria both in control and chromate grown cells. **Figure 4.20** shows the fluorescence emission spectra after excitation of phycobilisome at 580 nm in all the samples. In both the cyanobacteria, control cells showed allophycocyanin and PSII characteristic peaks at 655 nm and 686 nm respectively. After light stress, PSII peak disappeared in both cyanobacteria. This indicated uncoupling of phycobilisomes and PSII.

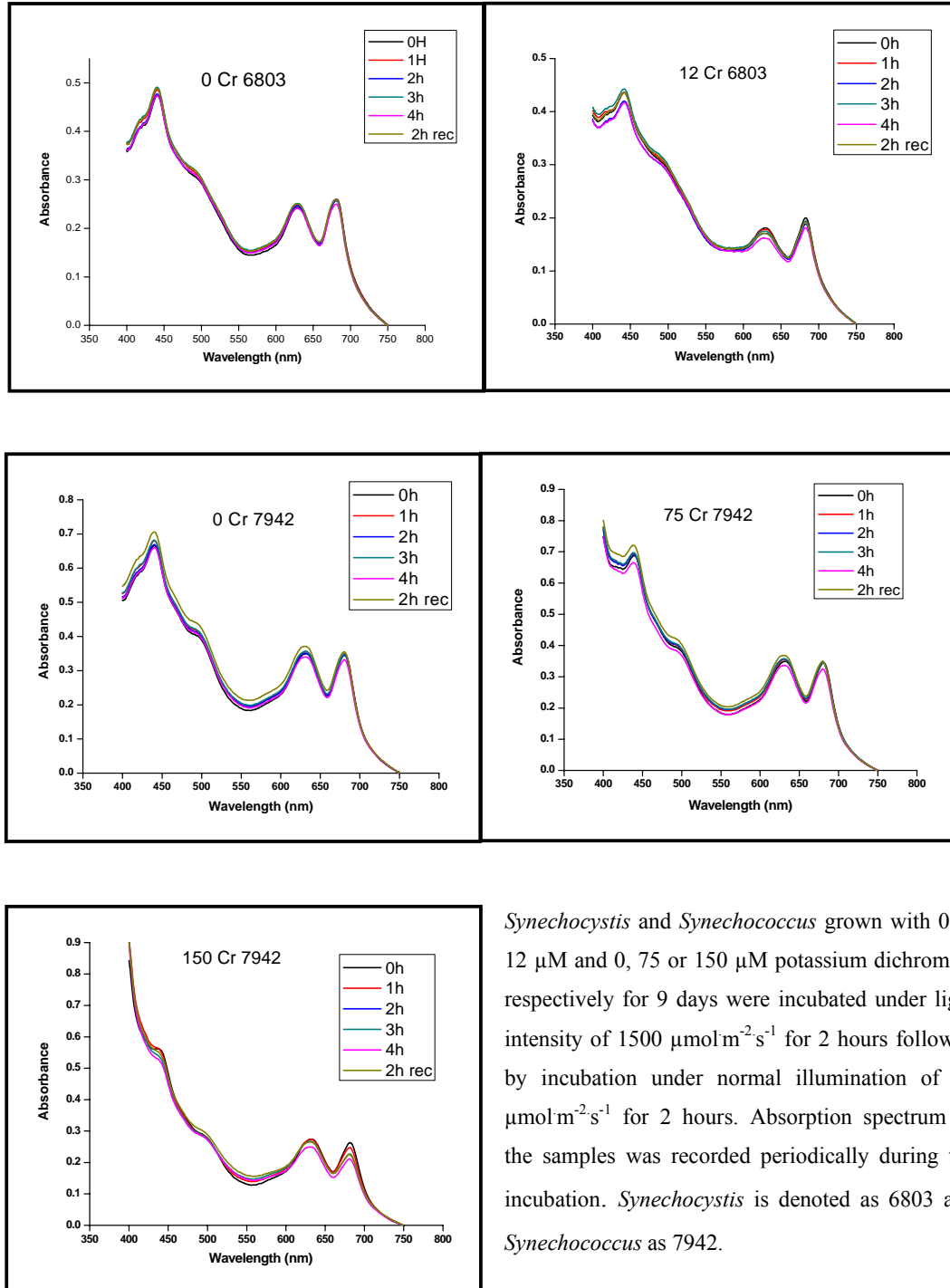
The changes in the fluorescence emission spectra along with study of $^{14}\text{CO}_2$ fixation rates showed that thylakoid membrane damage and repair is affected in the cells grown with chromate and the two cyanobacteria showed differences in the extent of damage and repair of thylakoid membranes.

Figure 4.17: $^{14}\text{CO}_2$ fixation rates after thylakoid membrane damage and repair in *Synechocystis* and *Synechococcus* grown with or without chromate



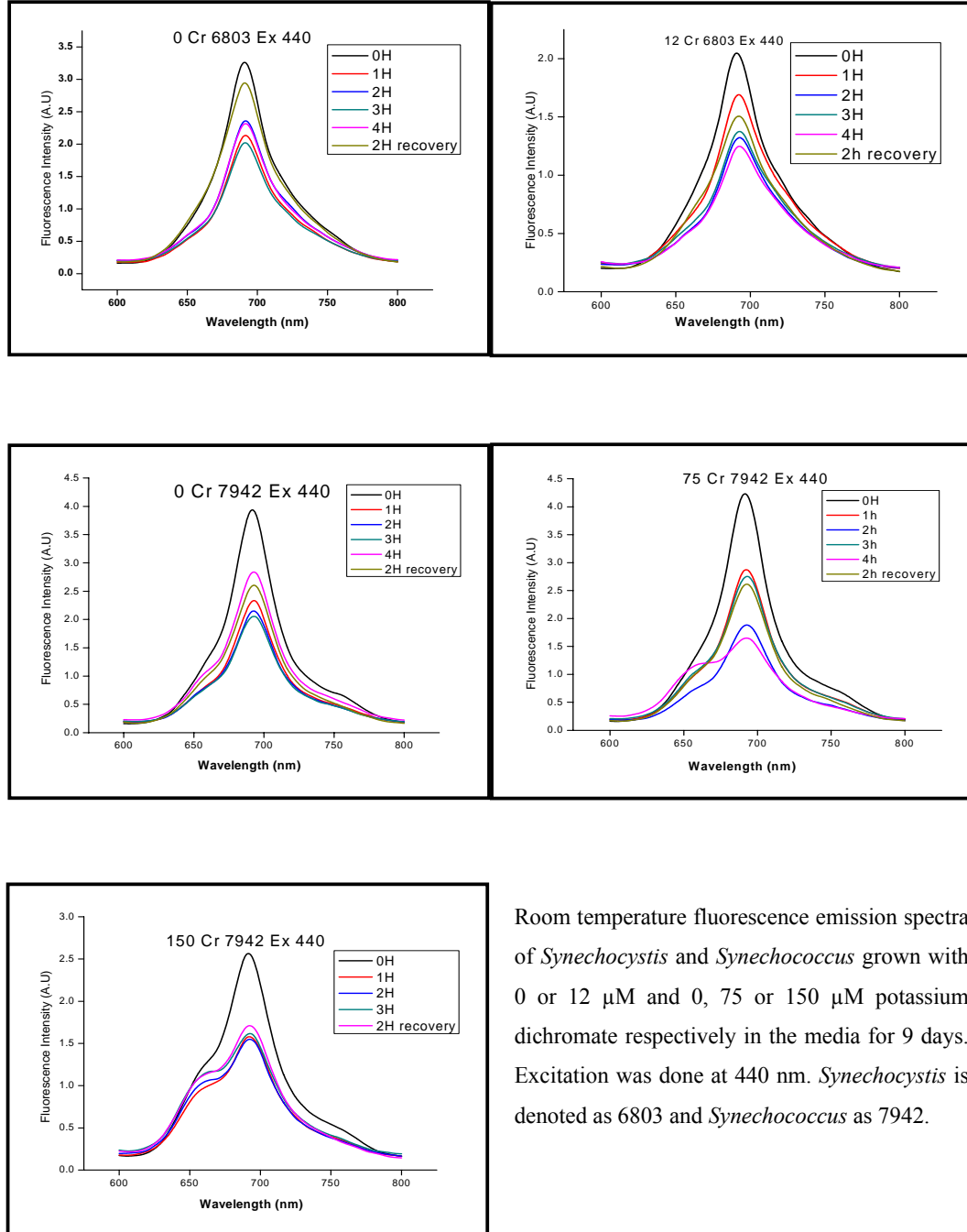
Synechocystis and *Synechococcus* grown with 0 or 12 μM and 0, 75 or 150 μM potassium dichromate respectively for 9 days were incubated under light intensity of $1500 \mu\text{mol m}^{-2} \text{s}^{-1}$ for 2 hours with or without chloramphenicol followed by incubation under normal illumination of $10 \mu\text{mol m}^{-2} \text{s}^{-1}$ for 2 hours. Total photosynthetic activity was determined as $^{14}\text{CO}_2$ fixation rate on chlorophyll basis during the incubation. *Synechocystis* is denoted as 6803 and *Synechococcus* as 7942.

Figure 4.18: Absorption spectra of *Synechocystis* and *Synechococcus* grown with or without chromate incubated under high light followed by incubation under normal illumination



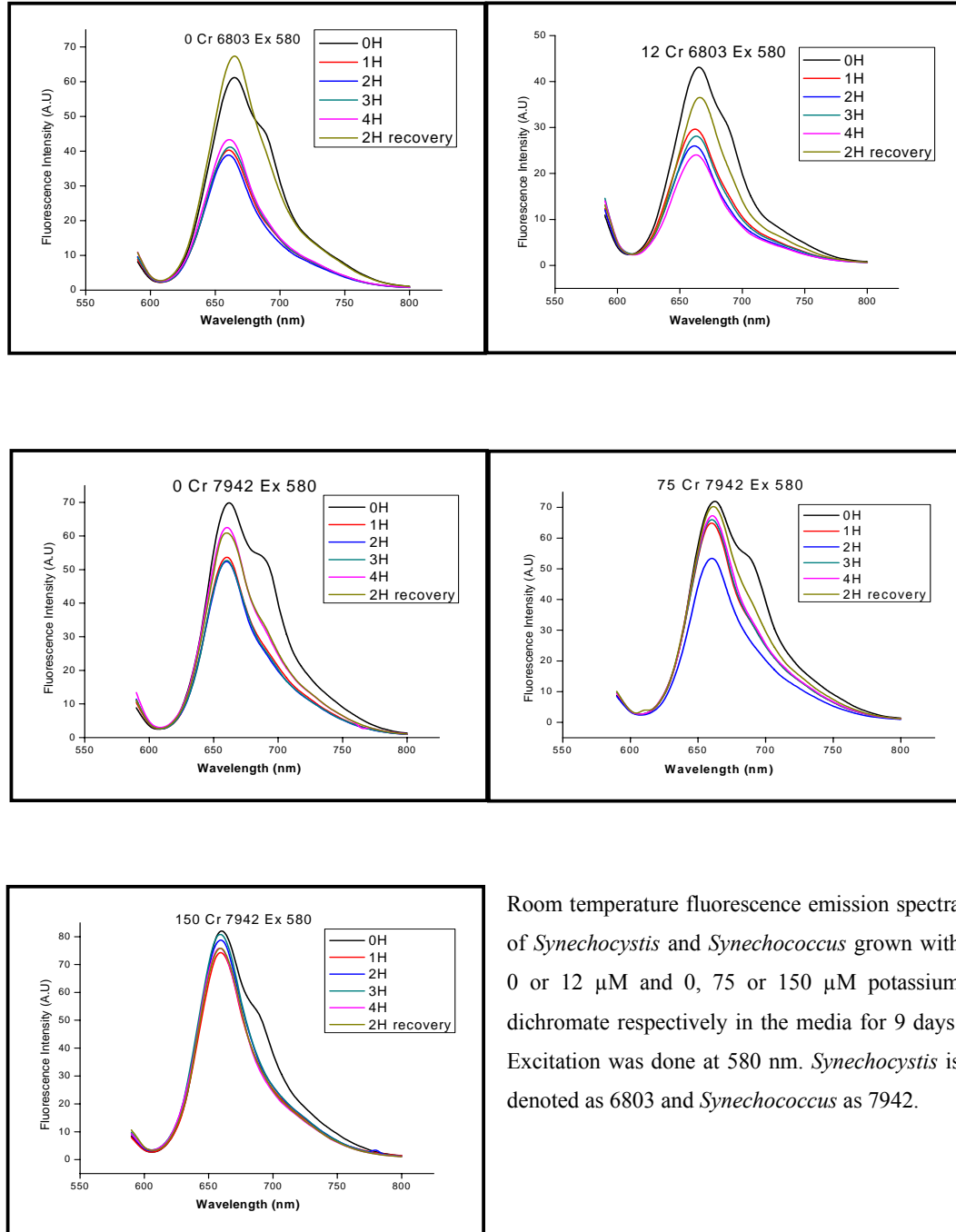
Synechocystis and *Synechococcus* grown with 0 or 12 μM and 0, 75 or 150 μM potassium dichromate respectively for 9 days were incubated under light intensity of $1500 \mu\text{mol m}^{-2} \text{s}^{-1}$ for 2 hours followed by incubation under normal illumination of $10 \mu\text{mol m}^{-2} \text{s}^{-1}$ for 2 hours. Absorption spectrum of the samples was recorded periodically during the incubation. *Synechocystis* is denoted as 6803 and *Synechococcus* as 7942.

Figure 4.19: Room temperature fluorescence emission spectra of *Synechocystis* and *Synechococcus* grown with or without chromate exposed to high light followed by recovery. Excitation wavelength = 440 nm



Room temperature fluorescence emission spectra of *Synechocystis* and *Synechococcus* grown with 0 or 12 μM and 0, 75 or 150 μM potassium dichromate respectively in the media for 9 days. Excitation was done at 440 nm. *Synechocystis* is denoted as 6803 and *Synechococcus* as 7942.

Figure 4.20: Room temperature fluorescence emission spectra of *Synechocystis* and *Synechococcus* grown with or without chromate exposed to high light followed by recovery. Excitation wavelength = 580 nm



Room temperature fluorescence emission spectra of *Synechocystis* and *Synechococcus* grown with 0 or 12 μM and 0, 75 or 150 μM potassium dichromate respectively in the media for 9 days. Excitation was done at 580 nm. *Synechocystis* is denoted as 6803 and *Synechococcus* as 7942.

4.4 Discussion

Cyanobacteria are the oldest photoautotrophs and carry out 'plant like' oxygenic photosynthesis. But unlike plants, they lack the compartmentalization and therefore photosynthesis and respiration take place in one and the same network of membranes known as thylakoids. The ever-changing and challenging environment in which these aquatic photoautotrophs thrive entail that their photosynthetic apparatus should have enough plasticity. In fact the secret of success of cyanobacteria to survive all kinds of harsh environments on the earth for billions of years lie in the adaptability of their metabolic, both anabolic and catabolic pathways to circumvent the stresses in their growth milieu such as acidity, alkalinity, nutritional imbalances, temperature variations, light conditions including exposure to UV etc. The studies on their adaptive responses, especially those on their photosynthetic apparatus therefore, form an interesting aspect of research in photosynthesis. Subtle changes in environmental and nutritional conditions would induce short and long term adaptive responses and may alter photosynthetic and electron transport activities. Since presence of chromate exerts oxidative stress and photosynthetic apparatus is sensitive to oxidative stress, the studies on structure-function of photosynthetic apparatus in *Synechocystis* and *Synechococcus* became interesting. Effects of growth with potassium dichromate were studied in these two cyanobacteria which showed differences in sensitivity to chromate. *Synechocystis* was grown with 0 and 12 μM potassium dichromate, whereas *Synechococcus* was grown with 0, 75 and 150 μM chromate for 9 days. The photosynthetic parameters were studied in these chromate adapted cultures versus control cultures not exposed to chromate. This study enabled us to compare and contrast the photosynthetic parameters of *Synechocystis* and *Synechococcus*, the two non-nitrogen fixing

unicellular aquatic cyanobacteria belonging to order Chroococcales, in addition to comparison of adaptation of photosynthetic apparatus to chromate.

Presence of chromate in growth medium affected the thylakoid membranes and ultrastructure in *Synechocystis* to a higher extent as compared to *Synechococcus*. Chromate also affected morphology of cells. Recently effects of chromate on cell morphology were reported in case of *Rhodobacter sphaeroides* by Italiano et al. (2012). *Synechocystis* showed higher rates of CO₂ fixation and PSII and PSI activities on chlorophyll basis as compared to *Synechococcus*.

Chromate up to 100 µM was found to stimulate growth in *Synechococcus* also showed higher rates of CO₂ fixation and PSII and PSI activities as compared to control. Earlier such stimulation of growth and photosynthesis has been observed by Tiwari et al. (1996) in case of *Synechocystis* at lower concentrations of cobalt chloride in growth media.

Photosynthetic pigment levels showed a decline in both the cyanobacteria at EC₅₀ concentration, with not much effect on *Synechococcus* grown with 75 µM. The shape of absorption spectra were maintained in all the conditions tested barring the decrease in peak intensities at characteristic wavelengths of the pigments. Signature fluorescence emission spectra were shown with few deviations indicating adjustments due to growth with potassium dichromate in both the cyanobacteria. A general decrease in chlorophyll fluorescence intensity was observed due to decrease in pigment content per cell. In *Synechococcus*, growth with 150 µM chromate caused dissociation of PSII indicated by reduction of the shoulder at 688nm on 580 nm excitation at room temperature. 77 K fluorescence emission studies also showed adjustments in the PBS-PSII/PSI association due to growth with chromate. Growth with chromate also caused decrease in phycobilisomes mobility in *Synechococcus*. Photochemical and biochemical studies showed that major photosynthetic functions

were maintained in *Synechococcus* cells on growth with chromate by making adjusting in the photosynthetic apparatus. In both the cyanobacteria, PSII was more sensitive to chromate stress as compared to PSI, which in agreement with reported literature. However, PSII in *Synechocystis* was more sensitive to chromate as compared to PSII in *Synechococcus* at the respective EC₅₀ concentrations. PSI in *Synechococcus* was not affected when cells were grown with 150 µM chromate. Thus the sensitivity of *Synechocystis* may be attributed to reduction in PSII.

Photosynthetic parameters were also studied *in vivo* in the cyanobacteria in response to chromate by the noninvasive technique of PAM fluorometry. Chlorophyll concentration of all the samples was adjusted to ~10 µg·ml⁻¹ and various parameters were studied. The two cyanobacteria showed variation with respect to response of photosynthetic apparatus to growth with chromate. Reduction in Fv/Fm is an index of the maximal photochemical efficiency of PSII. On growth with chromate, both the cyanobacteria showed significant decrease in Fv/Fm. Chromate decreased active PSI in *Synechocystis* but did not affect PSI in *Synechococcus*, instead an increase in active PSI was observed in *Synechococcus* grown with 75 µM dichromate indicated by higher value of Pm. Chromate has been reported to have different sites of inhibition, associating with PSII, PSI and electron transport sink beyond photosystems (Perreault et al. 2009) when acute exposure is given, a sign of photoinhibition or defective PSII functioning. The present study, however, has been carried out on the cyanobacteria grown in presence of chromate in the media in the concentrations which allowed them to grow at a slower rate. Therefore, in addition to indication of chromate toxicity, photosynthetic parameters signaled adjustments or adaptations which were different in the two cyanobacteria. Deeper insight on the sites of action of chromate was provided parameters obtained by slow kinetics and light curves. PSII in *Synechocystis* was affected by chromate and not PSI as shown

by decrease in the effective quantum yield of PSII, although disturbances do happened as shown by changes in the Y(ND) and Y(NA). Y(NO) has been suggested to be an indicator of PSII damage (Huang et al., 2010; Perreault et al., 2009; Suzuki et al. 2011). This value was found to be slightly higher in *Synechocystis* in response to chromate. Decrease in the value of Y(II)/Y(I) in *Synechocystis* and increase in *Synechococcus* indicated shift in the balance of distribution of quantum yield between two photosystems with PSII inhibited in *Synechocystis* in response to chromate. CEF was stimulated in both the cyanobacteria causing a rise in Y(CEF)/Y(I) which was also shown by higher ETR(I) in response to chromate. In addition, ETR(II) of *Synechocystis* decreased in response to chromate. These results altogether suggested that in *Synechocystis*, PSII was functionally altered by chromate. The light curves probed the effect of light on the electron transport rates in PSII and PSI in presence of chromate. ETR(II) in *Synechocystis* was shown to be affected the most in response to chromate whereas ETR(I) remained almost like control culture. Interestingly, *Synechococcus* grown with chromate showed a rise in both ETR(II) and ETR(I) with increasing light indicating an adaptive response which did not vary with increase in chromate from 75 to 150 μM dichromate. The index of light adaptation (**table 4.7**) in PSII showed a decline in *Synechocystis* and an increase in PSI in both the cyanobacteria as shown by the light curves. Similar trends like drop in $\text{ETR}_{\text{max}}(\text{I})$, maximum photochemical efficiency (α) in *Synechocystis* in response to chromate were observed.

Analysis of heterogeneity in thylakoids isolated from cells grown in presence or absence of chromate carried out by BN PAGE analysis showed alterations in pigment protein complexes. The studies in thylakoid membrane damage and repair revealed a new paradigm. *Synechocystis* which was more sensitive to chromate showed decreased sensitivity to high light stress in its chromate grown cells.

However, *Synechococcus* which was inherently more resistant to photoinhibition succumbed more to high light if cells were grown with chromate. The results suggested that in *Synechococcus* the cellular machinery was engaged in tolerating high levels of chromate in medium and therefore did not have enough resources to tolerate any additional oxidative stress.

Thus these studies on structure–function of photosynthetic machinery in *Synechocystis* and *Synechococcus* showed that there are differences in the photosynthetic super complexes and their *in vivo* functions. *Synechocystis* and *Synechococcus* also showed differences in the adjustments of the components of their photosynthetic machinery after prolonged exposure to chromate exerting extra oxidative stress. The adaptability of the photosynthetic apparatus to chromate especially in *Synechococcus* showed the sturdiness and stress tolerance of this strain of cyanobacteria. Higher tolerance of *Synechococcus* led us to analyze its major component of its light harvesting complex, phycocyanin in cultures grown in presence of chromate which is described in the next chapter.

Chapter 5

Analysis of Phycocyanin Isolated from Cyanobacteria Grown With or Without Chromate

5.1 Introduction

Management of resources is a striking feature of all living organisms. Photosynthetic organisms such as bacteria, algae and plants use antenna systems to capture light energy available in environment and transfer the energy to reaction centers where photochemistry occurs. Reaction centers are conserved across photosynthetic organisms *per se*, but antenna systems are diverse and have evolved according to the environmental conditions. Antenna system's absorption range covers wider range of solar spectrum; this allows the organisms to utilize the photon energy of the wavelengths which otherwise would not be utilized as the reaction centers are photo excitable by specific wavelengths.

Photosynthesis is essentially photo-energy dependent charge separation and further generation of chemical potential which is converted to chemical bond energy of long term storage molecules, carbohydrates. The very first step of photosynthesis has inspired a major field of research of artificial photosynthesis. There is considerable interest in exploring the natural light harvesting complexes (LHC) for their potential use in artificial photosynthesis. The aim is to use these antenna complexes in "fabrication of robust micron-scale biohybrid light harvesting systems to drive chemical processes or to generate photocurrent". Plants have chlorophyll and carotenoid containing light harvesting complexes which are embedded in thylakoid membranes. In cyanobacteria the antenna system comprises of water soluble mobile pigment protein complexes *viz* phycocyanin and allophycocyanin organized in phycobilisomes. These pigment protein complexes have covalently attached chromophore phycocyanobilin which is an open chain tetrapyrrole. In the earlier chapters, we have observed that *Synechococcus* is able to maintain its major photosynthetic functions at relatively higher dichromate concentrations by making adjustments in the photosynthetic apparatus. Therefore, in

this chapter, pigments of the antenna complex from control and chromate grown cells of *Synechococcus* were isolated and analyzed. In addition, isolation of phycocyanobilin (PCB) and phycocyanin-allophycocyanin (PC-APC) was carried out from *Synechococcus* sp., *A. nidulans* BD1. The PC-APC and PCB from *A. nidulans* BD1 were used to study their antenna functionality and charge transfer capability to semiconductor material by Verma et al. (2009, 2011).

5.2 Materials and Methods

5.2.1 Isolation of phycocyanobilin

Phycocyanobilin was isolated from mass culture of *Synechococcus* sp., *A. nidulans* BD1. Cells were harvested from 5 litres of log phase culture by centrifugation at 6000 x g for 10 minutes at room temperature. First phycocyanin-allophycocyanin (PC-APC) was isolated by lysozyme treatment of the cells. Cells were washed with HEPES buffer (100 mM HEPES, pH 8.0) and finally suspended in 20 ml of the buffer containing 20mg of lysozyme. This slurry was incubated at 37 °C for 16 h at 80 rpm. Cell debris was removed by centrifugation at 6000 x g for 15 minutes at 4 °C and the supernatant containing PC-APC was used for isolation of phycocyanobilin.

Phycocyanobilin pigment is covalently attached to the protein; it was isolated by HCl treatment as described by hEocha (1963) with some modifications. 20 ml of PC-APC obtained by lysozyme treatment was divided into 5 ml aliquots in 50 ml tubes and precipitated using chilled acetone. The blue colored precipitate in each tube was mixed with 2 ml of 11 N HCl and incubated at 18 °C for 20 minutes under shaking. The cleavage reaction was stopped by addition of 6 ml of distilled water to each tube followed by addition of 2 ml of chloroform. This mixture was shaken vigorously and centrifuged at 6000 x g for 10 minutes at 4 °C. The blue phycocyanobilin containing

chloroform phase was separated and pooled from all the tubes. It was given 2 - 3 washes with distilled water to remove traces of HCl. The phycocyanobilin preparation was maintained in dark on ice and used the same day for analysis. The yield of PCB was calculated from Beer Lambert law using molar extinction coefficient of 20588 M⁻¹·cm⁻¹ at 365 nm and molecular weight as 588.

5.2.2 Characterization of phycocyanobilin

The phycocyanobilin preparation was analyzed by spectrophotometry and HPLC. Absorption spectrum was recorded from 220 – 800 nm for determining integrity and quantification of the pigment; HPLC was carried out to ascertain the quality of the preparation according to Fu et al. (1979) with some modifications. HPLC separation was performed on 4.8 x 260 mm 5 µm particle size column (Symmetry 300 C18) at a flow rate of 1 ml·min⁻¹. The chromatographic solvent was acetone/water/acetic acid (150:50:1, by volume). Phycocyanobilin was detected spectrophotometrically at 365 nm using online detector.

5.2.3 Isolation of phycocyanin

Isolation and purification of phycocyanin was carried out from *A. nidulans* BD1 and *Synechococcus* 7942 grown with or without 150 µM potassium dichromate as described in earlier chapters. Cells were harvested from log phase culture by centrifugation at 6,000 × g at room temperature for 10 minutes. The cell pellet (corresponding to ~10 mg dry biomass) was washed with distilled water and resuspended in 1 ml HEPES buffer (100 mM HEPES, pH 8.0) containing 1 mg·ml⁻¹ of lysozyme and incubated at 37 °C for 16 h with shaking. The slurry obtained was centrifuged at 6,000 × g at 4 °C for 15 minutes to separate the blue supernatant containing phycocyanin from the cell mass.

Ten milligrams of activated charcoal powder and 15 μl of 2 % chitosan solution prepared in distilled water was added per milliliter of crude extract containing $\sim 1 \text{ mg}\cdot\text{ml}^{-1}$ phycocyanin and incubated at 4 $^{\circ}\text{C}$ for 4 h with gentle vortexing in between. Activated charcoal powder was washed thoroughly with distilled water before usage. The extract was centrifuged at $11,000 \times g$ at 4 $^{\circ}\text{C}$ for 10 min.

5.2.4 Characterization of phycocyanin

The contents of phycocyanin and allophycocyanin were calculated by spectrophotometric absorption at 650 and 620 nm, using the following equation (Bennett and Bogorad 1973; Bryant et al. 1979):

$$\text{PC (mg}\cdot\text{ml}^{-1}) = [A_{620} - (0.7 \times A_{650})]/7.38$$

$$\text{APC (mg}\cdot\text{ml}^{-1}) = [A_{650} - (0.19 \times A_{620})]/5.65$$

The purity of phycocyanin was monitored by measuring the A_{620}/A_{280} ratio. Absorption spectrum of the phycocyanin extract was recorded from 400 to 800 nm. Fluorescence emission spectra were obtained by excitation at 620 nm and emission was recorded from 630–800 nm. SDS-PAGE was done using 15 % acrylamide (Laemmli 1970).

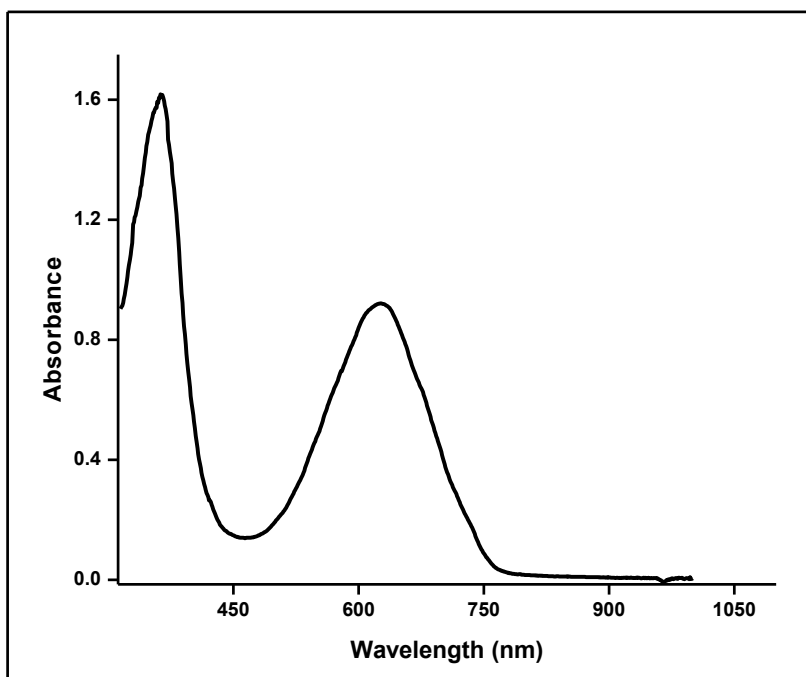
5.3 Results

5.3.1 Isolation and characterization of phycocyanobilin

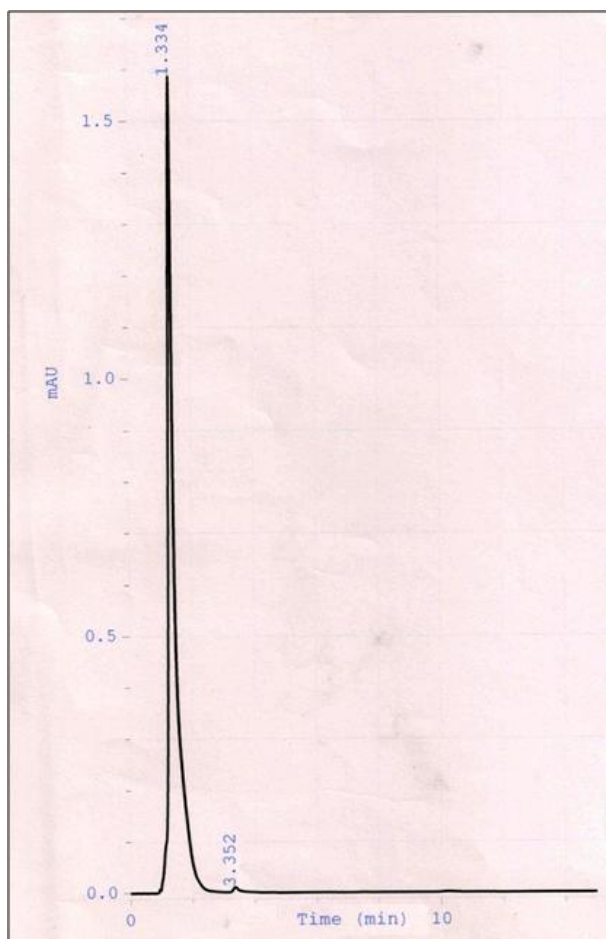
Phycocyanobilin was isolated by acid hydrolysis of the phycocyanin-allophycocyanin; this method retained its two carboxyl groups. Absorption spectrum of phycocyanobilin in chloroform was recorded to determine the integrity and yield of the pigment. Characteristic spectrum profile with peaks at 365 and 630 nm were observed as shown in **figure 5.1**. From 1 L of 20 day old culture, about 15 mg phycocyanin and 10 μg of

phycocyanobilin could be obtained. Further, purity of phycocyanobilin was also determined by HPLC. A single major peak at a retention time of 1.3 minutes was obtained indicating that the preparation was a pure compound was obtained in the elution profile as shown in **figure 5.2**.

Figure 5.1: Absorption spectrum of phycocyanobilin in chloroform



Absorption spectrum of phycocyanobilin cleaved off from protein by acid hydrolysis followed by extraction in chloroform was recorded to determine the integrity and yield of the pigment. Characteristic peaks at 365 and 630 nm were observed. X axis represents wavelength in nm and Y axis represents absorbance.

Figure 5.2: Elution profile of phycocyanobilin in chloroform

The separation was carried out on 4.8 x 260 mm 5 μm particle size Symmetry 300 C18 column with acetone/water/acetic acid (150:50:1, by vol) as mobile phase at a flow rate of 1 ml min^{-1} . Phycocyanobilin was detected spectrophotometrically at 365 nm using online detector. X axis represents time of elution and Y axis represents milli-absorbance at 365 nm.

5.3.2 Isolation of phycocyanin from *Synechococcus* grown with or without chromate

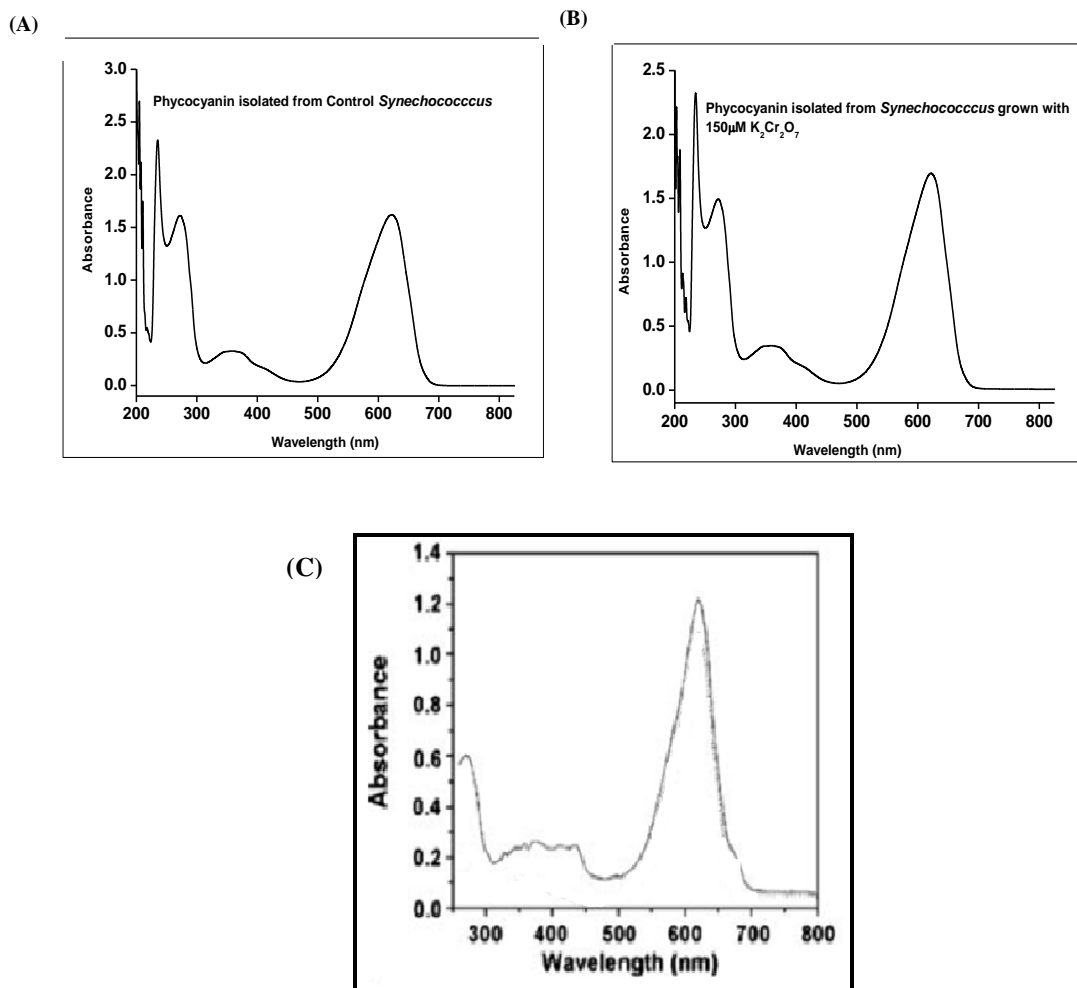
Table 5.1 shows the yield and purity of the phycocyanin obtained after lysozyme treatment and adsorption on charcoal-chitosan from *A. nidulans* BD1 and *Synechococcus* cells grown with or without chromate. In case of *Synechococcus*, the crude extracts showed purity ratio ($A_{620/280}$) of 1.05 and 1.41 from control and chromate grown cells which improved to 2.69 and 3.68 respectively after charcoal-chitosan treatment. The samples also got enriched in phycocyanin with respect to allophycocyanin after the charcoal-chitosan treatment as shown by increase in $A_{620/650}$, especially for *A. nidulans* BD1.

The absorption spectra of the phycocyanin-allophycocyanin preparation from *A. nidulans* and *Synechococcus* (control or chromate grown) showed a single peak at 620 nm (**figure 5.3**). Characteristic fluorescence emission at 660 nm was observed from phycocyanin–allophycocyanin isolated from *Synechococcus* and at 645 nm in case of phycocyanin from *A. nidulans* BD1 (**figure 5.4**). SDS-PAGE analysis showed two main bands corresponding to α and β subunits of phycocyanin between 18 to 20kDa (**figure 5.5**). Native PAGE showed a single band of phycobiliproteins comprising of phycocyanin and allophycocyanin. There was no difference in mobility and subunit composition between phycocyanin-allophycocyanin isolated from control and chromate grown cells. The spectral properties also did not show any discernable differences across the preparations indicating that growth with chromate does not bring about any change in spectral and compositional properties of phycobiliproteins in *Synechococcus*. Also phycocyanin-allophycocyanin from *A. nidulans* BD1 was found to be similar in composition to that of *Synechococcus*.

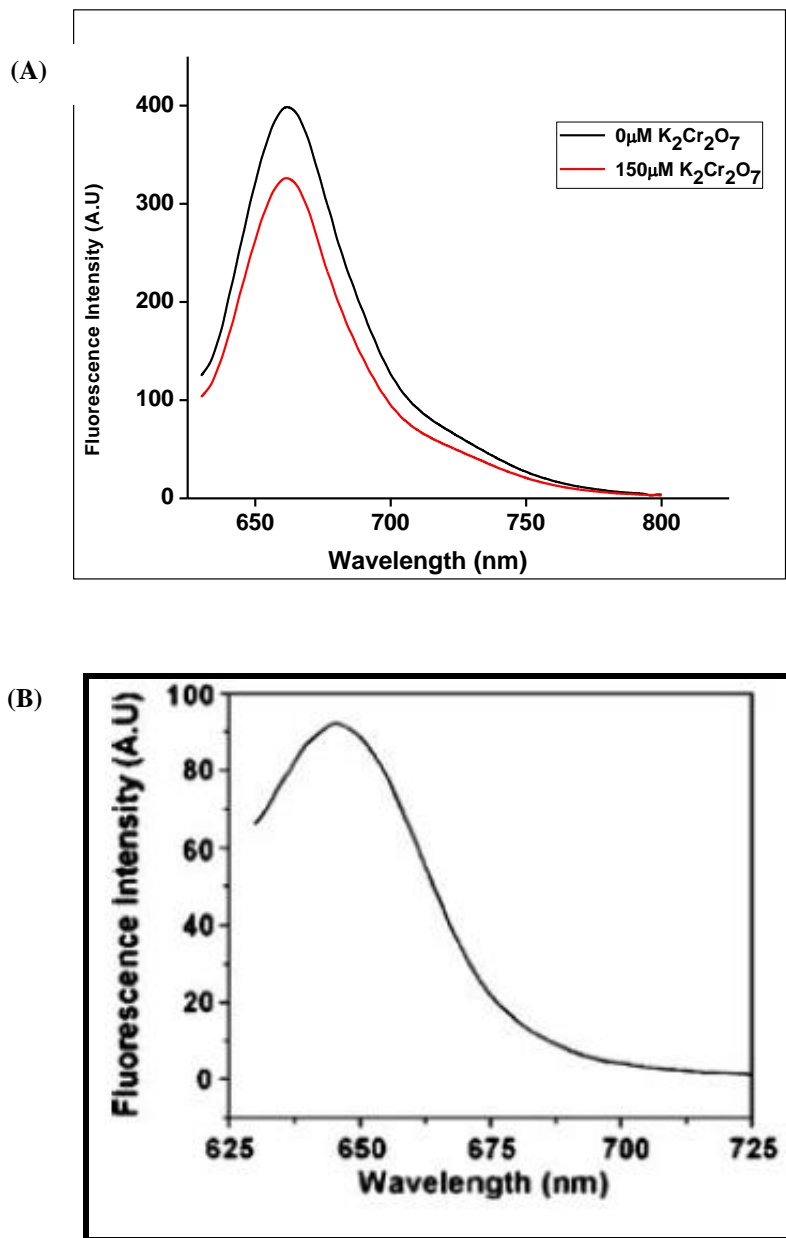
Table 5.1: Isolation and purification of phycocyanin

Sample	Purity (A _{620/280})	Purity (A _{620/650})	PC(mg·ml ⁻¹)	Yield (%)
<i>Synechococcus</i> Control crude	1.05	1.71	0.50	100
<i>Synechococcus</i> _150 μM K ₂ Cr ₂ O ₇ crude	1.41	1.85	0.57	100
<i>Synechococcus</i> Control_charcoal-chitosan	2.69	1.91	0.19	37.1
<i>Synechococcus</i> _150 μM K ₂ Cr ₂ O ₇ _charcoal-chitosan	3.18	1.93	0.19	32.8
<i>Anacystis nidulans</i> BD1	2.18	0.97	1.12	100
<i>Anacystis nidulans</i> BD1_charcoal-chitosan	4.72	2.3	1.01	90.1

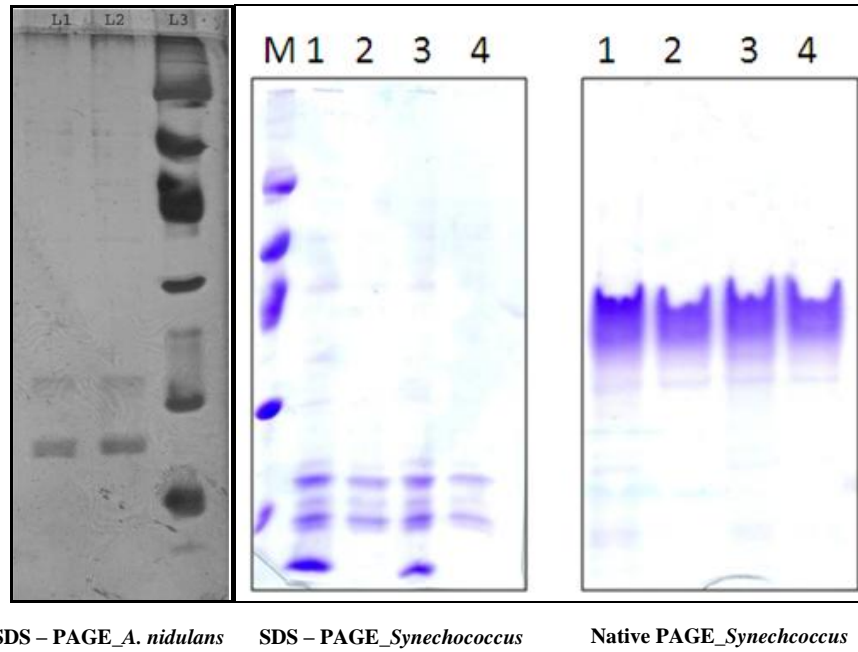
PC-APC isolated from *Synechococcus* grown with or without 150 μM potassium dichromate and also from also from *Anacystis nidulans* BD1 was subjected to charcoal chitosan purification step. A_{620/280} indicates purity of phycocyanin against total protein and A_{620/650} indicates purity against allophycocyanin.

Figure 5.3: Absorption spectra of phycocyanin

Absorption spectra of phycocyanin isolated from (A) *Synechococcus* control cells, (B) *Synechococcus* cells from culture grown with 150 μM dichromate and (C) *Anacystis nidulans* BD1 after charcoal-chitosan treatment. All three phycocyanin preparations showed characteristic absorption peak at 620 nm.

Figure 5.4: Fluorescence emission spectra of phycocyanin

Fluorescence emission spectra of phycocyanin purified from (A) *Synechococcus* grown with or without chromate and (B) *Anacystis nidulans* BD1 were recorded by exciting the sample at 620 nm. Characteristic emission at 660 nm was observed from phycocyanin isolated from *Synechococcus* and at 645 nm in case of phycocyanin from *Anacystis*.

Figure 5.5: Protein profile of the phycocyanin

SDS PAGE of the phycocyanin isolated from *Anacystis nidulans* BD1 and *Synechococcus* grown with or without chromate was carried out. SDS PAGE showed purification of the preparation before and after charcoal-chitosan treatment. Native PAGE of phycocyanin isolated from *Synechococcus* showed no difference between the samples obtained from control and chromate grown cells.

Phycocyanin from *Anacystis nidulans* L1: Phycocyanin after charcoal chitosan treatment; L2: before charcoal chitosan treatment; L3: Molecular weight markers: 94, 67, 43, 30, 20, 14 kDa.

Synechococcus SDS and Native gels: M: Molecular weight marker; 1: Phycocyanin from crude control cells; 2: Phycocyanin from control cells after charcoal chitosan treatment; 3: Phycocyanin from crude from cells grown with chromate; 4: Phycocyanin from chromate grown cells after charcoal chitosan treatment.

Molecular weight markers: 94, 67, 43, 30, 20, 14 kDa.

5.4 Discussion

Phycocyanin has been extracted and purified from *Spirulina platensis*, *S. fusiformis*, *S. maxima*, *Synechococcus sp.*, *Oscillatoria quadripunctulata*, *Aphanizomenon flos-aquae*, and *Phormidium fragile* and it is produced commercially from *S. platensis*, *Anabena*, and *Galdieria sulphuraria* (Eriksen 2008). About 50–90 % of the production cost of phycobilins resides in the purification steps (Patil et al. 2006). There exists a need for high-yielding strains and cost-effective simple methods to produce phycocyanin (Singh et al. 2009). The procedure described here was initially standardized for *A. nidulans* BD1 which uses lysozyme and charcoal–chitosan treatment takes only one day to obtain phycocyanin with purity ratio (A620/280) of 4.72 and yield (Gupta and Sainis 2010). The purity of phycocyanin can further be enhanced by various chromatographic methods, if required.

The phycocyanin isolated from chromate grown *Synechococcus* did not show differences in composition and spectral properties, although purity was less as compared to phycocyanin isolated from *A. nidulans*. The fluorescence emission peak of phycocyanin isolated from *Synechococcus* was red shifted as compared to the phycocyanin preparation obtained from *A. nidulans* BD1. In addition, the yield of phycocyanin from *Synechococcus* was poorer. The cell walls of *A. nidulans* BD1 appeared to be more susceptible to lysozyme.

Thus although phycobilisome mobility was affected in *Synechococcus* cells after growth with chromate, there was no change in their composition as well as spectral properties studied. Therefore, the mobility change may be due to some other structural alterations in thylakoid membranes. More sensitive methods may be applied to study changes, if any, brought about in the phycobiliproteins of *Synechococcus* in response to growth with chromate.

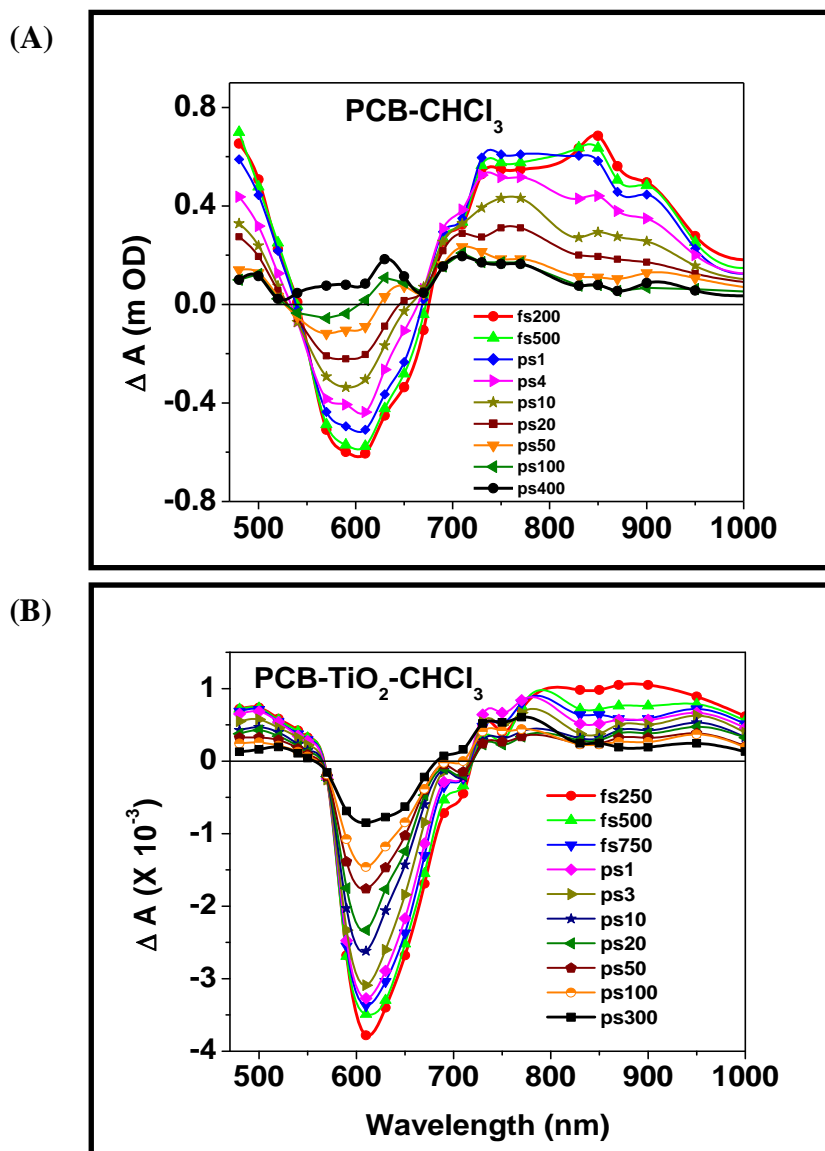
5.5 Application of the phycocyanobilin and phycocyanin

The natural photosynthetic systems present in all photosynthetic organisms are the product of an extremely long (>2.5 billion years) process of evolutionary refinement. It has inspired novel approaches to research and development of technologies for nonpolluting electricity generation, fuel production and carbon sequestration using solar energy; this area research has been named as ‘artificial photosynthesis’ (Collings and Critchley 2005). As the name implies, the inspiration is drawn from natural photosynthetic systems which were developed in organisms that were among the earliest known to exist on earth. The advent of dye sensitized solar cells (DSSC) or Grätzel cells is one such popular inspiration from natural photosynthesis. In contrast to conventional photovoltaic cells where light absorption and charge separation take place in the semiconductor itself, these two events are carried by ‘photosensitizer dye’ and conjugated semiconductor material in a DSSC as it happens in natural photosynthesis. Light absorption is carried out by light harvesting antenna complexes and charge separation function is carried out at the reaction center complexes.

Ruthenium complexes are the most widely used sensitizers in DSSCs because of their stability, strong absorption in visible region, high affinity to semiconductor material like TiO₂ etc. These dyes show absorption in 400 – 600 nm region generally.

The rationale behind isolation of phycocyanobilin was to use it for the study of electron transfer dynamics of PCB-TiO₂ conjugates. The method of acid hydrolysis used for PCB isolation retained its two carboxyl groups through which conjugation to TiO₂ takes place. The potential of phycocyanobilin to act as a sensitizer of the TiO₂ nanoparticles was studied by Verma et al. (2009) using ultrafast transient absorption spectroscopy. PCB as a candidate for a sensitizer in DSSC would be useful as it has broad absorption band beyond 600 nm so that almost whole of the visible spectrum.

In order to compete with other pathways of energy dissipation, the energy and electron transfer processes that fix the excited-state energy in photosynthesis are extremely fast. The advent of ultrafast laser systems that produce pulses with femtosecond duration have opened up a new area of research and enabled investigation of ultrafast photophysical and photochemical reactions in real time (Berera et al. 2009). Femtosecond (fs) time resolved pump – probe technique was used to study the excited state dynamics of PCB and PCB-TiO₂ in chloroform (**figure 5.6**).

Figure 5.6: Excited state dynamics of PCB and PCB-TiO₂ in chloroform

Transient absorption spectrum of (A) PCB and (B) PCB-TiO₂ in chloroform was obtained by the femto second ultrafast transient absorption spectroscopy recorded at the denoted time delay times after 400 nm laser pulse excitation (ΔA = transient absorbance). Changes in the transient spectra after conjugation with TiO₂ nanoparticles suggested electron transfer from excited PCB to conduction band of TiO₂; although back electron transfer process between conduction band electron and oxidized PCB was also indicated Verma et al. 2009.

The results showed conjugation to TiO₂ nanoparticles and electron injection into the conduction band of the nanoparticle, but back electron transfer by recombination of the electron and oxidized PCB was observed. PCB also did not show good photo stability, an important requisite for any practical use.

Phycobiliproteins are the most sought after natural chromophores containing proteins that have several applications in food, diagnostic, therapeutic, biotechnology, and cosmetic industry. They are stable highly abundant proteins in the cyanobacteria. Therefore, its isolation and purification in a single step from *A. nidulans* BD1 was optimized and its antenna functionality was studied with water soluble ZnO quantum dots by Verma et al. (2011) using ultrafast transient absorption spectroscopy. The study displayed the antenna function of PC – APC across the semiconductor interface which make them potential photosensitizers in interfacial electron-transfer processes.

Chapter 6

Summary and Future Directions

Cyanobacteria are the oldest photoautotrophs and carry out 'plant like' oxygenic photosynthesis. However, unlike plants, they lack the compartmentalization and therefore photosynthesis and respiration take place in the same network of membranes known as thylakoids. The ever-changing and challenging environment in which these aquatic photoautotrophs thrive entail that their photosynthetic apparatus should have enough plasticity. In fact the secret of success of cyanobacteria to survive all kinds of harsh environments on the Earth for billions of years lies in the adaptability of their metabolic pathways to circumvent the stresses in their growth milieu such as acidity, alkalinity, nutritional imbalances, temperature variations, light conditions including exposure to UV etc. The studies on their adaptive responses, especially those on their photosynthetic apparatus therefore, form an interesting aspect of research in photosynthesis.

Comparative analysis of chromate tolerance in *Synechococcus elongatus* PCC 7942 and *Synechocystis* PCC 6803 revealed that the former showed ~12 times higher tolerance to chromate than the latter, with EC_{50} values of $150 \pm 15 \mu\text{M}$ and $12 \pm 2 \mu\text{M}$ respectively. The EC_{50} values were dependent on the inoculum size in both cases indicating stoichiometric relation between chromate receptors per cell and number of chromate ions available in the growth medium. Interestingly, stimulation in growth at less than $100 \mu\text{M}$ potassium dichromate was observed in *Synechococcus*. Thompson et al. (2002) have compared *Synechococcus* PCC 7942 and *Nostoc* PCC 7120 for resistance to chromate under high and low density conditions and have shown that there is general decrease in toxicity in dense cultures. But studies on chromate uptake and/or efflux mechanism in the cyanobacteria have not been carried out. In the present study di-phenyl carbazide (DPC) assay showed that these two cyanobacteria were not chromate reducers, and hence uptake studies using ^{51}Cr chromate were carried out as it is more

sensitive method than DPC assay. Only nanomolar concentration of chromate accumulation was detected in *Synechocystis* over 24 hours by its log phase culture. Although in *Synechococcus*, no chromate accumulation could be observed under the conditions tested, stimulation of growth at lower chromate concentration entailed that *Synechococcus* was able to sense the presence of low concentration of chromate in the growth medium. Lesser extent of ultrastructural damage in *Synechococcus* supported this argument.

It is known that chromate ion enters the cells using sulfate transporters present in cell membrane as chromate ion is nearly identical in size, shape and charge as sulfate ion (Riedel 1985). Also, chromate efflux by *chr* homologues has been reported in some cyanobacteria including the strains used in the present study. Therefore, inhibition of sulfate uptake due to presence of chromate in the growth medium was determined using ³⁵sulfate and IC₅₀ values were calculated. IC₅₀ values of chromate in both *Synechococcus* and *Synechocystis* were dependent on sulfate concentration in medium indicating that sulfate uptake was competitively inhibited by chromate in both the cases. The inhibition of sulfate uptake by chromate suggested an interaction of chromate ions with sulfate uptake mechanism. However, the IC₅₀ value of chromate was much higher in *Synechococcus* as compared to *Synechocystis* showing that sulfate uptake receptors of *Synechocystis* have higher affinity for chromate as compared to those of *Synechococcus*.

Intracellular chromate content was monitored in *Synechocystis* and *Synechococcus* after growth for 9 days in the medium containing respective EC₅₀ concentrations i.e. 12 and 150 μM of potassium dichromate with ⁵¹chromate as tracer. Both *Synechococcus* and *Synechocystis* showed chromate concentration of 4-6 nmoles/10⁸ cells showing that *Synechococcus* accumulated proportionately lesser chromate at 150 μM; while

Synechocystis accumulated more at a much lower concentration of 12 μM potassium dichromate. Chromate is known to impart oxidative stress to living organisms. Oxidative stress markers were monitored in *Synechocystis* and *Synechococcus* after growth for 9 days in the medium containing respective EC_{50} concentrations i.e. 12 and 150 μM of potassium dichromate. Basal levels of antioxidant activities in the two cyanobacteria were also compared to understand the basis of contrasting tolerance. Further, whether growth with chromate gives additional advantage to the cyanobacteria to deal with oxidative stress was examined. A relatively tolerant response to potassium dichromate was observed in *Synechococcus* with stimulation in growth at low concentration of chromate. The increase in ROS at higher chromate concentrations where growth is reduced in *Synechococcus* indicated that the reason for such a response could be the inability of *Synechococcus* to cope with the chromate toxicity which manifests itself by causing oxidative stress inside the cells. Also, one more plausible reason could be a better chromate efflux mechanism working in *Synechococcus* which keeps chromium out or under tolerable limits up to 150 μM concentration in the medium. Therefore, a better machinery to keep chromate out and a better machinery to take care of oxidative stress make it more tolerant. In contrast, *Synechocystis* showed higher chromium content inside cells which probably led to free radical generation and hence the response was observed from low chromate concentrations itself. It may be concluded that chromate efflux system of *Synechocystis* may not be as strong as in *Synechococcus*.

Free radicals are byproducts of aerobic metabolism; for cyanobacteria it is respiratory and photosynthetic electron transport chains which are the sources of free radicals and are vulnerable to the damage caused by them. The effect of prolonged oxidative stress due to growth with chromate on structure function of photosynthetic apparatus in

Synechocystis and *Synechococcus* was explored. In addition, sulfate imbalance caused due to presence of chromate in the medium could also cause metabolic adjustments. Therefore photosynthetic parameters were studied in the chromate adapted versus control cultures of the two cyanobacteria. Although, previously effects of chromate have been investigated in different photoautotrophs on various aspects of photosynthesis, they mainly dealt with effect of acute chromate stress. We therefore undertook detailed analysis of photosynthetic machinery in response to growth with chromate in *Synechocystis* and *Synechococcus*.

This comparison enabled identification of similarities and contrast in the photosynthetic parameters of *Synechocystis* and *Synechococcus* as well as effect of chronic oxidative stress in the two cyanobacteria.

Presence of chromate in growth medium affected the thylakoid membranes and ultrastructure in *Synechocystis* to a higher extent as compared to *Synechococcus*. Chromate also affected morphology of cells. *Synechocystis* showed higher rates of CO₂ fixation and PSII and PSI activities on chlorophyll basis as compared to *Synechococcus*. Chromate up to 100 µM was found to stimulate growth in *Synechococcus* also showed higher rates of CO₂ fixation and PSII and PSI activities as compared to control. Earlier such stimulation of growth and photosynthesis has been observed by Tiwari et al. (1996) in case of *Synechocystis* at lower concentrations of Cobalt chloride in growth media.

Photochemical and biochemical studies showed that major photosynthetic functions were maintained in *Synechococcus* cells on growth with chromate by making adjustments in the photosynthetic apparatus. Photosynthetic pigment levels showed a decline in both the cyanobacteria at EC₅₀ concentration, with not much effect on *Synechococcus* grown with 75 µM concentration. Signature fluorescence emission

spectra with general decrease in chlorophyll fluorescence intensity were observed due to decrease in pigment content per cell. In *Synechococcus*, growth with 150 μM chromate caused dissociation of PSII. 77 K fluorescence emission studies also showed adjustments in the PBS-PSII/PSI association due to growth with chromate. In *Synechococcus*, growth with chromate also caused decrease in mobility of phycobilisomes.

In both the cyanobacteria, PSII was more sensitive to chromate stress as compared to PSI, which is in agreement with the earlier studies on effect of chromate on photosynthesis. PSII in *Synechocystis* was more sensitive to chromate as compared to PSII in *Synechococcus* at the respective EC_{50} concentrations showing the inherent differences in PSII from the two cyanobacteria. Thus the sensitivity of *Synechocystis* may be attributed also to damage to PSII. These differences also entailed that the damage and repair of PSII may be different in the two cyanobacteria.

Photosynthetic parameters were also studied *in vivo* in response to chromate by the noninvasive technique of PAM fluorometry which signaled adjustments or adaptation in *Synechococcus* and *Synechocystis* in response to growth with chromate. On growth with chromate, both the cyanobacteria showed significant decrease in F_v/F_m , an index of maximal photochemical efficiency. PSII in *Synechocystis* was affected by chromate and not PSI as shown by decrease in the effective quantum yield of PSII. The results suggested that in *Synechocystis*, PSII was more affected when cells were grown in presence of chromate as compared to *Synechococcus*. The light curves which probe the effect of light on the electron transport rates in PSII and PSI in presence of chromate indicated that ETR(II) in *Synechocystis* was shown to be affected the most in response to chromate whereas ETR(I) remained similar to control. *Synechococcus* grown with chromate showed a rise in both ETR(II) and ETR(I) with increasing light indicating an

adaptive response which did not vary with increase in chromate from 75 to 150 μM dichromate. PSII showed a decline in *Synechocystis* and an increase in PSI in both the cyanobacteria as shown by the light curves.

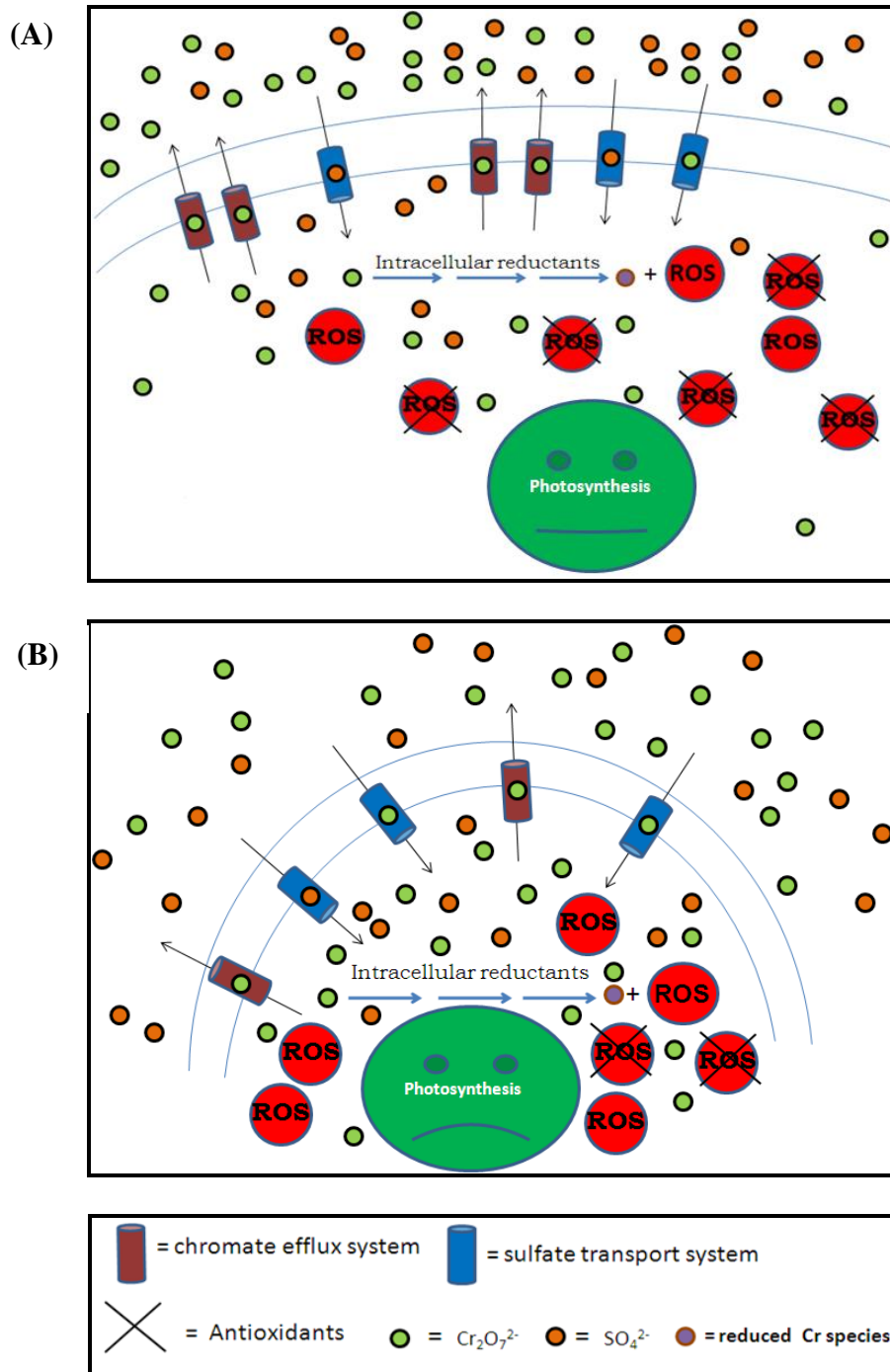
Chromate decreased active PSI in *Synechocystis* but not in *Synechococcus* suggesting adjustments or adaptations which were different in the two cyanobacteria. Deeper insight was provided by slow kinetics and light curves. PSII in *Synechocystis* was affected by chromate and not PSI as shown by decrease in the effective quantum yield of PSII, although Y(ND) and Y(NA) were affected. Y(NO), an indicator of PSII damage was found to be slightly higher in *Synechocystis* in response to chromate. Decrease in the value of Y(II)/Y(I) in *Synechocystis* and increase in *Synechococcus* indicated shift in the balance of distribution of quantum yield between two photosystems. CEF was stimulated in both the cyanobacteria causing a rise in Y(CEF)/Y(I) which was also shown by higher ETR(I) in response to chromate.

The studies in thylakoid membrane damage and repair, however, revealed a new paradigm. *Synechocystis* which was more sensitive to chromate showed decreased sensitivity to high light stress in its chromate grown cells. *Synechococcus* which was inherently more resistant to photoinhibition succumbed more to high light if cells were grown with chromate. The results suggested that in *Synechococcus* the cellular machinery was engaged in tolerating high levels of chromate in medium and therefore did not have enough resources to tolerate any additional oxidative stress.

Thus the studies on structure –function of photosynthetic machinery in *Synechocystis* and *Synechococcus* showed that there were differences in their photosynthetic super complexes and their *in vivo* functions. These two unicellular cyanobacteria also showed differences in the components of their photosynthetic machinery after prolonged exposure to chromate. The adaptability of the photosynthetic apparatus to chromate

especially in *Synechococcus* showed the sturdiness and stress tolerance of this strain of cyanobacteria. The results and the possible inferences are summarized in **figure 6.1**. The figure shows that in *Synechococcus* because of lower affinity of sulfate transporters to chromate, less of chromate gets in the cells, and because of efficient ROS scavenging machinery, the oxidative stress is managed better and hence photosynthetic parameters and in turn photosynthetic machinery is less affected at higher chromate concentration. On the contrary, in *Synechocystis* the sulfate transporters have higher affinity for chromate and allow more chromate ions inside the cell which would cause higher oxidative damage to photosynthetic apparatus affecting growth even at lower chromate concentration. Additionally the chromate efflux systems also could be playing important role in differential chromate tolerance in the two cyanobacteria.

Thus the studies showed that growth with chromate resulted in differential metabolic adjustments in these two cyanobacteria affecting the structure-function of photosynthetic machinery. This is first report on detailed investigations on the effect of chromate on growth, chromate and sulfate uptake and photosynthetic machinery in *Synechocystis vis a vis Synechococcus*.

Figure 6.1: Interaction of chromate with *Synechococcus* and *Synechocystis*

Schematic representation of the inferences drawn from the experimental results obtained. The sizes of ions and other entities may not be up to scale. (A) Events in *Synechococcus* grown with 150 μM of potassium dichromate. (B) Events in *Synechocystis* grown with 12 μM of potassium dichromate.

The very first step of photosynthesis; charge separation and transfer of excitation energy has inspired extensive research in exploring the natural light harvesting complexes (LHC) for their potential use in artificial photosynthesis. Mulder et al. (2009) have shown use of phycobilisomes in luminescent solar concentrators. Therefore isolation of phycocyanobilin (PCB) and phycocyanin-allophycocyanin (PC-APC) from a local isolate of *Synechococcus*, *Anacystis nidulans* BD1 was optimized. Higher tolerance of *Synechococcus* to chromate led us to analyze PC-APC from cultures grown in presence of chromate using the methods optimized in *A. nidulans* BD1. The PC-APC complex did not show any differences in terms of subunit composition and basic biophysical characteristics. However, the antenna functionality and energy transfer by PC-APC (from *A. nidulans* BD1) to ZnO quantum dots and also studies on electron transfer from PCB to TiO₂ nanoparticles can be new vistas of research. Efforts can be channelized to find out ways to stabilize these natural light harvesters for their practical use.

The contrasting characteristics observed in the two cyanobacteria would be useful in understanding the complex relationship of chromate and sulfate transporters. Further studies are needed to comprehend the phenomenon of stimulation of growth and morphological changes in *Synechococcus* at low concentration of chromate although no chromate uptake was observed in this organism. Identification of chromate sensitive mutant of *Synechococcus* or chromate resistant mutant in *Synechocystis* may be an approach to identify gene(s) for chromate tolerance. Although at this stage it appears that the multifarious interaction of sulfate/chromate transporters could be the basis of contrasting response of *Synechococcus* and *Synechocystis* to chromate and isolation of single mutations may not be possible. It will be interesting to explore the transcriptome, proteomes and metabolome in these two cyanobacteria in response to chromate stress.

List of references

Abed RM, Dobretsov S, Sudesh K. Applications of cyanobacteria in biotechnology. *J Appl Microbiol*. 2009;106(1):1-12. doi: 10.1111/j.1365-2672.2008.03918.x.

Agarwal R, Matros A, Melzer M, Mock HP, Sainis JK. Heterogeneity in thylakoid membrane proteome of *Synechocystis* 6803. *J Proteomics*. 2010;73(5):976-91.

Agarwal R. Physico-chemical Characterization and Biogenesis of Photosomes and Thylakoid Membranes from *Synechocystis* 6803, Ph D Thesis HBNI, Mumbai, (LIFE01200704003). 2011; 5: 140-166.

Agarwal R, Maralihalli G, Sudarsan V, Choudhury SD, Vatsa RK, Pal H, Melzer M, Sainis JK. Differential distribution of pigment-protein complexes in the Thylakoid membranes of *Synechocystis* 6803. *J Bioenerg Biomembr*. 2012;44(4):399-409.

Aguilar-Barajas E, Ce'sar Di'az-Pe'rez C, Ramirez-Diaz M, Riveros-Rosas H, Cervantes C (2011) Bacterial transport of sulfate, molybdate, and related Oxyanions. *Biometals*. 2011;24:687-707.

Aguilar-Barajas E, Jeronimo-Rodriguez P, Ramirez-Diaz MI, Rensing C, Cervantes C. The ChrA homologue from a sulfur-regulated gene cluster in cyanobacterial plasmid pANL confers chromate resistance. *World J Microbiol Biotechnol*. 2012;28: 865-869.

Ali NA, Ater M, Sunahara GI, Robidoux PY. Phytotoxicity and bioaccumulation of copper and chromium using barley (*Hordeum vulgare* L.) in spiked artificial and natural forest soils. *Ecotox Environ Safe*. 2004;57(3):363-374.

Ali NA, Dewez D, Didur O, Popovic R. Inhibition of photosystem II photochemistry by Cr is caused by the alteration of both D1 protein and oxygen evolving complex. *Photosynth Res*. 2006;89(2-3):81-7.

Allen JF, Forsberg J. Molecular recognition in thylakoid structure and function. *Trends Plant Sci*. 2001;6(7):317-26.

Alvarez AH, Moreno-Sanchez R, Cervantes C. Chromate efflux by means of the ChrA chromate resistance protein from *Pseudomonas aeruginosa*. *J Bact.* 1999;181:7398–7400.

Anjana K, Anubha K, Kiran B, Nisha R. Biosorption of Cr (VI) by immobilized biomass of two indigenous strains of cyanobacteria isolated from metal contaminated soil. *J Hazard Matter.* 2007;148:383–386.

Appenroth KJ, Stöckel J, Srivastava A, Strasser RJ. Multiple effects of chromate on the photosynthetic apparatus of *Spirodela polyrhiza* as probed by OJIP chlorophyll a fluorescence measurements. *Environ Pollut.* 2001;115(1):49-64.

Ashraf M, Harris PJC. Photosynthesis under stressful environments: An overview. *Photosynthetica.* 2013; 51 (2): 163-190.

Beauchamp C, Fridovich. Superoxide dismutase: improved assays and an assay applicable to acrylamide gels. *Anal. Biochem.* 1971;44:276–287.

Bennett A, Bogorad L. Complementary chromatic adaptation in a filamentous blue-green alga. *J Cell Biol.* 1973;58:419–435.

Berry EA, Guergova-Kuras M, Huang L, Crofts LR. Structure and function of cytochrome *bc* complexes. *Annu. Rev. Biochem.* 2000; 69: 1005–75.

Berera R, Grondelle R, Kennis JTM. Ultrafast transient absorption spectroscopy: principles and application to photosynthetic systems. *Photosynth Res.* 2009;101:105–118.

Bertrand M and Poirier I. Photosynthetic organisms and excess of metals. *Photosynthetica.* 2005; 43 (3): 345-353.

Bielicka A, Bojanowska I, Wiśniewski A. Two faces of chromium - Pollutant and Bioelement. *Pol J Environ Stud.* 2005;14(1):5-10.

Biesiadka J, Loll B, Kern J, Irrgang KD and Zouni A. Crystal structure of cyanobacterial photosystem II at 3.2 Å resolution: a closer look at the Mn-cluster. *Phys. Chem. Chem. Phys.* 2004;6: 4733 – 36.

Blankenship RE. *Molecular mechanisms of photosynthesis*. Blackwell Science, Oxford 2002.

Boyer PD. Catalytic site forms and controls in ATP synthase catalysis. *Biochim Biophys Acta.* 2000;1458(2-3):252-62.

Bryant DA, Guglielmi G, Tandeau de marsac N, Castlets AM, Cohen-Bazire G. The structure of cyanobacterial phycobilisomes:a model. *Arch Microbiol.* 1979;123:113–127.

Campbell D, Eriksson MJ, Oquist G, Gustafsson P, Clarke AK. The cyanobacterium *Synechococcus* resists UV-B by exchanging photosystem II reaction-center D1 proteins. *Proc Natl Acad Sci U S A.* 1998;95(1):364-9.

Campbell D, Zhou G, Gustafsson P, Oquist G, Clarke AK. Electron transport regulates exchange of two forms of photosystem II D1 protein in the cyanobacterium *Synechococcus*. *EMBO J.* 1995;14(22):5457-66.

Cervantes C, Campos-García J, Devars S, Gutiérrez-Corona F, Loza-Tavera H, Torres-Guzmán JC, Moreno-Sánchez R. Interactions of chromium with microorganisms and plants. *FEMS Microbiol Rev.* 2001;(3):335-47.

Cheung KH, Gu J. Mechanism of hexavalent chromium detoxification by microorganisms and bioremediation application potential: A review. *Int Biodeterior Biodegrad.* 2007;59: 8–15.

Choo TP, Lee CK, Low KS, Hishamuddin O. Accumulation of chromium (VI) from aqueous solutions using water lilies (*Nymphaea spontanea*). *Chemosphere.* 2006;62(6):961-7.

Collings AF, Critchley C. Artificial photosynthesis. From basic biology to industrial application. 2005, Wiley-VCH Verlag GmbH and Co. KGaA.

Dani DN, Sainis JK. Isolation and characterization of a thylakoid membrane module showing partial light and dark reactions. *Biochim Biophys Acta*. 2005;1669(1):43-52.

Davies Jr. FT, Puryear JD, Newton RJ, Egilla JN, Saraiva Grossi JA. Mycorrhizal fungi enhance accumulation and tolerance of chromium in sunflower (*Helianthus annuus*). *J Plant Physiol*. 2001;158:177-186.

Dismukes GC, Klimov VV, Baranov SV, Kozlov YN, DasGupta J, Tyrshkin A. The origin of atmospheric oxygen on Earth: the innovation of oxygenic photosynthesis. *Proc Natl Acad Sci USA*. 2001;98(5):2170-5.

Duffus JH. Heavy metals – meaningless term? *IUPAC, Pure Appl. Chem*. 2002;74:793-807.

Eocha C Ó. Spectral properties of the phycobilins. I. phycocyanobilin. *Biochemistry*. 1963;2(2):375–382.

Eriksen NT. Production of phycocyanin—a pigment with applications in biology biotechnology foods and medicine. *Appl Microbiol Biotechnol*. 2008; 80:1–14.

Fiore MF, Trevors JT. Cell composition and metal tolerance in cyanobacteria. *Biometals* 1994;7(2):83-103.

Foyer CH, Shigeoka S. Understanding oxidative stress and antioxidant functions to enhance photosynthesis. *Plant Physiol*. 2011;155(1):93-100. doi: 10.1104/pp.110.166181.

Fromme P, Jordan P, Krauss N. Structure of photosystemI. *Biochim. Biophys. Acta*. 2001; 1507: 5-31.

Fu E, Friedman L, Siegelman HW. Mass-spectral identification and purification of phycoerythrobilin and phycocyanobilin. *Biochem J.* 1979;179:1–6.

Garnham MW, Green M. Chromate (VI) uptake and interactions with cyanobacteria. *J Ind Microbiol.* 1995;14: 247-251.

Govindjee, Shevela D. Adventures with cyanobacteria: a personal perspective. *Front Plant Sci.* 2011;2:28. doi: 10.3389/fpls.2011.00028.

Grossman AR, Schaefer MR, Chiang GG, Collier JL. The phycobilisome, a light-harvesting complex responsive to environmental conditions. *Microbiol Rev.* 1993;57(3):725-49.

*Gupta A, Sainis JK. Isolation of C-phycocyanin from *Synechococcus* sp., *Anacystis nidulans* BD1. *J Appl Phycol.* 2010; 22(3): 231-233.

*Gupta A Bhagwat SG, Sainis JK. *Synechococcus elongatus* PCC 7942 is more tolerant to chromate as compared to *Synechocystis* sp. PCC 6803; *Biometals.* 2013 DOI 10.1007/s10534-013-9614-6.

Hagemann M. Molecular biology of cyanobacterial salt acclimation. *FEMS Microbiol Rev.* 2011;35(1):87-123. doi: 10.1111/j.1574-6976.2010.00234.x.

He YY, Häder DP. UV-B-induced formation of reactive oxygen species and oxidative damage of the cyanobacterium *Anabaena* sp.: protective effects of ascorbic acid and N-acetyl-L-cysteine. *J Photochem Photobiol B.* 2002;66(2):115-24.

Huang W, Zhang SB, Cao KF. Stimulation of cyclic electron flow during recovery after chilling-induced photoinhibition of PSII. *Plant Cell Physiol.* 2010;51:1922–1928.

Italiano F, Rinalducci S, Agostiano A, Zolla L, De Leo F, Ceci L, Trotta M. Changes in morphology, cell wall composition and soluble proteome in *Rhodobacter sphaeroides* cells exposed to chromate. *Biometals.* 2012. doi 10.1007/s10534-012-9561-7.

Jeanjean R, Matthijs HCP, Onana B, Havaux M, Joset F. Exposure of the Cyanobacterium *Synechocystis* PCC6803 to Salt Stress Induces Concerted Changes in Respiration and Photosynthesis Plant Cell Physiol. 1993; 34 (7): 1073-1079.

Kamaludeen SP, Arunkumar KR, Avudainayagam S, Ramasamy K. Bioremediation of chromium contaminated environments. Indian J Exp Biol. 2003;41(9):972-85.

Khattar JIS, Sarma TA, Sharma A. Effect of Cr⁶⁺ Stress on Photosynthetic Pigments and Certain Physiological Processes in the Cyanobacterium *Anacystis nidulans* and its Chromium Resistant Strain. J Microbial Biotechnol. 2004;14:1211-1216.

Kiran B, Kaushik A and Kaushik CP. Response surface methodological approach for optimizing removal of Cr (VI) from aqueous solution using immobilized cyanobacterium. Chem Eng J. 2007;126:147–153.

Kiran B, Kaushik A, Kaushik CP. Chromium (VI) tolerance in two halotolerant strains of Nostoc. J Environ Biol. 2008;29:155-158.

Klughammer C, Schreiber U. An improved method, using saturating light pulses, for the determination of photosystem I quantum yield via P700⁺-absorbance changes at 830nm. Planta. 1994;192:261–268.

Klughammer C, Schreiber U. Saturation pulse method for assessment of energy conversion in PS I. PAM Appl. Notes. 2008b;1:11–14.

Krieger A, Rutherford AW. The involvement of H₂O₂ produced by photosystem II in photoinhibition. In G Garab, ed, Photosynthesis: Mechanisms and Effects, Kluwer Academic Publishers, Dordrecht, The Netherlands. 1998; 3:2135–2213.

Laemmli UK. Cleavage of structural protein during assembly of the head of Bacteriophage T4. Nature. 1970;227:680–685.

Langård S. One hundred years of chromium and cancer: a review of epidemiological evidence and selected case reports. Am J Ind Med. 1990;17(2):189-215.

Latifi A, Ruiz M, Zhang CC. Oxidative stress in cyanobacteria. *FEMS Microbiol Rev.* 2009;33(2):258-78.

Liochev SI, Fridovich I. Superoxide and iron: partners in crime. *IUBMB Life.* 1999;48(2):157-61.

Liu XG, Zhao JJ, Wu QY. Oxidative stress and metal ions effects on the cores of phycobilisomes in *Synechocystis* sp. PCC 6803. *FEBS Lett.* 2005;579(21):4571-6.

Lowry OH, Rosebrough NJ, Farr AL, Randall RJ. Protein measurement with the Folin phenol reagent. *J Biol Chem.* 1951;193(1):265-75.

Mulder CL, Theogarajan L, Currie M, Mapel JK, Baldo MA, Vaughn M, Willard P, Bruce BD, Moss MW, McLain CE, Morseman JP. Luminescent solar concentrators employing phycobilisomes. *Adv Mater.* 2009;21:1-5.

Murata N, Sato N, Omata T, Kuwabara T. Separation and characterization of thylakoid and cell envelope of the blue-green Alga (Cyanobacterium) *Anacystis nidulans*. *Plant Cell Physiol.* 1981;22(5):855-866.

Nies DH, Koch S, Wachi NP, Saier MJ. CHR, a Novel Family of Prokaryotic Proton Motive Force-Driven Transporters Probably Containing Chromate/Sulfate Antiporters. *J Bact.* 1995;180: 5799-5802.

Nishiyama Y, Allakhverdiev SI, Yamamoto H, Hayashi H, Murata N. Singlet oxygen inhibits the repair of photosystem II by suppressing the translation elongation of the D1 protein in *Synechocystis* sp. PCC 6803. *Biochemistry.* 2004;43(35):11321-30.

Nishiyama Y, Allakhverdiev SI, Murata N. A new paradigm for the action of reactive oxygen species in the photoinhibition of photosystem II. *Biochim Biophys Acta.* 2006;1757(7):742-9.

Nixon PJ, Michoux F, Yu J, Boehm M, Komenda J. Recent advances in understanding the assembly and repair of photosystem II. *Ann Bot.* 2010;106:1-16.

Oláh V, Lakatos G, Bertók C, Kanalas P, Szöllősi E, Kis J, Mészáros I. Short-term chromium(VI) stress induces different photosynthetic responses in two duckweed species, *Lemna gibba* L. and *Lemna minor* L. *Photosynthetica*. 2010;48(4):513-520.

Ozturk S, Aslim B, Suludere Z. Evaluation of chromium (VI) removal behavior by two isolates of *Synechocystis* sp. in terms of exopolysaccharide (EPS) production and monomer composition. *Bioresource Technology*. 2009;100:5588-5593.

Pan XL, Chen X, Zhang DY, Wang JL, Deng CN, Mu GJ, Zhu HS. Effect of chromium(VI) on photosystem II activity and heterogeneity of *Synechocystis* sp. (cyanophyta): studied with in vivo chlorophyll fluorescence tests. *J Phycol.* 2009;45:386–394.

Pascual MB, Mata-Cabana A, Florencio FJ, Lindahl M, Cejudo FJ. Overoxidation of 2-Cys peroxiredoxin in prokaryotes: cyanobacterial 2-Cys peroxiredoxins sensitive to oxidative stress. *J Biol Chem*. 2010;285(45):34485-92.

Perreault F, Ait Ali N, Saison C, Popovic R, Juneau P. Dichromate effect on energy dissipation of photosystem II and photosystem I in *Chlamydomonas reinhardtii*. *J Photochem Photobiol B*. 2009;96(1):24-9.

Pospíšil P, Arató A, Krieger-Liszkay A, Rutherford AW. Hydroxyl radical generation by photosystem II. *Biochemistry*. 2004;43(21):6783-92.

Patil G, Chethana S, Sridevi AS, Raghavarao KSMS. Method to obtain C-phycoyanin of high purity. *J Chromatogr A*. 2006;1127:76–81.

Prasad SM, Singh JB, Rai LC, Kumar HD. Metal-induced inhibition of photosynthetic electron transport chain of the cyanobacterium *Nostoc muscorum*. *FEMS Microbiol Lett*. 1991; 82(1):95–100.

Rami´rez-Dí´az MI, Diaz-Perez C, Cervantes C. Mechanisms of bacterial resistance to chromium compounds. *Biometals*. 2008;21:321-332.

Reynolds ES. The use of lead citrate at high pH as electron-opaque stain for electron microscopy. *J Cell Biol.* 1963;17: 208-212.

Riedel GF. The relationship between chromium (VI) uptake, sulfate uptake and chromium (VI) toxicity in the estuarine diatom *Thalassiosira pseudonana*. *Aquat Toxicol.* 1985;7:191-204.

Rippka R, Deruelles J, Waterbury J, Herdman M, Stanier R. Generic assignments strain histories and properties of pure cultures of cyanobacteria. *J Gen Microbiol.* 1979;111: 1-61.

Sainis JK, Melzer M. Supramolecular organization of water-soluble photosynthetic enzymes along the thylakoid membranes in chloroplasts. In Pessaraki M, ed, *Handbook on Photosynthesis*, Boca Raton, CRC Press Taylor & Francis. 2005; 259–272.

Shcolnick S, Keren N. Metal homeostasis in cyanobacteria and chloroplasts. Balancing benefits and risks to the photosynthetic apparatus. *Plant Physiol.* 2006;141(3):805-10.

Stanier RY, Cohen-Bazire G. Phototrophic prokaryotes: the cyanobacteria. *Annu Rev Microbiol.* 1977;31:225-74.

Singh NK, Parmar A, Madamwar D. Optimization of medium components for increased production of C-phycoerythrin from *Phormidium ceylanicum* and its purification by single step process. *Bioresour Technol.* 2009;100:1663–1669.

Suzuki K, Ohmori, Y, Ratel E. High root temperature blocks both linear and cyclic electron transport in the dark during chilling of the leaves of rice seedlings. *Plant Cell Physiol.* 2011;52: 1697–1707.

Tabita FR, Caruso P, Whitman W. Facile assay of enzymes unique to the Calvin cycle in intact cells, with special reference to ribulose 1,5-bisphosphate carboxylase. *Anal Biochem.* 1978;84(2):462-72.

- Tandeau de Marsac N, Houmard J. Adaptation of cyanobacteria to environmental stimuli: new steps towards molecular mechanisms. *FEMS Microbiol Rev.* 1993;104: 119-190.
- Tandeau de Marsac N, Houmard J. Complementary chromatic adaptation: Physiological conditions and action spectra. In: *Methods in Enzymology, Cyanobacteria.* eds: Packer L and Glazer AN. 1988;167:318-328, Academic Press Inc.
- Thompson SL, Manning FCR, McColl SM. Comparison of the Toxicity of Chromium III and Chromium VI to Cyanobacteria. *Bull Environ Contam and Toxicol.* 2002;69: 286-293.
- Tiwari S, Mohanty P. Cobalt induced changes in photosystem activity in *Synechocystis* PCC 6803: alterations in energy distribution and stoichiometry. *Photosynth Res.* 1996;50(3): pp 243-256.
- Turrens JF. Mitochondrial formation of reactive oxygen species. *J Physiol.* 2003;552(2):335-44.
- Urone PF. Stability of Colorimetric Reagent for Chromium, s-Diphenylcarbazide, in various solvents. *Anal Chem.* 1955; 27:1354-1355.
- USEPA. Toxicological Review of Hexavalent Chromium. USEPA. 1998.
- Vajpayee P, Sharma SC, Tripathi RD, Rai UN, Yunus M. Bioaccumulation of chromium and toxicity to photosynthetic pigments, nitrate reductase activity and protein content of *Nelumbo nucifera* Gaertn. *Chemosphere.* 1999; 39(12):2159–2169.
- Vajpayee P, Tripathi RD, Rai UN, Ali MB, Singh SN. Chromium (VI) accumulation reduces chlorophyll biosynthesis, nitrate reductase activity and protein content in *Nymphaea alba* L. *Chemosphere.* 2000;41:1075-1082.
- Vermaas WFJ. Photosynthesis and respiration in cyanobacteria. *Enc Lif Sci.* 2001; doi: 10.1038/npg.els.0001670.

Verma S, Gupta A, Sainis JK, Ghosh HN. "Interfacial electron transfer dynamics in phycocyanobilin sensitized TiO₂ nanoparticles" at Conference-Frontiers in Photobiology, B.A.R.C, Mumbai. August 24 – 26, 2009; Abstract No. PB – 23:88.

Verma S, Gupta A, Sainis JK, Ghosh HN. Employing a photosynthetic antenna complex to interfacial electron transfer on ZnO quantum dot. *J Phys Chem Lett.* 2011;2:858-862.

Wang S, Chen F, Mu S, Zhang D, Pan X, Lee DJ. Simultaneous analysis of photosystem responses of *Microcystis aeruginosa* under chromium stress. *Ecotoxicol Environ Saf.* 2013;88:163-8.

Weydert CJ, Cullen JJ. Measurement of superoxide dismutase, catalase and glutathione peroxidase in cultured cells and tissue. *Nat Protoc.* 2010;5(1):51-66.

Wittig I, Braun HP, Schägger H. Blue native PAGE. *Nat Protoc.* 2006;1(1):418-28.

Xiao R, Ghosh S, Tanaka AR, Greenberg BM, Dumbroff EB. A rapid spectrophotometric method for measuring photosystem I and photosystem II activities in a single sample. *Plant Physiol Biochem.* 1997;359(5):411-417.

Yewalkar SN, Dhumal KN, Sainis JK. Chromium (VI)-reducing *Chlorella* spp. isolated from disposal sites of paper-pulp and electroplating industry. *J Appl Phycol.* 2007;19: 459-465.

* Published from the thesis work

Reprints of published articles
(from the thesis)

Isolation of C-phycoyanin from *Synechococcus* sp., (*Anacystis nidulans* BD1)

Alka Gupta · Jayashree K. Sainis

Received: 8 April 2009 / Revised and accepted: 4 May 2009 / Published online: 23 May 2009
© Springer Science + Business Media B.V. 2009

Abstract We report a procedure for obtaining fairly pure phycocyanin from a local isolate of the cyanobacterium *Synechococcus* sp (*Anacystis nidulans* BD1). Cells were incubated with $1 \text{ mg}\cdot\text{mL}^{-1}$ of lysozyme at 37°C for 16 h with shaking. The cell-free extract was treated with activated charcoal and chitosan. The purity (A_{620}/A_{280}) of phycocyanin obtained after lysozyme treatment was up to 2.18, which could be improved to 4.72 after incubation with activated charcoal and chitosan. The yield of phycocyanin was $80\text{--}100 \text{ mg}\cdot\text{g}^{-1}$ dry weight of cells. The method reported here is a single-step and efficient procedure and has the potential to be adopted for large-scale production of phycocyanin.

Keywords *Anacystis nidulans* · Cyanobacteria · Charcoal · Chitosan · Lysozyme · Phycocyanin-isolation · *Synechococcus* sp.

Introduction

In the Cyanobacteria, Cryptophyta, and Rhodophyta, phycocyanin and related phycobiliproteins are assembled in supramolecular aggregates known as phycobilisomes for efficient energy transfer to chlorophyll–protein complexes located at the thylakoid membrane. Phycocyanin (PC) is a blue-colored, major light harvesting pigment in these organisms. Phycocyanin and related phycobiliproteins are used in the food, biotechnology, and cosmetic industry because of their color and fluorescent and antioxidant

properties (Sekar and Chandramohan 2007). Phycocyanin has been extracted and purified from *Spirulina platensis*, *S. fusiformis*, *S. maxima*, *Synechococcus* sp., *Oscillatoria quadripunctulata*, *Aphanizomenon flos-aquae*, and *Phormidium fragile* and it is produced commercially from *S. platensis*, *Anabena*, and *Galdieria sulphuraria* (Eriksen 2008). About 50–90% of the production cost of phycobilins resides in the purification steps (Patil et al. 2006). There exists a need for high-yielding strains and cost-effective simple methods to produce phycocyanin (Singh et al. 2009).

Extraction of phycocyanin from cyanobacteria involves disintegration of cells using sonication, freeze thawing, occasionally enzymatic treatment and also using dried cells for extraction. The purification of this pigment protein complex is done by ammonium sulfate precipitation combined with a variety of procedures using hydrophobic, ion exchange, and size exclusion, and hydroxyapatite chromatography and also aqueous two-phase extraction (Eriksen 2008). The efficiency of phycocyanin extraction is dependent on the level of cell-wall disintegration as these proteins are regularly arranged in parallel rows on the thylakoid membrane. Since phycobiliproteins are water soluble, harsh cell disruption procedures release several other proteins resulting in a lower purity ratio (A_{620}/A_{280}) in crude extracts which leads to increase in number of purification steps with concomitant decrease in yield.

In the present study, we report a single-step procedure to isolate and purify phycocyanin with relatively higher purity ratio and better yield from *Anacystis nidulans*.

Materials and methods

A local isolate of freshwater cyanobacterium, *Anacystis nidulans* BD1, (now classified as *Synechococcus* sp.

A. Gupta · J. K. Sainis (✉)
Molecular Biology Division, Bhabha Atomic Research Centre,
Mumbai 400 085, India
e-mail: jksainis@barc.gov.in

Table 1 Isolation and purification of C-Phycocyanin from *Anacystis nidulans* BD1

Sample	Purity ($A_{620/280}$)	Purity ($A_{620/650}$)	CPC ($\text{mg}\cdot\text{mL}^{-1}$)	Yield of CPC (%)
Crude extract	2.18	0.97	1.12	100
After activated charcoal and chitosan treatment	4.72	2.3	1.01	90.1

$A_{620/280}$ indicates purity of phycocyanin against total protein and $A_{620/650}$ indicates purity against allophycocyanin.

according to Rippka et al. 1979) obtained from rice fields of Trombay, Mumbai and other standard strains of unicellular cyanobacteria *Synechococcus* 7942 and *Synechocystis* 6803 were cultured in BG 11 medium (Rippka et al. 1979) at $26\pm 2^\circ\text{C}$ under continuous illumination provided by cool white fluorescent lights with intensity of $21\text{ W}\cdot\text{m}^{-2}$. For rapid growth, the cultures were continuously bubbled with sterile air.

The cells were grown for 5 days and were harvested by centrifugation at $6,000\times g$ at room temperature for 15 min. The cell pellet (corresponding to $\sim 10\text{ mg}$ dry biomass) was washed with distilled water and re-suspended in 1 mL HEPES buffer (100 mM HEPES, 1 mM EDTA, pH 8.0) containing $1\text{ mg}\cdot\text{mL}^{-1}$ of lysozyme (Sigma-Aldrich; $50,000\text{ units mg}^{-1}$ protein, 95% protein) and incubated at 37°C for 16 h with shaking. The slurry obtained was centrifuged at $6,000\times g$ at 4°C for 15 min to separate the blue supernatant containing phycocyanin from the cell mass. Ten milligrams of activated charcoal powder and $15\ \mu\text{L}$ of 2% chitosan solution prepared in distilled water was added per milliliter of crude extract containing $\sim 1\text{ mg}\cdot\text{mL}^{-1}$ phycocyanin and incubated at 4°C for 4 h with gentle vortexing in between. Activated charcoal powder was washed thoroughly with distilled water before usage. The extract was centrifuged at $11,000\times g$ at 4°C for 10 min. The contents of phycocyanin and allophycocyanin were calculated by spectrophotometric absorption at 650 and 620 nm, using the following equation (Bennett and Bogorad 1973; Bryant et al. 1979):

$$\text{PC}(\text{mg}\cdot\text{mL}^{-1}) = \{A_{620} - (0.7 \times A_{650})\}/7.38$$

$$\text{APC}(\text{mg}\cdot\text{mL}^{-1}) = \{A_{650} - (0.19 \times A_{620})\}/5.65$$

The purity of phycocyanin was monitored by measuring the A_{620}/A_{280} ratio. Absorption spectrum of the phycocyanin extract was recorded from 400 to 800 nm. Fluorescence emission spectra were obtained by excitation at 620 nm and emission was recorded from 630–800 nm. SDS-PAGE was done using 15% acrylamide (Laemmli 1970).

Results and discussion

Phycobiliproteins are the most sought after natural chromophores containing proteins that have several applications in food, diagnostic, therapeutic, biotechnology, and cosmetic industry. It is therefore important to optimize their isolation and purification procedure. Table 1 shows the yield and purity of the phycocyanin obtained after lysozyme treatment and adsorption on charcoal and chitosan. The extract showed the purity ratio ($A_{620/280}$) of 2.16 and the yield was about $100\text{ mg}\cdot\text{g}^{-1}$ dry

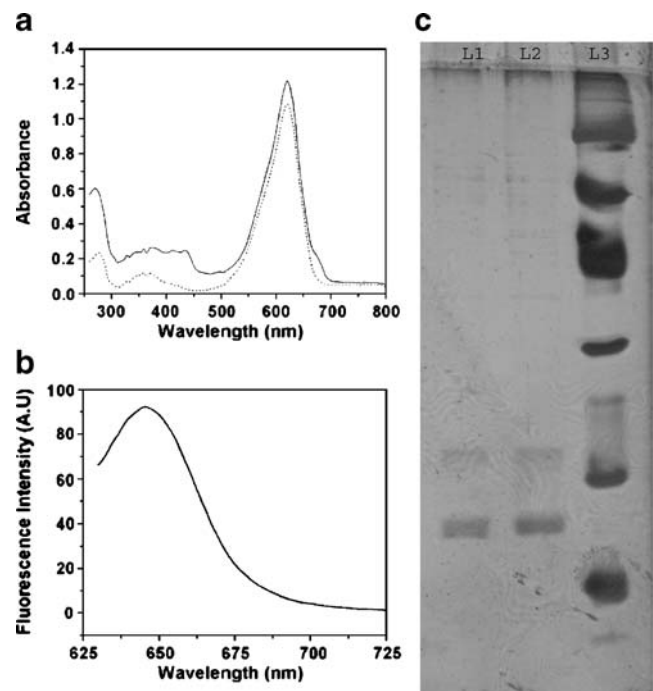


Fig. 1 Spectroscopic characterization and SDS-PAGE of purified phycocyanin; **a** absorption spectra of phycocyanin. Crude extract (solid line) and after treatment with activated charcoal and chitosan (dotted line). **b** Fluorescence emission spectrum of the phycocyanin obtained after treatment with activated charcoal and chitosan. The excitation was done at 620 nm. **c** SDS PAGE of phycocyanin. L2 Crude extract obtained after lysozyme treatment, L1 phycocyanin obtained after treatment with activated charcoal and chitosan, L3 protein molecular weight markers (94.0, 67.0, 43.0, 30.0, 20.1, 14.4 kDa)

weight of the cell biomass. After treatment with charcoal and chitosan, the purity ratio ($A_{620/280}$) improved further to 4.72 with negligible loss of phycocyanin. The phycocyanin/allophycocyanin ratio also improved to 2.3 after this step. The absorption spectra showed a single peak at 620 nm (Fig. 1a). The fluorescence emission spectra showed a peak at 645 nm, which is characteristic of phycocyanin (Fig. 1b). SDS-PAGE analysis of purified phycocyanin showed two main bands corresponding to α and β subunits of phycocyanin (Fig. 1c).

Previously phycocyanins have been extracted and purified from a several cyanobacteria using variety of steps which required longer time and deterioration in yield (Eriksen 2008). Lysozyme was used to produce spheroplasts from *Spirulina* (Gan et al. 2004). Santiago-Santos et al. (2004) treated *Calothrix* sp. with lysozyme for extraction of phycocyanins which were further purified using Q-Sepharose and hydrophobic interaction chromatography to obtain a purity ratio ($A_{620/280}$) of 3.5. In the case of *Synechococcus* sp. IO9201, a marine cyanobacterium, phycocyanin with a purity ratio of 4.85 was obtained using hydrophobic and ion exchange chromatography (Abalde et al. 1998). Patil et al. (2006) used charcoal–chitosan adsorption and aqueous two-phase extraction for purification of phycocyanin from *S. platensis* with purity ratio ($A_{620/280}$) of 3.96. Doke (2005) isolated phycocyanin from dry powder of *Spirulina* sp. with yield of about 80 mg·g⁻¹ dry weight with purity ratio ($A_{620/280}$) of 1.8.

The procedure described here which uses lysozyme and charcoal–chitosan treatment takes only one day to obtain phycocyanin with purity ratio ($A_{620/280}$) of 4.72 and yield up to 100 mg·g⁻¹ dry weight. The purity of phycocyanin can further be enhanced by various chromatographic methods, if required.

Interestingly, lysozyme treatment described above did not work efficiently with the standard strains such as *Synechococcus* 7942 and *Synechocystis* 6803. The cell walls of ‘*Anacystis nidulans* BD1’ appeared to be more susceptible to lysozyme. Since this organism belongs to *Synechococcus* sp., it does not have phycoerythrin and hence mere lysozyme treatment yielded reasonably pure phycocyanin in a single step. The cultures of this cyanobacterium were grown on minimal micronutrient-containing medium. Since this organism yielded appreciably pure phycocyanin, we conclude that

the proposed method can be adopted for large-scale production of phycocyanin from ‘*Anacystis nidulans* BD1’ (*Synechococcus* sp.)

Acknowledgments We sincerely thank Mr. N. Tekade and Mr. V. R. Jadhav, BARC for technical help, Ms. R. Agarwal, Drs. C. Rajanikant and G. Maralihalli, BARC for discussions and Dr. K. A. V. David for supplying *Anacystis nidulans* BD1.

References

- Abalde J, Betancourt L, Torres E, Cid A, Barwell C (1998) Purification and characterization of phycocyanin from the marine cyanobacterium *Synechococcus* sp. IO9201. *Plant Sci* 136:109–120. doi:10.1016/S0168-9452(98)00113-7
- Bennett A, Bogorad L (1973) Complementary chromatic adaptation in a filamentous blue-green alga. *J Cell Biol* 58:419–435. doi:10.1083/jcb.58.2.419
- Bryant DA, Guglielmi G, Tandeau de marsac N, Castlets AM, Cohen-Bazire G (1979) The structure of cyanobacterial phycobilisomes: a model. *Arch Microbiol* 123:113–127. doi:10.1007/BF00446810
- Doke JM Jr (2005) An improved and efficient method for extraction of phycocyanin from *Spirulina* sp. *Int J Food Eng* 1:1–13
- Eriksen NT (2008) Production of phycocyanin—a pigment with applications in biology biotechnology foods and medicine. *Appl Microbiol Biotechnol* 80:1–14. doi:10.1007/s00253-008-1542-y
- Gan X, Tang X, Shi C, Wang B, Cao Y, Zhao L (2004) Preparation and regeneration of spheroplasts from *Arthrospira platensis* (*Spirulina*). *J Appl Phycol* 16:513–517. doi:10.1007/s10811-004-5522-z
- Laemmli UK (1970) Cleavage of structural protein during assembly of the head of Bacteriophage T4. *Nature* 227:680–685. doi:10.1038/227680a0
- Patil G, Chethana S, Sridevi AS, Raghavarao KSMS (2006) Method to obtain C-phycocyanin of high purity. *J Chromatogr A* 1127:76–81. doi:10.1016/j.chroma.2006.05.073
- Rippka R, Deruelles J, Waterbury J, Herdman M, Stanier RY (1979) Generic assignments, strain histories and properties of pure cultures of cyanobacteria. *J Gen Microbiol* 111:1–61
- Santiago-Santos, M. C., Ponce-Noyola, T., Olvera-Ramirez, R., Ortega-Lopez, J., Canizares-Villanueva, R.O. (2004). Extraction and purification of phycocyanin from *Calothrix* sp. 39, 2047–2052.
- Sekar S, Chandramohan M (2007) Phycobiliproteins as a commodity: trends in applied research, patents and commercialization. *J Appl Phycol* 20:113–136. doi:10.1007/s10811-007-9188-1
- Singh NK, Parmar A, Madamwar D (2009) Optimization of medium components for increased production of C-phycocyanin from *Phormidium ceylanicum* and its purification by single step process. *Bioresour Technol* 100:1663–1669. doi:10.1016/j.biortech.2008.09.021

Synechococcus elongatus PCC 7942 is more tolerant to chromate as compared to Synechocystis sp. PCC 6803

Alka Gupta, Suresh G. Bhagwat & Jayashree K. Sainis

BioMetals

An International Journal on the Role of Metal Ions in Biology, Biochemistry and Medicine

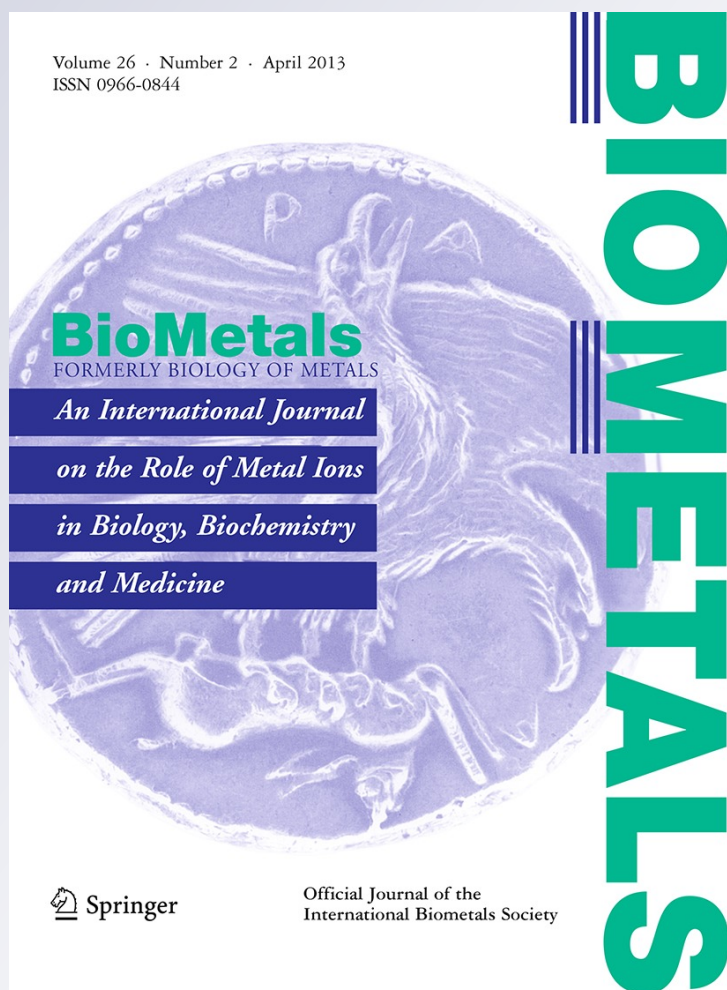
ISSN 0966-0844

Volume 26

Number 2

Biometals (2013) 26:309-319

DOI 10.1007/s10534-013-9614-6



Your article is protected by copyright and all rights are held exclusively by Springer Science +Business Media New York. This e-offprint is for personal use only and shall not be self-archived in electronic repositories. If you wish to self-archive your article, please use the accepted manuscript version for posting on your own website. You may further deposit the accepted manuscript version in any repository, provided it is only made publicly available 12 months after official publication or later and provided acknowledgement is given to the original source of publication and a link is inserted to the published article on Springer's website. The link must be accompanied by the following text: "The final publication is available at link.springer.com".

Synechococcus elongatus PCC 7942 is more tolerant to chromate as compared to *Synechocystis* sp. PCC 6803

Alka Gupta · Suresh G. Bhagwat · Jayashree K. Sainis

Received: 1 November 2012 / Accepted: 7 February 2013 / Published online: 21 February 2013
© Springer Science+Business Media New York 2013

Abstract Two unicellular cyanobacteria *Synechocystis* sp. PCC 6803 and *Synechococcus elongatus* PCC 7942 showed contrasting responses to chromate stress with EC_{50} of 12 ± 2 and 150 ± 15 μM potassium dichromate respectively. There was no depletion of chromate in growth medium in both the cases. Using labeled chromate, very low accumulation (<1 nmol/ 10^8 cells) was observed in *Synechocystis* after incubation for 24 h in light. No accumulation of chromate could be observed in *Synechococcus* under these conditions. Chromate oxyanion is known to enter the cells using sulfate uptake channels. Therefore, inhibition of sulfate uptake caused by chromate was monitored using ^{35}S labeled sulfate. IC_{50} values of chromate for ^{35}S sulfate uptake were higher in

Synechococcus as compared to *Synechocystis*. The results suggested that the sulfate transporters in *Synechococcus* have lower affinity to chromate than those from *Synechocystis* possibly due to differences in affinity of sulfate receptors for chromate. Bioinformatic analyses revealed presence of sulfate and chromate transporters with considerable similarity; however, minor differences in these may play a role in their differential response to chromate. In both cases the IC_{50} values decreased when sulfate concentration was reduced in the medium indicating competitive inhibition of sulfate uptake by chromate. Interestingly, *Synechococcus* showed stimulation of growth at concentrations of chromate less than 100 μM , which affected its cell size without disturbing the ultrastructure and thylakoid organization. In *Synechocystis*, growth with 12 μM potassium dichromate damaged the ultrastructure and thylakoid organization with slight elongation of the cells. The results suggested that *Synechococcus* possesses efficient strategies to prevent entry and to remove chromate from the cell as compared to *Synechocystis*. This is the first time a differential response of *Synechococcus* 7942 and *Synechocystis* 6803 to chromate is reported. The contrasting characteristics observed in the two cyanobacteria will be useful in understanding the basis of resistance or susceptibility to chromate.

Electronic supplementary material The online version of this article (doi:10.1007/s10534-013-9614-6) contains supplementary material, which is available to authorized users.

A. Gupta · J. K. Sainis (✉)
Molecular Biology Division, Bhabha Atomic Research Centre, Trombay, Mumbai 400085, India
e-mail: jksainis@barc.gov.in

S. G. Bhagwat
Nuclear Agriculture and Biotechnology Division, Bhabha Atomic Research Centre, Trombay, Mumbai 400085, India

Keywords Chromate-resistance · Cyanobacteria · IC_{50} chromate · Sulfate-uptake · *Synechococcus* PCC 7942 · *Synechocystis* PCC 6803

Abbreviations

EC ₅₀ of chromate	Concentration of potassium dichromate at which number of cells ml ⁻¹ was 50 % as compared to control
IC ₅₀ of chromate	Concentration of chromate required for 50 % reduction in uptake of sulfate as compared to control
OD	Optical density

Introduction

Chromium is a member of transition metals and exhibits various oxidation states from +2 to +6, of which +3 and +6 are predominant in chromium compounds. Hexavalent chromium (Cr⁶⁺) is highly soluble and hence toxic; it usually exists as oxyanions such as chromate (CrO₄²⁻) and dichromate (Cr₂O₇²⁻) whereas the trivalent form (Cr³⁺) is less soluble, less toxic and is found in the form of oxides, hydroxides or sulfates (Cheung and Gu 2007). The hexavalent form is released in the environment as aqueous waste from leather, paints, electroplating and other industries. Chromate is highly mobile and hence available, resulting in biological toxicity mainly due to oxidative damage to biomolecules (Cervantes et al. 2001). Microorganisms have developed different strategies to thrive in the presence of chromate in the aquatic environment. One of these strategies deals with reduction of chromate to the less toxic chromium(III) by chromate reductase identified in diverse bacterial species (Cervantes et al. 2001). Another strategy in prokaryotes uses chromate efflux system using a plasmid encoded gene, *chrA*. ChrA belongs to a small family of proteins (CHR), which occur in bacteria and archaea and represents a novel kind of prokaryotic proton motive force driven chromate transporters. Several members of CHR superfamily have been shown to confer resistance to chromate (Nies et al. 1998; Alvarez et al. 1999; Rami' rez-Diaz et al. 2008).

Among photoautotrophs, cyanobacteria and algae isolated from chromate contaminated sites or some mutants are able to tolerate chromate to varied extent (Garnham and Green 1995; Khattar et al. 2004; Anjana et al. 2007; Yewalkar et al. 2007; Kiran et al.

2007, 2008; Ozturk et al. 2009). Some of these adsorb chromate on the surface or reduce chromate to chromium(III). Recently an investigation into mechanism of chromate resistance in *Synechococcus elongatus* showed that it possesses a homologue of chromate transporter gene *srpC* on pANL plasmid which harbors genes of sulfur metabolism (Aguilar-Barajas et al. 2012). Although overexpression of *srpC* conferred chromate resistance to *E. coli* by reducing chromate uptake, it did not complement *E. coli cysA* sulfate uptake mutant, suggesting that *srpC* is not sulfate transporter. Since chromate oxyanion is structurally related to sulfate, chromate actively crosses biological membranes by means of the sulfate uptake pathway (Rami' rez-Diaz et al. 2008; Aguilar-Barajas et al. 2011). This results in sulfate deficiency as well as in creating oxidative stress in cells. Thus a complex relation is known to exist between sulfate and chromate transporters vis a vis the effect of chromate in prokaryotes.

Cyanobacteria are some of the oldest organisms living on the earth and have evolved mechanisms to combat various environmental stresses. The comparative study on the relative responses of different cyanobacteria to variety of stresses is an interesting field of research. The standard cultures of two taxonomically related cyanobacteria *Synechococcus* PCC 7942 and *Synechocystis* sp. PCC 6803 are known to differ in their responses to salt, light and oxidative stress (Fulda et al. 1999; Stork et al. 2005). We observed these two standard strains also showed contrasting tolerance to chromate, *Synechococcus* being more tolerant than *Synechocystis*. In this paper we report differential responses of these two cyanobacteria to chromate with respect to its effect on growth, ultrastructure, chromate and sulfate uptake. The bioinformatic analysis of chromate and sulfate transporters is also presented.

Materials and methods

Analysis of chromate toxicity

The two strains of unicellular cyanobacteria, *S. elongatus* PCC 7942 and *Synechocystis* sp. PCC 6803 (referred to as *Synechococcus* and *Synechocystis* respectively hereafter) were inoculated in 50 ml of BG-11 medium (Rippka et al. 1979) and grown at 30 °C under continuous white light of intensity

21 W m⁻². To study the effect of chromate on growth, ~10⁸ cells of log phase culture were inoculated in BG-11 medium containing K₂Cr₂O₇ ranging from 0 to 200 μM and growth was monitored periodically as cell density and expressed as number of cell ml⁻¹ using Neubauer's hemacytometer in the Zeiss Axio imager digital microscope. Growth was monitored as OD₇₃₀ up to 30 days. EC₅₀ value represents the concentration of potassium dichromate at which number of cells ml⁻¹ was 50 % as compared to control.

Determination of ⁵¹chromate accumulation

Chromate uptake was determined by using ⁵¹chromium labeled chromate as a tracer. Log phase cultures of *Synechococcus* and *Synechocystis* were washed and incubated (10⁸ cells ml⁻¹) in light (21 W m⁻²) for 24 h at room temperature in fresh BG-11 medium containing 10 or 100 μM K₂Cr₂O₇ with 20 μCi ⁵¹Cr labeled sodium chromate (0.24 μCi nmol⁻¹). Cells were washed with BG-11 medium followed by 1 mM EDTA, resuspended in 90 % methanol and mixed with 175 μl of Perkin-Elmer's Hidex aqualight cocktail. ⁵¹Chromate in the cells was estimated by counting β emission by using liquid scintillation counter.

Determination of IC₅₀ of chromate for ³⁵sulfate uptake

Inhibitory concentration (IC₅₀) of chromate for sulfate uptake was determined by monitoring uptake of ³⁵S labeled sodium sulfate. Log phase cultures of *Synechococcus* and *Synechocystis* were washed and suspended in fresh BG-11 medium (10⁸ cells ml⁻¹) containing 30 or 300 μM sulfate along with 40 μCi ³⁵sodium sulfate (28.6 μCi μmol⁻¹) and increasing concentration of chromate (0–10 mM) for 2 h in light at room temperature. Cell pellets were washed with BG-11 medium followed by 1 mM EDTA. The washed cells were resuspended in 90 % methanol and mixed with 175 μl of Perkin-Elmer's Hidex aqualight cocktail. ³⁵Sulfate in the cells was measured by liquid scintillation counting.

Transmission electron microscopy

Synechococcus and *Synechocystis* cells were grown with different concentrations of potassium dichromate for 9 days as indicated in figures. The cells were

harvested and washed with sodium phosphate buffer (100 mM, pH 7.4), fixed with 0.5 % glutaraldehyde—2 % paraformaldehyde for 2 h at room temperature followed by washing with water. Serial dehydration was carried out using 35, 50, 75 and 100 % ethanol for 30 min each. Ethanol was removed by incubation with propylene oxide for 3 h followed by further incubation with 3:1, 1:1, 1:3 (v/v propylene oxide:araldite) for 2 h each. The samples were infiltrated with Araldite for 16 h and embedded in it by incubation at 60 °C for 72 h. Thin (70 nm) sections were contrasted for 15 min with 10 % uranyl acetate in 50 % methanol followed by staining with lead citrate (Reynolds 1963) for 2 min. The sections were viewed under Libra 120 keV transmission electron microscope.

Sequence comparison of sulfate and chromate transporters

Amino acid sequences of sulfate and chromate transporters from *Synechococcus* and *Synechocystis* were downloaded from cyanobase (<http://genome.kazusa.or.jp/cyanobase>) and compared with similar well characterized genes from other bacteria. Alignment and analyses of proteins were performed using BioEdit v7.0.8. Conserved domains were obtained using conserved domain database (CDD) available at <http://www.ncbi.nlm.nih.gov/Structure/cdd/cdd.shtml> with CDDv2.3.CDD) and simple modular architecture research tool (SMART) available at <http://smart.embl-heidelberg.de>.

Results

Differential effect of chromate on growth of *Synechococcus* and *Synechocystis*

When log phase culture of *Synechococcus* and *Synechocystis* were inoculated in 50 ml of BG-11 medium, the exponential growth phase started after 4 days and lasted for about 30 days in untreated *Synechococcus* where as in case of untreated *Synechocystis* the log phase lasted for 15 days after which slow decline in growth was observed under similar growth conditions. The two organisms showed comparable growth rates in absence of chromate with doubling time in the range of 40–50 h till 15 days period indicating that both were growing normally

under the conditions used for their growth. Growth was monitored as OD_{730} and also by measuring number of cells ml^{-1} . *Synechococcus* cultures showed over twice the number of cells at equivalent OD_{730} as compared to *Synechocystis* culture suggesting difference in scattering properties of the cells.

To measure the effect of chromate on cell survival and growth, $\sim 10^8$ cells were inoculated in BG-11 medium containing different concentrations of chromate and growth was monitored by cell count.

In case of *Synechocystis* survival was reduced in the presence of potassium dichromate at concentration as low as 10–20 μM . On the contrary in case of *Synechococcus*, cells could grow even in presence of 200 μM potassium dichromate (Fig. 1). In *Synechococcus* inclusion of potassium dichromate up to 100 μM in growth medium stimulated growth; highest stimulation was observed with 70–80 μM potassium dichromate. Concentration of potassium dichromate required to inhibit growth completely in *Synechococcus* was 300 μM . In case of *Synechocystis*, survival declined with increasing concentration of chromate and was completely inhibited in presence of 30 μM potassium dichromate. Since the growth rates of *Synechocystis* and *Synechococcus* were comparable under the experimental conditions, the growth inhibition seen in *Synechocystis* in presence of

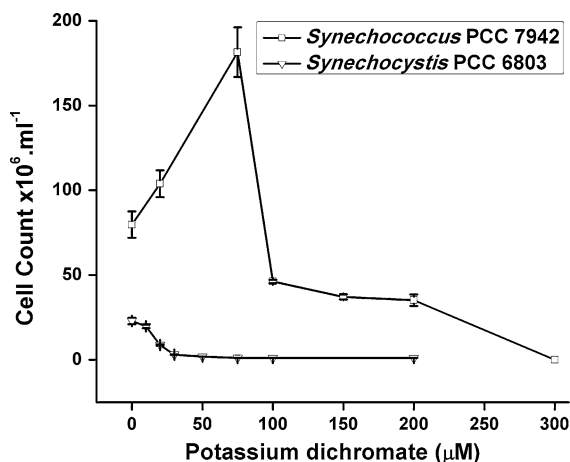


Fig. 1 Tolerance of *Synechococcus* and *Synechocystis* to potassium dichromate. BG11 medium containing increasing concentration of potassium dichromate was inoculated with log phase cultures of *Synechococcus* and *Synechocystis* containing $\sim 10^8$ cells ml^{-1} . Growth was monitored as number of cells ml^{-1} . EC_{50} for potassium dichromate was calculated after growth for 9 days. The points represent average of four experiments and bars represent SE

chromate was due to chromate toxicity rather than difference in growth characteristics between the two under normal conditions.

Since both cultures showed exponential growth from 4 to 15 days, the concentration of potassium dichromate at which number of cells ml^{-1} was 50 % as compared to control was monitored after 9 days of inoculation and was used to compare the tolerance of *Synechococcus* and *Synechocystis* to chromium stress. The 9 days EC_{50} of potassium dichromate was $12 \pm 2 \mu M$ for *Synechocystis* and $150 \pm 15 \mu M$ for *Synechococcus* (Fig. 1). The EC_{50} values increased with time after inoculation as well as with increase in the size of inoculum (Table 1 on line resource; Fig. 1 on line resource).

Differential accumulation of chromate by *Synechococcus* and *Synechocystis*

Synechococcus and *Synechocystis* were grown in the presence of increasing concentration of potassium dichromate. Cell free medium from each culture was obtained and chromate concentration in the medium was determined using di phenyl carbazide (DPC) reduction assay as described by Urone (1955). There was no change in chromate concentration in the supernatant of the growth medium indicating that chromate was not absorbed or reduced by both the cyanobacteria (data not shown). Chromate accumulation was also monitored using radiolabeled chromate as a tracer. In *Synechocystis* after 24 h of incubation in light, the chromate accumulation up to 0.04–0.05 $nmol 10^8$ cells $^{-1}$ was observed when extracellular concentration of chromate was 10 μM . This increased to 0.4 $nmol 10^8$ cells $^{-1}$ when chromate concentration in the medium was increased to 100 μM (Fig. 2). In contrast, there was no accumulation of chromate in *Synechococcus* cells under these conditions (Fig. 2). In *Synechocystis* there was no accumulation of chromate when the cells were boiled in the medium or when they were incubated in dark (data not shown).

Differential effect of chromate on uptake of sulfate by *Synechococcus* and *Synechocystis*

Sulfate uptake using ^{35}S labeled sodium sulfate in the presence of varying concentrations of chromate was monitored in *Synechococcus* (Fig. 3a, b) and *Synechocystis* (Fig. 3c, d) incubated in medium

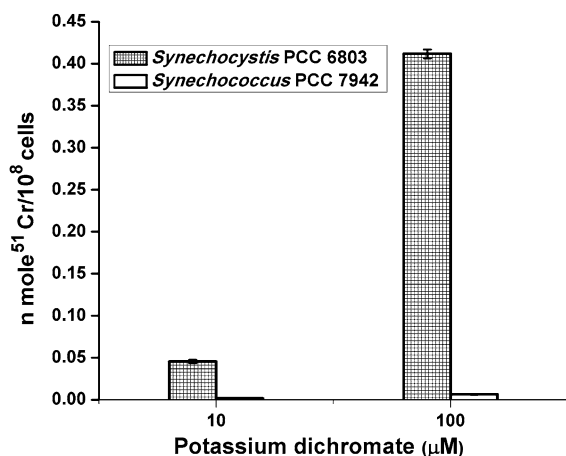


Fig. 2 Uptake of ⁵¹chromate by *Synechococcus* and *Synechocystis* in light Log phase cultures of *Synechococcus* and *Synechocystis* (10^8 cells ml^{-1}) were incubated in BG11 medium containing 10 or 100 μM of potassium dichromate with ⁵¹Cr as tracer. The intracellular ⁵¹Cr was measured after incubation for 24 h in light at room temperature

containing 30 and 300 μM sodium sulfate. Chromate was found to decrease the uptake of sulfate in *Synechococcus* and *Synechocystis*. When concentration of sulfate was increased from 30 to 300 μM the concentration of chromate required for IC_{50} was increased from 30.35 μM to 1.7 mM in case of *Synechococcus*. In *Synechocystis* when concentration of sulfate was increased from 30 to 300 μM the concentration of chromate required for IC_{50} was increased from 8.6 to 99 μM .

Differential effect of chromate on ultrastructure of *Synechococcus* and *Synechocystis*

Ultrastructural changes in *Synechococcus* and *Synechocystis* grown with EC_{50} concentration of potassium dichromate were observed by transmission electron microscopy. The length of cells in case of *Synechococcus* was reduced whereas there was slight elongation of cells in case of *Synechocystis* while the cell width was not affected. In *Synechococcus* the cells grown with chromate did not show extensive damage to ultrastructure (Fig. 4a, b, c). The cell wall, thylakoids and carboxysomes were not affected by the presence of dichromate in medium. However, growth in the presence of chromate resulted in reduction of length to breadth (L/B) ratio (Fig. 4f). In *Synechocystis* growth in the presence of chromate resulted in distortions in thylakoid membranes and damage to

cell wall in addition to slight elongation of regular spherical shape with increase in L/B ratio (Fig. 4d, e, f).

Bioinformatic analysis of sulfate and chromate transporters in *Synechococcus elongatus* PCC 7942 and *Synechocystis* sp. PCC 6803

To investigate if the differences in the IC_{50} of chromate for sulfate uptake in the two organisms could be attributed to the differences in primary structure of the sulfate and chromate transporters, a comparative bioinformatic analysis of amino acid sequences of these proteins from *Synechococcus* and *Synechocystis* was carried out (Tables 1, 2); (Figs. 2, 3, 4, 5, 6 on line resource). The analysis included SulT permease constituting the permease, membrane proteins and ATPase; and chromate transporter ChrA. Their sequences were also compared with the sequences of well characterized sulfate and chromate uptake related proteins from other prokaryotic organisms.

Sulfate-thiosulfate transporters

Sulfate-thiosulfate (SulT) permease complex from some bacteria is well characterized and typically consists of sulfate or thiosulfate binding protein Sbp or CysP, and the proteins of ABC transporter viz CysA, ATPase, CysW and CysT. These were used as reference to identify differences among the corresponding proteins in the two organisms under study. Ten and nine genes for sulfate transporters are identified in *Synechococcus* and *Synechocystis* respectively in cyanobase (Tables 1, 2). The sulfate binding proteins (SbpA) in *Synechococcus* and *Synechocystis* have ~58.9 % identity. SbpA from these organisms showed 99 conserved amino acid residues with SbpA from *Salmonella typhimurium* (Fig. 2 on line resource). Cys A, the ATPase subunit of the SulT permease of *Synechococcus* and *Synechocystis* have ~63 % identity (Tables 1, 2). Figure 3 (on line resource) shows that there were 148 conserved amino acid residues among them and the CysA from *Pseudomonas syringae*. Bacterial CysT and CysW constitute the transport channel of the SulT permease typically with six transmembrane helices which are also present in CysT and CysW from *Synechocystis*. *Synechococcus* CysT and CysW show ~46–64 % identities with homologs from *Synechocystis*. All of

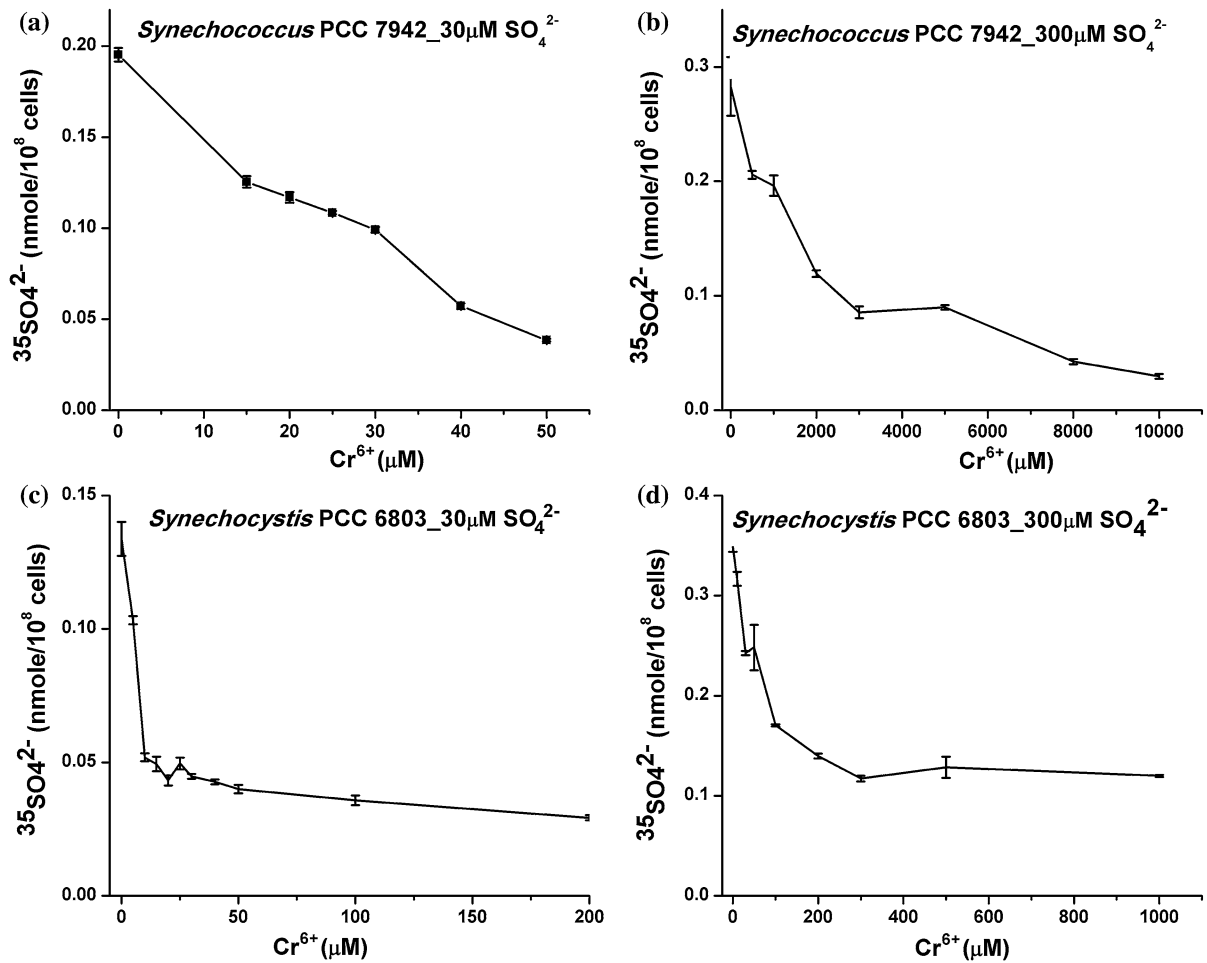


Fig. 3 Effect of chromate on uptake of ^{35}S labeled sulfate by *Synechococcus* and *Synechocystis*. Log phase cultures of *Synechococcus* and *Synechocystis* (10^8 cells ml^{-1}) were incubated in BG11 medium containing 30 or 300 μM sodium sulfate with ^{35}S labeled sodium sulfate as tracer and different concentrations of potassium dichromate as mentioned in figure. Uptake of ^{35}S sulfate was monitored after 2 h. The average of four

estimations is shown. Bars represent SE. **a** *Synechococcus* incubated in medium containing 30 μM sodium sulfate. **b** *Synechococcus* incubated in medium containing 300 μM sodium sulfate. **c** *Synechocystis* incubated in medium containing 30 μM sodium sulfate and **d** *Synechocystis* incubated in medium containing 300 μM sodium sulfate

these have six transmembrane helices except Synpcc7942_1687 (Cys T) which has seven transmembrane helices. *Synechocystis* and *Synechococcus* CysT and CysW showed 70 and 96 conserved amino acid residues with CysT and CysW from *E. coli*. (Figs. 4, 5 on line resource).

In addition to the conserved SulT components, the genomes of *Synechococcus* PCC 7942 and *Synechocystis* PCC 6803 show presence of some putative sulfate transporters, thiosulfate binding protein, low and high affinity sulfate transporter and sulfate

permease (Tables 1, 2). Some of these have transmembrane domains suggesting a possible membrane location for them.

Chromate transporters

Chromate resistance in prokaryotes has been attributed to ChrA which is a chemiosmotic pump responsible for chromate efflux using proton motive pump (Alvarez et al. 1999). Two ORFs have been annotated as chromate transporters in *Synechococcus* and

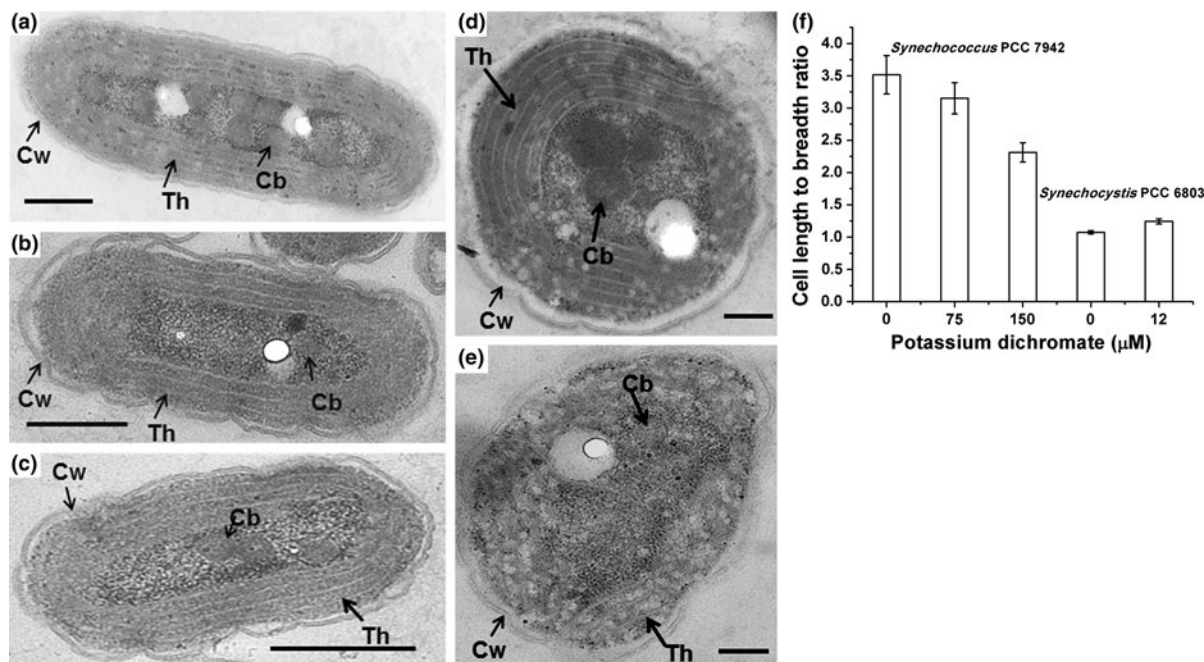


Fig. 4 Ultrastructure of *Synechococcus* and *Synechocystis* cells grown with or without potassium dichromate. Log phase cultures of *Synechococcus* and *Synechocystis* containing 10^8 cells ml^{-1} were inoculated in BG11 medium containing potassium dichromate as mentioned below. Cells were harvested after 9 days of growth and were processed for transmission electron microscopy as described in “Materials and methods” section. **a** *Synechococcus* control. **b** *Synechococcus* grown with 75 μM of potassium dichromate **c** *Synechococcus* grown with 150 μM of

potassium dichromate. *Bars* represent 500 nm. **d** *Synechocystis* control. **e** *Synechocystis* grown with 12 μM of potassium dichromate. *Bars* represent 200 nm. **f** Length to breadth ratio of *Synechococcus* and *Synechocystis* grown with above mentioned chromate concentrations in the growth medium. The *values* represent mean ratio obtained from electron micrographs of 15–20 cells and *bars* represent SE. *Th* thylakoids, *Cb* carboxysomes, *Cw* cell wall

Synechocystis, one on plasmid and other on chromosome (Tables 1, 2). These showed ~29–40 % identity, and presence of two CHR domains containing homologous halves with membrane spanning regions which is a feature of long chain CHR family proteins in bacteria. The cyanobacterial chromate transporters showed 37 conserved amino acid residues when compared with chromate transporter from *Pseudomonas aeruginosa* (Fig. 6 on line resource).

Discussion

Chromate toxicity in aquatic organisms is mainly examined by exposing cultures to different concentrations of chromate for a given time, followed by investigations on physiological parameters. We compared two non-nitrogen fixing unicellular aquatic cyanobacteria belonging to order *Chroococcales* for their sensitivity to chromate when included in their

growth media. Comparative analysis of chromate tolerance in *S. elongatus* PCC 7942 and *Synechocystis* PCC 6803 revealed that the former showed ~12 times higher tolerance to chromate than the latter, with EC_{50} values of 150 ± 15 and 12 ± 2 μM respectively. The EC_{50} values were dependent on the inoculum size in both cases indicating stoichiometric relation between chromate receptors per cell and number of chromate ions available in the growth medium. Thompson et al. (2002) have compared *Synechococcus* PCC 7942 and *Nostoc* PCC 7120 for resistance to chromate under high and low density conditions and have shown that there is general decrease in toxicity in dense cultures. Interestingly, stimulation in growth at less than 100 μM potassium dichromate was observed in *Synechococcus*. Lesser extent of ultrastructural damage in *Synechococcus* supports this argument.

In bacteria, two mechanisms of chromate tolerance are known: reduction of Cr(VI)–Cr(III) and efflux of chromate ions from cytoplasm (Rami’rez-Diaz et al. 2008).

Table 1 Comparative analysis of sulfate and chromate transporter genes in *Synechococcus*

Sulfate transporters in <i>Synechococcus</i> PCC 7942							
Sr. no.	ORF ID	Gene symbol	Definition	Aa	TM	Homologue in <i>Synechocystis</i>	% Identity
1	Synpcc7942_1681	<i>sbpA</i>	Thiosulfate-binding protein	350	Nil	slr1452	58.9
2	Synpcc7942_1680	<i>cysA</i>	Sulfate transport system permease protein 1	338	Nil	slr1455	63.3
3	Synpcc7942_1688	<i>cysW</i>	Sulfate ABC transporter, permease protein CysW	286	6	slr1454	51.9
4	Synpcc7942_1685	<i>cysW</i>	Sulfate transport system permease protein 2	286	6	slr1454	62.8
5	Synpcc7942_1682	<i>cysT</i>	Sulfate transport system permease protein 2	278	6	slr1453	62.5
6	Synpcc7942_1687	<i>cysT</i>	Sulfate ABC transporter, permease protein CysT	288	7	slr1453	46.1
7	Synpcc7942_1722		Thiosulfate-binding protein	361	Nil	slr1452	54.5
8	Synpcc7942_1686		Thiosulfate-binding protein	341	Nil	slr1452	42.4
9	Synpcc7942_0366		Putative sulfate transporter	727	11	slr0096	22.9
10	Synpcc7942_1380		Sulfate permease	574	11	slr1776	32.8

Chromate transporters in *Synechococcus* PCC 7942

1	Synpcc7942_0390		Chromate transporter			383 9	slr1457 40.2
2	Synpcc7942_B2622_ plasmid 1 ^a	<i>srpC</i>	Probable chromate transport transmembrane protein			393 12	slr1457 29.2

Translated amino acid sequences annotated as sulfate and chromate transporters as given in cyanobase were used for comparative analysis of *Synechococcus* PCC 7942 with *Synechocystis* PCC 6803. The values of amino acid chain length (Aa), number of transmembrane helices (TM) and % identity (as in orthologue search) for individual genes have been obtained from cyanobase

ORF ID open reading frame identity

^a Gene is located on plasmid

Table 2 Comparative analysis of sulfate and chromate transporter genes in *Synechocystis*

Sulfate transporters in <i>Synechocystis</i> PCC 6803							
Sr. no.	ORF ID	Gene symbol	Definition	Aa	TM	Homologue in <i>Synechococcus</i>	% Identity
1	slr1452	<i>sbpA</i>	Sulfate transport system substrate-binding protein	352	Nil	Synpcc7942_1681	58.9
2	slr1455	<i>cysA</i>	Sulfate transport system ATP-binding protein	355	Nil	Synpcc7942_1680	63.3
3	slr11041	<i>cysA</i>	Similar to sulfate transport ATP-binding protein CysA	260	Nil	Synpcc7942_0350	53.1
4	slr1454	<i>cysW</i>	Sulfate transport system permease protein	276	6	Synpcc7942_1685	62.8
5	slr1453	<i>cysT</i>	Sulfate transport system permease protein	286	6	Synpcc7942_1682	62.5
6	slr1229		Sulfate permease	453	9	Synpcc7942_1380	22.7
7	slr0096		Low affinity sulfate transporter	556	11	Synpcc7942_1380	25
8	slr0834		Low affinity sulfate transporter	564	12	Synpcc7942_1380	29.1
9	slr1776		High affinity sulfate transporter	566	11	Synpcc7942_1380	32.9

Chromate transporters in *Synechocystis* PCC 6803

1	slr1457	<i>chrA</i>	Chromate transport protein	399	9	Synpcc7942_0390	40.5
2	slr5038 pSYSM ^a		Chromate transporter	412	11	Synpcc7942_0390	36.4

Translated amino acid sequences annotated as sulfate and chromate transporters as given in cyanobase were used for comparative analysis of *Synechocystis* PCC 6803 with *Synechococcus* PCC 7942. The values of amino acid chain length (Aa), number of transmembrane helices (TM) and % identity (as in orthologue search) for individual genes have been obtained from cyanobase

ORF ID open reading frame identity

^a Gene is located on plasmid

DPC assays showed that these two cyanobacteria were not chromate reducers. Only nanomolar concentration of chromate accumulation was detected in *Synechocystis* using ^{51}Cr chromate and accumulation was not observed if cells were killed or incubated in dark indicating involvement of an active process in uptake of chromate (data not shown). Although in *Synechococcus*, no chromate accumulation was observed under these conditions, there was stimulation of growth along with reduction of cell length when chromate concentration in medium was less than 100 μM . This entailed that *Synechococcus* was able to sense the presence of low concentration of chromate in the growth medium. These observations indicated that in *Synechococcus* there are efficient mechanisms for sensing and efflux of chromate. In contrast, *Synechocystis* cells showed deterioration of ultrastructure, reduction in growth and elongation of cells with 12 μM chromate in medium. Recently effects of chromate on cell morphology are reported in case of *Rhodobacter sphaeroides* by Italiano et al. (2012).

It is known that chromate ion enters the cells using sulfate transporters present in cell membrane as chromate ion is nearly identical in size shape and charge as sulfate ion (Riedel 1985). IC_{50} values of chromate in both *Synechococcus* and *Synechocystis* were dependent on sulfate concentration in medium indicating that sulfate uptake was competitively inhibited by chromate in both the cases. The inhibition of sulfate uptake by chromate suggested an interaction of chromate ions with sulfate uptake mechanism. However, the IC_{50} value of chromate was much higher in *Synechococcus* as compared to *Synechocystis* showing that *Synechocystis* has higher affinity for chromate as compared to *Synechococcus*. Sequence analysis showed that both the cyanobacteria have similar type of sulfate uptake channels and also contain similar genes related to efflux of chromate having typical bi-domain structure of LCHR. The differences in IC_{50} value of chromate suggested that the sequence variation in the non-conserved regions of sulfate uptake systems in both these organisms may be contributing to higher affinity of the sulfate uptake system for chromate in *Synechocystis* 6803 as compared to *Synechococcus* 7942. *Synechococcus elongatus* PCC 7942 possesses a plasmid (pANL) that contains a gene (*srpC/chrA*) conferring chromate resistance. The higher chromate susceptibility of *Synechocystis* cannot be attributed to absence of

pANL as the sequence analysis shows that it has *chrA* homologues on its chromosome. Whether the location of *chrA* is responsible for the differential tolerance remains to be explored.

IC_{50} of chromate for sulfate uptake was higher in *Synechococcus* as compared to *Synechocystis* indicating that differential affinity of sulfate transporters for chromate may be contributing to the chromate tolerance in *Synechococcus* 7942 as compared to *Synechocystis* 6803. While IC_{50} for chromate at 10-fold increase in sulfate needed ~ 50 -fold increase in chromate in case of *Synechococcus*, in case of *Synechocystis* with similar increase in sulfate, IC_{50} was attained by only ~ 12 -fold increase in chromate concentration. Thus in *Synechococcus* the sulfate limitation by chromate would be avoided by the its sulfate transporters which have lower affinity to chromate as well as by the efficient chromate efflux systems resulting in higher EC_{50} for chromate. Although bioinformatic comparison of chromate and sulfate transporters revealed identity to a varying extent, the differences in their primary sequences could account for the difference in IC_{50} of chromate. Thus in addition to differences mentioned above, the different putative sulfate permease in these two organisms may play a role in their distinct chromate response. Chromate resistance of *Synechococcus* would give it growth advantage in chromate contaminated sites over *Synechocystis*.

Thus the multifarious interaction of sulfate/chromate transporters could be the basis of contrasting response of *Synechococcus* and *Synechocystis* to chromate.

In case of *Synechococcus* there was stimulation of growth at concentrations of chromate lower than 100 μM . It may be due to hormetic response characterized by low dose stimulation and high dose inhibition resulting in typical inverted U type dose response. Although biochemical mechanism of hormesis is not well understood it is possible that at low doses, the stressor activates repair processes which can repair the damage caused by chromate as well as other accumulated damages. Even though no chromate accumulation was seen in *Synechococcus* at low concentration, the effect on morphology and ultrastructure indicated presence of sensing mechanism and response. Another possibility may be that the reduced sulphate uptake due to chromate and subsequent adjustment of metabolic rate in *Synechococcus* has

effect on growth. Also at low concentration, chromate may interact with growth regulators, a possibility which needs to be addressed in future.

Bioinformatic analysis of sulfate and chromate transporters of *Synechococcus* and *Synechocystis* shows the complexity of these transporters. Chromate resistance is a manifestation of numerous biochemical processes governed by different genes and their homologues. The complexity in composition of sulfate and chromate transporters and subsequent metabolic adjustments to sulfate deficiency in these two strains may be the cause of differential response of these two cyanobacteria. On this back ground, exploring the molecular basis of the contrasting chromate resistance in these two organisms and also to comprehend the phenomenon of stimulation of growth and induction of morphological changes in *Synechococcus* at low concentration of chromate is a challenge in future.

Summary

The standard strains of *S. elongatus* PCC 7942 and *Synechocystis* sp. PCC 6803 showed significant differences in the EC₅₀ to chromate. There was difference in uptake of chromate; the resistant *Synechococcus* prevented entry by virtue of lower affinity of its sulfate transporters to chromate (IC₅₀ was higher). *Synechococcus* probably also removed chromate from the cells more efficiently as no chromium was detected in the cells. The resistant type sensed chromate at low concentration and possibly brought about changes in metabolism which resulted in stimulation of growth in terms of cell numbers. Bioinformatic analysis showed that chromate transporters are present in both the organisms; however the location of the responsible genes is different. Also, there is 29–40 % identity in the chromate transporter genes. Whether and how much, the differences in location and sequence variations contribute to the functioning of chromate transporter needs to be seen. The components of sulphate transporters from the two organisms also revealed identity in the range of ~40–60 % indicating that there is adequate scope for variation which can account for the observed differences. Although the cell length in the resistant type was reduced, the ultrastructure of the cell was protected in presence of chromate. The results indicate that the large difference in response to

chromate by the two organisms was due to a multi-component process. Although the comparison is between two genera, the large difference between the two makes it a suitable system for investigations on the resistance contributing factors and their interplay.

Acknowledgments The authors thank Dr. A. Ballal and Dr. R. Agarwal MBD, BARC, Mumbai for critical reading of the manuscript. We also thank Drs. S.F. D'Souza and J.S. Melo for useful suggestions. We thank Ms. N. Jadhav for sample preparation for Electron Microscopy. JKS acknowledges Department of Atomic Energy, India for Raja Ramanna Fellowship.

References

- Aguilar-Barajas E, Di'az-Pe'rez C, Ramirez-Diaz M, Riveros-Rosas H, Cervantes C (2011) Bacterial transport of sulfate, molybdate, and related oxyanions. *Biometals* 24:687–707
- Aguilar-Barajas E, Jeronimo-Rodriguez P, Ramirez-Diaz MI, Rensing C, Cervantes C (2012) The ChrA homologue from a sulfur-regulated gene cluster in cyanobacterial plasmid pANL confers chromate resistance. *World J Microbiol Biotechnol* 28:865–869
- Alvarez AH, Moreno-Sanchez R, Cervantes C (1999) Chromate efflux by means of the ChrA chromate resistance protein from *Pseudomonas aeruginosa*. *J Bacteriol* 181:7398–7400
- Anjana K, Kaushik A, Kiran B, Nisha R (2007) Biosorption of Cr(VI) by immobilized biomass of two indigenous strains of cyanobacteria isolated from metal contaminated soil. *J Hazard Mater* 148:383–386
- Cervantes C, Compos-Garcia J, Devars S, Gutie'rrez-Corona F, Loza-Tavera H, Torres-Guzman JC, Moreno-Sanchez R (2001) Interactions of chromium with microorganisms and plants. *FEMS Microbiol Rev* 25:335–347
- Cheung KH, Gu JD (2007) Mechanism of hexavalent chromium detoxification by microorganisms and bioremediation application potential: a review. *Int Biodeter Biodegrad* 59:8–15
- Fulda S, Huckauf J, Schoor A, Hagemann M (1999) Analysis of stress responses in the cyanobacterial strains *Synechococcus* sp. PCC 7942, *Synechocystis* sp. PCC 6803, and *Synechococcus* sp. PCC 7418: osmolyte accumulation and stress protein synthesis. *J Plant Physiol* 154:240–249
- Garnham GW, Green M (1995) Chromate(VI) uptake and interactions with cyanobacteria. *J Ind Microbiol* 14: 247–251
- Italiano F, Rinalducci S, Agostiano A, Zolla L, Leo DF, Ceci LR, Trotta M (2012) Changes in morphology, cell wall composition and soluble proteome in *Rhodobacter sphaeroides* cells exposed to chromate. *Biometals*. doi: 10.1007/s10534-012-9561-7
- Khattar JIS, Sarma TA, Sharma A (2004) Effect of Cr⁶⁺ stress on photosynthetic pigments and certain physiological processes in the cyanobacterium *Anacystis nidulans* and its chromium resistant strain. *J Microbiol Biotechnol* 14: 1211–1216

- Kiran B, Kaushik A, Kaushik CP (2007) Response surface methodological approach for optimizing removal of Cr(VI) from aqueous solution using immobilized cyanobacterium. *Chem Eng J* 126:147–153
- Kiran B, Rani N, Kaushik A (2008) Chromium(VI) tolerance in two halotolerant strains of *Nostoc*. *J Environ Biol* 29: 155–158
- Nies DH, Koch S, Wachi S, Pietzsch N, Saier MH (1998) CHR, a novel family of prokaryotic proton motive force-driven transporters probably containing chromate/sulfate antiporters. *J Bacteriol* 180:5799–5802
- Ozturk S, Aslim B, Suludere Z (2009) Evaluation of chromium(VI) removal behavior by two isolates of *Synechocystis* sp. in terms of exopolysaccharide (EPS) production and monomer composition. *Bioresource Technol* 100: 5588–5593
- Rami'ez-Diaz MI, Diaz-Perez C, Vargas E, Riveros-Rosa H, Compos-Garcia J, Cervantes C (2008) Mechanisms of bacterial resistance to chromium compounds. *Biometals* 21:321–332
- Reynolds ES (1963) The use of lead citrate at high pH as electron-opaque stain for electron microscopy. *J Cell Biol* 17:208–212
- Riedel GF (1985) The relationship between chromium(VI) uptake, sulfate uptake and chromium (VI) toxicity in the estuarine diatom *Thalassiosira pseudonana*. *Aquatic Toxicol* 7:191–204
- Rippka R, Deruelles J, Waterbury J, Herdman M, Stanier R (1979) Generic assignments strain histories and properties of pure cultures of cyanobacteria. *J Gen Microbiol* 111: 1–61
- Stork T, Michel KP, Pistorius EK, Dietz KJ (2005) Bioinformatic analysis of the genomes of the cyanobacteria *Synechocystis* sp. PCC 6803 and *Synechococcus elongatus* PCC 7942 for the presence of peroxiredoxins and their transcript regulation under stress. *J Exp Bot* 56:3193–3206
- Thompson SL, Manning FCR, McColl SM (2002) Comparison of the toxicity of chromium(III) and chromium(VI) to cyanobacteria. *Bull Environ Contam Toxicol* 69:286–293
- Urone PF (1955) Stability of colorimetric reagent for chromium, s-diphenylcarbazide, in various solvents. *Anal Chem* 27: 1354–1355
- Yewalkar SN, Dhumal KN, Sainis JK (2007) Chromium(VI)-reducing *Chlorella* spp. isolated from disposal sites of paper-pulp and electroplating industry. *J Appl Phycol* 19: 459–465

*Reprints of published articles
(related to the thesis)*

Employing a Photosynthetic Antenna Complex to Interfacial Electron Transfer on ZnO Quantum Dot

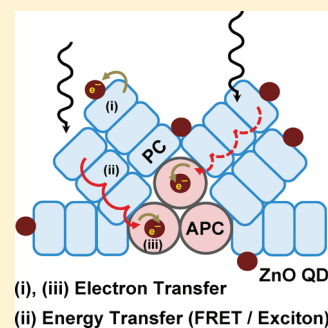
Sandeep Verma,[†] Alka Gupta,[‡] Jayashree K. Sainis,[‡] and Hirendra N. Ghosh^{*,†}

[†]Radiation and Photochemistry Division and [‡]Molecular Biology Division, Bhabha Atomic Research Centre, Mumbai, 400085, India

S Supporting Information

ABSTRACT: Photosynthetic antenna complexes exhibit unidirectional energy-transport phenomena, which make them potential photosensitizers in interfacial electron-transfer processes. In the present study, we show the antenna function of phycocyanin-allophycocyanin (PC–APC) complex using transient emission and absorption spectroscopy. Interfacial electron-transfer dynamics in the PC–APC complex sensitized ZnO semiconductor quantum dot material is compared in native and denatured conditions. The downhill sequential energy transfer from a peripheral phycocyanin disk to a core allophycocyanin disk opens a new electron injection pathway from the allophycocyanin disk in addition to primary electron injection from directly photoexcited phycocyanin disk. Further, the large association of phycocyanobilin chromophores in PC–APC conjugates stabilizes the positive charge within the sensitizer, which leads to slower charge recombination in comparison to that in denatured condition. This study displays the antenna function of energy-efficient biomolecules in favor of better charge separation across the semiconductor interface.

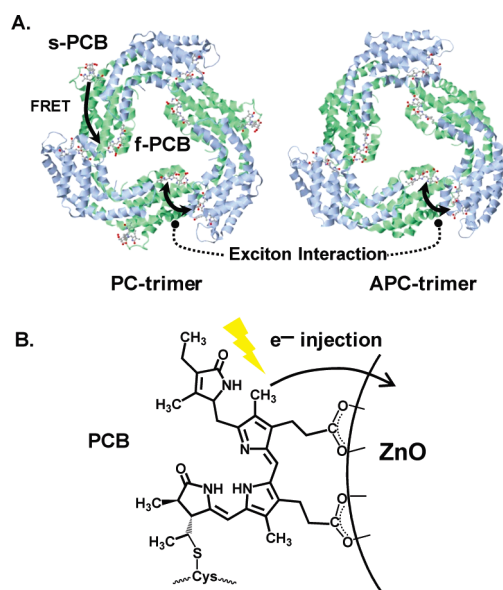
SECTION: Nanoparticles and Nanostructures



The light-harvesting mechanisms in cyanobacteria have enlightened a very important aspect of energy migration in closely coupled protein pigments.¹ The energy migration in light-harvesting pigment phycobilisome (PBS) takes place with an overall efficiency of 95%.² The multilayer interfacing of phycocyanin (PC) disks in the rod region to the allophycocyanin (APC) core region makes a large association of light-absorbing phycocyanobilin (PCB) chromophores in PBS.³ The excitonic interaction and dipole–dipole interaction between PCB chromophores lay the foundation of downhill energy transfer from the peripheral PC pigment to the APC core on a ~ 100 ps time scale.^{4–8} According to the structure–function relationship,⁹ the $\alpha\beta$ -polypeptide pair (monomer) assembles in a ring symmetry (trimer/hexamer), which expresses the genesis of sub-picosecond energy transfer in coherently aligned PCB chromophores ($\alpha 84$ and $\beta 84$ cysteine residue) within PC and APC core pigments.^{10,11} Further, the Förster energy-transfer cascade from the outer core PCB chromophore ($\beta 155$) to the inner core PCB chromophore ($\alpha 84$) in a multitude of PC disks sets an upper limit of ~ 100 ps for energy transfer in the PBS complex.¹² Accordingly, the Förster coupled chromophores devise a subset of “sensitizing (s)” and “fluorescing (f)” chromophores which covers a broad spectral region (visible) on account of a gradual energetics shift (PCB chromophores) from the peripheral to core region of the PBS entity.¹³

The PBS complex can formulate antenna functions^{14,15} as a result of a unique energy-directing property and broad spectral response, which are suitable for light-harvesting devices, sensors, and photocatalytic applications. Recently, PBSs, as extracted in the native form, are employed in a luminescent solar

Scheme 1. (A) Ring Assembly of the PC and APC Units for Coherent and Incoherent Energy Transfer and (B) Phycocyanobilin–apoprotein Sensitization of ZnO



concentrator¹⁶ with a function in redirecting captured photon energy onto an optically coupled solar cell unit. However, direct

Received: February 24, 2011

Accepted: March 24, 2011

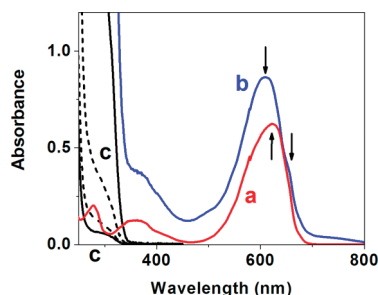


Figure 1. Optical absorption spectra of (a) PC-APC conjugates in HEPES aqueous buffer at 8.0 pH, (b) PC-APC/ZnO QDs and (c) ZnO QDs at different concentrations. (Peak positions are indicated by arrows.)

involvement of a PBS antenna complex in an interfacial electron-transfer (IET) process is hindered by a multitude of parallel and sequential energy-transfer^{1–13} processes in PBS antenna complexes. In principle, the pigment protein has a high potential to develop into an efficient photosensitizer for semiconductor nanocrystal or quantum dot materials due to its high molecular extinction coefficient ($\sim 10^5 \text{ M}^{-1} \text{ cm}^{-1}$) and phenomenal unidirectional energy-transport property.¹⁷ In this work, we present antenna functionality of PC-APC conjugates to generate interfacial charge separation on ZnO semiconductor quantum dot (QD) materials. Herein, the “PC-APC conjugates” term refers to a PBS antenna complex extracted from *Synechococcus BDI*¹⁸ in HEPES buffer solution at pH 8.0. The labeling PC-APC conjugate postulates an energy-transfer function from PC to APC units. The ZnO semiconductor material is selected for its good pH compatibility with PBS buffer solution (8.0pH) and suitable conduction band (CB $\approx -0.45 \text{ eV}$ vs. NHE) energetics.¹⁹ The carboxylate functionality of the PCB chromophore helps in binding on the ZnO surface, as depicted in Scheme 1.

In the PC-APC conjugate sensitized ZnO system, the electron injection process can be initiated directly from the photoexcited PC entity (PCB chromophore²⁰). The significant PC-APC coupling can help in achieving an additional electron-transfer pathway from the APC unit by receiving captured photoenergy from the nonparticipating PC entity. In this way, the PBS antenna functionality may circumvent the loss of nonparticipating photoexcited states of the PC complex and can provide better charge separation.

Figure 1 shows the optical absorption spectra of the PC-APC conjugate ($\sim 1.75 \mu\text{M}$) that increases after addition of ZnO QDs (60 g/L). An absorbance peak at 623 nm with a small shoulder at 655 nm is observed in the 475–690 nm region, which corresponds to the lowest excited/exciton state of PC and the APC trimer, respectively. The high intensity peak at 623 nm suggests a larger content of PC entities as compared to APC units in the PBS complex. The trimer form of PC and APC disks and the higher content of PC entities are confirmed by native PAGE analysis,¹⁸ which is provided in the Supporting Information. The higher energetic band in the 300–450 nm region is characteristic of a second excited state (Soret-type band) of PCB chromophores (linear tetrapyrrole).²¹ The photoexcitation in this region mainly populates the PCB chromophore located on the peripheral PC pigment. The significant increase in absorption spectra of the conjugated PC-APC complex after addition of ZnO QDs represents the efficient sensitization of the ZnO QDs.

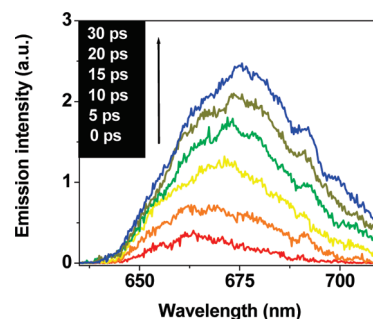


Figure 2. Transient emission spectra of conjugated PC-APC complex in buffer solution at 8.0 pH on a 0–30 ps time scale by using laser pulse excitation at 400 nm.

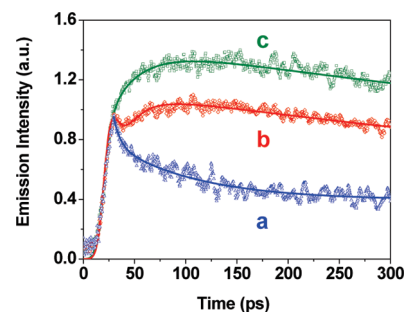


Figure 3. Transient emission decay kinetics of conjugated PC-APC complex at (a) 615, (b) 655, and (c) 675 nm (normalized for comparison purpose).

The observation of efficient spectral sensitization of ZnO QDs prompts us to look into the antenna functionality of the PC-APC conjugate. The energy-transfer pathways in the conjugated PC-APC complex are explored by time-resolved emission measurements (Figure 2) using a streak camera with a temporal resolution of ~ 6 ps.

Figure 2 shows the transient emission spectrum of a native PC-APC complex. Initially, an emission maximum is observed at 663 nm, which red shifts to 675 nm with increasing intensity in a 0–30 ps delay time. The transient emission spectrum is assigned to the APC trimer. In the literature,^{4,12} the emission due to the pure PC entity is reported in the 620–650 nm region. In the present study, the absence of prominent PC complex emission is sign of an efficient PC \rightarrow APC energy-transfer process. The 400 nm photoexcitation leads to Förster energy transfer from the peripheral *s*-PCB chromophore ($\beta 155$) to the inner core *f*-PCB chromophore ($\beta 84$) of the PC pigment. The whole process is traced by leaked emission (low) of the *s*-PCB chromophore in the 615–620 nm region.

Figure 3 shows the transient emission decay profile of the PC-APC conjugate at 615, 655, and 675 nm wavelengths. The fitting time constants are provided in Table 1. The 6.5 ps decay component of the 615 nm emission kinetics closely matches the rise of the 655 nm emission (~ 8 ps) and hence is assigned to the *s*-PCB \rightarrow *f*-PCB energy-transfer process. The 30 ps evolution time in the 675 nm emission kinetics represents the solvation (diffusive protein matrix response) process²² of the PC-APC complex, which explains the increasing emission intensity during peak shift (~ 12 nm) on a 0–30 ps time scale (Figure 2). The ultrafast (~ 8 –30 ps) solvation process inhibits the back energy

Table 1. Fitting Parameter for Time-Resolved Emission Traces of the Native PC–APC Complex with Instrument Response Function (IRF) ≤ 6 ps

615 nm	655 nm	675 nm
IRF (+100%)	IRF (+85%)	IRF (+68%)
6.5 ps (−25%)	6.5 ps (−5.7%)	30 ps (+32%)
82 ps (−32%)	8 ps (+10.7%)	>400 ps (−100%)
>400 ps (−43%)	20 ps (+4.3%)	
	>400 ps (−94.3%)	

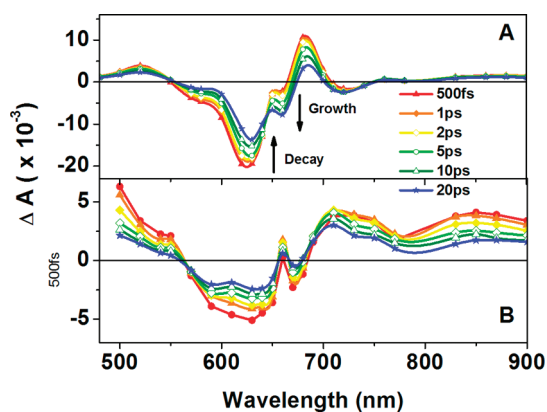


Figure 4. TA spectra of native PC–APC conjugates (A) and a denatured PC–APC complex (B) recorded at 500 fs and 1, 2, 5, 10, and 20 ps delay times after 400 nm laser pulse excitation (ΔA = transient absorbance).

transfer and thus ensures a unidirectional energy transfer in the PC–APC complex. The longer decay component (~ 80 ps), observed only at 615 nm, represents the heterogeneous relaxation channel of the PC complex. Similar heterogeneous relaxation processes were observed earlier on a 40–100 ps time scale for the PC complex (bare) obtained from different cyanobacteria systems and recognized as a characteristic of the PC complex.^{5,23} The longer component (>400 ps) is assigned to the long-lived APC complex reported earlier with a 1–2 ns lifetime.^{1–13}

The energy transfer function of the PC–APC conjugate is confirmed by another complementary technique, femtosecond time-resolved transient absorption (TA) spectroscopy²⁴ using 400 nm pump excitation and 480–900 nm probe detection of PC–APC transient species. The TA spectrum of the PC–APC conjugate is presented in Figure 4A (top panel). The early 500 fs TA spectrum comprises a strong negative band in the 600–640 nm region. The negative absorption represents photobleach or stimulated emission or both on the grounds that absorption and emission of the PC complex appear in this region (Figure 1 and earlier literature^{4,12}). The photobleach/stimulated emission band exhibits a salient feature of a decreasing 630 nm peak with concomitant growth of another 660 nm peak in a 20 ps time window. The presence of an isosbestic point at 645 nm signifies the PC \rightarrow APC energy-transfer process in the conjugated PC–APC complex. The energy-transfer process is further supported by a monotonously decaying excited-state absorption band (positive band) of PC units in the 480–550 nm region and corresponding growth of the stimulated emission band of APC

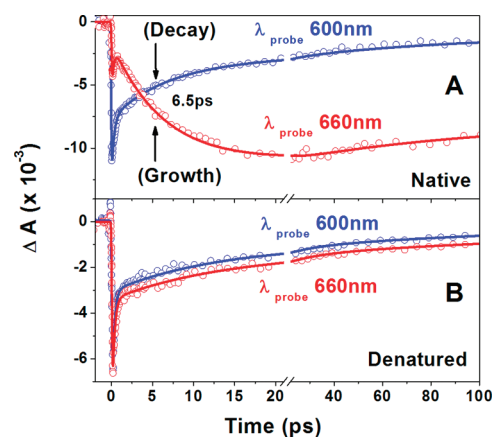


Figure 5. TA kinetics at 600 and 660 nm, which respectively probes (A) the PC and APC entities of the native PC–APC conjugate and (B) the denatured PC–APC complex. (Kinetics are normalized for comparison purpose.)

units in the 700–750 nm region. The energy-transfer kinetics are monitored accordingly in the selected TA spectral region.

Figure 5 shows the TA kinetics at 600 and 660 nm probing wavelengths. The fitting time constants are provided separately in Supporting Information Table S2. The shortest ~ 300 fs time component of the 600 and 660 nm TA kinetics can be assigned to an exciton relaxation^{7,8} process in the PC–APC conjugate. A second decay component on a 6.5 ps time scale in the 600 nm photobleach/stimulated emission kinetics of the PC segment matches well with the growth component of the 660 nm photobleach/stimulated emission signal of the APC segment. Such features are not observed in TA analysis of a denatured PC–APC mixture (Figures 4B and 5B and Supporting Information Figures S11 and S12). This reaffirms the 6.5 ps time domain for the PC \rightarrow APC energy-transfer process, which was observed earlier in transient emission studies. It is further supported by TA decay kinetics of the PC segment at 520 nm and stimulated emission growth kinetics of the APC segment at 700 nm, which are provided in the Supporting Information. The longer ~ 70 ps and >1 ns time components in the TA decay (of the native PC–APC complex) represents heterogeneous relaxation and natural lifetime of the PC and APC segments, respectively.

The TA and emission studies establish the antenna functioning of the PC–APC conjugate in the sub-picosecond to ~ 10 ps time domain. Therefore, it is appropriate to carry out an IET study on the sensitized ZnO QD system, which also occurs in the same time domain.²⁵ Figure 6A (top panel) shows the TA spectra of the conjugated PC–APC complex sensitized ZnO QDs. The prominent difference of the TA spectrum of PC–APC conjugates in the absence (Figure 4A) and presence (Figure 6A) of ZnO QDs corresponds to transient species generated by the IET process. The positive TA band in the 650–770 nm region resembles the cation $[\text{PC-APC}]^{+\bullet}$ spectrum. The assignment is based on the $[\text{PC-APC}]^{+\bullet}$ cation spectrum ascertained in selective one-electron oxidation in pulse radiolysis studies (Supporting Information Figures S15 and S16). Another positive TA band in the 830–950 nm region represents an electron (transient species) in the CB of ZnO QDs.²⁶ The negative TA band in the 575–640 nm region corresponds to bleach recovery by charge recombination and exciton relaxation processes.

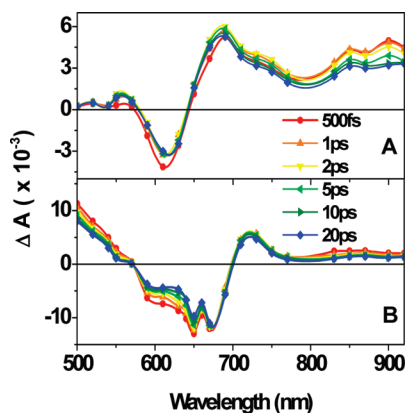


Figure 6. TA spectra of the native PC–APC conjugate sensitized ZnO QD (A) and the denatured PC–APC complex sensitized ZnO QD (B) recorded at 500 fs and 1, 2, 5, 10, and 20 ps delay times after 400 nm laser pulse excitation.

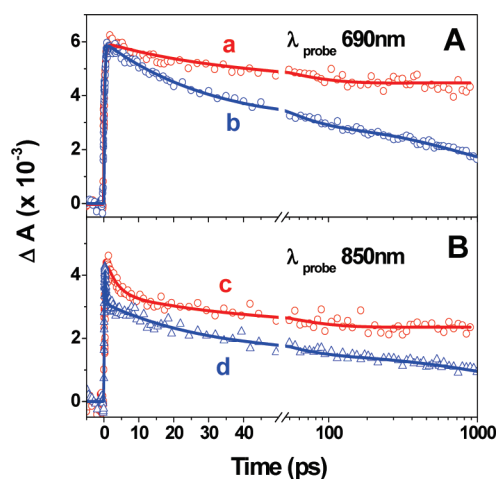


Figure 7. TA kinetics at (A) 690 nm probing the (PC–APC)⁺⁺ cation in (a) the native PC–APC/ZnO QD and (b) the denatured PC–APC/ZnO QD system and at (B) 850 nm probing the e[−] CB (ZnO QD) in (c) the native PC–APC/ZnO system and (d) the denatured PC–APC/ZnO system. (Kinetics are normalized for comparison purpose.)

The role of the PC–APC conjugate function in achieving a better charge separation across the ZnO QD interface is understood by comparing the IET dynamics (690 nm cation or 850 nm e[−] CB (ZnO)) in native and denatured conditions. The details of TA spectrum of a denatured PC–APC mixture/ZnO QD system (Figure 6B (bottom panel)) is provided in the Supporting Information (Figure S13).

Figure 7 shows a comparison of the IET dynamics in native and denatured conditions. The fitting time constants are given separately in the Supporting Information in Table S2. In both cases, the cation formation kinetics (rise of the 690 nm TA signal) are observed to be multiexponential (<80 fs (+50%) and 400 fs (+50%)). This is attributed to the low density of the acceptor states (in the CB) of the ZnO QD. More importantly, the cation decay kinetics (1 ps to 1 ns) is observed to be slower in the native PC–APC/ZnO QD system (40 ps (−25%), >1 ns (−75%)) in comparison to that in the denatured PC–APC/ZnO QD system (30 ps (−49%), >1 ns (−51%)). The trend is

further observed in the decay profile of e[−] CB (ZnO) recorded at 850 nm.

In conclusion, the comparison of native and denatured PC–APC/ZnO systems reveals a higher electron injection yield (~2.4 times) and a slow BET in native conditions. The antenna function of the native PC–APC conjugate bestows a higher electron injection yield due to a largely associated network of PCB chromophores. In any IET reaction (like this one), the photoexcitation energy of the sensitizer molecule is not fully utilized in view of certain energy loss caused by nonradiative or radiative decay to the ground state. In this regard, the conjugate function of the PC–APC complex enlightens a way to intervene the energy loss by redirecting the excitation energy from the noninjecting primary source (PC pigment) to the secondary source (APC pigment). The success relies on the fact that the energy-transfer process (6.5 ps in the PC–APC conjugate) is sufficiently faster to compete with the heterogeneous relaxation channel (~80 ps for the PC pigment) but slower than the IET process (≤400 fs) related to either electron injecting source (PC pigment or APC pigment). The importance of the antenna function is further realized when breaking of long-range association (denatured PC–APC mixture) causes a fast back electron-transfer process. In the conjugated system (native PC–APC conjugate), the cation ([conjugate PC–APC]⁺⁺) is stabilized by a large network of electron-donor units (associated PCB chromophores). Therefore, the back electron-transfer process is accordingly slowed down in the conjugated system (native PC–APC complex) in comparison to that in the nonconjugated system (denatured PC–APC mixture). This apparently displays the antenna function of energy-efficient biomolecules in favor of better charge separation across the semiconductor interface.

■ ASSOCIATED CONTENT

S Supporting Information. Details about the tabulated form of the fitting time constants of TA kinetics, sample preparation, excitation and emission spectra, the CD spectrum of the sample in the native and denatured conditions, TA spectra of the denatured PC–APC complex and the denatured PC–APC sensitized ZnO system, the cation spectrum of the native and denatured PC–APC complexes in a pulse radiolysis study, and the experimental setup for TA and emission studies. This material is available free of charge via the Internet at <http://pubs.acs.org>.

■ AUTHOR INFORMATION

Corresponding Author

*E-mail: hngshosh@barc.gov.in. Fax: (+) 91-22-25505331/25505151.

■ ACKNOWLEDGMENT

The authors thank Dr. D. K. Palit, Dr. S.K. Sarkar, and Dr. T. Mukherjee for their encouragement and continuous support.

■ REFERENCES

- (1) Glazer, A. N.; Chan, C.; Williams, R. C.; Yeh, S. W.; Clark, J. H. Kinetics of Energy Flow in the Phycobilisome Core. *Science* **1985**, *230*, 1051–1053.

- (2) Glazer, A. N.; Yeh, S. W.; Webb, S. P.; Clark, J. H. Disk-to-Disk Transfer as the Rate-Limiting Step for Energy Flow in Phycobilisomes. *Science* **1985**, *227*, 419–423.
- (3) Glazer, A. N. Phycobilisomes: Structure and Dynamics. *Annu. Rev. Microbiol.* **1982**, *36*, 173–198.
- (4) Yamazaki, I.; Tamai, N.; Yamazaki, T.; Murakami, A.; Mimuro, M.; Fujita, Y. Sequential Excitation Energy Transport in Stacking Multilayers: Comparative Study between Photosynthetic Antenna and Langmuir–Blodgett Multilayers. *J. Phys. Chem.* **1988**, *92*, 5035–5044.
- (5) Beck, W. F.; Sauer, K. Energy-Transfer and Exciton-State Relaxation Processes in Allophycocyanin. *J. Phys. Chem.* **1992**, *96*, 4658–4666.
- (6) Debreczeny, M. P.; Sauer, K.; Zhou, J.; Bryant, D. A. Comparison of Calculated and Experimentally Resolved Rate Constants for Excitation Energy Transfer in C-Phycocyanin. 2. Trimers. *J. Phys. Chem.* **1995**, *99*, 8420–8431.
- (7) Womick, J. M.; Moran, A. M. Exciton Coherence and Energy Transport in the Light-Harvesting Dimers of Allophycocyanin. *J. Phys. Chem. B* **2009**, *113*, 15747–15759.
- (8) Womick, J. M.; Miller, S. A.; Moran, A. M. Toward the Origin of Exciton Electronic Structure in Phycobiliproteins. *J. Chem. Phys.* **2010**, *133*, 024507/1–024507/10.
- (9) Huber, R. A Structural Basis of Light Energy and Electron Transfer in Biology (Noble Lecture). *Angew. Chem., Int. Ed. Engl.* **1989**, *28*, 848–869.
- (10) MacColl, R. Cyanobacterial Phycobilisomes. *J. Str. Biol.* **1998**, *124*, 311–334.
- (11) Edington, M. D.; Riter, R. E.; Beck, W. F. Interexciton-State Relaxation and Exciton Localization in Allophycocyanin Trimers. *J. Phys. Chem.* **1996**, *100*, 14206–14217.
- (12) Suter, G. W.; Holzwarth, A. R. A Kinetic Model for the Energy Transfer in Phycobilisomes. *Biophys. J.* **1987**, *52*, 673–683.
- (13) Glazer, A. N.; Clark, J. H. Phycobilisomes: Macromolecular Structure and Energy Flow Dynamics. *Biophys. J.* **1986**, *49*, 115–116.
- (14) Scholes, G. D. Quantum-Coherent Electronic Energy Transfer: Did Nature Think of It First? *J. Phys. Chem. Lett.* **2010**, *1*, 2–8.
- (15) Das, R.; Kiley, P. J.; Segal, M.; Norville, J.; Amy, Yu, A.; Wang, L.; Trammell, S. A.; Reddick, L. E.; Kumar, R.; Stellacci, F.; et al. Integration of Photosynthetic Protein Molecular Complexes in Solid-State Electronic Devices. *Nano Lett.* **2004**, *4*, 1079–1083.
- (16) Mulder, C. L.; Theogarajan, L.; Currie, M.; Mapel, J. K.; Baldo, M. A.; Vaughn, M.; Willard, P.; Bruce, B. D.; Moss, M. W.; McLain, C. E.; et al. Luminescent Solar Concentrators Employing Phycobilisomes. *Adv. Mater.* **2009**, *21*, 3181–3185.
- (17) Glazer, A. N. Light Guides. *J. Biol. Chem.* **1989**, *264*, 1–4.
- (18) Gupta, A.; Sainis, J. K. Isolation of C-phycocyanin from *Synechococcus* sp., (*Anacystis nidulans* BD1). *J. Appl. Phycol.* **2010**, *22*, 231–233.
- (19) Van de Walle, C. G.; Neugebauer, J. Universal Alignment of Hydrogen Levels in Semiconductors, Insulators and Solutions. *Nature* **2003**, *433*, 626–628.
- (20) Liu, Z. Theoretical Studies of Natural Pigments Relevant to Dye-Sensitized Solar Cells. *J. Mol. Struct.: THEOCHEM* **2008**, *862*, 44–48.
- (21) Gouterman, M. *The Porphyrins*; Dolphin, D, Ed.; Academic Press: New York, 1978; Vol. III, p 1.
- (22) Riter, R. R.; Edington, M. D.; Beck, W. F. Protein-Matrix Solvation Dynamics in the α Subunit of C-Phycocyanin. *J. Phys. Chem.* **1996**, *100*, 14198–14205.
- (23) Debreczeny, M. P.; Sauer, K.; Zhou, J.; Bryant, D. A. Comparison of Calculated and Experimentally Resolved Rate Constants for Excitation Energy Transfer in C-Phycocyanin. 1. Monomers. *J. Phys. Chem.* **1995**, *99*, 8412–8419.
- (24) Verma, S.; Kar, P.; Das, A.; Ghosh, H. N. Efficient Charge Separation in TiO₂ Films Sensitized with Ruthenium(II)–Polypyridyl Complexes: Hole Stabilization by Ligand-Localized Charge-Transfer States. *Chem.—Eur. J.* **2011**, *17*, 1561–1568.
- (25) Katoh, R.; Furube, A.; Hara, K.; Murata, S.; Sugihara, H.; Arakawa, H.; Tachiya, M. Efficiencies of Electron Injection from Excited Sensitizer Dyes to Nanocrystalline ZnO Films as Studied by Near-IR Optical Absorption of Injected Electrons. *J. Phys. Chem. B* **2002**, *106*, 12957–12964.
- (26) Bauer, C.; Boschloo, G.; Mukhtar, E.; Hagfeldt, A. Electron Injection and Recombination in Ru(dcbpy)₂(NCS)₂ Sensitized Nanostructured ZnO. *J. Phys. Chem. B* **2001**, *105*, 5585–5588.